

**The effect of heat and chemical  
penetration enhancers on the follicular  
absorption of topically applied drugs**

**Hassan Abdi Farah**

Submitted to the University of Hertfordshire in partial fulfilment of the  
requirements of the degree of Doctors of Philosophy

**January 2018**

# Abstract

The stratum corneum (SC) is the primary barrier regulating the penetration of substances into the lower layers of skin. A number of strategies have been used to increase drug transport across skin, with chemical penetration enhancers (CPEs) being the most common approach. Heat is another strategy that has been shown to render skin more permeable to drugs. The synergistic effects of heat in combination with CPEs is an under-investigated and promising strategy to enhance the dermal delivery of drugs. In this thesis, the effect of physiologically tolerable heat ( $\leq 45$  °C) on the *in vitro* percutaneous absorption of minocycline, isotretinoin and finasteride was investigated, with an aim to develop an optimised delivery system. Furthermore, the employment of heat coupled with CPEs as a targeting strategy for improving follicular transport and skin penetration of drugs with a wide range of lipophilicities was investigated.

Three active pharmaceutical ingredients; minocycline, isotretinoin and finasteride were selected based their differing lipophilic properties (minocycline: Log P = -0.61, isotretinoin: Log P = 6.6 and finasteride: Log P= 3.2). All drugs were delivered from saturated suspensions from various dermatological vehicles commonly used as CPEs. Two of the major parameters influencing percutaneous absorption, the diffusion and partition coefficients (as pathlength normalised), were determined with a view to gain insight into the mechanisms through which heat can enhance drug delivery to the skin.

The findings of this thesis have shown that the application heat ( $\leq 45$  °C) can significantly enhance skin permeation of hydrophilic and hydrophobic drugs (up to 27-fold when isotretinoin was delivered from EtOH) mainly through improvements in partitioning of the drug from the formulation into the SC. Heat was found to enhance the flux of hydrophobic drugs more when delivered from diisopropyl adipate (DPA) and propylene glycol (PG). Therefore, the level of enhancement achieved was found to be dependent on both the physicochemical properties of the drugs and formulation components

(CPEs). In the presence of magnesium chloride, the majority of minocycline was recovered from the epidermis. However, the application of heat was found alter the skin distribution of minocycline (in the presence of magnesium chloride) so that most of the drug was recovered from the dermis (the target site for minocycline), potentially improving its efficacy. Also, localised heating for short periods (15-25 min) in combination with fatty acid esters and alcohols and their derivatives demonstrated the positive impact heat and CPEs can have on follicular transport (up to 2-fold increase). This strategy potentially allows for targeted delivery through hair follicles which is likely to be a significant advance for drugs like isotretinoin, which have significant side effects profiles.

In conclusion, this work has demonstrated that the novel strategy employing the customised use of physiologically tolerable heat ( $\leq 45^{\circ}\text{C}$ ) to target the follicular structures and enhance drug delivery is a highly promising approach which, following further investigations will be highly beneficial in the optimisation of current topical formulations and the development of new drug delivery systems.

# Acknowledgments

Firstly, I would like to express my heartfelt gratitude to my supervisors, Dr. William McAuley and Prof. Marc Brown for their advice and guidance over the last few years. I am deeply grateful to MedPharm Ltd for sponsoring this PhD and for allowing me to spend time working in their organisation.

I would like to thank all the technical staff at UH, especially Mr James Stanley without whom the HPLC instrument would have been constantly out of order. I must also extend a special and most sincere thanks to Dr. Victoria Hutter whom trained me on how to use the confocal microscope, Prof. Rob Chilcott and Dr. Julie Sanderson for allowing me to use their cryostats at BioPark and the University of East Anglia respectively.

I must also thank all my colleagues and friends at UH for their advice, words of encouragement and for making my experience memorable.

Finally, I must thank all my family members for their continual support. I especially thank my wife Yasmin, for her patience and many sacrifices. I would like to give an extra thank you to my parents and children for their constant support and encouragement throughout this journey.

# Table of Contents

<b>ABSTRACT.....</b>	<b>I</b>
<b>ACKNOWLEDGMENTS .....</b>	<b>III</b>
<b>TABLE OF CONTENTS.....</b>	<b>IV</b>
<b>ABBREVIATIONS.....</b>	<b>VIII</b>
<b>1 INTRODUCTION.....</b>	<b>1</b>
1.1 INTRODUCTION .....	2
1.2 SKIN STRUCTURE AND FUNCTION .....	6
1.2.1 EPIDERMIS .....	7
1.2.2 DERMIS .....	9
1.2.3 HYPODERMIS.....	10
1.2.4 SKIN APPENDAGES .....	10
1.3 PILOSEBACEOUS UNIT .....	12
1.3.1 ANATOMY OF THE PILOSEBACEOUS UNIT.....	12
1.3.2 HAIR FOLLICLE- ASSOCIATED SKIN DISORDERS .....	16
1.3.3 GENERAL ASPECTS OF FOLLICULAR DRUG DELIVERY .....	22
1.4 ROUTES OF DRUG PENETRATION ACROSS SKIN .....	24
1.4.1 TRANSEPIDERMAL ROUTE FOR DRUG PERMEATION .....	25
1.4.2 TRANSAPPENDAGEAL ROUTE (SWEAT GLANDS) .....	26
1.5 FACTORS AFFECTING PERCUTANEOUS ABSORPTION.....	27
1.5.1 PHYSIOLOGICAL FACTORS AFFECTING DERMAL ABSORPTION OF DRUGS .....	27
1.5.2 PHYSICOCHEMICAL FACTORS INFLUENCING PERCUTANEOUS ABSORPTION.....	28
1.5.3 ENVIRONMENTAL FACTORS AFFECTING DERMAL ABSORPTION.....	29
1.6 MATHEMATICS OF SKIN PERMEATION .....	30
1.7 PERCUTANEOUS ABSORPTION ENHANCEMENT OF TOPICAL AND TRANSDERMAL FORMULATIONS .....	32
1.7.1 PASSIVE METHODS.....	33
1.7.2 ACTIVE METHODS .....	39
1.8 SUMMARY .....	48
1.9 THE AIM AND OBJECTIVES OF THESIS .....	49

<b>2</b>	<b><u>ANALYTICAL VALIDATION OF GENERAL METHODS</u></b>	<b>50</b>
<b>2.1</b>	<b>INTRODUCTION</b>	<b>51</b>
2.1.1	ACTIVE PHARMACEUTICAL INGREDIENTS (APIs) OF INTEREST	51
2.1.2	REVERSE PHASE HIGH PERFORMANCE LIQUID CHROMATOGRAPHY (HPLC) FOR QUANTIFICATION OF APIs	54
2.1.3	<i>IN VITRO</i> SKIN PERMEATION ASSESSMENT	55
<b>2.2</b>	<b>MATERIALS AND METHODS</b>	<b>56</b>
2.2.1	HPLC ASSAY METHOD DEVELOPMENT	57
2.2.2	<i>IN VITRO</i> SKIN PERMEATION METHOD DEVELOPMENT	65
<b>2.3</b>	<b>RESULTS AND DISCUSSION</b>	<b>68</b>
2.3.1	HPLC METHOD VALIDATION	68
2.3.2	<i>IN VITRO</i> SKIN PERMEATION METHOD DEVELOPMENT	78
<b>2.4</b>	<b>CONCLUSION</b>	<b>102</b>
<b>3</b>	<b><u>EFFECT OF HEAT, CPES AND MAGNESIUM CHLORIDE ON THE SKIN PERMEATION AND DISTRIBUTION OF MINOCYCLINE</u></b>	<b>103</b>
<b>3.1</b>	<b>INTRODUCTION</b>	<b>104</b>
<b>3.2</b>	<b>MATERIALS AND METHODS</b>	<b>106</b>
3.2.1	QUANTITATIVE ANALYSIS OF MINOCYCLINE	106
3.2.2	EFFECT OF MAGNESIUM ON THE SATURATED SOLUBILITY OF MINOCYCLINE	106
3.2.3	<i>IN VITRO</i> SKIN PERMEATION EXPERIMENTS	107
3.2.4	DRUG SKIN DISTRIBUTION STUDIES	108
3.2.5	PENETRATION OF MINOCYCLINE AND MAGNESIUM-MINOCYCLINE COMPLEX INTO SKIN: CONFOCAL LASER SCANNING MICROSCOPY STUDIES	109
3.2.6	DETERMINATION OF MAGNESIUM AND MINOCYCLINE STOICHIOMETRY	111
3.2.7	VISCOSITY MEASUREMENTS OF MINOCYCLINE FORMULATIONS WITH AND WITHOUT MAGNESIUM AT 32 °C AND 45 °C	112
3.2.8	<i>IN VITRO</i> RELEASE RATE STUDY USING CELLULOSE MEMBRANE	112
3.2.9	<i>IN VITRO</i> RELEASE RATE OF MINOCYCLINE AND MAGNESIUM-MINOCYCLINE COMPLEX ACROSS CELLULOSE MEMBRANE: COMPLETE SYSTEM HEATING VS HEAT APPLIED FROM TOP	114
3.2.10	DATA TREATMENT AND STATISTICS	115
<b>3.3</b>	<b>RESULTS AND DISCUSSION</b>	<b>116</b>
3.3.1	THE EFFECT OF MAGNESIUM ON THE SATURATED SOLUBILITY OF MINOCYCLINE	116
3.3.2	<i>IN VITRO</i> SKIN PERMEATION AND DISTRIBUTION ACROSS FULL THICKNESS ABDOMINAL SKIN	117

3.3.3	DISTRIBUTION OF MINOCYCLINE AND MAGNESIUM-MINOCYCLINE COMPLEX ACROSS FULL THICKNESS HUMAN ABDOMINAL SKIN: CONFOCAL LASER SCANNING MICROSCOPY STUDIES.....	127
3.3.4	DETERMINATION OF MAGNESIUM AND MINOCYCLINE STOICHIOMETRY .....	130
3.3.5	VISCOSITY MEASUREMENTS OF MINOCYCLINE FORMULATIONS WITH AND WITHOUT MAGNESIUM AT 32 °C AND 45 °C	132
3.3.6	<i>IN VITRO</i> RELEASE STUDIES USING CELLULOSE MEMBRANE.....	134
3.3.7	<i>IN VITRO</i> RELEASE OF MINOCYCLINE AND MAGNESIUM-MINOCYCLINE COMPLEX: COMPLETE SYSTEM HEATING VS HEAT APPLIED FROM TOP .....	144
<b>3.4</b>	<b>CONCLUSION .....</b>	<b>150</b>

**4 EFFECT OF HEAT AND CPES ON THE *IN VITRO* PERCUTANEOUS ABSORPTION OF ISOTRETINOIN**  
**152**

<b>4.1</b>	<b>INTRODUCTION .....</b>	<b>153</b>
<b>4.2</b>	<b>MATERIALS AND METHODS.....</b>	<b>155</b>
4.2.1	QUANTITATIVE ANALYSIS OF ISOTRETINOIN .....	155
4.2.2	<i>IN VITRO</i> EXPERIMENTS.....	156
4.2.3	DATA TREATMENT AND STATISTICS .....	159
<b>4.3</b>	<b>RESULTS AND DISCUSSION .....</b>	<b>160</b>
4.3.1	INFINITE DOSE <i>IN VITRO</i> SKIN PERMEATION AND DISTRIBUTION STUDIES .....	160
4.3.2	FINITE DOSE <i>IN VITRO</i> SKIN PERMEATION AND DISTRIBUTION STUDIES .....	167
4.3.3	THE EFFECTS OF HEAT APPLIED FROM TOP ON DRUG DELIVERY INTO THE HAIR FOLLICLES, SKIN TISSUE AND RECEIVER FLUID OVER 24 HR.....	175
4.3.4	THE EFFECTS OF HEAT FROM TOP ON DRUG DELIVERY INTO THE HAIR FOLLICLES, SKIN TISSUE AND RECEIVER FLUID OVER 1 HR .....	180
<b>4.4</b>	<b>CONCLUSION .....</b>	<b>183</b>

**5 INFLUENCE OF CPES AND HEAT ON THE SKIN PERMEATION, DISTRIBUTION AND FOLLICULAR ABSORPTION OF FINASTERIDE.....**  
**185**

<b>5.1</b>	<b>INTRODUCTION .....</b>	<b>186</b>
<b>5.2</b>	<b>MATERIALS AND METHODS.....</b>	<b>188</b>
5.2.1	HPLC ANALYSIS OF FINASTERIDE .....	188
5.2.2	<i>IN VITRO</i> EXPERIMENTS.....	189
5.2.3	DATA TREATMENT AND STATISTICS .....	191
<b>5.3</b>	<b>RESULTS AND DISCUSSION .....</b>	<b>192</b>
5.3.1	INFINITE DOSE <i>IN VITRO</i> SKIN PERMEATION AND DISTRIBUTION STUDIES .....	192

5.3.2	THE EFFECT OF HEAT APPLIED FROM TOP ON DRUG DELIVERY INTO THE HAIR FOLLICLES, SKIN TISSUE AND RECEIVER FLUID OVER 24 HR: <i>IN VITRO</i> FINITE DOSE STUDIES .....	199
5.3.3	THE EFFECT OF HEAT APPLIED FROM TOP ON DRUG DELIVERY INTO THE HAIR FOLLICLES, SKIN TISSUE AND RECEIVER FLUID OVER 1 HR: <i>IN VITRO</i> FINITE DOSE STUDIES .....	206
5.4	CONCLUSION .....	210
6	<b><u>GENERAL DISCUSSION .....</u></b>	<b><u>212</u></b>
6.1	GENERAL DISCUSSION.....	213
7	<b><u>REFERENCES.....</u></b>	<b><u>224</u></b>

# Abbreviations

Abbreviation	Definition
%	Percent
°C	Degrees Celsius
$\Delta T$	Thermal gradient
$\alpha$	Thermodynamic activity
$\eta$	Viscosity
$\gamma$	Activity coefficient
$\Delta Abs$	Change in absorbance
$\mu g$	Microgram
$\mu l$	Microlitre
$\mu g/mL$	Microgram per millilitre
$\mu m$	Micrometre
ANOVA	Analysis of variance
APIs	Active pharmaceutical ingredients
$C_0$	Concentration of drug in superficial layer of skin
$C_1$	Drug concentration in the outermost layers of the membrane
$C_2$	Drug concentration in the innermost layers of the membrane
CHADD	Controlled heat aided drug delivery
cm	Centimetre
CLSM	Confocal laser scanning microscopy
CPEs	Chemical penetration enhancers
$C_r$	Concentration within the receptor solution
$C_s$	Saturated solubility of the drug in the applied vehicle
$C_v$	Concentration in donor solution/vehicle
CV	Coefficient variation
D	Diffusion coefficient
Da	Dalton
$D/h^2$	Pathlength normalised diffusion coefficient
DHT	Dihydrotestosterone
DMI	Dimethyl isosorbide
DPA	Diisopropyl adipate

$D_T$	Thermophoretic mobility
EDTA	Ethylenediaminetetraacetic acid
EtOH	Ethanol
$E_R$	Enhancement ratio
$f$	Distance between peak maximum and peak front at $W_x$
FDA	Food and Drug Administration
FNS	Finasteride
$g$	Gram
GRAS	Generally Recognised as Safe
GTCC	Crodamol™ GTCC
$h$	Diffusional pathlength/membrane thickness
HPLC	High Performance Liquid Chromatography
hr	Hour
ICH	International Conference on Harmonisation
IPA	Isopropyl alcohol
IPM	Isopropyl myristate
ITN	Isotretinoin
$J$	Flux
$K$	Partition coefficient
$K'$	Capacity Factor
$K_B$	Boltzmann constant
kDa	Kilodalton
$Kh$	Pathlength normalised partition coefficient
$K_p$	Permeability constant
L	Litre
LOD	Limit of detection
Log P (o/w)	Logarithm of partition coefficient octanol/water
LOQ	Limit of quantification
M	Molar
MC	Mean concentration
MCN	Minocycline hydrochloride
min	Minute
mg	Milligram
mg/mL	Milligram per millilitre

mL	Millilitre
mL/min	Millilitre per minute
Mg <sup>2+</sup>	Magnesium ion
mm	Millimetre
MW	Molecular weight
MWCO	Molecular weight cut-off
N	Theoretical Plate Number
nm	Nanometre
NMF	Natural moisturising factor
OECD	Organisation for Economic Co-operation and Development
PBS	Phosphate buffer solution
PG	Propylene glycol
PGML 90	Propylene glycol monolaurate 90
PSU	Pilosebaceous Unit
PTFE	Polytetrafluoroethylene
Q	Cumulative amount of drug permeated
Q(C)	Amount of drug permeated into and across the skin when using no additional heat and CPEs (the control)
Q(E)	Amount of drug permeated into and across the skin when using enhancement strategies (i.e. heat and CPEs)
r	radius
R <sup>2</sup>	Coefficient of determination of a linear regression
RSD	Relative standard deviation
SB	Stratum basale
SC	Stratum corneum
SD	Standard deviation
SEM	Standard error of mean
SG	Stratum granulosum
SL	Stratum lucidum
SS	Stratum spinosum
ST	Sodium thiosulfate pentahydrate
ST 15	Sodium thiosulfate solution producing heat (45°C) for 15 min
ST 25	Sodium thiosulfate solution producing heat (45°C) for 25 min
T	Absolute temperature (Kelvin)

t	Time
TC	Theoretical concentration
TF	Tailing Factor
$T_L$	Lag time
$t_0$	Elution time of the void volume
$t_R$	Retention time of analyte
$t_w$	Peak width measured at baseline of the extrapolated sides to baseline
TP	Transcutol® P
UV	Ultraviolet
V	Molecular volume
$V_T$	Drift mobility
$W_x$	Width of the peak determined at 5% from the baseline of the peak height
X=0	Outermost membrane layer
X=h	Innermost membrane layer

# **1 Introduction**

## 1.1 Introduction

The skin offers a route of administration for topical and systemic delivery of therapeutic compounds. Where the target site is the skin, local delivery reduces systemic exposure potentially eliminating unwanted systemic side-effects (Colin Long, 2002; Kornick, Santiago-Palma, Moryl, Payne, & Obbens, 2003). Delivery of drugs via the skin for systemic effect is beneficial, because it avoids hepatic first pass metabolism and the risks associated with intravenous therapy and the issues associated with varying gastric pH, and emptying time (Henzl & Loomba, 2003). In addition, this route of drug administration can provide the controlled release of drugs into the systemic circulation and can be useful for patients with swallowing difficulties.

The skin is affected by more diseases than any other organ with figures of more than 1000 different conditions frequently quoted (Schofield, Grindlay, & Williams, 2009). In the United Kingdom (UK), the prevalence of skin disease is very common with one-quarter to one-third of the population affected at any particular point in time (Williams, 1997). Around 6 % of all GP diagnoses involve the skin (Williams, 1997) and approximately 15 % of the population per year in England and Wales seek GP advice regarding conditions relating to skin (making it the fourth commonest reason for seeking GP advice), indicating the large burden of skin disease on the healthcare system (Schofield et al., 2009).

The impact of skin disease is often underestimated and has been accorded low priority because most skin conditions are not life threatening. However, they have a major impact on psychological wellbeing, social functioning and everyday activities of patients and their families and carers (Hay et al., 2014; Hollestein & Nijsten, 2014). It has been reported that skin conditions such as acne vulgaris, alopecia, atopic eczema, psoriasis and rosacea have a greater impact on quality of life than other long term conditions such as angina, asthma and hypertension (Parks, Balkrishnan, Hamel-Gariépy, & Feldman, 2003; Rapp, Feldman, Exum, Fleischer, & Reboussin, 1999; Sampogna, Tabolli, & Abeni, 2013). Moreover, conditions such as acne, alopecia and eczema are often a source of hidden financial

burden on patients and their carers (Basra & Finlay, 2007; Parks et al., 2003; Seidler, Bayoumi, Goldstein, Cruz, & Chen, 2012).

To alleviate the burden imposed by skin diseases more work is needed to improve the efficacy and reduce the side effects of topically applied medicines, whilst also increasing the range of drugs that can be delivered via the skin to produce therapeutic drug concentrations at the biological target site. However, delivery of drugs into the skin is difficult because of its barrier function, which is largely attributed to the outer most layer of skin, the stratum corneum (SC) as described in Section 1.2. Other factors also affect the absorption of drugs into and across the skin and can be defined as physiological, physicochemical and environmental (Keith & Chilcott, 2008; Williams, 2003).

Over the years, research has focused on finding ways to perturb the SC barrier to improve drug delivery into and through the skin. These enhancement strategies can be divided into active or passive methods, which seek to render existing routes for drug diffusion more permeable or create new routes/channels across the SC barrier (Barry, 2001).

Active methods involve the use of external energy to act as driving mechanism and/or to render the SC more permeable. Example methods include iontophoresis, ultrasound (phonophoresis) and heat (thermophoresis). Other active strategies such as microneedles completely bypass the SC through puncturing it. These strategies have been shown to improve the transport of drugs through skin and are described in more detail in Section 1.7.2. However, patients are yet to benefit fully from much of the success achieved in research utilising these enhancement strategies, as their translation into the clinic has been extremely slow. Moreover, those products utilising active strategies that have made it on to the market have had very limited commercial success despite their often superior therapeutic benefits because in most cases they are considerably more expensive than the usual dermal formulations (Perumal, Murthy, & Kalia, 2013; Yeoh, 2012).

Passive methods typically involve the use of formulation vehicles/chemical penetration enhancers (CPEs) to increase the driving force for drug diffusion and/or increase skin permeability to drugs. This strategy has been shown to promote the permeation of drugs across the SC and is known to be effective for particular types of drug molecule (Katrin Moser, Kriwet, Naik, Kalia, & Guy, 2001). However, the use of numerous CPEs has been associated with skin sensitisation/irritation, with irritation occurring more frequently when high levels of CPEs are used (Arora, Kisak, Karande, Newsam, & Mitragotri, 2010; Benson, 2005; Finnin & Morgan, 1999; Kanikkannan & Singh, 2002).

Therefore, combining active and passive strategies (such as heat and CPEs, respectively) may allow the levels of CPEs to be reduced, thus avoiding/reducing skin sensitisation. In addition, both strategies are reasonably inexpensive and could work well together to promote drug permeation across the SC. Whilst the effect of heat on drug diffusion across skin has been investigated in the literature as early as the 1960s (Blank, Scheuplein, & Macfarlane, 1967; Cummings, 1969; Fritsch, Stoughton, & Stapelfeldt, 1963), only one product is currently licensed that utilises physiologically tolerable heat ( $\leq 45$  °C) as an enhancement strategy. Synera™/Rapydan™ a topical patch that contains lidocaine and tetracaine, using the proprietary Controlled Heat-Assisted Drug Delivery (CHADD™) is licensed in the US and Europe (Sawyer, Febbraro, Masud, Ashburn, & Campbell, 2009) to increase topical anaesthetic delivery into the skin to reduce the time delay between application and anaesthesia. Although, heat as an enhancement strategy is underutilised, it is an inexpensive and effective strategy, which needs further investigation in order to realise the potential of this mode of delivery.

Although the majority of drug delivery research to the skin has focused on increasing drug permeation across the continuous SC, interest in targeted follicular drug delivery is growing because investigations have highlighted that hair follicles can play a greater role in drug transport than previously assumed (Dokka, Cooper, Kelly, Hardee, & Karras, 2005; Grams, Whitehead, Lamers, Sturmman, & Bouwstra, 2005; Jacobi, Toll, Sterry, & Lademann, 2005; Ogiso et al., 2002; Teichmann, Ossadnik, Richter, Sterry, & Lademann, 2006; Alexa Teichmann et al., 2005). In addition, delivery of therapeutic agents to the

pilosebaceous unit is essential for particular skin conditions such as acne, alopecia and certain cancers. Whilst the influence of active strategies such as iontophoresis and ultrasound on targeted follicular delivery of drugs is documented (Gelfuso, Gratieri, Delgado-Charro, Guy, & Vianna Lopez, 2013; Han, Kim, & Kim, 2004; Meidan, Docker, Walmsley, & Irwin, 1998; Rastogi, Anand, Dinda, & Koul, 2010; Sarheed & Frum, 2012), the combined influence of delivery strategies such as heat ( $\leq 45$  °C) and vehicle composition (CPEs) on follicular absorption of topically applied drugs is a novel and potentially highly promising strategy yet to be investigated.

The design of optimal topical and transdermal dosage forms requires an understanding of the structure and function of human skin. Therefore, a detailed description of the distinct layers, cell types and their functions are provided in Section 1.2 .

## 1.2 Skin structure and function

The skin is the largest organ of the human body and accounts for approximately 10 % of the total body mass of an average adult (Walters & Roberts, 2002). By forming a barrier between the body and environment, the skin protects against the external invasion of allergens, chemicals, microorganisms, ultraviolet (UV) radiation and the loss of water and nutrients. The skin has an important role in homeostasis by regulating body temperature and blood pressure. The skin also functions as an important sensory organ in touch with the environment, sensing stimulation in the form of temperature, pressure and pain (Benson, 2012).

The anatomical structure of the skin is complex and crucial for its various functions. It consists of three main layers: epidermis, dermis and hypodermis. Nerves, blood and lymphatic vessels pervade the last two layers. Furthermore, different appendages are associated with the skin: hair follicles, eccrine glands and apocrine glands (Benson, 2012; Walters & Roberts, 2002). The generic structure of mammalian skin is depicted in Figure 1-1.

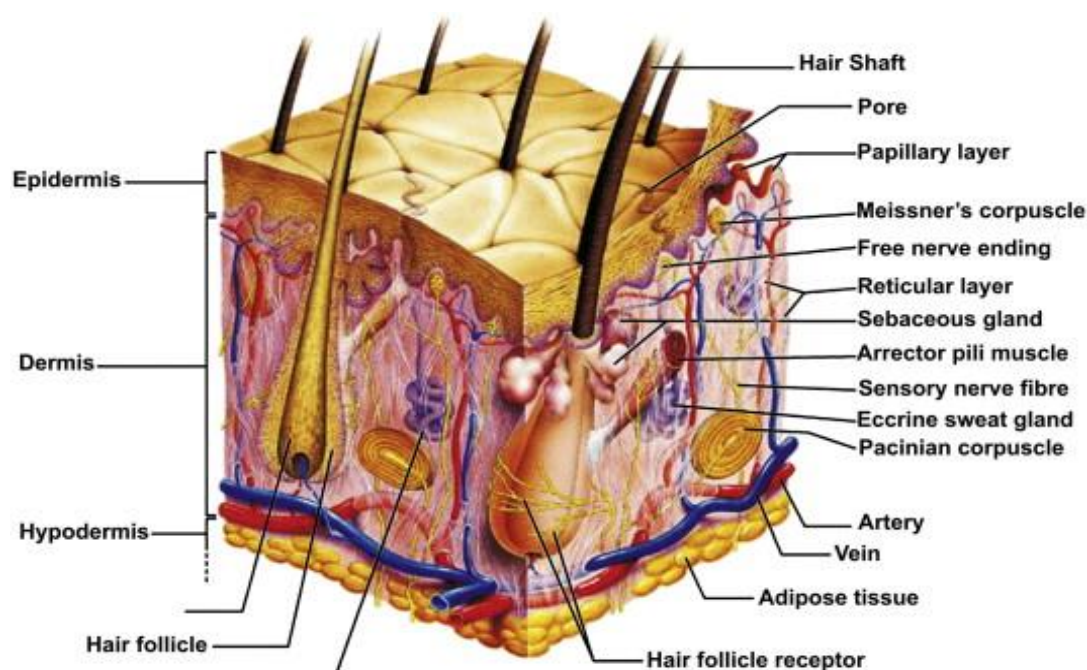


**Figure 1-1: Generic structure of mammalian skin consisting of three main layers (epidermis, dermis, hypodermis) and typical structures like hairs, sweat and sebaceous glands (Alexander et al., 2012).**

### 1.2.1 Epidermis

The epidermis does not contain blood vessels and is composed of stratified squamous epithelium. It varies in thickness depending on the area of the body (approximately 0.06 mm on the eyelids to about 0.8 mm on the palms of hand and soles of the feet) and consists of four main strata (Walters & Roberts, 2002). From the outside to inside, they are known as the stratum corneum (SC), stratum lucidum (SL), stratum granulosum (SG), stratum spinosum (SS) and stratum basale (SB) as shown schematically in Figure 1-2. Each layer represents different levels of cellular differentiation. The keratinocytes, which are the primary cell type in the epidermis, undergo an orderly pattern of proliferation, differentiation and keratinization from the SB through to the SC where they finally shed through a process known as desquamation. The journey of the keratinocytes from the basal layer to the skin surface takes approximately 14 days, during which time the cells synthesise various proteinaceous materials collectively termed keratin, they become thin, hard and dehydrated and die. The SC cells are typically retained for a further 14 days prior to shedding. These cells together with the intercellular lipids synthesised by the keratinocytes form the SC. The Langerhans cells, melanocytes and Merkel cells are the other cell types present in the epidermis. Langerhans are commonly found in the SS. They are also found in hair follicles, sebaceous glands and apocrine glands where they play an important role as part of the immune system. Melanocytes are located in the basal layer and produce melanin, which provides protection against ultraviolet radiation and defines the colour of skin. Merkel cells (sensory cells) are also found in the SB and sense mechanical stimuli (Elias, 2005; Riviere, 2011; Ryan, Gerberick, & Kern, 2010).

The SC, also known as the non-viable epidermis is 10-20  $\mu\text{m}$  thick depending on the region of human body. The SC provides the main barrier function of skin as shown by progressive tape stripping, which leads to significantly increased skin permeability (Blank, 1953). One of its main functions is to protect the body against external materials and molecules as well as loss of water from the body. The SC consists of 15-20 layers of completely keratinized flattened cells (bricks) without nuclei and organelles, which are embedded in a lipid matrix (mortar), with desmosomes acting as rivets between the

corneocytes. The corneocytes are surrounded by cornified cell envelopes formed of protein/lipid structures. The intercellular lipid phase of the SC is rich in ceramides (40-50 %), cholesterol (20-33 %), cholesterol esters (0-20 %) and saturated free fatty acids (7-13 %). This unique composition contributes to the skin barrier function (Scheuplin & Blank, 1971; van Smeden, Janssens, Gooris, & Bouwstra, 2014). The role of the SC lipids in the barrier function has been demonstrated further by their removal with solvent extraction, which lead to increased transepidermal water loss (Scheuplin & Blank, 1971) and enhanced skin permeability (Sweeney & Downing, 1970; Squier, Cox, & Wertz, 1991). The SC intercellular lipid lamellae are highly structured and exhibit two coexisting phases, the short periodicity phase (with repeat distance of 6.4 nm) and the long periodicity phase (with repeat distance of 13.4 nm). Three states of lipid organisation (lateral packing) have been identified within these phases, an ordered densely packed orthorhombic phase which is crystalline and exhibits low permeability to drug molecules, an ordered less densely packed, gel-like, more permeable hexagonal phase and a disordered, highly permeable liquid phase (Janssens et al., 2012). Within the SC, the orthorhombic packing is thought to be the dominant phase in healthy skin. Thus, the arrangement of lipids within the SC intercellular lipid lamellae is believed to contribute to its barrier function. The hydration of the SC is also an important consideration from a barrier function and pharmaceutical point of view. Natural moisturising factor (NMF) in the SC acts as a humectant and plasticizer in the SC and therefore plays an important role in maintaining its hydration as it binds to water to aid swelling of the corneocytes (Benson, 2012). Dry skin is associated with dermatological conditions, whilst increased skin hydration has been reported to promote the percutaneous absorption of certain compounds and enhance skin appearance (Harding, 2004). The SL is only present in plantar and palmar skin and is more commonly considered to be the lower layers of the SC.

The SG is 1-3 cells layers thick. This layer is characterised by the presence of keratohyalin granules and membrane-coating granules that contain the precursors for the intercellular lipid lamellae seen in the SC are synthesised (Menon, 2002). Within these granules, lamellar subunits arranged in parallel stacks are observed. In the uppermost cells of the SG, the lamellar granules are extruded into the intercellular

space. At this stage lysing enzymes are released which start to degrade viable cell components such as nuclei and organelles. After this the keratinocytes become flattened and compacted to form the SC (Walters & Roberts, 2002).

The SS is located above the basal layer and consists of two to six rows of keratinocytes that change morphology from columnar to polygonal cells. In this layer the keratinocytes begin to differentiate and synthesise keratins that form tonofilaments (Fuchs, 1990). The shortening of these tonofilaments leads to the formation of desmosomes, which form anchors between the cell membranes of adjacent keratinocytes (Walters & Roberts, 2002).

The SB is a single cell layer of columnar or cuboidal cells anchored to the basement membrane (which makes the boundary between the epidermis and dermis) and the adjacent cell layer (the SS) by hemidesmosomes and desmosomes respectively. Cells of the SB contain organelles such as mitochondria and ribosomes and are metabolically active (Benson, 2012). Keratinocytes within this layer undergo cell division, after replication one daughter cell remains in this layer whilst the other migrates upwards through the epidermis towards the skin surface (Watt, 1989).

### **1.2.2 Dermis**

The dermis which is about 3-5 mm thick lies immediately below the epidermis and forms the major part of mammalian skin (Walters & Roberts, 2002). This layer houses numerous structures such as, blood and lymphatic vessels, nerve endings, pilosebaceous units (hair follicles and sebaceous glands), and sweat glands (eccrine and apocrine). The network of connective tissue is mainly composed of collagen fibrils and elastic tissue providing support and flexibility respectively. Its extensive vasculature allows it to perform vital roles of thermoregulation, the delivery of oxygen and nutrients to the epidermis and the removal of toxins and waste products. The dermis is the site responsible for transdermal drug uptake into the systemic circulation and clearance of topically applied drugs (Walters & Roberts, 2002).

### **1.2.3 Hypodermis**

The hypodermis is the deepest layer of the skin and houses major blood vessels and nerves. It acts as an insulator, a shock absorber and serves as a fat store. This layer is composed of loose, fibrous connective tissue, which contains adipose tissue and fibroblasts. One of its main roles is in anchoring the skin to the underlying muscles, thus providing it with mechanical support (Benson, 2012; Walters & Roberts, 2002).

### **1.2.4 Skin appendages**

There are three types of skin appendages, the pilosebaceous unit, eccrine and apocrine sweat glands. Dense capillary networks closely envelope the base of both the hair follicles and sweat ducts. The eccrine glands are epidermal structures that are simple, coiled tubes arising from a coiled ball, of approximately 100  $\mu\text{m}$  in diameter, located in the lower dermis. They secrete a dilute salt solution with a pH of about 5 in response to temperature-controlling determinants, such as exercise and high environmental temperature, as well as emotional stress through the autonomic (sympathetic) nervous system. The apocrine glands are limited to specific body regions (axillae, nipples and anogenital areas) and are also coiled tubes. These glands are about ten times the size of the eccrine ducts, extend as low as the subcutaneous tissue and are paired with hair follicles (Walters & Roberts, 2002). The pilosebaceous unit is discussed in more detail in the Section 1.3 below.

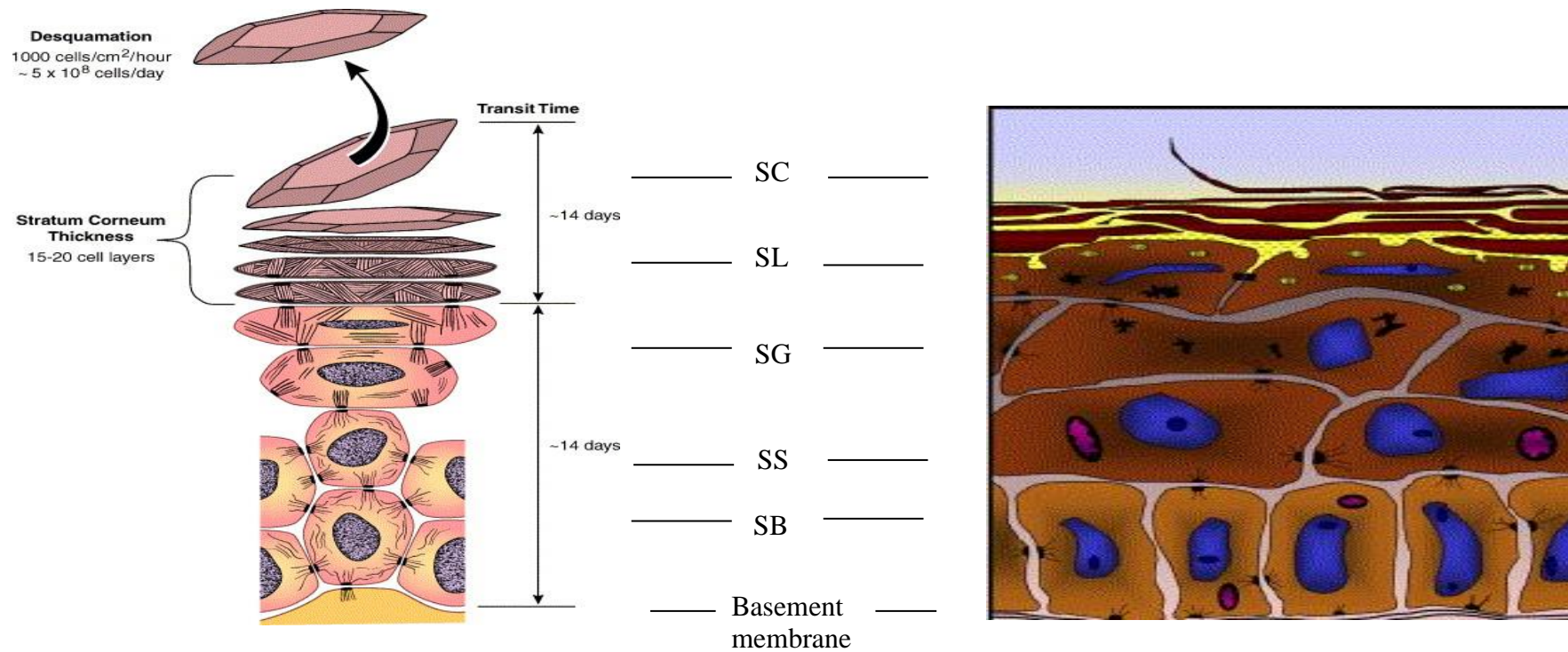


Figure 1-2: Structure of epidermal layers: stratum basale (SB), spinosum (SS), granulosum (SG), lucidum (SL) and corneum (SC) illustrating the differentiation process from basal cells to the completely keratinized cells of the stratum corneum leading to final event of epidermal desquamation (adapted from Milstone, 2004; Proksch, Fölster-Holst, & Jensen, 2006).

### **1.3 Pilosebaceous unit**

The pilosebaceous unit, which consists of the hair follicle, the hair shaft, the adjoining arrector pili muscle and the associated sebaceous glands, is linked with the aetiology of numerous skin conditions. Examples include acne vulgaris, alopecia areata, androgenic alopecia, folliculitis, hirsutism and some skin tumours (Patzelt, Knorr, Blume-Peytavi, Sterry, & Lademann, 2008). Consequently, they are increasingly considered important targets for locally active therapeutic agents. The hair follicle is also thought to provide a potentially important drug delivery route through the SC into the deeper layers of skin as discussed in Section 1.3.3. This section will discuss the anatomical considerations, drug delivery opportunities and the pilosebaceous unit- associated skin disorders acne vulgaris and androgenic alopecia.

#### **1.3.1 Anatomy of the pilosebaceous unit**

As described previously the pilosebaceous unit consists of the hair follicle, the hair shaft, the adjoining arrector pili muscle and the associated sebaceous gland. The structure of human hair follicle is depicted in Figure 1-3.

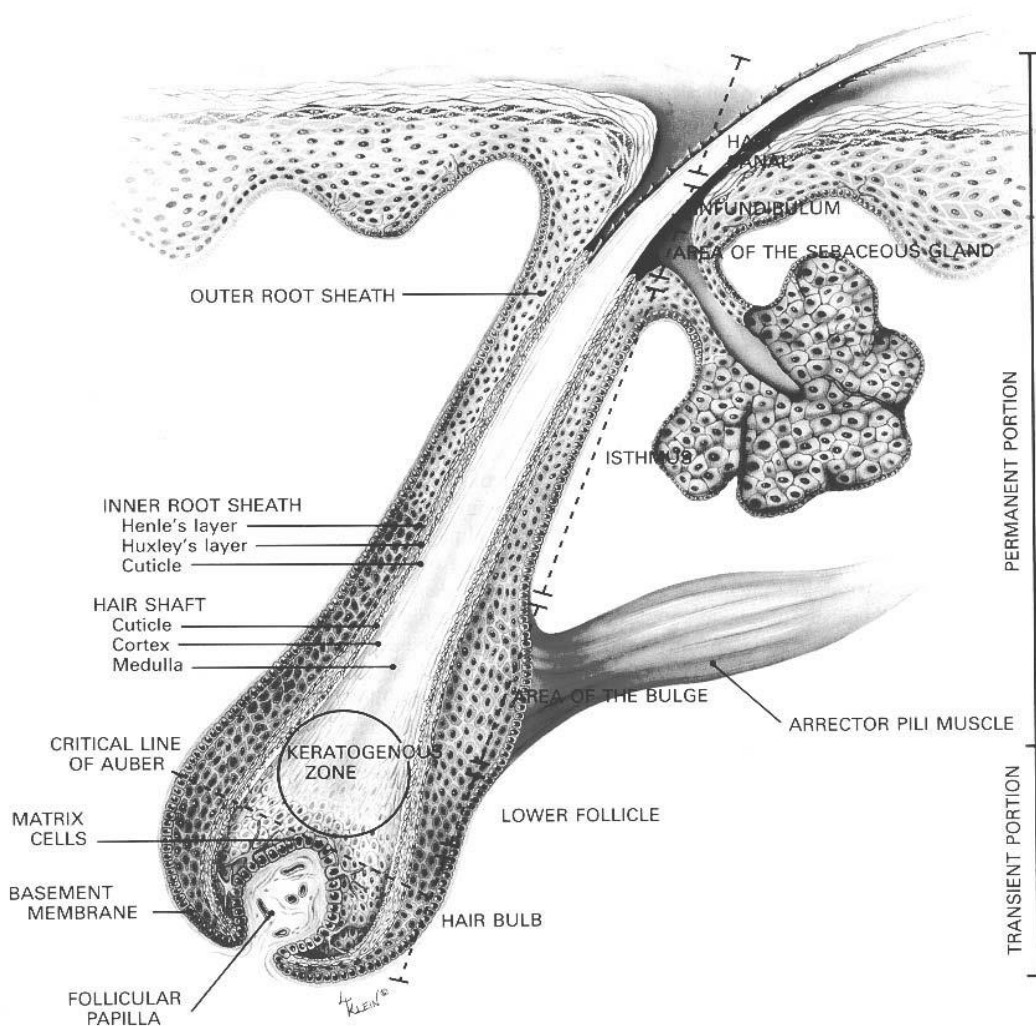


**Figure 1-3: Structure of human hair follicle. The hair follicle is divided into several regions from the skin surface to the lower layers: hair canal, infundibulum, isthmus, the bulge area, lower follicle and hair bulb (Grams & Bouwstra, 2005).**

Hair follicles consist of concentric cylinders that surround the hair shaft. From the outside to the centre of the follicle, these layers are the outer root sheath, the inner root sheath including the Henle's layer, Huxley's layer and the cuticle. The hair shaft from the outermost layer to the centre is composed of a cuticle, cortex and a medulla. The outer root sheath is a keratinised layer that is continuous with the epidermis (Meidan, Bonner, & Michniak, 2005) and is thereby of greatest importance with regard to drug delivery, as it increases the skin surface area susceptible to penetration. The function of the outer root sheath is the protection and moulding of the inner layers (Lauer, Ramachandran, Lieb, Niemiec, & Weiner, 1996). Each hair follicle is associated with one or more sebaceous glands, which are

outgrowths of epithelial cells. Ducts join these glands to the upper part of follicular canal (Meidan et al., 2005), from which they release sebum (Lauer et al., 1996).

The hair follicle can be divided into several regions starting from the skin surface. The infundibulum is the upper part of the hair follicle up to the sebaceous duct. In this area, tight connection between the hair shaft and the skin is absent. Therefore, the hair shaft can move freely with the skin. This gap is called the follicular duct and is filled with sebum from the sebaceous gland. Due to the loss of epidermal differentiation, the thickness of the SC decreases deeper in the infundibulum, which results in a weaker barrier for penetration compared to the SC at the surface (Schaefer & Lademann, 2001).

The isthmus is located between the sebaceous gland opening and the area of the bulge where the arrector pili muscle is connected to the hair follicle (Sperling, 1991). Above the isthmus, the hair follicle is permanent and does not disintegrate during the growth of the hair follicle (Grams & Bouwstra, 2005).

The bulge area is located where the arrector pili muscle is in contact with the hair follicle. Below the bulge area starts the lower follicle with the keratogenous zone, which is where keratin is produced. The lowest part of the hair follicle is the hair bulb, where the matrix cells, the basement membrane and follicular papilla are located. These structures play an important role in the regulation of hair growth cycles and hair pigmentation (Grams & Bouwstra, 2005; Wosicka & Cal, 2010).

#### **1.3.1.1 Growth cycle of the hair**

Two types of human hairs exist which are categorised by size. They are the terminal and vellus hairs. Terminal hairs are macroscopically long and distinctively have a length of > 2 cm, are at least 60 µm in diameter, pigmented and usually extend more than 3 mm into the hypodermis. They are typically found on the scalp, eyebrows, and eyelashes. In contrast, vellus hairs are usually short < 2 cm are thin with a diameter of 30 µm, often unpigmented and normally extend just 1 mm into the dermis. These hairs are found throughout the body and become terminal hairs in the beard area, trunk, axillae, and genitalia under the influence of male sex hormones at puberty (Patzelt, Knorr, et al., 2008).

Hair follicles undergo a specific growth cycle of alternating proliferative and rest stages. The actively growing phase is termed anagen, in which matrix cells proliferate in response to further signals from the dermal papilla, and begin the process of terminal differentiation, moving upwards in the follicle to form the hair shaft and inner root sheath (Cotsarelis, 2006). Pigmentation of hair results from the activity of melanocytes, which reside in the hair bulb and deposit pigment granules into the hair shaft (Millar, 2002). Anagen is followed by catagen, a brief destructive phase whereby the matrix cells stop proliferating and hair shaft and inner root sheath differentiation slow. This drags the dermal papilla upward to rest just below the permanent, non-cycling upper follicle (Fuchs, 2007). The follicle then enters a resting period termed telogen, in which it lies dormant prior to the hair being shed. Anagen subsequently reoccurs as the hair matrix cells start dividing and lower follicle redevelops (Meidan et al., 2005). In the non-bald scalp up to 90 % of follicles are within the anagen phase (lasting for 2-6 years), up to 2 % are within the catagen phase (2 weeks) and about 10 % are in the telogen phase (2-4 months) (Wosicka & Cal, 2010).

#### **1.3.1.2 Sebaceous glands**

Throughout the body each hair follicle is associated with sebaceous gland to form the pilosebaceous unit (Patzelt, Knorr, et al., 2008). Sebaceous glands are composed of lobules of lipid producing sebocytes lining sebaceous ducts. Non-hair bearing sites including the mouth, the eyelids, the nipples, and the genitals also have sebaceous glands. The greatest density of these glands is on the face and scalp. Only the palms and soles, which also have no hair follicles, are completely devoid of sebaceous glands (Benson, 2012).

Sebaceous glands release lipids through holocrine secretion, a process in which the entire cell disintegrates to extrude its contents in the upper third of the follicular canal (Clarys & Barel, 1995). Human sebum reaching the surface of the skin consists of a mixture of lipids including cholesterol, squalene, triglycerides and free fatty acids (Patzelt & Lademann, 2013). Sebum is speculated to maintain hydration of the skin's surface, to keep the skin soft, to protect it from infection by bacteria

and fungi (Meidan et al., 2005) and maintain a skin pH of about 5.5 (Walters & Roberts, 2002). The role of sebaceous gland in acne and androgenic alopecia is discussed in Sections 1.3.2.1 and 1.3.2.2 respectively.

### **1.3.1.3 Arrector pili**

The arrector pili muscle is a smooth muscle bundle that is attached to the hair follicle (Meidan et al., 2005; Patzelt, Knorr, et al., 2008). The sympathetic nerve fibres mediate contraction of this muscle causing the hairs to stand. In humans, this may occur in response to cold or fear (Cutts et al., 2002; Poblet, Ortega, & Jiménez, 2002).

## **1.3.2 Hair follicle- associated skin disorders**

A broad range of skin conditions are associated with the hair follicles as described briefly in Section 1.3. However, this thesis will focus on two disorders acne vulgaris and androgenetic alopecia.

### **1.3.2.1 Acne Vulgaris**

Acne vulgaris is a common disorder of the pilosebaceous units located in the face, chest and back (Aslam, Fleischer, & Feldman, 2015). It affects over 80 % of teenagers (Zauli et al., 2014) and up to 9.4 % of the global population (Tan & Bhate, 2015). Whilst, the prevalence of severe acne has decreased owing to improved treatment, the number of adults with acne appears to be increasing. However, the reasons for this are uncertain (Stathakis, Kilkenny, & Marks, 1997). The causes of acne have not been fully elucidated, but familial history and hormones are thought to be heavily involved (Thiboutot, 2001; Shinjita & Reynolds, 2013).

Clinically, acne is classified into mild, moderate, moderate severe and severe, depending on the presence of inflammation, scarring and type of lesions (Gollnick, 2003). The clinical classifications are indicated below (Table 1-1).

**Table 1-1: Simplified clinical severity grading for acne vulgaris and the accompanying symptoms.**

Symptoms	Severity grade			
	Mild	Moderate	Moderate severe	Severe
Comedones	✓	✓✓	✓✓	✓✓✓
Papules/pustules	x/✓	✓/✓✓	✓✓✓	✓✓✓
Small nodules/cysts	x	x/✓	✓✓	✓✓
Nodules	x	x	x/✓	✓✓
Inflammation	x	✓	✓✓	✓✓✓
Scar formation	x	x	✓	✓

Key: Absent; x    few; ✓    many; ✓✓    very numerous; ✓✓✓

In its mild to moderate form, acne is characterised by slight spotty skin irritations with or without mild inflammation (Gollnick, 2003). Treatment with a lower strength preparation (e.g. azelaic acid, benzyl peroxide and topical retinoid) is recommended as first line therapy (Nast et al., 2016). However, in the more inflammatory types of acne, bacterial invasion of the pilosebaceous follicle occurs and pustules, infected cysts and in extreme cases inflamed and infected sacs appear. Without treatment, these lesions may become extensive and leave permanent, disfiguring scars (Jacob, Dover, & Kaminer, 2001). This adverse effect on physical appearance can potentially contribute to significant psychological distress, as the sufferer is constantly aware of the obvious facial blemishes (Mancini, 2008). Thus, the immediate goals of treatment are to limit the physical and psychological scarring.

The causes of acne are complex and not fully understood. However, several factors such as androgens, altered sebum production, *Propionibacterium acnes* (*P. acnes*) proliferation and abnormal keratinization or sloughing of the cells within the pilosebaceous unit are believed to contribute to acne formation (Shinjita & Reynolds, 2013). The role of each factor in the development of acne will be discussed next.

#### **1.3.2.1.1 Role of androgens in acne development**

Androgens are produced in the adrenal glands, gonads and locally within the sebaceous glands. Evidence for their involvement in acne stem from clinically higher acne rates seen in patients in puberty (Burton, Cunliffe, Stafford, & Shuster, 1971) and in patients with conditions where there is overproduction of androgens e.g. polycystic ovarian syndrome, congenital adrenal hyperplasia and certain tumours (Shinjita & Reynolds, 2013). The influence of androgens in acne pathogenesis was also highlighted by Hamilton (1941), who showed that castrated males with no acne could develop the disease after administration of testosterone. Additionally, patients with androgen insensitivity syndromes (from lack of functional androgen receptors) do not produce sebum and do not develop acne (Sansone & Reisner, 1971).

Androgens such as testosterone and dihydrotestosterone (DHT) are considered to affect acne by promoting growth of sebaceous glands. Testosterone is converted to DHT in the skin by type I 5-alpha reductase (Thiboutot, 2001). The rise in androgens in puberty stimulates sebum production by binding androgen receptors on the pilosebaceous ducts and sebaceous glands. Also, acne prone skin has higher androgen receptor density and higher 5-alpha reductase activity (Sansone & Reisner, 1971). Finally androgens induce keratinocyte proliferation mediated by growth factors and IL-1 $\alpha$  that can result in hyperkeratinisation in the ductal and infundibular regions leading to the formation of comedones (Shinjita & Reynolds, 2013).

#### **1.3.2.1.2 Altered sebum production leading to acne formation**

Excessive hormonal stimulation and genetically enhanced responsiveness has been observed in acne prone patients (Pochi & Strauss, 1964). These two factors increase lipid cell production and sebaceous gland size, causing an increase in sebum excretion (Plewig, 1974). This increase in sebum excretion has been related to acne severity (Cunliffe & Shuster, 1969). However, increased sebum excretion/production alone is not sufficient to explain all cases of acne. According to Kligman & Katz (1968) 'sebum may fuel the process but not everyone catches fire'. Thus, other features in combination with elevated sebum production are understood to influence the pathogenesis of acne.

For example, the composition of sebum lipids and presence of *P. acnes* are believed to be important in comedo formation and impact inflammation. There are increased free fatty acids, squalene, squalene oxidase and decreased linoleic acid in acne patients. These changes promote hypercornification of the follicle through direct and indirect modulation of the innate immune system. Oxidized squalene can also stimulate hyper-proliferation of keratinocytes via IL-1 $\alpha$  up-regulation (Shinjita & Reynolds, 2013). Reduced linoleic acid within the sphingolipids of the follicle may also lead to hyperkeratinisation (Letawe, Boone, & Pierard, 1998).

#### **1.3.2.1.3 Role of *Propionibacterium acnes* in the development of acne**

*P. acnes* (a commensal anaerobic, gram-positive rod bacterium) plays a significant role in acne pathogenesis (Dessinioti & Katsambas, 2010). This bacterium is the source of lipolytic enzymes that convert sebum triglycerides into free fatty acids, which stimulates the release of antimicrobial peptides and therefore inflammation and comedogenesis (Shinjita & Reynolds, 2013). Also, *P. acnes* stimulates the release of a variety of signalling molecules that promote inflammation and rupture of the follicular wall, which may lead to scar formation (Kim et al., 2002). Additionally, *P. acnes* produce a biofilm, a polysaccharide lining around a collection of microbes that enhances adherence within the follicle. The biofilm can also increase the stickiness of sebum and impede keratinocyte desquamation, leading to the keratin plug seen in a comedone. The biofilm also increases *P. acnes* resistance to antibiotics (Coenye, Peeters, & Nelis, 2007).

#### **1.3.2.1.4 Abnormal Keratinization in acne formation**

Hyperkeratinisation is the result of both hyper-proliferation and retention of keratinocytes within the follicle (Holmes, Williams, & Cunliffe, 1972). Factors that promote hyper-proliferation include changes in lipid composition of sebum, response to androgens, inflammation from local cytokines, and *P. acnes*. Normally, flow of sebum out of the pilosebaceous duct carries with it desquamated keratinocytes. However, normal flow is impeded by factors such as the *P. acnes* biofilm adhering to follicular lining and the “bottleneck” effect of microcomedo that limit extrusion of sebaceous material

(Gollnick, 2003). This, in turn, leads to increased adhesion of keratinocytes and decreased ductal keratinocyte shedding (Shinjita & Reynolds, 2013).

### **1.3.2.2 Androgenetic alopecia**

Androgenetic alopecia is termed male pattern and female pattern hair loss in men and women respectively. It is a common condition that is characterised by progressive thinning and shrinking of scalp hair, which ultimately leads to reduced hair density over the crown and frontal scalp. Androgenetic alopecia affects approximately 30 % of men under 30 years of age, 50 % under 50 years and 70 % under 70 years of age. In women, the prevalence before menopause is 5-10 %, rising to 20-30 % after the menopause (Wolff, 2008). The causes of androgenetic alopecia have not been fully elucidated, but familial history (genetic factors) and hormones (androgens) are thought to be important factors in the pathophysiology of androgenetic alopecia (Kaufman, 2002; Trüeb, 2002).

Although pattern hair loss is a biologically normal trait, hair loss in humans can adversely affect body image, self-esteem and quality of life of sufferers (Cash, 1992; Cash, Santos, & Williams, 2005). Although this condition is not gender specific, impairment of psychosocial wellbeing is more frequent and severe in women (Cash, Price, & Savin, 1993).

Clinically the different patterns of hair loss associated with androgenetic alopecia have been classified using the Hamilton-Norwood (Figure 1-4) and the Ludwig scales of pattern hair loss (Figure 1-5). Traditionally the Hamilton-Norwood scale is used to describe the pattern of hair loss in men and the Ludwig scale in women. However, the different patterns are not gender specific and can be used interchangeably (Monselise, Cohen, Wanser, & Shapiro, 2015).

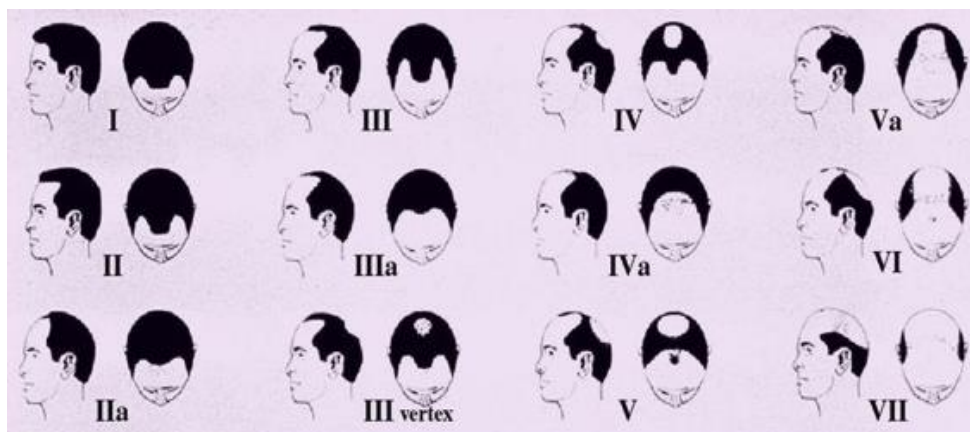


**Figure 1-4: The Hamilton-Norwood scale of male-pattern hair loss (Monselise et al., 2015).**

Most men with androgenetic alopecia show a typical pattern of hair loss, often beginning at the temples and in the vertex area as depicted in Figure 1-4.

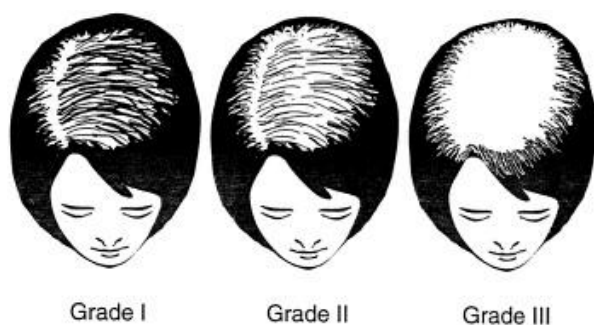


**Figure 1-5: The Ludwig scale of female-pattern hair loss (Unger & Unger, 2003).**

In contrast, most women with androgenic alopecia have diffuse thinning in the midline of the scalp as illustrated in Figure 1-5. In both men and women, androgenetic alopecia is accompanied by acceleration of hair growth cycle, as reflected by reduction of anagen growth phase and increased shedding of telogen hair (Unger & Unger, 2003). The normal hair growth cycle, including anagen, catagen and telogen stages was described in Section 1.3.1.1.

The exact controls of the hair follicle growth cycle still remain unknown. However, the discovery of the role played by type II 5-alpha reductase in the peripheral conversion of testosterone to DHT has been a breakthrough in hair research. Androgenetic alopecia is considered to have a strong genetic component (Ioannides & Lazaridou, 2015; Trüeb, 2002). Although all of the genes involved are not yet known, its mode of inheritance is complex due the great number of genes involved. Androgenetic alopecia is induced by androgens in genetically susceptible men and women. DHT, which is formed by

the peripheral conversion of testosterone by type II 5-alpha reductase, is thought to be responsible for the characteristic miniaturisation of scalp hair follicle (Kaufman, 2002). In genetically susceptible hair follicles, DHT binds to the androgen receptor and the hormone receptor complex then activates the genes responsible for the gradual transformation of large, terminal follicles to small-miniaturised follicles (Inui & Itami, 2011). Over successive hair cycles, the duration of anagen shortens and matrix size decreases, resulting in smaller follicles that produce shorter, finer, miniaturised hairs of various lengths and diameters, which are the hallmark of androgenetic alopecia (Rebora, 2004).

### **1.3.3 General aspects of follicular drug delivery**

The hair follicles constitute a break in the continuity of the SC and act as channels for drugs to reach deeper skin layers. The hair follicle openings are continuous with the epidermis and the SC is still intact and present in the uppermost region the infundibulum (see Figure 1-3). However, in the lower part of the infundibulum the SC is much thinner and less developed. This thinner SC provides a reduced barrier to percutaneous absorption, whilst providing a large surface area for absorption at the same time (Schaefer & Lademann, 2001; Vogt, Mandt, Lademann, Schaefer, & Blume-Peytavi, 2005). Moreover, hair follicles allow the possibility of targeted drug delivery as they potentially provide direct access to sebaceous glands and lower regions of the hair follicle, which are important drug targets in conditions such as acne and alopecia respectively. Additionally, applied formulations may accumulate and deposit in the follicular openings, consequently forming a reservoir for long term delivery (Lademann et al., 2006, 2011). The pilosebaceous unit also has rich blood supply as a result of being surrounded by a high density of blood vessels (Montagna & Ellis, 1958), which could potentially increase clearance of topically applied drugs and contribute to systemic delivery.

The parameters that govern follicular drug delivery are not yet fully clear. A potential barrier to follicular drug delivery is that the hair follicle orifices account for only 0.1 % of the total skin surface (Meidan et al., 2005; Otberg et al., 2004). However, the density of hair follicles on the scalp and face

can reach as much as 10 % of the total skin surface, creating a higher local surface area (Lieb, Liimatta, Bryan, Brown, & Krueger, 1997).

In addition, the slow upward flowing sebum may pose a physical as well as a chemical barrier for drug penetration into the hair follicles. At the same time, sebum may serve as a vehicle for drugs that are soluble in it. The incorporation of CPEs, which can potentially interact with sebum and alter its solubility parameter so that follicular transport is favoured, is likely to reduce the potential barrier posed by sebum (Motwani, Rhein, & Zatz, 2004). Similarly, moderate levels of heat ( $\leq 45$  °C) may reduce sebum viscosity or unblock pores clogged with sebum and debris, which could result in increased follicular absorption of topically applied drugs.

From the literature, drug delivery via the follicular route is thought to predominate in the early stages of the transport process, with the transepidermal route becoming more important in the later stages (Maghraby, Williams, & Barry, 2001). More recently, support for the importance of the follicular pathway in the initial phase of drug diffusion was shown using stimulated Raman scattering microscopy, with steady state achieved within less than 30 min post application of formulation (Saar, Contreras-Rojas, Xie, & Guy, 2011).

Overall, there is limited information available on the contribution of the hair follicles to the total transport across the skin and even less is known about the combined effect of heat ( $\leq 45$  °C) and CPEs on this contribution. Therefore, more research is needed to investigate the influence of the combined effects of heat ( $\leq 45$  °C) and CPEs on follicular drug delivery, particularly in the early stages of drug transport (< 30 min).

#### **1.3.3.1 Local target areas for hair follicles**

Despite their limited surface area, hair follicles are still regarded as important drug delivery targets. Various targets within the hair follicles are of interest for topically applied drugs; these include the sebaceous gland, the bulge area, the bulb and the various concentric layers in the follicle (Meidan, Bonner, & Michniak, 2005; Wosicka & Cal, 2010). Sebaceous gland dysfunction has been implicated in

aetiology of androgenetic alopecia and acne (Patzelt et al., 2011). Therefore, delivery of drugs directly to this area with limited systemic delivery is desirable to maximise therapeutic efficacy and minimise side effects (Agarwal, Katare, & Vyas, 2000; Lu, Ciotti, Valiveti, Grice, & Cross, 2008). Similarly, the bulge area is thought to initiate and/or is responsible for hair growth and various forms of cancer have been thought to originate from this region (Lavker et al., 2003). In the bulb region melanocytes are present, which are responsible for the hair colour and thus for greying of the hair. Treatment of these melanocytes in albino mice has demonstrated that it is possible to treat hair pigment deficiencies (Alexeev, Igoucheva, Domashenko, Cotsarelis, & Yoon, 2000).

#### 1.4 Routes of drug penetration across skin

It is possible for drugs to cross the SC through the transepidermal route (consisting of the transcellular and paracellular routes) and the transappendageal route, which involves permeation through sweat ducts and follicles. These routes of penetration are schematically illustrated in Figure 1-6. The role of hair follicles in drug penetration into skin was covered in Section 1.3.3, therefore the transepidermal route and sweat glands will be discussed in more detail.

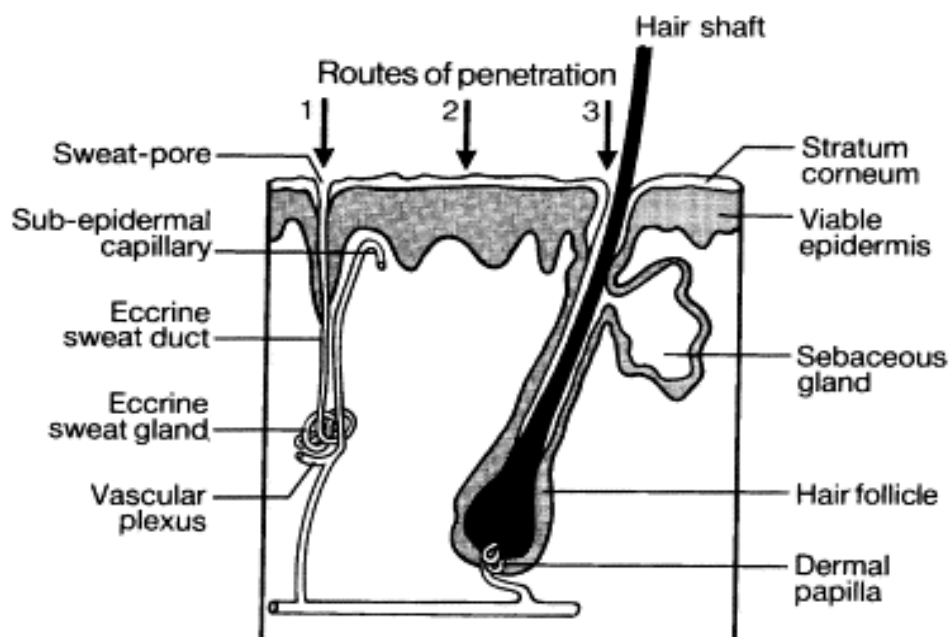
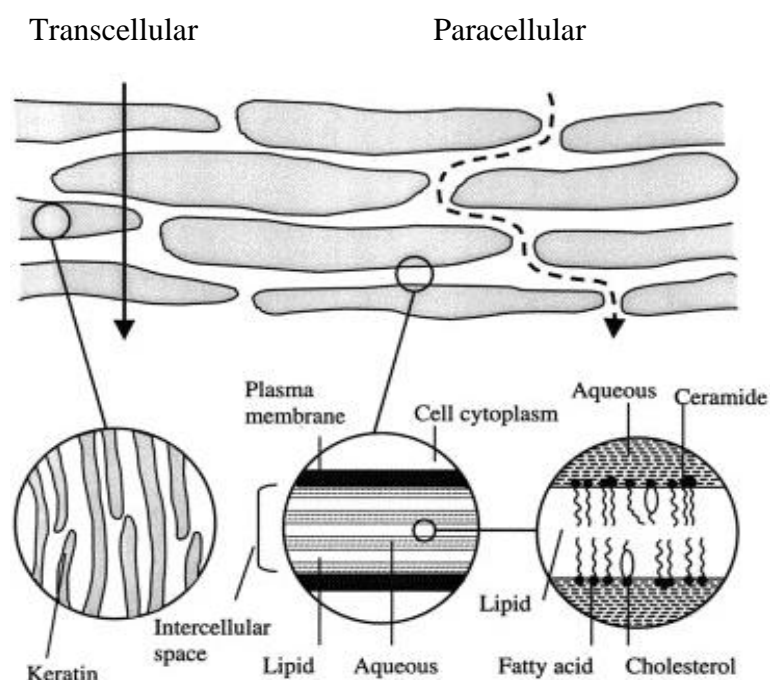


Figure 1-6: Simplified diagram of skin structure and drug penetration routes: (1) via the sweat ducts (2) across the continuous SC or (3) through the hair follicles with their associated sebaceous glands (Barry, 2002).

### 1.4.1 Transepidermal route for drug permeation

The transepidermal route is often considered the predominant drug permeation route in the literature (Benson, 2005). It consists of the transcellular and paracellular routes, with this latter route thought to be the primary pathway for drugs to cross the SC (Roberts & Cross, 2002). Both routes are depicted in **Figure 1-7** shown below.



**Figure 1-7: Permeation routes through the SC: (1) across the corneocytes and the intercellular lipid matrix (transcellular route) and (2) via the lipid matrix between the corneocytes (paracellular route) (Katrin Moser et al., 2001).**

#### 1.4.1.1 Transepidermal - Transcellular route

The transcellular route involves the repeated partitioning and diffusion across the hydrophilic corneocytes and the hydrophobic intercellular lipid matrix surrounding the corneocytes. It has been hypothesised that this route favours more polar solutes. However, the existence of this route of permeation could not be proven experimentally (Roberts & Cross, 2002). Furthermore, Potts and Francoeur could not prove diffusion of water through corneocytes. Therefore, it was argued that the transcellular pathway is unlikely for polar organic molecules in general, when not even water utilises this pathway (Potts & Francoeur, 1991; Pugh, 2001). These issues, coupled with the fact that this route requires repeated partitioning from hydrophilic to lipophilic regions, makes this route very unlikely to be important for transport of drugs across the SC (Scheuplein, 1967).

#### **1.4.1.2 Transepidermal - Paracellular route**

The paracellular route involves a tortuous path through the continuous lipid matrix around the corneocytes. This route is considered to be the dominant pathway during steady state-permeation of compounds (Roberts & Cross, 2002). The existence of the paracellular pathway was shown by histological localisation of topically applied compounds within the intercellular space (Boddé, van den Brink, Koerten, & de Haan, 1991). Also the importance of lipids to the barrier function of the SC also indicates this lipid pathway to be the dominant route (Harada, Murakami, Yata, & Yamamoto, 1992). The actual path length taken by a compound diffusing through the SC is considerably larger than the thickness of the SC, which further points the tortuous intercellular space as the dominant route (Albery & Hadgraft, 1979; Potts & Francoeur, 1991).

#### **1.4.2 Transappendageal route (sweat glands)**

The transappendageal routes consist of the hair follicles and sweat glands. The potential contribution of hair follicles to drug transport across skin is discussed in Section 1.3.3, therefore the role of sweat glands in drug transport will be covered herein. Sweat glands offer a way of bypassing the SC and enabling direct penetration into the dermis. Drug transport through this route is considered to be rapid compared to the transepidermal route, particularly in the early stages of diffusion until the amount of drug penetrating through this route becomes insignificant compared to that passing through the transepidermal route when steady state conditions are attained (Scheuplin & Blank, 1971). However, the overall contribution of this route to total drug delivery into and across skin remains unclear. This is because diffusion through sweat glands would have to occur against a flow of sweat in the outward direction and there is evidence that sweat glands are only open when sweating occurs (Hadgraft, 1983). Nevertheless, this route maybe important for the transport of charged and large polar molecules (Lauer et al 1995).

## 1.5 Factors affecting percutaneous absorption

Percutaneous absorption of solutes across skin is affected by many factors. Generally, they can be categorised as physiological, physicochemical and environmental factors and will be discussed in more detail.

### 1.5.1 Physiological factors affecting dermal absorption of drugs

The non-homogeneous nature of skin will influence the extent of dermal absorption. Due to inherent variability, wide variations in permeability are expected. *In vitro* a coefficient variation (CV) of about 43 % was observed for a single donor (Southwell, Barry, & Woodford, 1984). Inter-individual variance was observed to be 6 to 110 % (CV) or 2- to 8-fold (Lee, Earl, & Williams, 2001; Diane Southwell et al., 1984; van de Sandt et al., 2004). To account for this donor effect the Organisation for Economic Co-operation and Development (OECD) guideline 428 recommends for one experiment, skin preparations from at least two different donors (OECD, 2004b). Intra-individual variations arise due to regional differences within the body. It was shown *in vivo*, that forearm, palm and ball of the foot provide larger barrier functions than that from the axilla (3 to 7-fold) and scrotum (11 to 42-fold). This affect was assigned to SC thickness, hair follicle density and skin flexibility (Maibach, Feldman, Milby, & Serat, 1971). Roberts et al (1982) further highlighted the influence of regional differences within the body on the percutaneous absorption of methyl salicylates, with higher permeability being observed for the abdominal area compared to the forearm. Age related changes in percutaneous absorption were observed for human volunteers, whereby the absorption rate decreased with increasing age (Roskos, Maibach, & Guy, 1989; Singh & Singh, 1993). This difference was attributed to a reduction in sebum production, increased dryness of SC and the decreased transportation capacities to the systemic circulation due to decreased blood flow and atrophy of capillaries only present *in vivo* (Christophers & Kilgman, 1965). SC hydration has been shown to increase percutaneous absorption (Potts & Francoeur, 1990). This effect could be due the general swelling of the corneocytes, which alters the motility of the attached lipids and disrupts the lamellar structures resulting in reduced SC barrier function (Hotchkiss, Miller, & Caldwell, 1992; Potts & Francoeur, 1990; Roberts & Walker, 1993;

Warner, Stone, & Boissy, 2003). High water content can also affect the solubility of the penetrant. Moreover, observed inter-individual variability between human volunteers was not clearly attributable to gender or race (Leopold & Maibach, 1996; Lotte, Wester, Rougier, & Maibach, 1993; Rougier, Lotte, Corcuff, & Maibach, 1988). The presences of catabolic enzymes within the viable epidermis and sebaceous glands may lead to dermal biotransformation, which in turn could affect the percutaneous absorption of solutes across skin. This could alter the physicochemical properties of the penetrant, which may result in accelerated or attenuated permeation. Finally, pathological variations like wounds, psoriasis or atopic eczema decrease the SC barrier function (Wiechers, 1989).

### **1.5.2 Physicochemical factors influencing percutaneous absorption**

Permeation and maximum flux decrease in an exponential manner with respect to the molecular volume of drug, imposing a limit on the size of the compound that may penetrate the SC (Potts & Guy, 1992). Although the molecular volume is more suitable to measure the bulk of a molecule, the molecular weight is often used for simplicity. Thus drugs with a molecular weight of less than 500 Da are thought to transverse the SC effectively (Bos & Meinardi, 2000). However, tacrolimus and pimecrolimus (MW=804 & MW=810, respectively) are two molecules that are therapeutically effective and are examples of exceptions to the '500 Da rule'.

The octanol/water partition coefficient ( $\log P_{(o/w)}$ ) is a physicochemical property that has been shown to be able to predict drug flux across skin. Kim, Lee, & Kim (2000) reported parabolic relationships between skin permeability and  $\log P$ . If a drug is too hydrophilic, it will not partition into the skin while lipophilic compounds will remain in the SC and not penetrate the deeper tissues. Thus, the ideal partition coefficient for transdermal drug delivery is when the  $\log P$  is between 1-3 (Finnin & Morgan, 1999), suggesting that a balance between hydrophilic and lipophilic properties is needed.

According to the pH-partition hypothesis (Swarbrick, Lee, Brom, & Gensmantel, 1984), non-ionised drugs penetrate the skin more rapidly than ionised form. The SC permeability coefficients for non-ionized compounds are frequently 1-2 orders of magnitude larger than permeability coefficients for

ionized forms of the same compound (Vecchia & Bunge, 2003). However, this may not always apply especially when solubility of non-ionised drug is too low. Additionally, the exact relationship between the non-ionized and ionized forms would be expected to depend upon the compound and the lipophilicity of the non-ionized chemical, in particular, but also on the vehicle and salt form of the chemical used, as ion pairing may also facilitate ionized drug transport (Hadgraft & Valenta, 2000).

### 1.5.3 Environmental factors affecting dermal absorption

Environmental factors are also important to consider. For example, contact area, contact time, occlusion, formulation/vehicle composition and temperature may influence the extent of percutaneous absorption. A summary of the physiological, physicochemical and environmental factors affecting percutaneous absorption are summarised in Table 1-2.

**Table 1-2: A summary of the physiological, physicochemical and environmental factors affecting percutaneous absorption of solutes.**

Physiological factors	Physicochemical factors	Environmental factors
Age/gender	Charge	Contact area/time
Blood flow	Melting point	Dose
Metabolism	Molecular weight	Formulation/vehicle
Hair follicle density	Partition coefficient ( $\log P_{(o/w)}$ )	Occlusion
Skin thickness/species	Solubility	Temperature

## 1.6 Mathematics of skin permeation

The SC is devoid of active transporters due to its the dead nature (Blank, 1953; Dancik, Thompson, Krishnan, & Roberts, 2010), so drug transport across human skin occurs via passive diffusion. The process of diffusion across skin is very complex because of its multi-layered structure and presence of skin appendages. Therefore, it is surprising that a simple Fickian diffusion mathematical model can be used to generate valuable approximates from transdermal drug delivery data given the heterogenous nature of the skin. Nonetheless, Fick's first law of diffusion (Equation 1-1) can be used to model drug diffusion processes, where the skin structure is assumed to act as a simple homogeneous membrane. Fick's first law of diffusion states that flux ( $J$ ) of a compound (the rate mass transfer per unit area) at a given time and position is proportional to the diffusion coefficient ( $D$ ) and concentration difference ( $dC/dx$ ) across the skin:

$$J = -D \frac{dC}{dx} \quad \text{Equation 1-1}$$

The negative sign signifies that diffusion occurs in the direction of decreasing concentration of penetrant. The classical description of transport process is shown in Figure 1-8.

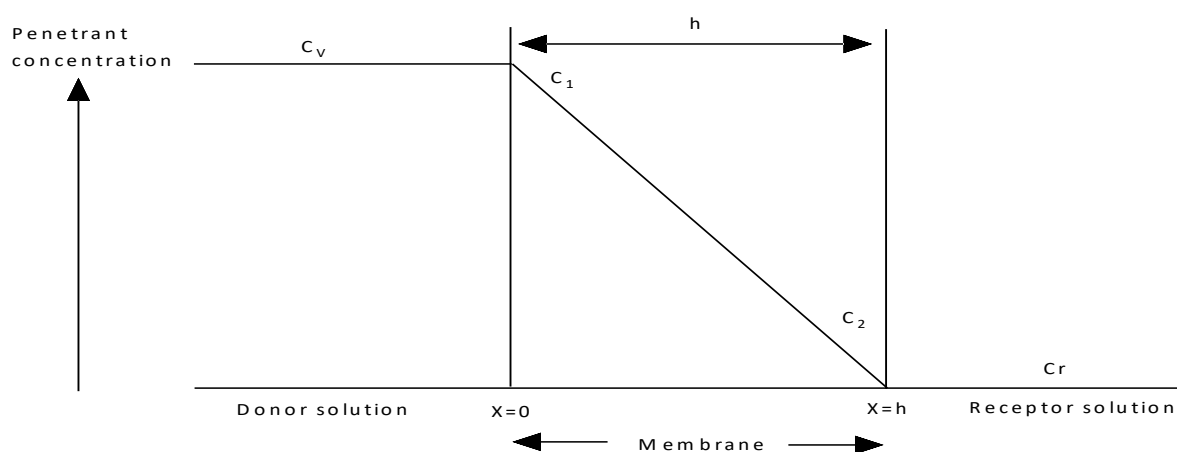


**Figure 1-8: Concentration profile across homogenous membrane at steady state zero order flux: ( $C_v$ ) concentration of penetrant in donor solution/vehicle, ( $C_r$ ) concentration of penetrant in receptor solution, ( $C_1$ ) concentration of penetrant in outermost membrane layer, ( $C_2$ ) concentration of penetrant in innermost membrane layer, ( $X=0$ ) outermost membrane layer, ( $X=h$ ) innermost membrane layer and ( $h$ ) membrane thickness (Barry, 1983).**

Adapting Equation 1-1 for steady flux over a membrane with thickness  $h$  and the concentrations  $C_1$  and  $C_2$  at the outermost ( $x=0$ ) and innermost layers ( $x=h$ ) respectively leads to:

$$J = \frac{D(C_1 - C_2)}{h} \quad \text{Equation 1-2}$$

If sink conditions hold in the receptor compartment, solute concentration at any time ( $t$ ), within the innermost membrane layer ( $x=h$ ) is assumed to be negligible ( $C_1 \gg C_2$ ). When using skin as the membrane it is not sufficient to measure its thickness and use it as  $h$ . The real length of the pathway through the SC depends on the drug and its preferences to take the transcellular, paracellular or transappendageal routes. In addition, considering the interactions that exist between the drug, the vehicle and the skin, it can be seen that that partition behaviour is very important. The drug concentration ( $C_1$ ) within the outermost membrane layer ( $X=0$ ) depends on the concentration within the donor solution ( $C_d$ ) and the partition coefficient ( $K$ ) between the membrane and vehicle:

$$C_1 = KC_v \quad \text{Equation 1-3}$$

Therefore, substituting Equation 1-3 into Equation 1-2 the flux ( $J$ ) across the membrane can be described as:

$$J = \frac{DKC_v}{h} \quad \text{Equation 1-4}$$

Flux ( $J$ ) of the penetrant can be calculated from the slope of the steady state diffusion curve (black curve in Figure 1-9). In most cases, it is difficult to determine  $D$ ,  $K$  or  $h$  independently. Therefore, they can be collected into single variable defined as:

$$K_p = \frac{KD}{h} \quad \text{Equation 1-5}$$

Where  $K_p$  is the permeability coefficient and substitution into Equation 1-4 gives Equation 1-6

$$J = K_p C_v \quad \text{Equation 1-6}$$

$K_p$  can be determined by dividing the steady state slope by the initial concentration of the drug applied to the donor phase. When the steady state portion of the line is extrapolated to the time axis (dashed line in Figure 1-9), the point of intersection is known as the lag time ( $T_L$ ), which is dependent on the membrane diffusion coefficient and the thickness of the membrane ( $h$ ).

$$T_L = \frac{h^2}{6D} \quad \text{Equation 1-7}$$

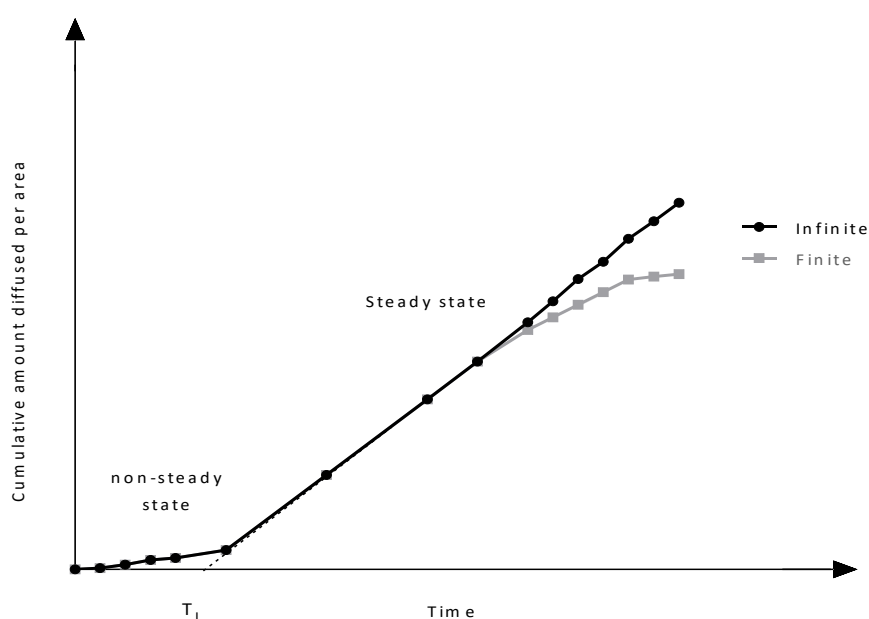


**Figure 1-9: Cumulative absorption of a solute through the skin as a function of time under infinite (black circles) and finite (grey squares) dose conditions. The slope of the linear portion of the curve represents the flux ( $J$ ) at steady state and the intercept of the extrapolated line with the x-axis gives the lag time ( $T_L$ ).**

Under finite dose conditions, the solute concentration is depleted over time leading to a sigmoidal-shaped diffusion curve (grey curve in Figure 1-9). Finite dose experiments are necessary for determining the percent absorbable dose and simulating in use conditions.

## 1.7 Percutaneous absorption enhancement of topical and transdermal formulations

The SC provides the primary barrier to the transport of topically applied molecules across skin. Over the years, much effort has been dedicated to finding ways to perturb its barrier properties in order to

optimise drug delivery. These enhancement strategies can be divided into passive or active methods, which seek to render existing routes more accessible or create new routes/channels across the SC barrier.

### **1.7.1 Passive methods**

The conventional means of applying drugs to skin include the use of vehicles such as ointments, creams, gels and patches. Such vehicles can be modified to enhance the driving force for diffusion and/or increasing skin permeability or bypass enzymatic activity. This includes the use of CPEs, supersaturated systems and by incorporating a prodrug as the diffusing species.

#### **1.7.1.1 Chemical penetration enhancers (CPEs)**

CPEs are often incorporated into formulations to promote permeation of poorly penetrating drugs by overcoming the barrier properties of the SC (Smith & Maibach, 2006). The exact mechanisms of action of CPEs can be very difficult to elucidate and often a single enhancer can have various modes of action. Therefore, CPEs are grouped based on their chemical structures rather than their complex modes of action. The modes of action of CPEs can be categorised based on whether the enhancer acts directly on the skin or whether it indirectly promotes drug flux by modification of the formulation (Lopez-Castellano & Merino, 2010).

The direct effects of enhancers on skin (illustrated in Figure 1-10) are described by the lipid protein partition theory (Barry, 2004), which states that chemical enhancers can overcome the barrier properties of the SC in numerous ways. Firstly, enhancers could disrupt the intercellular lipid domains. This disruption in the lipid bilayer could be homogeneous whereby the enhancer distributes evenly within the complex bilayer lipids or heterogeneous whereby the enhancer is concentrated within regions of the bilayer lipids leading to pooling of the enhancer in these areas. With such interactions, lipids in the bilayer may fluidise, alter polarity, phase separate or could be extracted causing the barrier resistance of the bilayer lipids to be reduced. Secondly, enhancers may change the solvent nature of the SC so that partitioning of the drug into the tissue becomes more favourable. This leads

to an increase in the amount of permeant in the skin. Thirdly, enhancers could act on the SC intercellular keratin (corneocytes) by denaturing or modifying its conformation causing swelling, increased hydration and vacuolisation. Fourthly, enhancers could denature or modify structure of the desmosomes that maintain cohesion between corneocytes causing splitting of SC, which is clinically unacceptable process (Barry, 2004; Goodman & Barry, 1989; Williams & Barry, 2004).

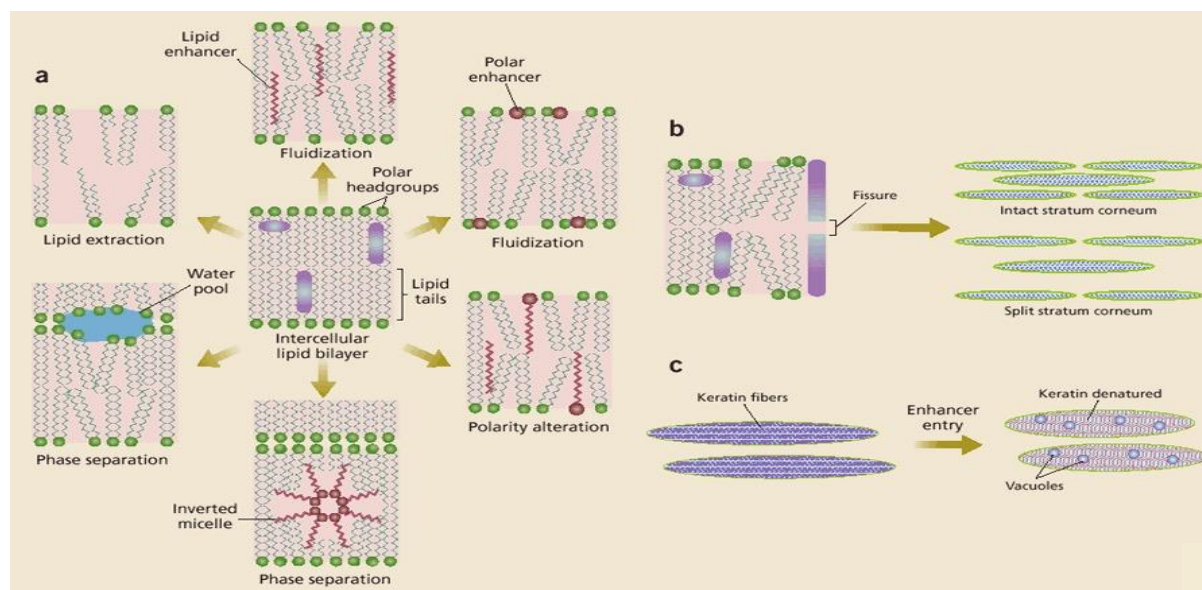


**Figure 1-10: Schematic representation of the mechanisms by which a chemical enhancer may interact with human stratum corneum: (a) action at intercellular lipids (b) action at protein component of the stratum corneum, leading to fissuring of intercellular lipids, splitting of stratum corneum squames (c) action within corneocytes, leading to further swelling, keratin denaturation and vacuole formation within individual corneocytes (Barry, 2004).**

As previously mentioned, CPEs can cause modifications to occur in formulations that promote drug flux, without directly disrupting the SC structure. These indirect effects can be categorised as follows: (a) change in the thermodynamic activity by increasing the degree of saturation in the vehicle and therefore increase the escaping tendency (see Section 1.8.1.4 for more detail); (b) Solubilising the permeant in the donor, especially where solubility is very low (e.g. steroids in aqueous donor solutions), can reduce depletion effects and prolong drug permeation; (c) the solvent permeating through the membrane could drag the permeant with it (Barry, 2005).

To be of clinical value a chemical penetration enhancer must exert its effects without injuring the underlying viable skin cells. Hence, enhancers should reduce SC barrier properties only temporarily

and act reversibly. Other desirable properties of CPEs include: they should be non-toxic, pharmacologically inert, the effect should be both predictable and reproducible and should work unidirectionally. Also they should be compatible with all formulation components including the active pharmaceutical ingredient and should be cosmetically acceptable (Williams & Barry, 2012).

CPEs reported in the literature include sulfoxides e.g. dimethylsulfoxide (Anigbogu, Williams, Barry, & Edwards, 1995); Azone (Hadgraft, Peck, Williams, Pugh, & Allan, 1996); pyrrolidones (Southwell & Barry, 1983); surfactants (Ribaud, Garson, Doucet, & Lévêque, 1994); Terpenes (Williams & Barry, 1992) ; phospholipids (Michel, Purmann, Mentrup, Seiller, & Kreuter, 1992) and water (Williams & Barry, 2004). However, this section will focus on fatty acids and alcohols/glycols as they are more commonly used CPEs.

Fatty acids are amongst the most studied group of penetration enhancers. They have been shown to be very effective in promoting the skin transport of many drugs including, propranolol (Ogiso & Shintani, 1990), flurbiprofen (Chi, Park, & Kim, 1995), naloxone (Aungst, J. Rogers, & Shefter, 1986), acyclovir (Cooper, Merritt, & Smith, 1985), thiamine disulphide (Komata, Inaoka, Kaneko, & Fujie, 1992) and tegafur (Lee et al., 1993). The major attraction of fatty acids is that Food and Drug Administration (FDA) classified some of these chemicals as Generally Recognised as Safe (GRAS). Structurally, fatty acids consist of an aliphatic hydrocarbon chain and a terminal carboxyl group. Structures within this group differ due to differences in chain length, in the number and position of double bonds in the molecule and whether the chains are branched and/or contain other substituents.

Altering fatty acid chain length has been shown to affect the level of enhancement of naloxone. A parabolic relationship was shown to exist between flux and saturated alkyl chain length, with C<sub>12</sub> being the most effective (Aungst et al., 1986). Similarly, Ogiso & Shintani, (1990) reported that medium chain length fatty acids lauric acid (C<sub>12</sub>) and myristic acid (C<sub>14</sub>) produced the maximum permeation for propranolol and enhancement was significantly larger than those in short and long chain fatty acids.

This suggests that medium chain length fatty acids are generally better enhancers than short and long chain fatty acids.

Additionally, the ability of fatty acids to enhance skin permeation is believed to be affected by other properties such as the number and position of double bonds and whether the fatty acid is branched or not (Narayanasamy Kanikkannan & Singh, 2005). Moreover, fatty acid esters such as isopropyl myristate have been investigated extensively in the literature and has been reported to enhance the skin permeation and penetration of many permeants (El-Nahas, Fakhry, El-Ghamry, Sabry, & Shereen, 2011; Furuishi, Fukami, Suzuki, Takayama, & Tomono, 2010; Hirata, Helal, Hadgraft, & Lane, 2013; Khan, ur-Rahman, Nawaz, & Khan, 2014; Nayak, Mohanty, & Sen, 2010; Sato, Sugibayashi, & Morimoto, 1988).

Fatty acids enhance permeant transport across skin by their direct action on the SC lipids. They are believed to disrupt the intercellular lipids (as illustrated in Figure 1-10) resulting in an increase in lipid fluidity and hence an increase in drug diffusivity or mobility across the SC (Williams & Barry, 2012b). Sato et al., (1988) examined the effects of a series of binary mixtures of isopropyl myristate (IPM) and propylene glycol (PG) on nicorandil permeation across skin and discovered that 10% IPM-PG enhance drug transport more than neat propylene glycol through full thickness skin. This difference disappeared when the SC was removed via tape stripping. Therefore, it was suggested that isopropyl myristate had a direct effect on the SC.

Alcohols and glycols are other important classes of CPEs that are commonly used as efficacious cosolvents for other penetration enhancers (Williams & Barry, 2012b). Examples include ethanol and propylene glycol respectively. They have been extensively investigated in the literature (Heard, 2015). Like fatty acids, alcohols and glycols can render the SC more permeable through their direct effects on the SC lipids. Propylene glycol is thought to enhance solute drug flux across skin by altering both intercellular lipids and corneocytes structures as well as enhancing permeant membrane solubility

thereby improving drug partitioning into the skin (Williams & Barry, 1992). Ethanol is believed to enhance solute flux across skin by extraction of intercellular lipids (Williams & Barry, 2012b).

Since fatty acids are generally believed to enhance permeant diffusivity by causing fluidisation of the intercellular lipids, clearly there is potential for synergistic or additive effect that may increase permeant flux when mixtures of these types of enhancers (alcohols/glycols and fatty acids) are concurrently applied to the skin. Several reports have documented the synergistic enhancements obtained from a mixture of propylene glycol with fatty acids for solutes of varying physicochemical (Hoelgaard, Møllgaard, & Baker, 1988; Karande & Mitragotri, 2009; T. Loftsson, Somogyi, & Bodor, 1989).

However, the enhancement effect of penetration enhancers can be highly influenced by other formulation components. For example, the addition of glycerol (another glycol) effectively reduced the effect of propylene glycol, whereas the permeation of estradiol was significantly enhanced by the addition of either hexadecanol or octadecanol (Møllgaard & Hoelgaard, 1983).

In addition, the concentration of penetration enhancer incorporated into the donor solution plays an important role in skin permeation enhancement of most penetration enhancers. It was found that the enhancement in the flux of nicorandil across skin from isopropyl myristate-propylene glycol vehicles was dependent on the isopropyl myristate content. Isopropyl myristate produced maximum enhancement at a concentration of about 10 %, the use of higher concentration of up to 50% produced similar enhancement with further increases to 90-100 % resulting in reduced drug flux (Sato et al., 1988).

Furthermore, individual CPEs may be limited in their efficacy in disrupting the skin barrier and may cause skin irritation and erythema at high concentrations (Finnin & Morgan, 1999). Also, CPEs might enhance concomitantly the percutaneous absorption of the excipients formulated with the drug product and this can lead to undesirable effects. Therefore, there is a critical need to develop topical

and transdermal formulations with reduced levels of skin irritation and excellent permeation enhancing effects. This could be achieved by selecting less irritating CPEs, combining CPEs to produce synergy and by introducing active methods such as controlled heat ( $\leq 45$  °C) (see Section 1.8.2.1).

#### **1.7.1.2 Ion pairing**

Charged drug molecules do not readily penetrate human skin (Roy & Flynn, 1990). This strategy involves adding oppositely charged species to the charged drug to form a more lipophilic ion pair, in which the charges are neutralised so that the complex can partition into and permeate through the SC. In the viable epidermis, the ion pair dissociates releasing the charged parent drug, which then continues to partition into the aqueous epidermis and diffuse onwards (Benaouda, Brown, Shah, Martin, & Jones, 2012; Benson, 2005).

#### **1.7.1.3 Prodrugs**

The molecule to be delivered can be chemically modified into a different more diffusible form by esterification of carboxylic function, which typically makes the molecule more lipophilic (prodrug) (Chan & Li Wan Po, 1989; Sloan, 1989). Once the prodrug has entered the skin, a conversion into its original, therapeutic form occurs as result of the action of the skin enzymes. Most prodrugs are in the form of esters, which are easily hydrolysed by esterases present in the skin (Johansen, Møllgaard, Wotton, Larsen, & Hoelgaard, 1986; Redasani & Bari, 2015). Therefore, the prodrug strategy utilises the metabolic activity of the skin to enhance permeation of topically applied compounds. An example of the successful application of this strategy is the well-established commercial product betamethasone valerate (Benson, 2005).

#### **1.7.1.4 Supersaturation**

Supersaturation offers the possibility of increasing drug delivery to the skin without affecting the skin's barrier, therefore avoiding any possible irritancy or side effects that are associated with other drug delivery enhancement approaches. Increasing the concentration of the drug above its saturated solubility in a particular solvent further increases the thermodynamic activity of the drug in its

formulation (Hadgraft and Walters, 1995). This can be demonstrated by rewriting Equation 1-4 (Fick's first law of diffusion) in terms of drug thermodynamic activity (Higuchi, 1960):

$$J = \frac{\alpha D}{\gamma h} \quad \text{Equation 1-8}$$

Where  $\alpha$  is the thermodynamic activity of the permeant in the vehicle and  $\gamma$  is the activity coefficient of the permeant in the membrane. As  $\alpha/\gamma$  is equivalent to  $KC_v$ , Equation 1-8 corresponds to Equation 1-4. Supersaturated systems have been used to enhance the penetration of various drugs through model silicone membranes as well as human skin (Davis & Hadgraft, 1991; Megrab, Williams, & Barry, 1995; Pellett, Davis, & Hadgraft, 1994). Supersaturated systems can be prepared by the evaporation of volatile solvent (Reid, Jones, & Brown, 2009) or by mixing of cosolvents (Davis & Hadgraft, 1991). This approach has been used to enhance the delivery of range of drugs such as hydrocortisone (Davis & Hadgraft, 1991), oestradiol (Megrab et al., 1995) and piroxicam (Pellett et al., 1994). The advantages associated with the use of supersaturated systems include being inexpensive and that they do not irreversibly alter the barrier property of the SC. The major limitation of this strategy is drug crystallisation, which leads to a decrease in the initial high drug flux. This inherent instability can be overcome by incorporation of anti-nucleating agents to improve stability (Reid et al., 2009).

## 1.7.2 Active methods

Several active strategies have been employed to enhance the transport of topically applied compounds across skin. Active methods involve the use of external force to act as driving mechanism and/or to render the SC more permeable. Active methods utilising the above mechanisms include, iontophoresis, ultrasound and heat. Other active strategies such as microneedles completely bypass the SC.

### 1.7.2.1 Iontophoresis

Iontophoresis involves application of a small direct current (approximately 0.5 mA/cm<sup>2</sup>) through a drug-containing electrode in contact with skin, with a grounding electrode completing the circuit (Merino & Lopez, 2010). The advantages of this mode of drug delivery over passive methods are the

following: (i) the ability to enhance the skin flux of large molecular weight (> 500 Da) compounds such as peptides and other macromolecules, (ii) the drug molecule can be delivered in a controlled and precise manner due to the direct proportional relationship between drug flux and the applied current, which in turn reduced the inter and intra-individual variations associated with percutaneous drug delivery and (iii) it can be used for systemic and/or topical delivery (Banga, 2011). The main limitations of this mode of application are its cost in comparison with that of more conventional therapies, burns and/or irritation produced by the application of electrical current to the skin and that the molecular weight of the active compound can act as the rate limiting factor as this mode of delivery has failed to significantly improve the transdermal delivery of macromolecules > 7 kDa (Kanikkannan, 2002).

#### **1.7.2.2 Ultrasound (Phonophoresis and Sonophoresis)**

Ultrasound also referred to as phonophoresis or sonophoresis involves the use of ultrasonic energy to enhance drug flux across the SC. The drug may be delivered simultaneously while ultrasound is being applied, or the skin may be pre-treated with ultrasound followed by application of the drug (Lavon & Kost, 2004; Ogura, Paliwal, & Mitragotri, 2008; Smith, 2007; Tyle & Agrawala, 1989). The main advantages of this mode of drug delivery over typical methods are; both local and systemic drug delivery can be achieved and its ability to enhance transdermal flux of large molecular weight compound (up to 48 kDa). The major disadvantage associated with the use of ultrasound are unwanted effects such as minor tingling, irritation and burning of skin, which can often be reduced or eliminated by optimising important parameters such as frequency, intensity, pulse length and application time (Escobar-Chávez, Bonilla-Martinez, & Villegas-González, 2010).

#### **1.7.2.3 Microneedles**

Microneedles can puncture the skin to create micron sized channels through which transport of molecules across skin are facilitated. This unique attribute of bypassing the SC has eliminated the physicochemical limitations on the type of molecule that can traverse the skin. Subsequently, microneedles have been used to enhance drug delivery of molecules with diverse properties including macromolecules (Olatunji, Al-Qallaf, & Das, 2010). With an average length of 50-900  $\mu\text{m}$ ,

microneedles can be used to facilitate both topical and transdermal delivery of molecules across skin (Quinn, Courtenay, Kearney, & Donnelly, 2015). Despite considering microneedles as promising strategy for enhancing drug transport across skin, they have some limitations: (i) unlikely to be useful in diseased skin (ii) the small size of the needles limits the therapeutic delivery rates of high-dose and low-potency molecules, (iii) it is very important to consider the variations of skin thickness while designing microneedles since this could affect the natural behaviour of the barrier and hence influence the drug delivery, (iv) microneedle tips can be broken off and left under the skin (v) microneedles can be difficult to apply on the skin, (vi) local inflammation may result if the amount of drug is high under the skin and (vii) after removal of the microneedle delivery system, pores in the SC remain open, which potentially increases the risk of infection (Escobar-Chávez et al., 2011). However, the risk of the latter occurring is thought to be low (Prausnitz, Mikszta, Cormier, & Andrianov, 2009). Also, whether the microneedles require sterilisation or not is an issue yet to be resolved.

Heat is an alternative enhancement strategy that does not offer some of the advantages (such as faster transport of drugs across skin and delivery of macromolecules/proteins) presented by the methods discussed above. However, heat is still an appealing strategy that could improve current/conventional topical dosage systems and is relatively inexpensive compared to these methods. Since the focus of the work described in this thesis is the influence of heat on the absorption of topically applied drugs, heat as an enhancement strategy will be extensively discussed in the following section. Covering important aspects such as the advantages, limitations, different methods of producing heat and the potential mechanisms by which heat enhances drug absorption across skin.

#### 1.7.2.4 Heat (Thermophoresis)

The use of heat as a strategy to enhance percutaneous absorption was reported in the 1960s (Blank et al., 1967; Cummings, 1969; Fritsch et al., 1963) and is generally known as thermophoresis. More recently, heat facilitated drug delivery has received considerable attention from numerous researchers (Akomeah, Nazir, Martin, & Brown, 2004; Chang & Riviere, 1991; Clarys et al., 1998; Klemsdal, Gjesdal, & Bredesen, 1992; Oliveira, Leverett, Emamzadeh, & Lane, 2014; Pattnaik, Swain, Rao, Varun, & Mallick, 2015; Peck, Ghanem, & Higuchi, 1995; Wood, Brown, & Jones, 2012).

It is important to note that heat energy has been physically produced using very different techniques. The first technique, thermal ablation, involves heating the skin surface (before administration of drugs) for a short period at a very high temperature ( $\geq 100$  °C), until tissues are vaporised, and removal of the SC occurs at the site of heating leading to the creation of channels, whereby the drug enters the skin. Heat energy for thermal ablation has been produced using thermoporation, radio frequency and lasers (Lee, Shen, Wang, Hu, & Fang, 2002). The second technique, involves using chemical mixtures to produce heat (Shahzad, Louw, Gerber, & du Plessis, 2015). It is this last technique of generating heat that will be investigated for its ability to enhance percutaneous absorption in this thesis.

This mode of delivery is non-invasive and involves the use of heat usually generated by chemical reaction ( $< 50$  °C) applied locally for short duration to temporarily and reversibly disrupt the barrier properties of the SC, resulting in enhanced drug transport across skin (Shahzad et al., 2015). This approach is especially enticing when synergistically combined with CPEs so as to expand the range of drugs with diverse properties that can be delivered across the skin.

The number of marketed products utilising chemically generated heat to facilitate drug transport across skin is very limited. Synera™/Rapydan™ a topical patch that combines lidocaine and tetracaine, using proprietary Controlled Heat-Assisted Drug Delivery (CHADD™) is licenced in the US and Europe (Sawyer et al., 2009). Similarly, Bioré® Warming Anti-Blackhead cleanser a topical cream, which

contains salicylic acid for the treatment of acne is available across Australia, Europe and the US (Horne, Kelly, Kirchhoffer, Koontz, & Young, 2011).

The CHADD™ heating patch (shown in Figure 1-11) uses iron oxidation as a source of heat energy and is able to generate skin surface temperature of 42 °C for up to 4 hr, or even longer (Stanely, Hull, & Rigby, 2001; J. Zhang, Hao, Hull, & Rigby, 2003).

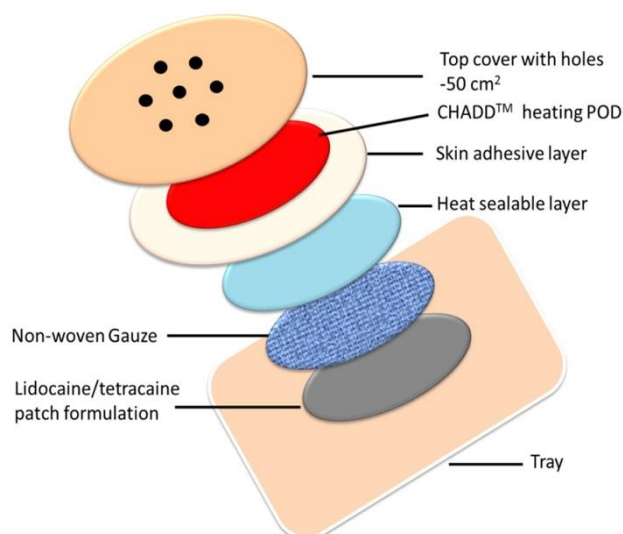


**Figure 1-11: Lidocaine/Tetracaine patch utilising CHADD™ technology developed by Zars Pharma Ltd (Shahzad et al., 2015).**

It consists of an outer semipermeable membrane that controls the temperature by allowing the ingress of oxygen to initiate iron oxidation. Below this outer semipermeable membrane is a semisynthetic air permeable pouch that contains heat-generating material: iron, carbon, sodium chloride, vermiculite and water. The next layer is a pressure sensitive skin adhesive layer. This is followed by a heat sealable barrier film, which separates the formulation from the temperature control components (Stanely et al., 2001; J. Zhang et al., 2003). Other non-drug containing and heat generating patches on the market that utilise similar heat-generating material as CHADD™ include: Cura-Heat® Patches, Deep Heat Pain Relief Heat Patch, Nurofen® Express Heat Patches, ThermaCare® and Voltarol® Thermal Patch Heat Patch. These patches are not used to deliver active drug molecules across skin, but are rather used for their therapeutic heat to help reduce muscular and joint pains (Nadler et al., 2002, 2003). Concerns have been raised about the suitability of heat facilitated drug

delivery using the exothermic oxidation of iron as a source of heat energy, due to a risk of dose variability and thermal burns, which could occur due to changes in air oxygen, humidity and pressure (Curran, McGuigan, & O'Broin, 2013; Raleigh, Rivard, & Fabus, 2005).

Bioré® Warming Anti-Blackhead cleanser consists of an anhydrous composition (e.g. surfactant, polymer, glycols and zeolite) that generates heat in the presence of water. Within this product, heat is generated using materials known as zeolites, which are capable of heating the temperature of skin up to 47 °C for less than 1 minute (Horne et al., 2011).

Phase change materials have been investigated for their suitability as an energy source for heat facilitated drug transport (Wood, Brown, Jones, & Murnane, 2011; Wood, Jones, & Brown, 2012). Supercooled salt solutions containing sodium acetate trihydrate and sodium thiosulfate pentahydrate have been identified as suitable phase change materials with excellent ability to store heat, high thermal conductivity, are relatively cheap, possesses the ability to remain stable in the supercooled state for years and are GRAS listed (Wood et al., 2011). Producing supercooled solutions involves: dissolving the phase change material in a vehicle (such as water) with simultaneous heating, followed by cooling of the mixture to generate a supersaturated salt system that remains in solution. The latent heat stored within the system can be released by a liquid to solid phase change (recrystallization), which can be initiated by introducing a nucleating agent (Wood et al., 2012). Like iron oxidation patches, supercooled systems are also commercially available as heat packs for various uses including muscle and joint pains e.g. ThermaClick Heat Pads.

Important parameters such as intensity and duration of heat (controlled by e.g. the mass/volume of heat generating material and presence of a trigger such as oxygen/nucleating agent) and exposure time are known to influence heat facilitated percutaneous absorption (Shahzad et al., 2015; Wood et al., 2011). Other factors such the rate of crystallisation and the level of saturation are thought to be important parameter for phase change materials (Wood et al., 2012). Therefore, these parameters

can be manipulated and optimised for either local or systemic drug delivery, whilst avoiding cutaneous damage or patient discomfort.

The heat generated by chemical techniques such as iron oxidation (Zhang et al., 2003) and supercooled solutions is generally less than 50 °C (Wood et al., 2012). Whilst there are no regulatory limits on the intensity and duration of heat produced by thermophoretic delivery systems, the scarce information on temperatures tolerated by the skin would suggest that an appropriate range for thermophoretic delivery system would be 44-47 °C (McAuley & Caserta, 2015; Moritz & Henriques, 1947). Consequently, most studies investigating heat facilitated percutaneous absorption have employed temperatures of  $\leq 45$  °C, which is within physiologically tolerable range.

The mechanism by which heat enhances percutaneous drug delivery are numerous. Heat may enhance dermal absorption by influencing the following parameters; the release of permeant from the formulation/vehicle, partitioning of the permeant into the SC and diffusion through it and finally partitioning from the SC to the viable epidermis and lower layers from where a permeant can be taken up systemically. Additionally, heat is believed to reversibly disrupt the SC barrier at temperatures of  $\leq 45$  °C by changing SC lipid organisation from ordered state (orthorhombic) to more disordered state (hexagonal), resulting in enhanced percutaneous delivery (Wood et al., 2012).

Drug release from the formulation/vehicle and partitioning are important rate limiting steps in the drug transport process (Lane, Santos, Watkinson, & Hadgraft, 2012), both of which are influenced by changes in temperature. Increasing the temperature can enhance the solubility of a drug in the vehicle, with increased drug vehicle solubility decreasing thermodynamic activity, which is the driving force for drugs to escape the vehicle and partition into the skin. However, this problem can be resolved by using volatile solvents in the formulation. Moreover, an inverse relationship between temperature and solubility has been reported for some drug compounds (such as erythromycin and lidocaine), in which case heat can be used to increase thermodynamic activity and drug flux by lowering the drug solubility in the vehicle (McAuley & Caserta, 2015). Heat can also increase the skin uptake of

formulation components such as CPEs, which could potentially lead to increased drug flux through synergistic effects. Improved drug transport due to solvent/enhancer uptake into model membranes has been reported (McAuley et al., 2010; Oliveira, Beezer, Hadgraft, & Lane, 2010; Twist & Zatz, 1988). Depending on the drug-vehicle-skin interactions, in some systems the partition coefficient increases as a function of temperature, whereas in others an increase in temperature may reduce the partition coefficient as its uptake would be enthalpically driven and facilitated at lower temperatures due to strong drug-SC components interactions (McAuley & Caserta, 2015). Finally, heat is known to increase the kinetic energy of the drug molecule within the formulation and the lipid bilayers, resulting in increased drug release from the formulation, as well as improved partitioning and diffusion through the skin.

The drug transport process is essentially a diffusion process, which is influenced by temperature. The Stoke-Einstein equation (Equation 1-9) relates the diffusion coefficient of a molecule directly to the absolute temperature:

$$D = \frac{K_B T}{6\pi\eta r} \quad \text{Equation 1-9}$$

Where  $D$  is the diffusion coefficient,  $K_B$  is the Boltzmann constant,  $T$  is the absolute temperature (Kelvin),  $\eta$  is the viscosity of the solvent and  $r$  is the radius of the diffusing species. The Stokes-Einstein equation suggests that diffusion coefficient ( $D$ ) is directly proportional to temperature ( $T$ ), provided that the other factors remain constant, which is unlikely due to the effects of temperature on viscosity ( $\eta$ ). Longworth (1954) whilst examining the temperature dependence of  $D$  of a series of compounds in aqueous solution, concluded that increase in  $D$  from 1 to 25 °C is primarily due to a decrease in the viscosity ( $\eta$ ) of the solvent, with kinetic energy changes ( $K_B T$ ) accounting for only 10 % of the enhancement effect of temperature. The same author has also found that the Stokes radius of few compounds tested decreased when applying heat as a result of the lower hydration of the solute molecules in water (Longworth, 1954).

In the clinical situation, a thermal gradient will exist between the heat-aided formulation (high temperature) and the skin surface (low temperature). In such a thermal gradient, the drug and other formulation components (e.g. CPEs) attain drift mobility ( $V_T$ ) in addition to Brownian diffusion, which is linearly dependent on the thermal gradient ( $\Delta T$ ) with a proportionality constant  $D_T$ , known as thermophoretic mobility or thermal diffusion coefficient:

$$V_T = -D_T \Delta T \quad \text{Equation 1-10}$$

This thermophoretic driving force is induced by the thermal gradient, which is influenced by the interactions between the particles and solvents in the system. Thus the thermal force is unique to each system, which means its magnitude is expected to vary depending on the vehicle response to the thermal gradient and the dependence on the molecule-vehicle interaction on temperature (McAuley & Caserta, 2015).

Heat is also known to have a direct effect on the skin through the fluidisation of the SC lipids. Within the physiologically tolerable temperature range (35-47 °C), the first lipid transition occurs, where the SC lipid lateral packing changes from the less permeable orthorhombic packing state to the more permeable hexagonal packing state (Gay, Guy, Golden, Mak, & Francoeur, 1994). This is likely to result in increased membrane permeability and diffusion coefficient (Park, Lee, Kim, & Prausnitz, 2008). Finally, raising the skin temperature is likely to increase cutaneous blood circulation, which leads to increased drug clearance into system circulation (Klemsdal et al., 1992). This increase in drug clearance is likely to maintain a concentration gradient for diffusion to occur, which is good for achieving transdermal drug delivery.

## 1.8 Summary

The outermost skin layer, the SC provides the rate-limiting barrier for drug delivery across skin. It is well established that drug diffusion across skin occurs predominately through the lipid matrix of the SC. Hair follicles also provide a route of entry into the lower layers of the skin and substantially contribute to drug transport in the initial stages ( $\leq 30$  min) of the drug transport process. Thus, there is developing interest in using the hair follicles and their associated pilosebaceous units as target structures for localised drug delivery, particularly for the treatment of skin diseases and hair growth abnormalities. The pilosebaceous units are implicated in the aetiology of acne, androgenetic alopecia and other sebaceous gland dysfunctions, and are thus obvious targets for locally active therapeutic agents. Whilst conditions such as acne and androgenetic alopecia are not life threatening, they can have a huge impact on the quality of life of individuals suffering from these conditions. The efficacies of current treatments for these conditions need to be improved to alleviate their burden on the patients, carers and healthcare system. The use of heat as an enhancement strategy may improve delivery of topical formulations for these conditions by limiting the exposure of the skin to high drug concentrations and by enhancing drug localisation in the hair follicles. Physiological tolerable heat ( $\leq 45^{\circ}\text{C}$ ) in particular may offer a suitable means of maximising the accumulation of drugs in the hair follicles and sebaceous glands, by reducing the viscosity of sebum which may pose as a chemical or physical barrier to drug transport or by unclogging pores or by removing debris/dead skin and oil from pores making them available for drug transport. This is likely to be particularly beneficial for conditions such as acne which are characterised by excessive sebum production. Moreover, heat as an enhancement strategy is non-invasive and considerably cheaper compared to other well established active strategies such as iontophoresis and sonophoresis. However, the influence of heat on follicular drug delivery is less researched and understood and heat remains an under-investigated and an under-utilised enhancement strategy in general.

## 1.9 The aim and objectives of thesis

The customised use of physiologically tolerable heat ( $\leq 45^{\circ}\text{C}$ ) to target the follicular structures is a novel and highly promising prospect. To date, no studies have been published investigating the effect of heat and CPEs on the follicular absorption of topically applied drugs. Therefore, the aim of this research project is to understand the effect of heat ( $\leq 45^{\circ}\text{C}$ ) and CPEs on the follicular absorption of topically applied drugs. Minocycline HCl, isotretinoin and finasteride were selected as relevant drugs with respect to follicular penetration. To achieve this aim, the following objectives were set:

- To develop and validate HPLC methods for the quantification of minocycline HCl, isotretinoin and finasteride following skin permeation and penetration experiments.
- To develop and validate *in vitro* permeation methods and drug extraction procedures that enable quantification of drugs located in the follicular canal and the different skin layers of human skin after topical application of these drugs.
- Examine the suitability of using sodium thiosulphate as a heating system to generate short burst of heat to facilitate drug delivery.
- Investigate the effect of heat ( $\leq 45^{\circ}\text{C}$ ) for various durations on the skin permeation, distribution and follicular absorption of all three drugs delivered from various neat or binary solvent systems.
- Study the effect of heat ( $\leq 45^{\circ}\text{C}$ ) and CPEs on  $Kh$  &  $D/h^2$  to gain better understanding of the mechanism of enhancement.

## **2 Analytical Validation of General Methods**

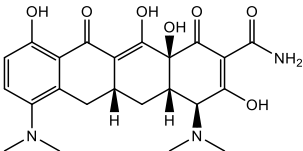
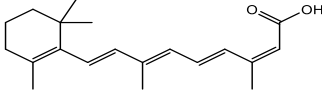
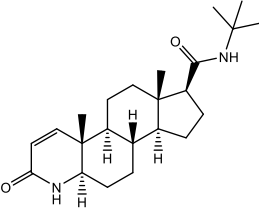
## 2.1 Introduction

This chapter describes the validation of high performance liquid chromatography (HPLC) methods used to quantify the three-selected active pharmaceutical ingredients (APIs) minocycline, isotretinoin and finasteride. This chapter also contains details of methods for *in vitro* skin permeation and distribution experiments, as well as drug solubility and stability studies in selected solvents and media. It was then intended that these initial pre-formulation data would be used to select suitable CPEs to investigate their *in vitro* influence on skin permeation, distribution and follicular absorption of topically applied drugs in combination or without heat.

### 2.1.1 Active Pharmaceutical Ingredients (APIs) of interest

The three APIs minocycline, isotretinoin and finasteride were chosen because of their pharmacological activities with respect to hair follicles, which are potential drug targets in conditions such as acne and alopecia (Lademann et al., 2006, 2011).

**Table 2-1: Chemical structures and physicochemical properties of APIs investigated (Log  $P_{(o/w)}$  & MW).**

	Minocycline	Isotretinoin	Finasteride
<i>Chemical structure</i>			
<i>Molecular weight</i>	493.9	300.4	372.6
<i>Log P* (octanol/water)</i>	-0.61	6.6	3.2

\*Experimental log P values obtained from published work (Di Stefano et al., 2008; Nankervis, Davis, Day, & Shaw, 1995; Loftsson, Hreinsdóttir, & Másson, 2005)

Also, these APIs were selected because they have similar molecular weights (< 500) and differing lipophilicities, which means the suitability of using heat ( $\leq 45$  °C) and CPEs as a targeting strategy for improving follicular transport and skin penetration of drugs with a wide range of lipophilicities can be

investigated. The chemical structures and physicochemical properties of the chosen drugs are shown in Table 2-1.

#### **2.1.1.1 Minocycline**

Minocycline is a second generation semisynthetic tetracycline antibiotic with broad-spectrum activity against aerobic and anaerobic Gram-positive and Gram-negative bacteria (BNF 66, 2013). It exhibits bacteriostatic properties by binding to the 30S ribosomal subunit, thus inhibiting protein synthesis (Garrido-Mesa, Zarzuelo, & Gálvez, 2013).

Minocycline's activity against *P. acnes* and its anti-inflammatory properties have made it an effective treatment for acne vulgaris (Ochsendorf, 2010). However, prolonged treatment involving systemic minocycline has been associated with multiple adverse effects which have been linked to its accumulation in fatty tissue and to its long half-life (Aronson, 2014). Examples of adverse effects include vestibular side-effects (dizziness, vertigo and nausea), pigmentation of a variety of tissues (skin, thyroid, nails, sclera, teeth, conjunctiva, tongue and bone) (Good & Hussey, 2003), hypersensitivity reactions, autoimmune disorders (systemic lupus erythematosus-like syndrome, autoimmune hepatitis, and polyarteritis nodosa) and disturbance of gastrointestinal micro flora (Elewski et al., 2011). Therefore, the potential toxicity of systemic minocycline highlights the need for a topical minocycline formulation. Topical therapy offers the advantage of minimising or eliminating these adverse effects by the use of a much lower topical dose compared to the oral dose and by confining the medication specifically to the lesion or affected skin site with limited systemic absorption. In addition, clinical efficacy maybe improved when high drug concentration is achieved in the lesion by site-specific topical drug delivery.

### 2.1.1.2 Isotretinoin

Isotretinoin (13-cis-retinoic acid) a derivative of retinoic acid is commonly used for conditions such as acne and can be administered topically or taken orally. Isotretinoin targets all four identified factors underlying acne pathogenesis. Therefore, its mechanism of action are decreased comedogenesis, sebum production, *P. acnes* proliferation and inflammation. Oral isotretinoin is associated with severe side effects such as extreme drying of skin and mucus membranes, photosensitivity, inflammatory bowel disease, depression, suicidal ideation and is also teratogenic and, therefore, reserved for severe acne only. The current marketed topical preparations show systemic absorption and skin irritation (Queille-Roussel et al., 2001). However, this irritation is mild to moderate compared to oral delivery. Therefore, there is a need to develop topical formulations with the ability to provide high drug concentrations in the pilosebaceous unit, achieved by utilising the possible synergistic effects of CPEs and heat. This could potentially improve the treatment of acne whilst decreasing side effects associated with both systemic delivery and existing topical formulations of isotretinoin.

### 2.1.1.3 Finasteride

Finasteride, a 5-alpha reductase inhibitor is currently only available as an oral preparation for the treatment of benign prostatic hyperplasia and androgenetic alopecia in men. Its mechanism of action is to block the conversion of testosterone to the more potent metabolite dihydrotestosterone (DHT). DHT has been implicated in the aetiology of a variety of skin disorders, including acne and androgenetic alopecia. Oral delivery of finasteride has been associated with significant systemic side effects such as impotence, decreased libido, ejaculation disorders, and breast tenderness and enlargement, with these adverse effects being encountered not only during therapy but also after treatment cessation (Traish, Melcangi, Bortolato, Garcia-Segura, & Zitzmann, 2015). Consequently, the topical application of finasteride to the hair follicles and associated sebaceous glands directly may eliminate these side effects by reducing systemic exposure. Additionally, topical formulations of finasteride may provide improved efficacy due to the high drug concentrations in the target site.

### 2.1.2 Reverse Phase High Performance Liquid Chromatography (HPLC) for quantification of APIs

The organisation for economic co-operation and development (OECD) guidelines for skin absorption *in vitro* tests, recommend the use of HPLC to measure the transport of non-radiolabelled drugs (OECD, 2004a, 2004b). When performing permeation experiments, a series of endogenous components released from skin may affect drug quantification. Hence, the use of an analytical technique such as, reverse phase HPLC (RP-HPLC), which allows the separation of the test analyte from these interfering substances and enables the precise and accurate quantification of the analyte is required. RP-HPLC chromatography involves the partitioning of a solute between a hydrophobic stationary phase (usually octadecylsilane which is bonded to a silica support) and a hydrophilic mobile phase (eluent) e.g. acetonitrile, methanol, aqueous buffers or a mixture thereof. This allows separation of the various components of a sample based on the relative affinity of the solute for the stationary and mobile phase. To achieve efficient separation an ideal combination of different parameters must be identified. These include; the composition and pH of the mobile phase, flow rate, injection volume, the nature of the stationary phase and the column temperature. The compounds are preferably detected by monitoring the absorbance of ultraviolet (UV) radiation assuming the drug molecule contains a chromophore. UV detectors function by monitoring light absorbed by the solute molecules, since each solute or chromophore may absorb light maximally at a characteristic wavelength which allows identification of the solute. Conversely, if two or more solutes absorb light at the same wavelength, the ability of RP-HPLC to separate the components allows both qualitative and quantitative analysis of respective compounds. The decision to use HPLC and UV detection together was therefore also based on the required sensitivity and specificity of the assay when conducting *in vitro* skin permeation and penetration studies, in comparison to other analytical techniques.

### 2.1.3 *In vitro* skin permeation assessment

The OECD guidelines on *in vitro* skin permeation studies recommend using Franz diffusion cells to investigate dermal absorption of test materials. It also states diffusion experiments should use appropriate skin models, receiver fluids and must be validated to ensure that the method is fit for purpose (OECD, 2004a, 2004b). Therefore, the aim of the work in this chapter was to:

- Develop and validate appropriate HPLC methods which would allow the precise quantification of the three APIs being studied, in the presence of human skin and receptor fluid used in Franz cell diffusion studies.
- Perform system suitability tests to confirm the performance of the chromatographic systems.
- Ensure all procedures/methods employed in the *in vitro* skin permeation and penetration studies were 'fit for purpose' to safeguard accuracy and reproducibility.

## 2.2 Materials and Methods

Minocycline HCl (99.9 %), Isotretinoin (99.9 %) and Finasteride (99.9 %) were purchased from Sequoia Research Products (Pangbourne, UK). Acetonitrile HPLC grade (99.9 %), ethanol HPLC grade (99.9 %), glycerol (>98.0 %), hydrochloric acid (37.0 %), formic acid (98.0-100.0 %), methanol HPLC grade (99.9 %), propan-2-ol (>99.5 %), propylene glycol (>99.0 %), propylene glycol diacetate (99.0 %), phosphate buffer solution (PBS) tablets, sodium hydroxide pellets ( $\geq 97.0$  %) ACS reagents certified, Dura Seal™ (Diversified Biotech, USA), Hamilton GASTIGHT® syringes (Hamilton®, Switzerland), Parafilm M® laboratory film (Bemis® Flexible packaging, USA) and Whatman® nylon filter paper 0.2  $\mu\text{m}$  (Whatman International Ltd, Maidstone, UK) were acquired from Fisher Scientific (Loughborough, UK). Ethylenediaminetetraacetic acid (EDTA, 99.0-101.0 %), hydrogen peroxide (30.0 %) were supplied by Sigma Aldrich (Gillingham, UK). Acetic acid (>99 %), ethylene glycol (>99 %), isopropyl myristate (>96 %), magnesium chloride hexahydrate (>99 %), sodium phosphate monobasic monohydrate (98.0-102.0%) and tetrabutylammonium hydroxide titrant, 0.4M in water HPLC grade was bought from Acros Organics (New Jersey, USA). Phenoxyethanol ( $\geq 99.0\%$ ) was purchased from Fluka (St Louis, USA). Diisopropyl adipate (> 99.8 %) and Crodamol™ GTCC (> 99.8 %), Crodamol™ ISIS (> 99.8 %), dimethyl isosorbide (> 99.8 %) and isopropyl palmitate (> 99.8 %) were supplied by Croda (Barcelona, Spain). Propylene glycol dipelargonate (> 99.8 %), Propylene glycol monolaurate 90 (> 99.8 %), propylene glycol monolaurate FCC (> 99.8 %) and Transcutol® P (>99.8%) was purchased from Gattefosse (France). Cotton buds (Johnson & Johnson Ltd, Maidenhead, UK) and Scotch® Magic™ Invisible Tape (3M, USA) were donated by UH campus pharmacy (Hatfield, UK). Polytetrafluoroethylene (PTFE) syringe filters 25mm 0.22 $\mu\text{m}$  was purchased from dot-red® analytical (Cambridgeshire, UK). Individually calibrated unjacketed upright Franz diffusion cells (volume 3.0 mL: diameter 1.0  $\text{cm}^2$ ) were acquired from Soham Scientific (UK). Deionised water (18.2  $\text{M}\Omega\cdot\text{cm}$ ) was from Millipore Milli-Q® water system.

## **2.2.1 HPLC assay method development**

### **2.2.1.1 HPLC chromatographic conditions**

Analytical method verification was carried out using a Shimadzu Prominence instrument (Shimadzu Corp., Kyoto, Japan) consisting of LC-20 AD pumps with DGU-20A<sub>5R</sub> degasser, SIL-20A HT auto-sampler, CTO-20 AC column oven, SPD-20A diode array detector, and CBM-20A communication module. Data acquisition was performed on Labsolutions software<sup>®</sup> version 5.54 SP2. The HPLC conditions used for the determination of minocycline, isotretinoin and finasteride are detailed in Table 2-2. The preparation of the mobile phase buffer used in the minocycline assay is described in Section 2.2.1.2. The pH of this buffer was measured using a Hanna pH 209 pH meter and all aqueous components of the mobile phase for all three APIs were filtered through 0.2 µm nylon filter before being used.

**Table 2-2: HPLC methods for analysis of minocycline isotretinoin and finasteride**

Parameter	Minocycline	Isotretinoin	Finasteride
Stationary phase	Phenomenex® Luna®, C18 (2), 150 mm x 4.6 mm (5 µm) (Phenomenex Ltd., Cheshire, UK)	Phenomenex® HyperClone™ 5 µm ODS (C18), 150 x 4.6 mm (5µm) (Phenomenex Ltd., Cheshire, UK)	Thermo Scientific™ Hypersil™ ODS (C18) 250 x 4.6 mm (5 µm) (Thermo Fisher Scientific, Leicestershire, UK)
Guard Column	Security Guard™ cartridge, C18 4 x 3.0 nm (Phenomenex Ltd., Cheshire, UK)	Security Guard™ cartridge, C18 4 x 3.0 nm (Phenomenex Ltd., Cheshire, UK)	Security Guard™ cartridge, C18 4 x 3.0 nm (Phenomenex Ltd., Cheshire, UK)
Mobile Phase	22 % Acetonitrile: 78 % Phosphate buffer (0.1 M NaH <sub>2</sub> PO <sub>4</sub> containing 10 mM tetrabutylammonium hydroxide and 2 mM EDTA, adjusted to pH 6.5 with 5 M sodium hydroxide)	76 % Acetonitrile (containing 0.1 % formic acid): 24 % Deionised water (containing 0.1 % formic acid)	60 % Acetonitrile: 40 % Deionised water
UV wavelength (nm)	272	355	210
Flow rate (mL/min)	1.0	1.0	0.5
Injection volume (µl)	20	10	10
Run time (min)	15.0	15.0	15.0
Column temperature	Room temperature (20 °C)		

### 2.2.1.2 Preparation of buffer solutions

The buffer solution used in the minocycline HPLC assay (0.1 M sodium phosphate, 10 mM tetrabutylammonium hydroxide, 2 mM EDTA, pH 6.50, 1 L) described in Table 2-2 was prepared according to the following procedure:

1. Sodium phosphate monobasic monohydrate (13.80g) was weighed onto a weigh boat and transferred to a 1 L volumetric flask. Any sodium phosphate monobasic monohydrate found to remain on the weigh boat was rinsed into the volumetric flask using deionised water (MilliQ, 18.2 M $\Omega$ ).
2. Ethylenediaminetetraacetic acid (EDTA, 0.585 g) was weighed onto a weigh boat and transferred to the volumetric flask from Step (1). Any EDTA remaining on the weigh boat was rinsed into the volumetric flask using deionised water (MilliQ, 18.2 M $\Omega$ •cm).
3. Using a glass bulb pipette, 25 mL of 0.4 M tetrabutylammonium hydroxide was transferred into the volumetric flask from Step (2).
4. Approximately 900 mL of deionised water (MilliQ, 18.2 M $\Omega$ •cm) was measured using a 1 L A-grade measuring cylinder and transferred to the 1 L volumetric flask from Step (3), and the solution was thoroughly mixed.
5. The pH of the buffer solution was measured using the Hanna Instruments pH 209 pH meter and was adjusted to 6.45 using 5 M sodium hydroxide solution.
6. The buffer solution was stirred until the EDTA had visually dissolved, after which time the solution was made to volume using deionised water (MilliQ, 18.2 M $\Omega$ •cm) and thoroughly mixed.
7. The pH of the buffer solution was measured and if required adjusted to pH 6.50 using the procedure previously summarised in Step (5).
8. The buffer solution was filtered through a 0.2  $\mu$ m nylon filter.
9. The buffer solution was stored for up to 1 week at room temperature (20 °C).
10. Volumes were scaled according to analytical requirements.

The buffer solutions investigated as potential receptor fluid systems in Sections 2.2.2.1 and 2.2.2.2 were prepared as follows:

To prepare 0.5 M acetate buffer (AB) solution at pH 4.5, acetic acid (3.0 g) was dissolved in approximately 90 mL of deionised, adjusting the pH of the solution to 4.5 (using 1 M sodium hydroxide) and then making the volumetric flask up to volume (100 mL) with deionised water. To prepare 0.5 M AB at pH 5.0, the procedure above was repeated but the pH was adjusted as required before making up to volume with deionised water.

Phosphate buffered saline (PBS) 0.15 M solution at pH 7.4 was prepared by dissolving one PBS tablet in 100 mL of deionised water.

### **2.2.1.3 Calibration curve (linearity, LOD and LOQ)**

A stock solution (500 µg/mL) was prepared by dissolving 0.01 g of the required API to 20 mL volume in methanol. A series of calibration standard solutions with varying concentrations were prepared by serial dilution from the stock solution using methanol as the diluent. For minocycline, the concentrations of these standards were: 50, 40, 20, 15, 10, 5, 3 µg/mL. In the case of isotretinoin, the concentrations of the calibration standards were: 30, 10, 5, 1, 0.5, 0.25, 0.1 µg/mL. With regards to finasteride the concentrations of the standards were: 40, 30, 20, 10, 5, 1, 0.5 µg/mL. All calibration standards and stocks solutions were prepared in amber volumetric flasks and additional precautions such as wrapping aluminium foil over glass weighing boats were taken to protect isotretinoin from light.

A calibration curve was constructed by plotting the response (peak area) against concentration of the standards. The correlation coefficient ( $R^2$ ) of this plot was determined. Also, the limit of detection (LOD) and limit of quantification (LOQ) were calculated from the standard error of the y-value (peak area) for each x-value (concentration) in the regression line of the calibration curve (STEYX) and its slope using Equation 2-1 and Equation 2-2, respectively:

$$LOD = \left( \frac{STEYX}{Slope} \right) \times 3.3 \quad \text{Equation 2-1}$$

$$LOQ = \left( \frac{STEYX}{Slope} \right) \times 10 \quad \text{Equation 2-2}$$

#### 2.2.1.4 System suitability

To evaluate the performance and effectiveness of the HPLC methods described in Table 2-2, system suitability parameters such as capacity factor ( $k'$ ), tailing factor (TF) and theoretical plates number (N) and injection repeatability were determined and compared against limits recommended by the FDA (FDA, 1994).

##### 2.2.1.4.1 Capacity factor ( $K'$ )

The capacity factor ( $K'$ ) is a measure of where the peak of interest is located with respect to the void volume. Generally, the peak should be well resolved from other peaks and the void volume. A capacity factor value of more than 2 is recommended as per ICH guidelines (ICH, 2005). Capacity factor ( $K'$ ) was calculated using Equation 2-3, where  $t_0$  = elution time of the void volume or non-retained components and  $t_R$  = retention time of the analyte.

$$K' = \frac{(t_R - t_0)}{(t_0)} \quad \text{Equation 2-3}$$

#### 2.2.1.4.2 Tailing factor (TF)

Tailing factor (TF) is an important system suitability parameter as the accuracy of quantification decreases with increase in peak tailing. Tailing factor was calculated using Equation 2-4, where  $W_x$  = width of the peak determined at 5 % from the baseline of the peak height and  $f$  = distance between peak maximum and peak front at  $W_x$ . It is recommended by the FDA that tailing factor should be less than or equal to 2 (FDA, 1994).

$$TF = \frac{W_x}{2f} \quad \text{Equation 2-4}$$

#### 2.2.1.4.3 Theoretical plate number (N)

The theoretical plate number (N) is a measure of column efficiency and was determined using Equation 2-5 where  $t_w$  = peak width measured at baseline of the extrapolated straight sides to baseline. The FDA recommend N value greater than 2000 should be achieved (FDA, 1994).

$$N = 5.54 \times \left( \frac{t_R}{t_w} \right)^2 \quad \text{Equation 2-5}$$

#### 2.2.1.4.4 Injection repeatability

The injection repeatability was calculated by examining the changes in peak area between 10 injections of the same calibration standard (10  $\mu\text{g}/\text{mL}$ ). The percentage relative standard deviation (% RSD) was calculated to determine whether the precision criterion set by FDA had been met. The FDA recommends % RSD of less than or equal to 1 is achieved (FDA, 1994).

#### 2.2.1.4.5 Repeatability and intermediate precision

Precision of the HPLC assays (described in Table 2-2) were measured as both repeatability (intra-day) and intermediate precision (inter-day). Intra-day precision was determined using three different concentrations in the calibration range (at low, medium and high) of each drug prepared as described in Section 2.2.1.3. These solutions were analysed on the day of preparation (day 1, with n=6 injections

per solution). The inter-day precision was assessed by evaluating chromatographic response from independently prepared standards (at low, medium and high concentrations) on three separate days (n=3 replicates, n=6 injections of each sample solution). The percentage relative standard deviation (% RSD) values were calculated and then compared to limits set by the ICH (ICH, 2005)

#### **2.2.1.4.6 Accuracy**

Accuracy was determined using calibration standard solutions at three different concentrations (at low, medium and high range) for each drug (n=6 injections per solution) using the calibration plot mean concentration (MC) and comparing these results with theoretical concentration (TC) calculated based on the weighed drug value (Equation 2-6). This was compared to limits set by the FDA.

$$\% \text{ Accuracy} = \left( \frac{MC}{TC} \right) \times 100 \quad \text{Equation 2-6}$$

#### **2.2.1.4.7 Stability of calibration standard solutions**

The stability of calibration standard solutions for each API was determined using three different concentrations low, high and medium level (as described in Section 2.2.1.3.) stored at 4 °C. These samples were analysed by the relevant HPLC method (described in Table 2-2) at 0, 1, 2 and 4 weeks (n=3 replicates, n=6 injections of each sample solution). The change in peak area with respect to the freshly prepared standard (t= 0 h) was then measured.

#### **2.2.1.4.8 Forced degradation of minocycline**

It is important that the HPLC assay for minocycline can separate and resolve the associated degradation peaks, as tetracyclines are known to be notoriously unstable in aqueous solutions or solvents containing hydroxyl groups (Kubis, Dybek, & Krutul, 1987; Liang, Denton, & Bates, 1998). Stress testing of the drug can help identify likely degradation products, the stability of the molecule and also validate specificity of the analytical procedure (ICH, 2003). Thus, to demonstrate assay specificity, the chemical stability of minocycline was studied by checking for changes in HPLC chromatograms (number of peaks, retention time, peak area) after maintaining minocycline under

stressed environments described below. Forced degradation, was conducted on a stock solution containing 40 mg of minocycline in 100 mL methanol. Methanol was used for the stress testing, as this is the diluent that was used to prepare the HPLC standards. The following conditions were employed and are based on stress degradation studies of minocycline conducted by Jain *et al.* (2007). To 5 mL of the stock solution:

1. 5 mL of 2M HCl was added and the mixture was heated in a water bath for 2 hr at 80 °C (acid induced degradation).
2. 5 mL of 2M NaOH was added and the mixture was heated in a water bath for 2 hr at 80 °C (base induced degradation).
3. 5 mL of hydrogen peroxide (H<sub>2</sub>O<sub>2</sub>) (6 %, v/v) was added and the mixture was heated in a water bath for 2 hr at 80 °C (hydrogen peroxide induced degradation).
4. 5 mL of methanol was added and the solution was placed at room temperature for 2 hr (Control)

Each degradation study was performed in triplicate (n=3) and aliquots of the resultant solutions were transferred into 2 mL borosilicate amber HPLC vials and analysed using the minocycline HPLC assay described in Table 2-2.

#### **2.2.1.4.9 Cotton bud/syringe filter binding study**

Cotton buds and syringe filters are commonly used in Franz cell studies to remove excess formulation from the skin surface and to clean samples by removing any contaminants present in the solutions prior to HPLC analysis, respectively. However, there is potential for the API to bind to the cotton bud or syringe filter. This possibility was investigated by preparing low, high and medium level concentrations of calibration standards (as described in Section 2.2.1.3). The drug content of each standard was analysed soon after preparation (starting point). This value was quoted as 100%. For the syringe filter binding study, each concentration was filtered through individual 0.2 µm PTFE syringe filters six times and analysed by HPLC to determine any change in concentration from the starting

point. With regards to the cotton bud binding study, 5.0 mL of each standard concentration was placed into individual amber glass vials (n=3). Then a cotton bud was cut in half and one half was placed into each vial. Samples (200  $\mu$ L) were removed at 48 hr and analysed by the relevant HPLC method described in Table 2-2. The change in peak area with respect to the freshly prepared (t=0 h) calibration standards was then measured.

## **2.2.2 *In vitro* skin permeation method development**

### **2.2.2.1 Chemical stability studies in donor (CPEs) and receptor solutions**

To characterize the dependence of the chemical stability of APIs on the various investigated vehicles (CPEs), stability studies were performed at different temperature (4  $^{\circ}$ C, 37  $^{\circ}$ C, 50  $^{\circ}$ C and room temperature, 20  $^{\circ}$ C). All samples were stored in amber glass vials for up to 4 weeks. With regards to the receptor fluids, stability studies were conducted at 37  $^{\circ}$ C and 50  $^{\circ}$ C over 24 hr and up to 4 weeks at 4  $^{\circ}$ C. All the vials were filled to the top and wrapped with parafilm to prevent evaporation. The drug content of each sample was analysed at the day of preparation (starting point). This value was quoted as 100 %. Afterwards samples were taken at regular intervals, where a defined amount of formulation was dissolved to 10 mL in methanol and vortexed for approximately 1 minute. Samples were then filtered using 0.2  $\mu$ m PTFE syringe filters and then analysed by HPLC as described in Table 2-2.

### **2.2.2.2 Solubility studies in donor (CPEs) and receptor solutions**

Solubility studies were conducted by introducing an excess amount of API into individual amber glass vials. Then 1.0 mL of each solvent (CPEs) to be tested was added into each vial at room temperature (20  $^{\circ}$ C). For the investigated receptor fluids, 1.0 mL of each receptor fluid was added to each individual vial at 37  $^{\circ}$ C and 50  $^{\circ}$ C (such temperatures were set on water bath to ensure skin temperatures of 32  $^{\circ}$ C and 45  $^{\circ}$ C during the *in vitro* permeation studies). The suspensions were stirred for 24 hr at the stated temperatures, after which samples were removed and filtered using 0.2  $\mu$ m PTFE syringe filters. Where appropriate the filtrate was diluted with methanol and analysed via the respective HPLC method described in Table 2-2.

### 2.2.2.3 Method validation for API extraction from skin tissue

The chemical stability of each API in two extraction solutions methanol: water (90:10 % v/v) and methanol was investigated. The chemical stability studies were performed at room temperature (20 °C) over 72 hr following the method described in Section 2.2.2.1.

The efficiency of extracting each API from the various skin layers, scotch tape and cotton buds on completion of the *in vitro* drug permeation experiments was investigated for both extraction solutions. A piece of abdominal skin (with a surface area of approximately 1 cm<sup>2</sup>) was dosed with known concentration of each drug in methanol (100 µL of a 1 mg/mL solution) and allowed to dry over 4 hr. The residual formulation was removed following three separate cleaning phases. The first cleaning phase was conducted by carefully rolling a dry cotton bud over the skin upwards three times, then downwards three times, then clockwise and anticlockwise along the edges once. For the second cleaning phase, the first cleaning phase was repeated using a wet cotton bud soaked in methanol. For the third cleaning phase, the first phase was repeated using a dry cotton bud. All three buds were placed into an individual amber glass vial. To remove any remaining surface formulation two tape strips were taken and placed into a separate amber glass vial. This was followed by a further ten tape strips taken to remove the SC and were transferred into another glass vial. After this the skin was heated at 60 °C using a benchtop oven (Binder, Binder GmbH, Germany) for 2 min which allowed the epidermis to be separated from the dermis more easily. Then the epidermis and dermis were transferred into individual glass vials. Also, a vial containing scotch tape, a vial containing three cotton buds, a vial containing 2-octyl cyanoacrylate and an empty vial were also dosed with the same known concentration of API and allowed to dry for 4 hr (controls). Then 2.0 mL of the extraction solution was added to each vial. Each vial was then sonicated for 20 min before being transferred to a Stuart® roller mixer SRT9 (Cole-Parmer, UK) overnight (16-18 hr). All samples were then filtered using 0.2 µm syringe filters before being analysed by HPLC as described in Table 2-2. The extraction procedure was repeated until the drug content in the extracted samples were no longer detectable or below the LOQ. This experiment was performed in triplicate for each drug.

#### 2.2.2.4 Assay interference study

To determine the effect of skin endogenous compounds on the HPLC assay for each API, Franz cell diffusion experiments were performed using human abdominal skin. Skin was prepared as described in Section 2.2.2.6.

Defatted full thickness human abdominal was removed from the freezer and carefully cut to the appropriate size using a scalpel. Then the skin was clamped between the donor and the receptor compartment of the Franz cells, with the SC facing the donor compartment. The receptor chamber was then filled with the relevant receiver fluid for each drug, whereas the donor chamber was left empty. The Franz cells were placed in a water bath at  $37\text{ }^{\circ}\text{C} \pm 1\text{ }^{\circ}\text{C}$  to achieve skin surface temperature of  $32\text{ }^{\circ}\text{C} \pm 1\text{ }^{\circ}\text{C}$ . At 24 hr, all the receiver fluid was removed and analysed using the appropriate HPLC method as described in Table 2-2.

#### 2.2.2.5 Preparation of donor solutions

To prepare formulations for the infinite *in vitro* permeation experiments, excess drug was added to the required CPE(s) and stirred for 24 hr in a water bath (Grant Instruments, UK) at appropriate temperatures ( $37\text{ }^{\circ}\text{C}$  or  $50\text{ }^{\circ}\text{C}$ ) to produce saturated solutions which were used directly. Where the formulations were required for finite *in vitro* permeation studies, the solutions were filtered using  $0.2\text{ }\mu\text{m}$  syringe filters before being applied.

#### 2.2.2.6 Preparation of skin

Full thickness human abdominal and scalp skin were supplied by ZenBio (USA). Using a class 2 laminar flow cabinet skin samples were prepared carefully by removing subcutaneous fat using forceps and scalpel. With regards to the scalp skin the hairs were carefully removed using Gillette Fusion Proglide Styler® trimmer prior to defatting. Then the defatted skin samples were stored in a freezer at  $-20\text{ }^{\circ}\text{C}$  until they were ready for use. The abdominal skin donors were Caucasian females and the scalp skin donors were Caucasian males.

## 2.3 Results and Discussion

### 2.3.1 HPLC method validation

#### 2.3.1.1 Calibration curve (linearity, LOD and LOQ)

Typical examples of HPLC chromatograms (intensity (mV) against time (min)) under the chromatographic conditions (described in Table 2-2) for all three penetrants are shown in Figure 2-1 (a-c). Under these chromatographic conditions the retention times for minocycline, isotretinoin and finasteride were: 9.8, 10.2 and 10.3 min respectively.

To validate the suitability of the HPLC methods: linearity, LOD, LOQ, precision and accuracy were measured. Linearity was investigated across the concentration range tested by constructing calibration curves (shown in Figure 2-2 (a-c)) by plotting the response (peak area) against concentration of the standards for each penetrant. These plots yielded correlation coefficient ( $R^2$ ) values exceeding the recommended limit of 0.9990 (ICH, 2005). In the concentration ranges investigated the data shows the direct proportional relationship between response (peak area) and the concentration of the penetrant present in solution.

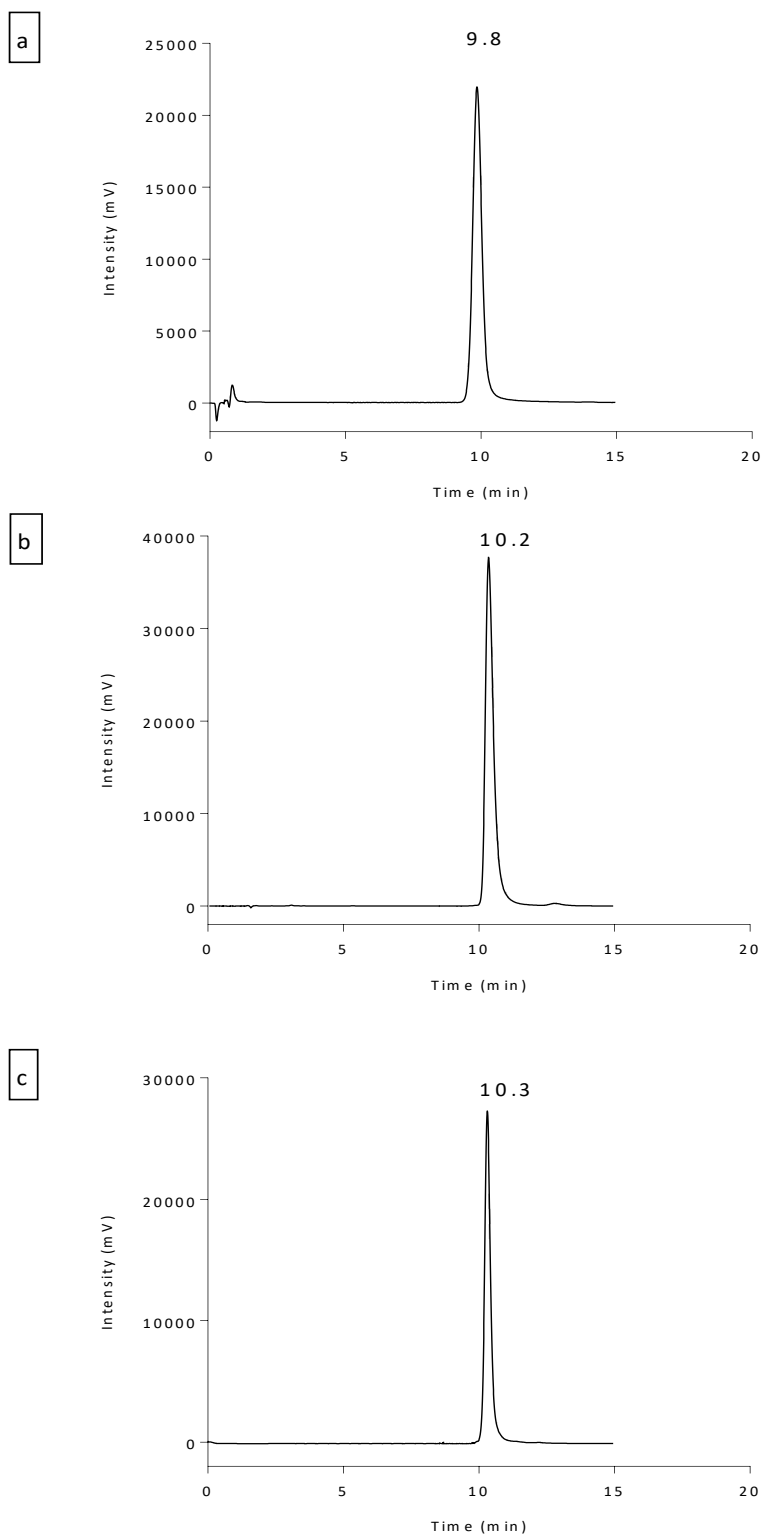


**Figure 2-1: HPLC chromatograms of (a) minocycline (20 µg/mL) calibration standard (b) isotretinoin (10 µg/mL) calibration standard and (c) finasteride (10 µg/mL) calibration standard.**

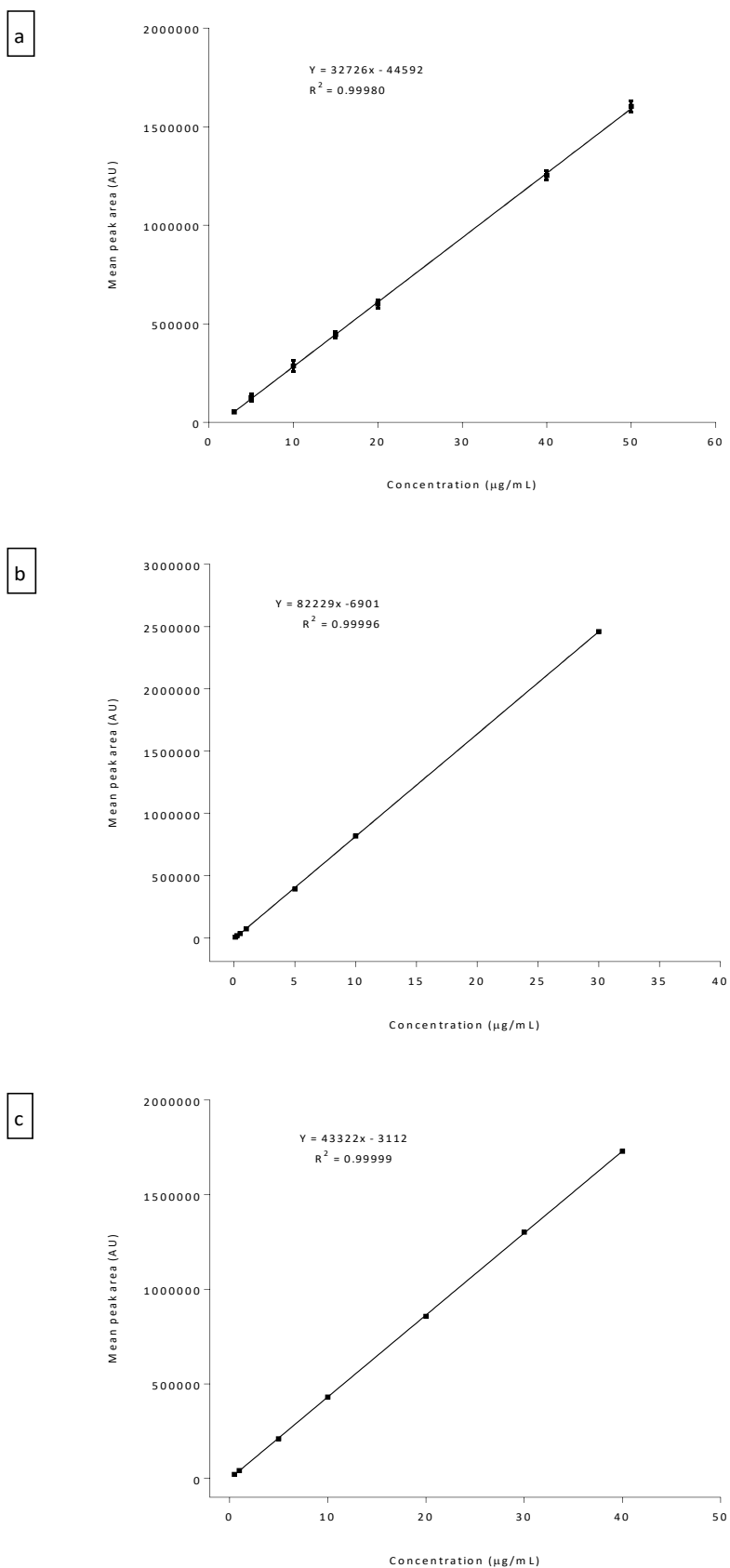


Figure 2-2: HPLC calibration curves showing mean peak areas as function of concentration of (a) minocycline (b) isotretinoin (c) finasteride in methanol ( $\pm$  S.D., n=6 injections).

The LOD of an analytical method is the lowest amount of analyte in a sample that can be reliably detected but not necessarily quantified as an exact value. Whereas, the LOQ is the lowest amount of analyte in a sample, which can be quantitatively determined with a suitable level of precision and accuracy (ICH, 2005). Both LOD and LOQ were calculated using Equation 2-1 and Equation 2-2, respectively. The LOD and LOQ values for minocycline, isotretinoin and finasteride are reported in Table 2-3.

### 2.3.1.2 System suitability

System suitability parameters such as capacity factor ( $K'$ ), tailing factor (TF), the number of theoretical plates (N) and injection repeatability were determined to evaluate the performance and effectiveness of the HPLC methods (Shabir, 2003) described in Table 2-2. Capacity factor ( $K'$ ) was calculated using Equation 2-3. Typically, the peaks associated with the three drugs were well resolved from the solvent peaks giving  $K'$  values greater than 2 (reported in Table 2-3) and meets the recommended acceptance criterion set by the FDA (FDA, 1994).

Tailing factor (TF) was calculated using Equation 2-4. This parameter highlights the significance of peak symmetry, as the accuracy of quantification decreases with an increase in peak tailing due to difficulties in determining where the peak ends, which in turn can cause errors in peak integration and therefore inaccurate quantification. The FDA recommend a value of T less than 2 should be obtained (FDA, 1994). For all three drugs, T was within the recommended limits (Table 2-3).

The theoretical plate number (N) is a measure of column efficiency and should be  $> 2000$  (FDA, 1994). Therefore, the greater the number of plates, the better the separation that is achieved due to reduced peak broadening (Moldoveanu & David, 2013). For all three methods N was found to be greater than 2000, indicating high column efficiency (Table 2-3).

**Table 2-3: Results from system suitability tests and validation of the HPLC methods developed to determine minocycline, isotretinoin and finasteride.**

	Active pharmaceutical ingredients			
	Minocycline	Isotretinoin	Finasteride	limits
<b>Capacity Factor (K')</b>	5.24	6.05	6.23	K' > 2
<b>Tailing Factor (TF)</b>	1.02	1.40	1.23	F ≤ 2
<b>Theoretical Plate Number (N)</b>	5182.57	5249.11	11727.00	N > 2000
<b>Injection Repeatability (% RSD)</b>	0.76	0.10	0.15	% RSD < 1%
<b>Linearity (R<sup>2</sup>)</b>	0.99980	0.99996	0.99999	R <sup>2</sup> > 0.9990
<b>Limit of detection (µg/mL)</b>	0.21	0.24	0.32	-
<b>Limit of quantification (µg/mL)</b>	0.64	0.73	0.97	-
<b>Repeatability</b>				
(% RSD at low, medium, high concentrations)	0.42, 0.38, 0.46	0.08, 0.13, 0.36	0.26, 0.04, 0.12	% RSD < 2%
<b>Intermediate precision</b>				
(% RSD at low, medium, high concentrations)	0.30, 1.39, 1.72	0.13, 0.68, 0.59	0.52, 0.46, 0.54	% RSD < 2%
<b>Accuracy</b>				
(% RSD at low, medium, high concentrations)	100.1%, 100.0%, 100.1%	100.7%, 98.9%, 99.1%	98.1%, 98.6%, 98.3%	100 ± 2 %

The injection repeatability was investigated by measuring the changes in peak area between 10 injections of one calibration standard (of each drug) at a concentration of 10 µg/mL (Section 2.2.1.3) followed by calculation of the % RSD. This test indicates the performance of the HPLC instrument under the chromatographic conditions employed for each method (described in Table 2-2). The

measured % RSD was within the precision limits set by the FDA ( $\leq 1\%$ ) (FDA, 1994), thus showing the good precision of the analytical instruments used.

#### **2.3.1.3 Repeatability and intermediate precision**

Precision of the HPLC methods were measured as both repeatability (intra-day) and intermediate precision (inter-day) by assaying three different concentrations of each penetrant (at low, medium and high concentration). Intra-day repeatability expresses the precision of an analytical method under the same operating conditions over a short interval of time, whereas inter-day intermediate precision provides information on the effects of random events (preparing standards on different days or different analyst) on the precision of the analytical method (Shabir, 2003). The acceptance criteria for the % RSD for both precision tests should be less than 2% (ICH, 2005). The measured % RSD values for all three HPLC methods are shown in Table 2-3 and were within the limits recommended by the ICH (% RSD < 2%), which indicates a suitable level of precision for all three HPLC methods.

#### **2.3.1.4 Accuracy**

The accuracy of an analytical procedure expresses the closeness of agreement between the experimentally determined concentration and the theoretical concentration calculated based on the weighed drug value (Equation 2-6). Accuracy is usually expressed as the % recovery and was determined using calibration standard solutions at three different concentrations (at low, middle and high range). The FDA reviewer guidance on validation of chromatographic methods advocate the mean recovery of the drug should be within  $100 \pm 2\%$  (FDA, 1994). The accuracy test results for all three methods is presented in Table 2-3, which demonstrates the accuracy of all three methods, as values fall within the acceptance criteria set by the FDA.

#### **2.3.1.5 Stability of calibration standard solutions**

It is important to determine the conditions and period of time analytical solutions remain stable. This is particularly important when delays (e.g. instrument breakdowns) occur during HPLC analysis (Shabir, 2003). The stability of calibration standard solutions was determined by preparing three

different standard concentrations at low, medium and high level and stored at 4 °C for four weeks. These samples were analysed by the relevant HPLC method (presented in Table 2-2) at 0, 1, 2 and 4 weeks (Table 2-4).

**Table 2-4: Stability of minocycline, isotretinoin and finasteride in methanol (calibration standard diluent) stored at 4°C for up to 4 weeks (n=6 injections of 10 µg/mL standard for each drug).**

Drug (µg/mL)	% Peak Area			
	t=0	t=1 week	t=2 weeks	t=4 weeks
Minocycline	100.00	99.10	98.47	95.52
Isotretinoin	100.00	99.79	99.23	98.68
Finasteride	100.00	99.67	99.58	99.21

The data in Table 2-4 shows the stability of 10 µg/mL standard solution (medium level concentration) for each analyte, when stored at 4 °C. Analysis of this data indicates that isotretinoin and finasteride samples were stable under the storage conditions selected with recovery values of  $\geq 98\%$  over the four-week period (Table 2-4). Recovery of minocycline was found to be 95.52 % at four weeks. Therefore, using these standard solutions could lead to inaccuracies in the quantification of minocycline. To overcome this, standard solutions for minocycline should be used for analysis within 2 weeks of preparation when stored at 4°C as recovery values of  $\geq 98\%$  were achieved within this period of time. All the other concentration ranges investigated (low and high-level concentrations) for all three analytes showed similar trends in stability over the four-week period at 4 °C (data not shown).

### 2.3.1.6 Forced degradation of minocycline

The specificity of the HPLC method for minocycline was examined by exposing the analyte to the stress conditions (shown in Table 2-5) to determine whether degradation peaks interfere with the retention time of minocycline.

**Table 2-5: The effect of different stress conditions on minocycline stability and assay specificity (n=3).**

Stress conditions	Recovery (% $\pm$ S.D., n=3)	Additional peaks retention times (min)
None (control sample)	99.74 $\pm$ 0.18	4.8
2 M HCl, 80 °C (2h)	13.29 $\pm$ 0.14	1.6, 2.6, 5.0, 6.6, 11.4, 13.2
2 M NaOH, 80 °C (2h)	48.55 $\pm$ 0.53	1.4, 1.5, 2.4, 3.6, 3.8, 5.0, 6.5, 8.2, 12.5
H <sub>2</sub> O <sub>2</sub> , 6 % v/v, 80 °C (2h)	2.47 $\pm$ 0.17	1.6, 2.4, 3.5, 4.2, 4.9, 6.0, 7.6, 8.3, 12.4, 13.1, 14.4

Minocycline was affected differently by exposure to the various stress conditions investigated. The % recovery was lowest for hydrogen peroxide, followed by hydrochloric acid and sodium hydroxide respectively (as shown in Table 2-5). Tetracyclines are known to be oxidatively unstable and often change colour over time from yellow to brown (Liang et al., 1998). Unsurprisingly therefore this data indicates that minocycline is more susceptible to hydrogen peroxide induced degradation (oxidation) compared to acid and base induced degradation. Under the stress conditions investigated, HPLC chromatograms with extra peaks compared to the control sample were produced as shown in Figure 2-3 and the retention times of these additional peaks are listed in Table 2-5. From Figure 2-3, the degradation products did not interfere with the minocycline peak at 9.8 min, which was well resolved.

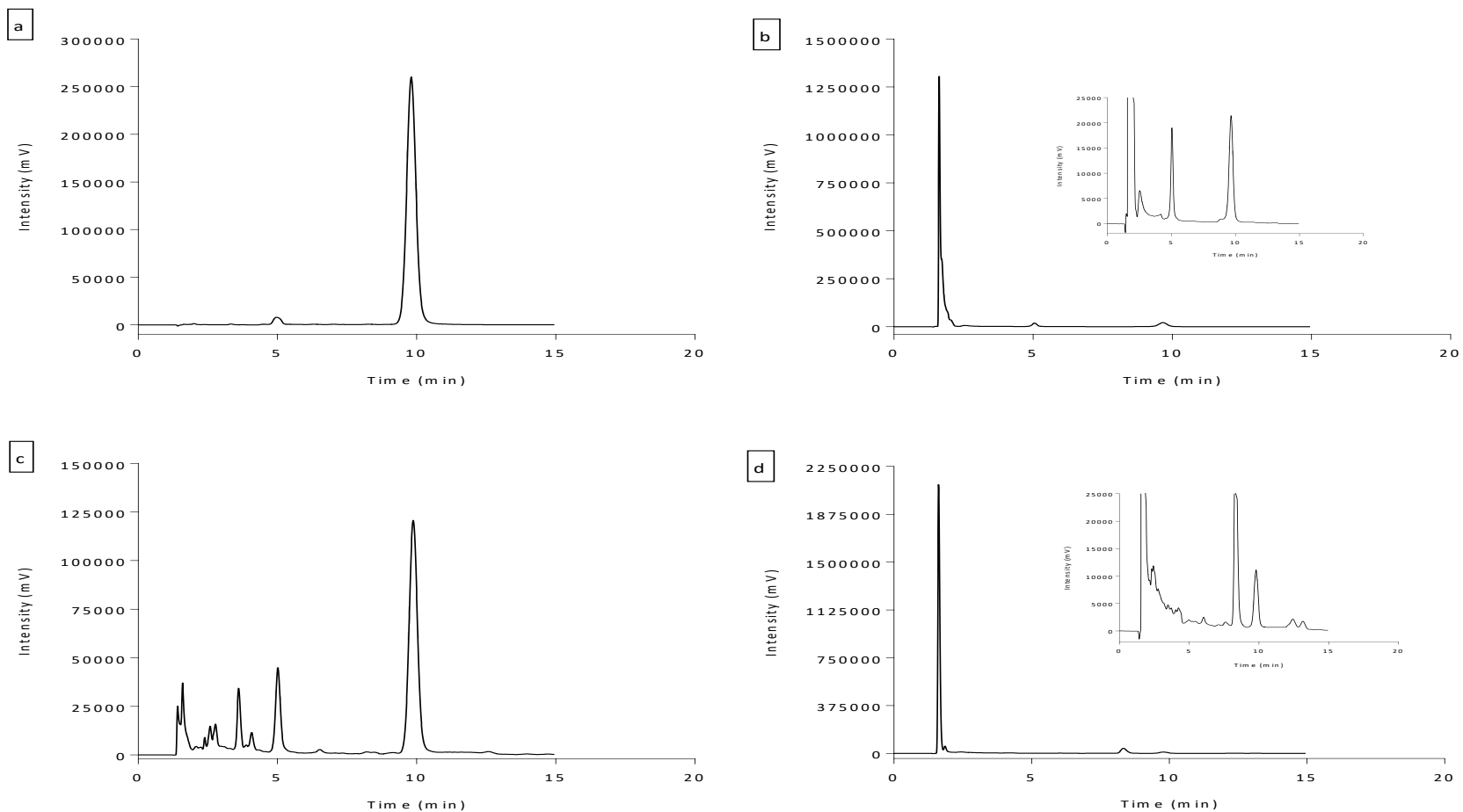


Figure 2-3: HPLC Chromatograms of (a) minocycline (200  $\mu\text{g/mL}$ ) control solution (b) minocycline exposed to 2 M HCl at 80  $^{\circ}\text{C}$  for 2 hr, (c) minocycline exposed to 2 M NaOH at 80  $^{\circ}\text{C}$  for 2 hr and (d) minocycline exposed to  $\text{H}_2\text{O}_2$  (6 % v/v) at 80  $^{\circ}\text{C}$  for 2 hr. All solutions placed under stress conditions contained 200  $\mu\text{g/mL}$  minocycline and were produced from a stock solution with nominal concentration of 400  $\mu\text{g/mL}$ .

### 2.3.1.7 Cotton bud/syringe filter binding study

This study was set up to investigate the potential binding of the analytes to cotton buds (used in skin penetration studies to remove excess formulation from the skin) and the PTFE syringe filters used as part of sample preparation. The binding of the analyte to the cotton bud or syringe filter can lead to low recoveries of the assay. Also, the use of organic solvents can sometimes extract contaminants out of the cotton bud or syringe filter, which could potentially interfere with the determination of the analyte. In this study, no extra peaks were observed in samples incubated with cotton buds. Similarly, the filtered samples compared to the un-filtered samples showed no extra peaks (data not shown). Data from the analyte - cotton bud binding experiment showed recovery values  $\geq 97\%$  over 48 hr time period (Table 2-6), implying analyte binding to the cotton buds was negligible.

**Table 2-6: Analyte-Cotton bud binding study after 48 hr incubation of cotton buds in different standard concentrations (% recovery  $\pm$  S.D., n=3).**

Standard concentration ( $\mu\text{g/mL}$ )	Minocycline	Isotretinoin	Finasteride
5	98.21 $\pm$ 1.24	99.34 $\pm$ 0.58	101.87 $\pm$ 3.98
10	97.39 $\pm$ 0.78	99.08 $\pm$ 0.32	99.66 $\pm$ 0.64
30/40	99.46 $\pm$ 0.49 <sup>b</sup>	99.22 $\pm$ 0.10 <sup>a</sup>	101.37 $\pm$ 1.86 <sup>a</sup>

<sup>a</sup> indicates recovery for 30  $\mu\text{g/mL}$  standard concentration, <sup>b</sup> indicates recovery for 40  $\mu\text{g/mL}$  standard concentration.

Analyte – PTFE syringe filter binding was investigated by comparing filtered and un-filtered samples for each analyte. The analyte – PTFE syringe filter binding experiment yielded recovery values  $\geq 99\%$  for the range of concentrations investigated (Table 2-7), indicating analyte binding to PTFE syringe filters was also negligible.

**Table 2-7: Analyte - PTFE syringe filter binding study, with each standard concentration filtered through 0.2 µm PTFE syringe filter six times (% recovery ± S.D., n=3).**

Standard concentration (µg/mL)	Minocycline	Isotretinoin	Finasteride
5	102.07 ± 1.34	102.01 ± 1.76	100.36 ± 0.84
10	100.00 ± 0.55	99.18 ± 0.65	100.94 ± 1.45
30/40	100.18 ± 0.45 <sup>b</sup>	99.61 ± 0.89 <sup>a</sup>	101.94 ± 0.99 <sup>a</sup>

<sup>a</sup> indicates recovery for 30 µg/mL standard concentration, <sup>b</sup> indicates recovery for 40 µg/mL standard concentration.

## 2.3.2 *In vitro* skin permeation method development

### 2.3.2.1 Chemical stability studies in donor (CPEs)/receptor fluids

The chemical stability of each drug in various donor and receptor fluids was investigated at 37 °C and 50 °C for 24 hr as these conditions were employed in the skin permeation experiments. Whereas, studies at 4 °C were performed for only receptors fluids and were conducted for a longer period (up to 4 weeks) to determine if the drugs remain stable under this storage condition, which would be employed if delays occurred during HPLC analysis.

The drug content of each sample was analysed at the day of preparation and quoted as 100%. Then samples were taken at 24 hr and 4 weeks (only for receptor fluids stored at 4°C), where a defined amount of formulation was dissolved to 10 mL in methanol and vortexed for approximately 1 minute. Samples were then filtered using 0.2 µm PTFE syringe filters prior to analysis by the appropriate HPLC method (described in Table 2-2). The results for the 24 hr stability study for the three drugs in various donor solutions/CPEs at 37 °C and 50 °C are shown in Figure 2-4. These CPEs were selected because they can exhibit a wide range of excipient effects (e.g. improving drug solubility and aesthetic traits such as odour, colour and texture) in addition to their primary function of participating in skin permeabilization (Karande & Mitragotri, 2009). Also, some of these enhancers such as dimethyl isosorbide (DMI), isopropyl myristate (IPM) and Transcutol® P (TP) have been shown to be effective at lowering the melting point of sebum (Motwani et al., 2004).

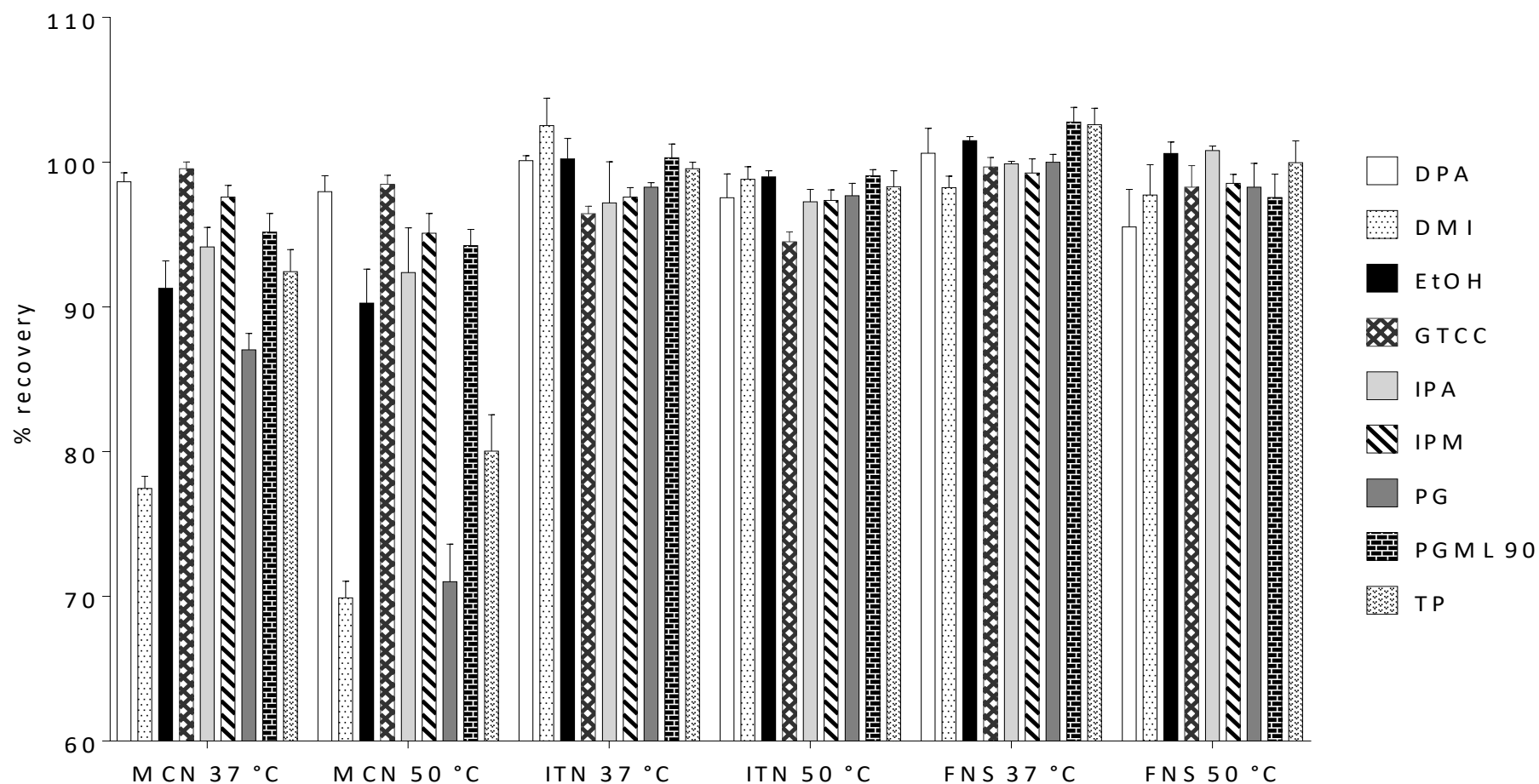


Figure 2-4: Stability of minocycline (MCN), isotretinoin (ITN) and finasteride (FNS) in various pharmaceutical vehicles at 37 °C and 50 °C for 24 hr. The vehicles investigated are Diisopropyl adipate (DPA), Dimethyl isorbidide (DMI), ethanol (EtOH), Crodamol™ GTCC (GTCC), Isopropyl alcohol (IPA), Isopropyl myristate (IPM), Propylene glycol (PG), Propylene glycol monolaurate 90 (PGML 90) and Transcutol® P (TP). Data represent mean + S.D. (n=3).

Therefore, they may act synergistically with heat ( $\leq 45\text{ }^{\circ}\text{C}$ ) to reduce sebum viscosity and alter its solubility parameter so that drug uptake into hair follicles is more favourable. These properties could potentially facilitate and promote the delivery of higher drug concentrations to the hair follicles and their associated sebaceous glands to produce localised drug delivery.

Overall, isotretinoin and finasteride were found to be more stable than minocycline in both the hydrophilic and hydrophobic vehicles investigated under the experimental conditions employed, with  $> 97\%$  recovery recorded for both drugs.

Minocycline was relatively more stable in the hydrophobic vehicles (GTCC, DPA, IPM and PGML 90) compared to hydrophilic vehicles with  $\geq 95\%$  recovery achieved at both temperatures; this is in good agreement with the literature as oil based formulations have been shown to improve minocycline stability (Ousler III, Chapin, Abelson, & Shapiro, 2012; Salman, Angel, & Swaminathan, 2014). In the hydrophilic vehicles (EtOH, IPA, PG and TP) at  $37\text{ }^{\circ}\text{C}$ , minocycline recovery ranged from  $87\%$  to  $94\%$ , with the highest recovery recorded for IPA ( $94.15 \pm 1.34\%$ ). Storage at a higher temperature ( $50\text{ }^{\circ}\text{C}$ ) resulted in further decline in the % minocycline recovered from PG ( $71.01 \pm 2.59\%$ ), TP ( $80.04 \pm 2.51\%$ ), EtOH ( $90.26 \pm 2.35\%$ ) and IPA ( $92.37 \pm 3.10\%$ ). This reduced chemical stability of minocycline was expected in hydrophilic vehicles. This is because minocycline (as with other tetracyclines) is notorious for its poor stability in aqueous/hydrophilic solutions (Ritter & Suffern, 1992). In such conditions, minocycline undergoes reversible epimerisation in solution to the less active 4-epiminocycline, with the rate of epimerisation increased with pH levels below 5.0 and higher temperatures (Pawelczyk & Matlak, 1982). Additionally, above pH 5.0 minocycline undergoes oxidation to produce degradation products showing little or no therapeutic activity (Pawelczyk & Matlak, 1982; Salman et al., 2014). Therefore, an attempt was made to stabilise minocycline under the experimental conditions employed in the skin permeation experiments so that accurate and reproducible results could be produced.

Thus, the influence of magnesium chloride hexahydrate on minocycline stability in hydrophilic vehicles such as EtOH, IPA, PG and TP at the conditions employed in the skin permeation experiment ( $37\text{ }^{\circ}\text{C}$

and 50 °C for 24 hr) was investigated. This was determined using 0.05 % w/v minocycline in hydrophilic vehicles containing 0.05 % w/v magnesium chloride. These concentrations were selected to ensure the solubility of both magnesium and minocycline was not an issue in the different solvents. Also, at these concentrations the molar ratio of magnesium-minocycline is 2.4:1, which means magnesium is in molar excess relative to minocycline.

From the literature, the tetracycline structure contains many potential metal-binding sites: oxygen atoms at the C10-C12 keto-phenol system, the enolic oxygen at C3 and nitrogen atoms at C4 and the carboxamide group in ring A (Arias et al., 2016; Doluisio & Martin, 1963; Sakaguchi, Toma, Yoshida, Omura, & Takasu, 1958; Schmitt & Schneider, 2000). In particular, the oxygen atoms in C11 and C12 were observed to be very important functional groups to stabilise with magnesium (Jin et al., 2007; Piccariello, 2013; Wessels, Ford, Szymczak, & Schneider, 1998). In the literature, stoichiometries of 1:1, 1:2 and 2:1 magnesium-tetracycline complexes have been reported (Jin et al., 2007; Piccariello, 2013; Wessels et al., 1998). Based on these stoichiometries, the following structures of magnesium-minocycline complexes (shown in Figure 2-5) are proposed.

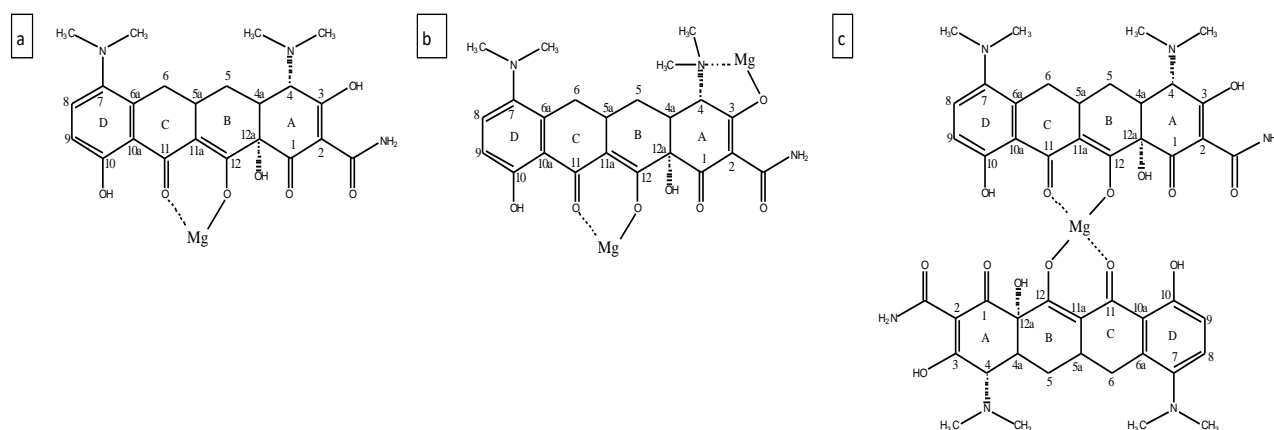


**Figure 2-5: proposed stoichiometry and structure of magnesium ( $Mg^{2+}$ )-minocycline complexes (a) 1:1 magnesium-minocycline (b) 2:1 magnesium-minocycline (c) 1:2 magnesium-minocycline. These anticipated structures are based on reported stoichiometries of magnesium with various tetracyclines in the literature (Jin et al., 2007; Piccariello, 2013; Schmitt & Schneider, 2000; Wessels et al., 1998).**

Currently, crystal or solution structures of Magnesium (or other alkaline earth metal) and tetracycline complexes are not available that could address the differences in stoichiometry or probable binding sites reported in the literature. A possible explanation for this disagreement may be the differences in the polarity and pH of the solvent systems employed since tetracycline may exist in different tautomers and conformations, which may influence the interaction/stoichiometry between the metal ions and tetracycline.

Interestingly, the coordination of magnesium to tetracyclines has been reported to be important for the antibacterial activity of tetracyclines in biological systems. This is because tetracyclines are thought to bind to the bacterial 30S ribosomal subunit as magnesium-tetracycline complex leading to inhibition of protein synthesis (Orth, Saenger, & Hinrichs, 1999; White & Cantor, 1971). However, despite the importance of metal ion interaction with tetracycline to explain its behaviour in biological systems, these interactions are not yet fully understood (Schmitt & Schneider, 2000).

Data from the magnesium-minocycline stability study showed recovery values  $\geq 94\%$  over both the temperatures studied implying that magnesium chloride improved the stability of minocycline in the vehicles tested (Figure 2-6).

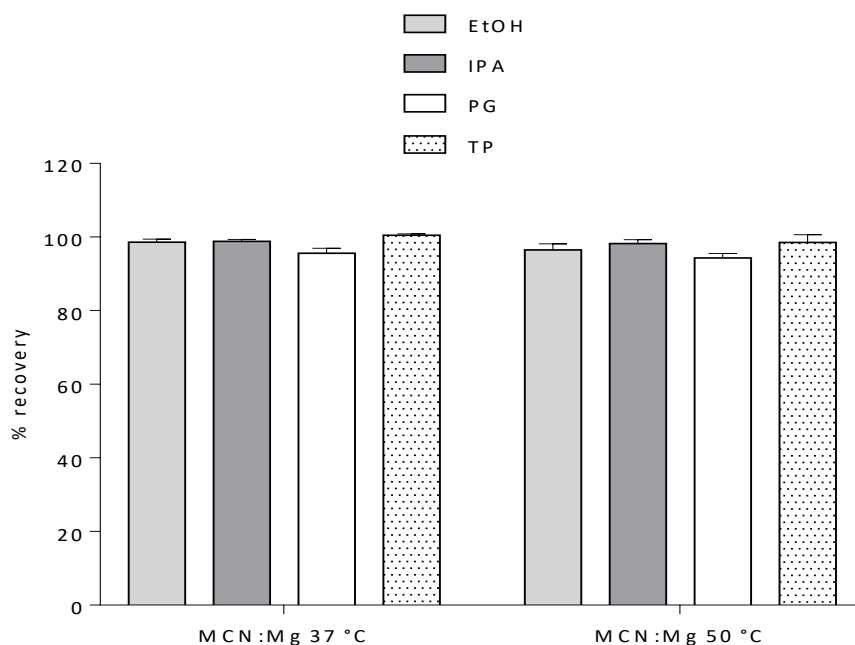


**Figure 2-6: Stability of 0.05 % w/v minocycline (MCN) in hydrophilic vehicles ethanol (EtOH), isopropyl alcohol (IPA), propylene glycol (PG) and Transcutol® P (TP) containing 0.05 % w/v magnesium chloride (Mg) at 37 °C and 50 °C for 24 hr. Data represent mean + S.D. (n=3).**

The greatest improvement in minocycline stability in the presence of magnesium chloride was observed for propylene glycol at 37 °C ( $95.57 \pm 1.40\%$ ) and 50 °C ( $94.30 \pm 1.23\%$ ). This corresponded to 8 % and 23 % increase in the % minocycline recovered at 37 °C and 50 °C respectively, compared to propylene glycol samples without magnesium (Figure 2-6). Improved minocycline stability in polyhydric alcohols containing magnesium chloride was previously reported in the literature (Hasegawa, Takatsuki, Takatsuki, & Osaka, 1987; Melvin, Noseworthy, & Spiegel, 1962). Magnesium is thought to stabilise minocycline by forming a complex, in which the conformational structure of minocycline becomes more rigid, thus preventing or reducing epimerisation (Novák-Pékli, el-Hadi Mesbah, & Pethó, 1996; Piccariello, 2013; Wessels et al., 1998). To further explore if magnesium chloride could provide longer periods of minocycline stabilisation, a stability study was conducted at 25 °C for four weeks (Table 2-8).

**Table 2-8: Stability of 0.05 % w/v minocycline in hydrophilic vehicles ethanol (EtOH), isopropyl alcohol (IPA), propylene glycol (PG) and Transcutol® P (TP) containing varying magnesium chloride concentrations at 25 °C for 4 weeks. Data represent mean  $\pm$  range (n= 3 injections).**

Vehicle	Magnesium chloride hexahydrate concentration (% w/v)					
	0.00	0.025	0.05	0.10	0.25	0.50
EtOH	60.02 $\pm$ 0.039	94.12 $\pm$ 0.004	94.82 $\pm$ 0.005	94.82 $\pm$ 0.001	92.49 $\pm$ 0.004	71.01 $\pm$ 0.002
IPA	42.96 $\pm$ 0.004	97.24 $\pm$ 0.028	97.83 $\pm$ 0.003	95.08 $\pm$ 0.001	91.82 $\pm$ 0.005	89.99 $\pm$ 0.001
PG	54.99 $\pm$ 0.006	96.70 $\pm$ 0.002	97.39 $\pm$ 0.003	96.07 $\pm$ 0.007	96.86 $\pm$ 0.009	82.47 $\pm$ 0.007
TP	53.21 $\pm$ 0.004	94.02 $\pm$ 0.001	97.10 $\pm$ 0.026	92.87 $\pm$ 0.002	96.96 $\pm$ 0.015	82.13 $\pm$ 0.002

Overall, the presence of magnesium chloride was able to improve minocycline stability in hydrophilic vehicles such as ethanol, isopropyl alcohol, propylene glycol and Transcutol® P markedly over four weeks at 25 °C as shown in Table 2-8. The data shows that the optimum effect was achieved with 0.05 % w/v magnesium chloride, with further increase in magnesium chloride leading to reduced minocycline recovery. A possible explanation for this trend is that the use of magnesium chloride hexahydrate produced solutions with greater water content as the concentration of magnesium was increased, with the increased water concentrations in the solutions triggering minocycline degradation possibly via oxidation. This is supported by the observation that solutions containing 0.5 % w/v magnesium chloride hexahydrate were darker in colour compared to the other solutions containing lower concentrations of magnesium chloride hexahydrate. To overcome this issue magnesium chloride (anhydrous) could be used to ensure the presence of water in the solutions is minimal. Nevertheless, the addition of magnesium chloride hexahydrate to the hydrophilic vehicles allowed the goal of stabilising minocycline under the conditions employed in the skin permeation experiments to be met.

The stability of minocycline in the different receptor fluids at 37 °C and 50 °C for 24 hr are shown in Figure 2-7, whereas the stability of isotretinoin and finasteride are presented in Figure 2-8 under the same conditions.

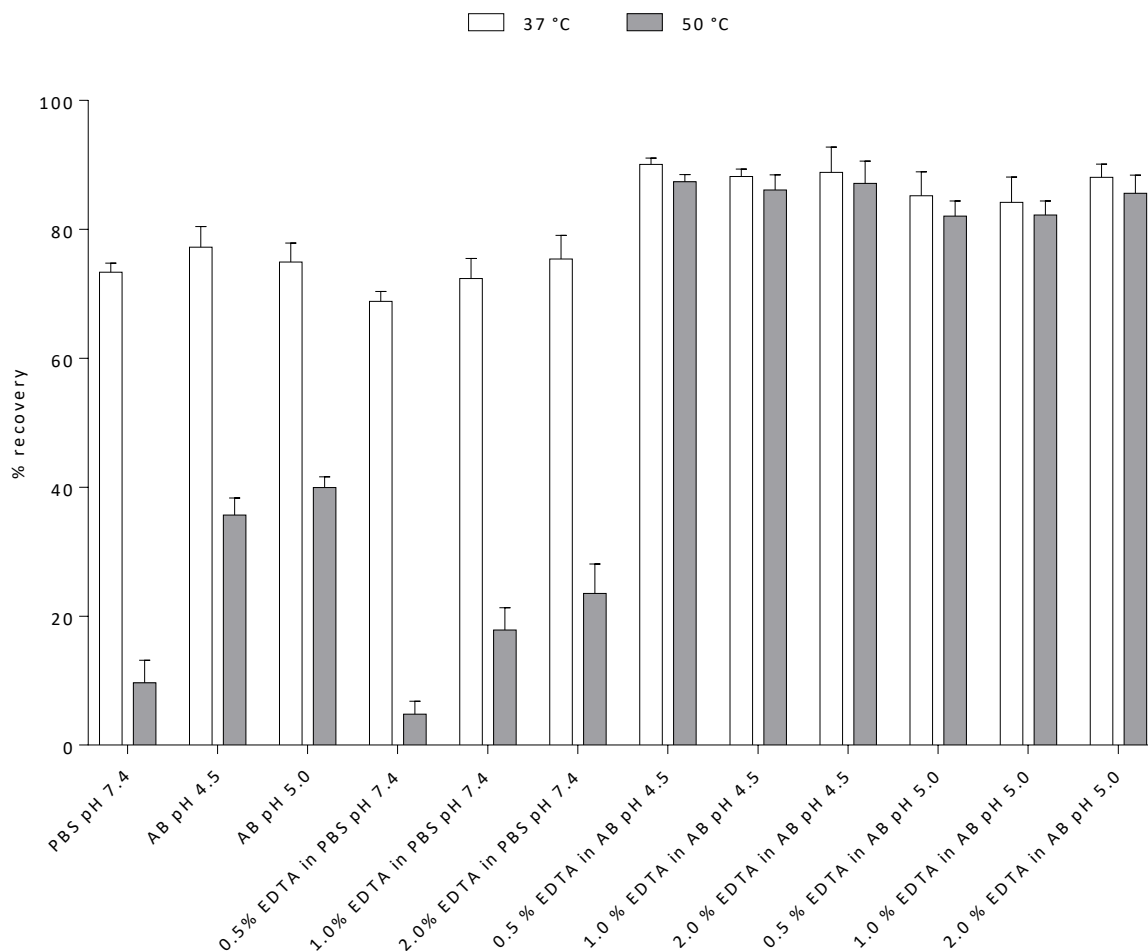


**Figure 2-7: Stability of minocycline in 0.15M PBS pH 7.4 and 0.5M acetate buffer(AB) pH 4.5 & pH 5.0 with varying EDTA content at 37 °C and 50 °C for 24 hr. Data are expressed as mean + S.D. (n=3). The concentration of EDTA is represented as % w/v.**

As mentioned previously, minocycline (as with other tetracyclines) degrades via epimerisation and oxidation. Oxidation of tetracyclines is associated with a change in colour from yellow to dark orange/brown/black. The rate and extent of degradation is influenced by moisture, light, pH and temperature. Also, the instability of minocycline in aqueous solutions has been shown to be accelerated by the presence of phosphate and citrate ions, whilst acetate ions were shown to impact minocycline stability in aqueous solutions less negatively (Pawelczyk & Matlak, 1982). Various stabilisers such as sodium metabisulfite, sodium sulphite and EDTA have been incorporated into minocycline solutions in an attempt to prevent its oxidation (Pawelczyk & Matlak, 1982).

In this study, acetate buffers pH 4.5 and 5.0 along with PBS pH 7.4 containing various concentrations of EDTA (0 - 2 %) were investigated as potential receptor fluids. In this study, EDTA was employed as an antioxidant. This data is presented in Figure 2-7. At 37 °C the maximum minocycline stability was recorded for acetate buffer pH 4.5 ( $77.26 \pm 3.16$  %) for solutions without EDTA. Increasing the temperature resulted in further reduction in minocycline stability, with recovery values of  $9.67 \pm 3.51$  %,  $35.68 \pm 2.64$  % and  $39.97 \pm 1.63$  % for PBS pH 7.4, acetate buffer pH 4.5 and acetate buffer pH 5.0, respectively. This level of stability was not sufficient for a potential receptor fluid. Also, for these samples, storage at 50 °C produced solutions with a black- dark brown colour, indicating that oxidation may have occurred. In PBS, the presence of EDTA did not have the desired effect, as the % minocycline recovered was lower compared to solutions without EDTA at both temperatures investigated. The reason for this is unclear, but a potential explanation is that the EDTA could have accelerated oxidation of minocycline in the presence of phosphate ions. On the other hand, acetate buffer solutions containing EDTA showed higher drug recovery compared to all the other receptor solutions investigated, with 0.5 % EDTA in acetate buffer pH 4.5 producing the maximum recoveries of  $90.08 \pm 0.99$  % and  $87.39 \pm 1.10$  % at 37 °C and 50 °C respectively. The stability of minocycline in the other EDTA containing acetate buffer solutions ranged from 82 % to 88 % across the temperatures investigated, with the lower recoveries occurring at 50 °C. Interestingly, it was observed that these solutions remained yellow (no colour change) at both temperatures investigated, suggesting that degradation may have mainly occurred via epimerisation, with the higher temperature shifting the equilibrium so that more of the epimer is formed. Hence, the % minocycline recovery was lower at 50 °C compared to 37 °C.

Therefore, 0.5 % EDTA in acetate buffer pH 4.5 was selected as the most appropriate receptor fluid for minocycline skin permeation experiments because it promoted drug stability, showed good solubility and contained the lowest concentration of EDTA.

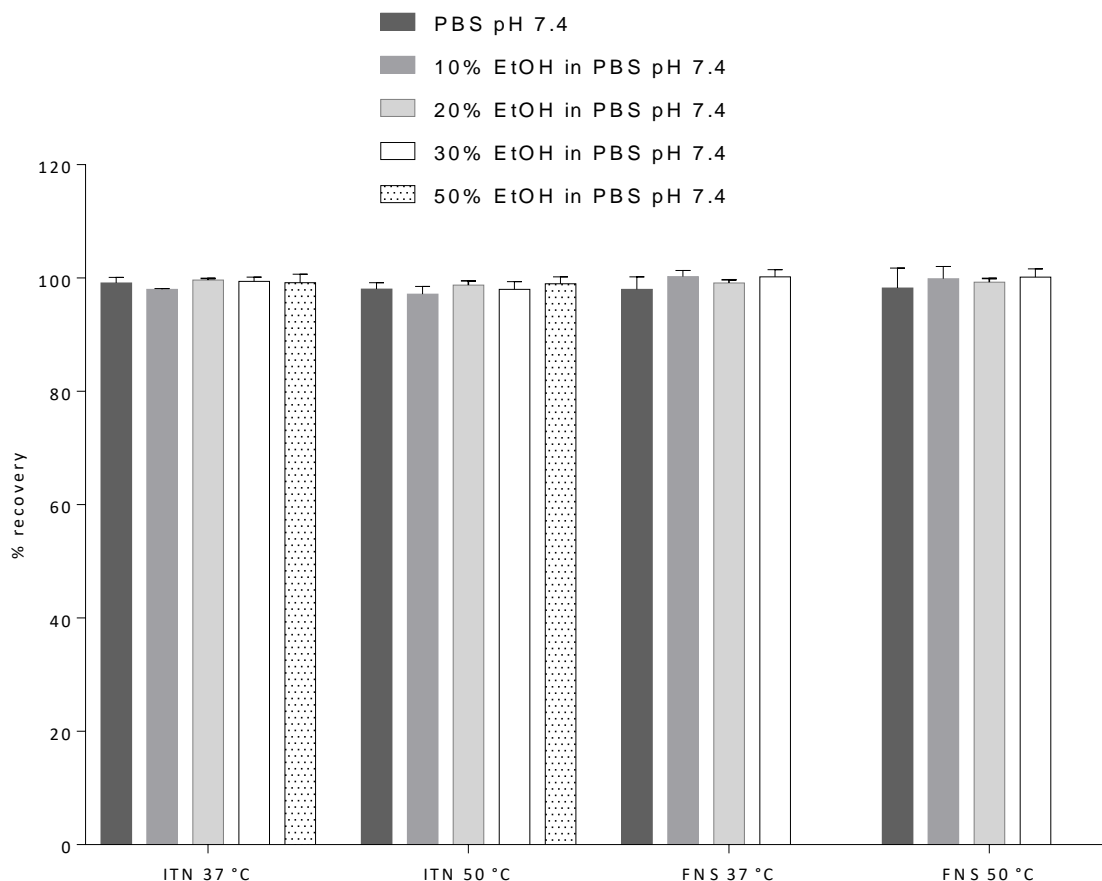


**Figure 2-8: Stability of isotretinoin (ITN) and finasteride (FNS) in 0.15M PBS pH 7.4 receptor fluids with varying ethanol (EtOH) content at 37 °C and 50 °C. Data represents mean  $\pm$  S.D. (n=3). Stability of FNS in EtOH-PBS (50:50 % v/v) was not determined.**

The stability of both isotretinoin (ITN) and finasteride (FNS) in different receptor solutions investigated at both 37 °C and 50 °C is shown in Figure 2-8. Both isotretinoin and finasteride demonstrated suitable stability in all the receptor fluids examined, with recovery values of  $\geq 98\%$  at both temperatures investigated. For isotretinoin, Ethanol-PBS (50:50 % v/v) was chosen as the receptor fluid as it displayed good drug solubility with the potential to maintain sink conditions under the experimental conditions employed. For the same reason, Ethanol-PBS (30:70 % v/v) was chosen as the receptor fluid for finasteride.

The stability of each drug in the chosen receptor fluid was determined at 4 °C for up to 4 weeks, in case of delays in analysis of samples due to breakdown of HPLC instrument. These results are shown in Figure 2-9.

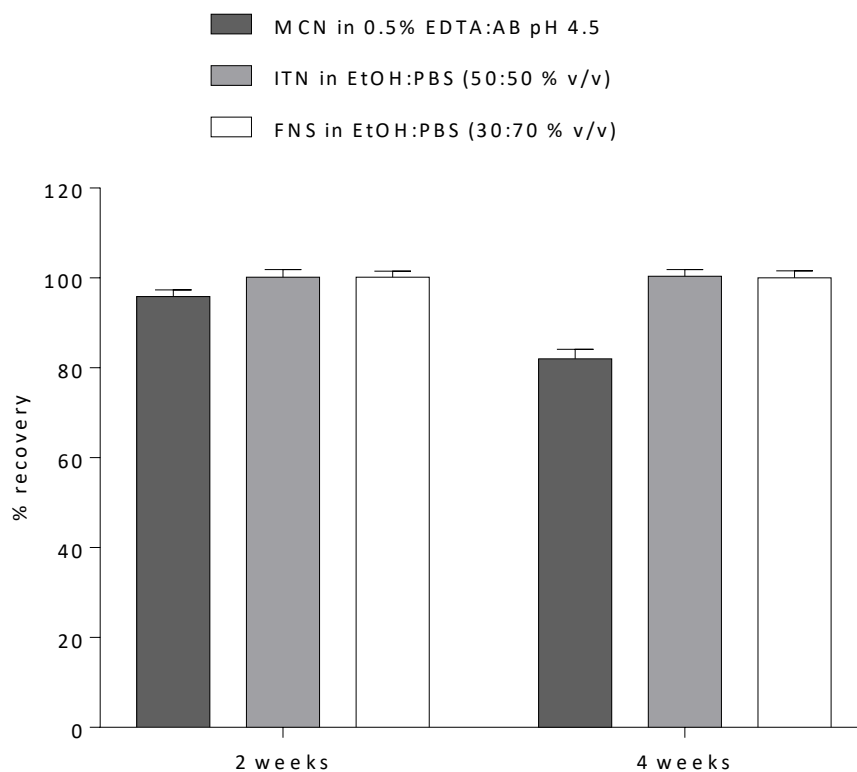


**Figure 2-9: Stability of minocycline (MCN), isotretinoin (ITN) and finasteride (FNS) in 0.5% EDTA in 0.5 M acetate buffer pH 4.5, EtOH: PBS (50:50 % v/v) and EtOH: PBS (30:70 % v/v) at 4°C, respectively. Data represents mean + S.D. (n=3).**

Under these conditions minocycline was stable for up to 2 weeks with recovery of  $\geq 95\%$  in 0.5% EDTA in AB pH 4.5, with recovery declining to  $82.00 \pm 2.15\%$  after 4 weeks. However, both isotretinoin and finasteride were stable throughout the entire study with recovery values  $> 99\%$  in Ethanol-PBS (50:50 % v/v) and Ethanol-PBS (30:70 % v/v), respectively.

### 2.3.2.2 Saturated solubility in donor (CPEs) and receptor fluid

As discussed previously in Chapter 1 (Section 1.7.1.4), altering the thermodynamic activity of a drug in vehicle by increasing the degree of saturation can improve drug flux across skin by increasing the escaping tendency. Consequently, the thermodynamic activity of a molecule in a vehicle is more important than its absolute concentration (Moser, Kriwet, Kalia, & Guy, 2001). Nonetheless, the knowledge of accurate drug solubility data is essential for the design of topical dosage forms, since poor drug solubility in the vehicle can limit a drug's bioavailability. Therefore, the saturated solubility of minocycline, isotretinoin and finasteride was determined in a range of hydrophilic and hydrophobic vehicles commonly used in topical/transdermal drug delivery formulations for their excipient or skin permeabilization properties. The solubility studies were conducted by adding excess amounts of drug to vials containing 1 mL of solvent. A PTFE coated magnetic stirrer bar was introduced into each vial, after which the vials were tightly sealed and para-filmed. The samples were left on magnetic stirrer plate at 500 rpm at room temperature for 24 hr to reach equilibrium. The saturated solutions were then filtered through 0.20  $\mu\text{m}$  PTFE syringe filters. The concentrations of each drug in the filtrates were determined by HPLC after appropriate dilution with methanol. The saturated solubility of each drug in the various vehicles is shown in Table 2-9.

**Table 2-9: Saturated solubility of minocycline, isotretinoin and finasteride in various hydrophilic and hydrophobic vehicles at room temperature (20 °C). Data represent mean  $\pm$  S.D. (n=3).**

Vehicles	Saturated Solubility (mg/mL)		
	Minocycline	Isotretinoin	Finasteride
Benzyl alcohol	23.4 $\pm$ 0.62	12.89 $\pm$ 0.05	229.85 $\pm$ 0.31
Crodamol® GTCC	0.04 $\pm$ 0.008	3.70 $\pm$ 0.01	1.83 $\pm$ 0.01
Crodamol® ISIS	0.04 $\pm$ 0.005	1.69 $\pm$ 0.03	0.39 $\pm$ 0.04
Dimethyl isosorbide	18.35 $\pm$ 1.36	23.66 $\pm$ 0.11	18.65 $\pm$ 0.21
Diisopropyl adipate	0.60 $\pm$ 0.15	8.42 $\pm$ 0.05	5.62 $\pm$ 0.34
Ethanol	8.49 $\pm$ 0.46	10.66 $\pm$ 0.15	296.43 $\pm$ 2.41
Ethylene glycol	15.57 $\pm$ 0.68	0.07 $\pm$ 0.005	24.82 $\pm$ 0.11
Glycerol	105.22 $\pm$ 1.28	0.10 $\pm$ 0.007	0.33 $\pm$ 0.01
Isopropyl alcohol	12.82 $\pm$ 0.63	10.18 $\pm$ 0.08	73.26 $\pm$ 0.15
Isopropyl myristate	0.60 $\pm$ 0.11	4.07 $\pm$ 0.02	1.82 $\pm$ 0.01
Isopropyl palmitate	0.31 $\pm$ 0.12	3.42 $\pm$ 0.01	0.64 $\pm$ 0.02
PEG 400	11.41 $\pm$ 0.85	5.25 $\pm$ 0.02	7.47 $\pm$ 0.13
Phenoxyethanol	21.75 $\pm$ 0.96	8.05 $\pm$ 0.41	81.34 $\pm$ 0.31
Propylene glycol	85.26 $\pm$ 1.58	0.71 $\pm$ 0.06	34.53 $\pm$ 0.14
Propylene glycol diacetate	2.50 $\pm$ 0.58	5.23 $\pm$ 0.15	6.13 $\pm$ 0.17
Propylene glycol dipelargonate	0.17 $\pm$ 0.08	4.79 $\pm$ 0.03	1.77 $\pm$ 0.02
Propylene glycol monolaurate 90	0.70 $\pm$ 0.12	10.71 $\pm$ 0.21	34.27 $\pm$ 0.20
Propylene glycol monolaurate FCC	0.32 $\pm$ 0.10	8.83 $\pm$ 0.27	15.13 $\pm$ 0.25
Transcutol® P	7.85 $\pm$ 0.35	27.63 $\pm$ 0.17	60.05 $\pm$ 0.40
Water	22.03 $\pm$ 0.45	0.01 $\pm$ 0.009	0.03 $\pm$ 0.004

Minocycline is a hydrophilic drug (Di Stefano et al., 2008) and so was expected to show good solubility in water. As such the data showed minocycline was very soluble in water ( $22.03 \pm 0.45$  mg/mL). Glycerol a hydrophilic vehicle was determined to have the largest minocycline saturated solubility ( $105.22 \pm 1.28$  mg/mL) closely followed by propylene glycol ( $85.26 \pm 1.58$  mg/mL), with other hydrophilic vehicles showing saturated solubilities ranging from 7 to 23 mg/mL. The more hydrophobic vehicles such as such Crodamol™ ISIS, Crodamol™ GTCC, Diisopropyl adipate, Isopropyl myristate, Isopropyl palmitate, Propylene glycol dipelargonate, Propylene glycol monolaurate 90 and Propylene glycol showed reduced minocycline saturated solubility ( $< 1$  mg/mL) compared to the hydrophilic vehicles. In contrast, isotretinoin and finasteride are more lipophilic than minocycline and so were expected to show reduced aqueous solubility (Thorsteinn Loftsson et al., 2005; Nankervis et al., 1995). The solubility study revealed that isotretinoin and finasteride saturated solubility in water as  $0.01 \pm 0.009$  mg/mL and  $0.03 \pm 0.004$  mg/mL, respectively. The saturated solubility of finasteride in Crodamol™ ISIS, glycerol and isopropyl palmitate was less than 1 mg/mL. Similarly, the saturated solubility of isotretinoin in ethylene glycol, glycerol and propylene glycol was less than 1 mg/mL. Both isotretinoin and finasteride showed good solubility in the other vehicles investigated with saturated solubility values ranging from 1 to 300 mg/mL approximately.

The saturated solubility of the three drugs in numerous receptor fluids was also investigated using the method described above and in Section 2.2.2.2 but at 37 °C and 50 °C. The selection of an appropriate receptor solution is essential for good *in vitro* experimental design. The choice of receptor fluid is influenced by the physicochemical properties of the drug being investigated and the type of analytical method employed to determine the concentration of the compound. For a hydrophilic compound, buffered saline solution is generally used. With lipophilic drugs, selection of receptor fluids is more complicated as these molecules will diffuse into the SC readily but may not partition from the skin into the receptor fluid. Thus, it is important to ensure the penetrant has sufficient solubility in receptor fluid to maintain a concentration gradient for diffusion. This is often achieved by using 50% aqueous ethanol as receptor fluid for highly lipophilic drugs (OECD, 2004a; Scott & Ramsey, 1987).

Alternatively, solubilising agents such as polyethylene glycol 20-oleyl ether (Volpo 20) and serum albumin can be introduced to improve penetrant solubility (Schaefer & Redelmeier, 1996). The selected receptor fluid should not alter the integrity of the skin barrier function (OECD, 2004b) and not interfere with the analytical method employed to determine the concentration of the penetrant. The OECD guidelines on percutaneous absorption studies state that the test material should be soluble up to ten times the likely maximum concentration achievable in the receptor fluid during the experiment to ensure that sink conditions are maintained (OECD, 2004b). Thus, solubility studies were conducted in various solvent systems to find appropriate receptor fluids to provide sink conditions for the skin permeation experiments.

The solubility of minocycline was determined in phosphate buffered saline (PBS) pH 7.4 and acetate buffer solutions (pH 4.5 and 5.0) containing a range of EDTA concentrations in an attempt to improve its aqueous stability at 37 °C and 50 °C (experimental temperatures used in the Franz diffusion cell experiments to achieve a skin surface temperature of 32 °C and 45 °C respectively). This data is displayed in Figure 2-10.

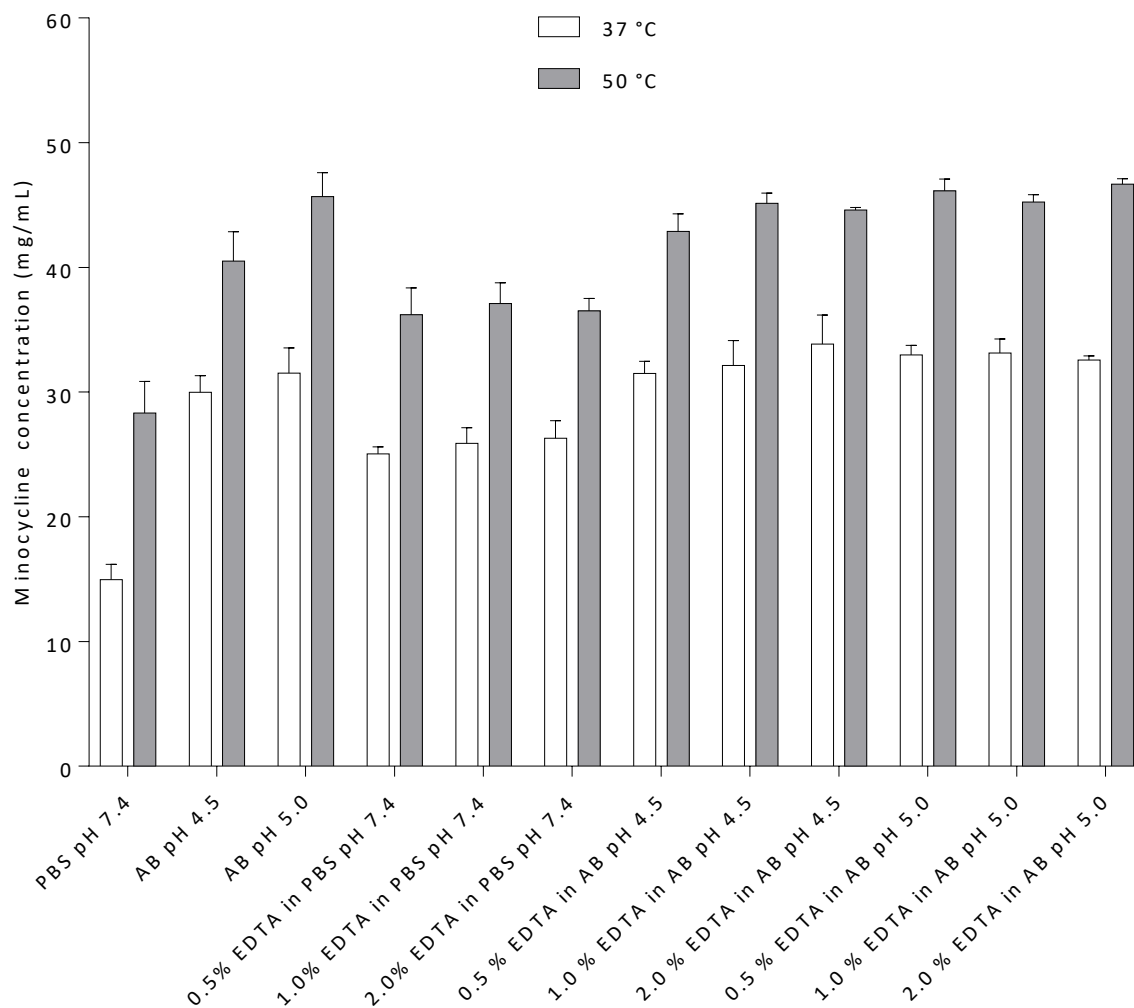


**Figure 2-10: Saturated solubility of minocycline in 0.15M PBS pH 7.4 and 0.5M acetate buffer (AB) based receptor fluids (with varying EDTA content and pH) at 37 °C and 50 °C. Data are expressed as mean + S.D. (n=3). The concentration of EDTA is represented as % w/v.**

Data from this experiment showed that minocycline was very soluble in all the vehicles studied (Figure 2-10). At 37 °C the solubility of minocycline in PBS pH 7.4 was  $14.96 \pm 1.24$  mg/mL, whereas in acetate buffers the solubility was double at the same temperature and ranged from approximately 31 to 35 mg/mL. However, increasing the temperature to 50 °C doubled minocycline solubility in PBS pH 7.4 to  $28.32 \pm 2.53$  mg/mL. Similarly, the solubility of minocycline increased with temperature for the acetate buffer solutions but not to the same extent, with solubility ranging from approximately 42 to 46 mg/mL. At the temperatures employed both the concentrations of EDTA and pH of acetate buffer solutions studied had no influence on the saturated solubility of minocycline.

With regards to isotretinoin and finasteride, their solubility in PBS pH 7.4 alone and PBS with varying ethanol content (10 to 50 % v/v) was investigated at the temperatures employed (37 °C and 50 °C) (Figure 2-11).

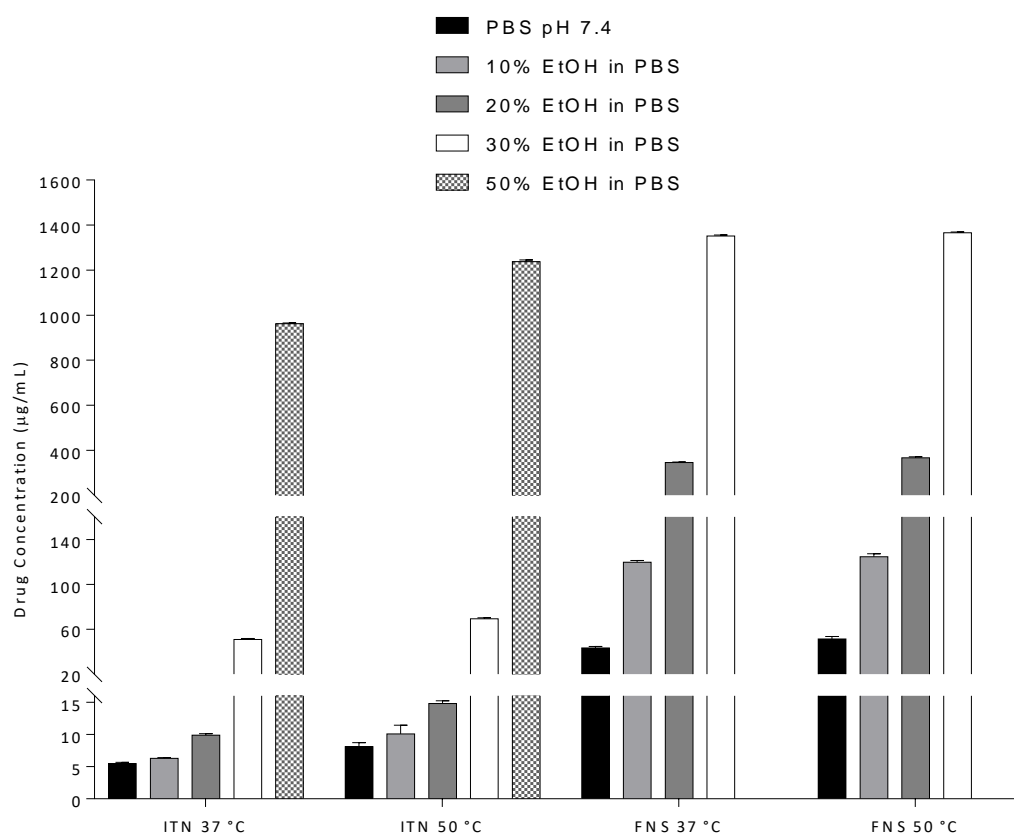


**Figure 2-11: Saturated solubility of isotretinoin (ITN) and finasteride (FNS) in 0.15M PBS pH 7.4 based receptor fluids with varying ethanol (EtOH) content at 37 °C and 50 °C. Data represents mean + S.D. (n=3). Solubility of FNS in EtOH-PBS (50:50 % v/v) was not determined.**

Analysis of this data showed that isotretinoin and finasteride solubility at 37 °C in PBS pH 7.4 was  $5.49 \pm 0.17 \mu\text{g/mL}$  and  $43.46 \pm 0.35 \mu\text{g/mL}$ , respectively. At the higher temperature (50 °C) the saturated solubility for both isotretinoin and finasteride increased to  $8.11 \pm 0.61 \mu\text{g/mL}$  and  $51.31 \pm 2.41 \mu\text{g/mL}$ , respectively. Increasing the ethanol content in the solution resulted in greater drug solubility for both drugs at the temperatures investigated, with solutions containing the most ethanol showing the greatest solubility. For isotretinoin, this corresponded to a solubility of  $961.74 \pm 3.23 \mu\text{g/mL}$  and  $1237.13 \pm 7.75 \mu\text{g/mL}$  in EtOH-PBS (50:50 % v/v) at 37 °C and 50 °C, respectively.

Whereas, for finasteride this coincided with a solubility of  $1352.09 \pm 4.27 \mu\text{g/mL}$  and  $1365.41 \pm 3.45 \mu\text{g/mL}$  in EtOH-PBS (30:70 % v/v) at 37 °C and 50 °C, respectively. The solubility of finasteride in EtOH-PBS (50:50 % v/v) was not determined because EtOH-PBS (30:70 % v/v) was believed would provide adequate solubility.

### 2.3.2.3 Method validation for penetrant extraction from skin tissue

The stability of each drug in both extraction fluids was investigated over 72 hr at room temperature (20 °C). The stability results for methanol: water (90:10 % v/v) is shown in Figure 2-12, whilst the methanol results are shown in Figure 2-13.

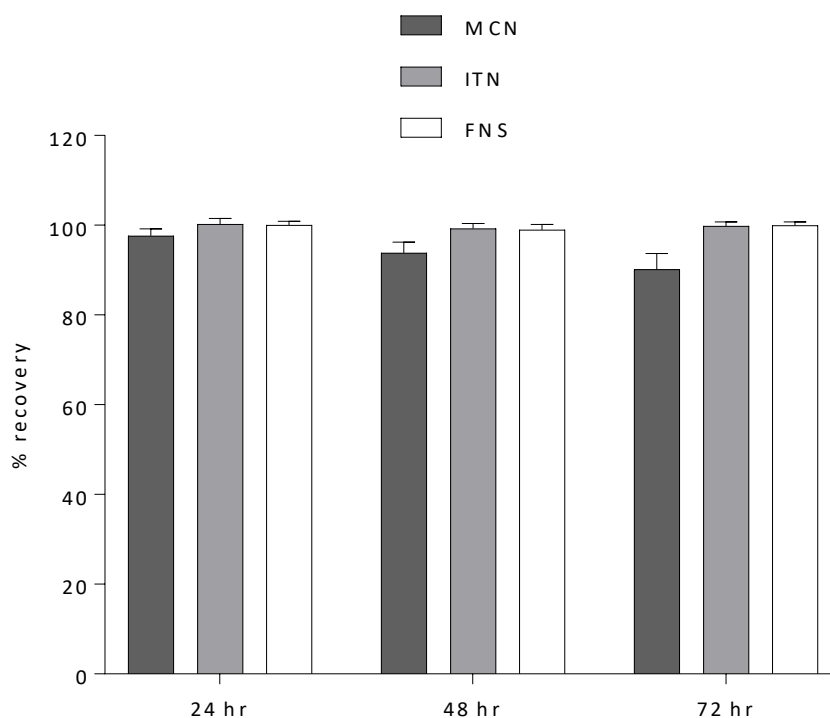


**Figure 2-12: Stability of minocycline (MCN), isotretinoin (ITN) and finasteride (FNS) in Methanol: Water (90:10 % v/v) at room temperature for 24, 48 and 72 hr. Data represents mean + S.D. (n=3).**

The stability of minocycline in methanol: water (90:10 % v/v) was > 97 % at 24 hr, with the percent recovery declining further to 90 % at 72 hr. In contrast, both isotretinoin and finasteride were stable over the 72 hr with recovery values of > 99 % and > 98 %, respectively.

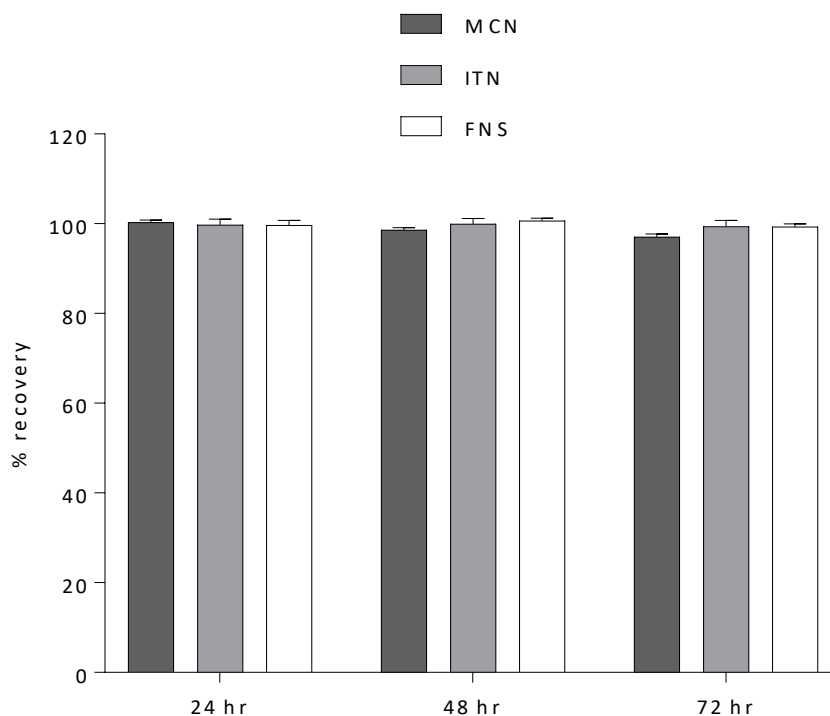


**Figure 2-13: Stability of minocycline (MCN), isotretinoin (ITN) and finasteride (FNS) in methanol at room temperature for 24, 48 and 72 hr. Data represents mean + S.D. (n=3).**

The stability of all three drugs in methanol over 72 hr at room temperature is shown in Figure 2-13.

The recovery values for minocycline, isotretinoin and finasteride after 72 hr was  $97.09 \pm 0.65 \%$ ,  $99.43 \pm 1.31 \%$  and  $99.31 \pm 0.65 \%$ , respectively. Thus, both isotretinoin and finasteride showed suitable stability in both extraction fluids over 72 hr at room temperature, whilst, minocycline showed appropriate stability in methanol alone over the investigated period.

**Table 2-10: Minocycline (MCN), isotretinoin (ITN) and finasteride (FNS) solubility in different extraction solutions and absolute recovery values for drug-spiked samples after 20 min of sonication, followed by 16-18 hr of shaking on a roller mixer. Data represents mean  $\pm$  S.D. (n=3).**

	Extraction Solutions					
	MeOH: Water (90:10 % v/v)			MeOH		
	MCN	ITN	FNS	MCN	ITN	FNS
Solubility (mg/mL)	8.28 $\pm$ 1.90	1.24 $\pm$ 0.18	247.38 $\pm$ 3.75	20.06 $\pm$ 2.20	6.07 $\pm$ 0.15	274.72 $\pm$ 1.28
<b>Control samples</b>						
Empty vial	94.70 $\pm$ 2.52	99.68 $\pm$ 1.10	98.70 $\pm$ 0.51	101.13 $\pm$ 0.25	99.39 $\pm$ 0.55	101.13 $\pm$ 2.10
Scotch tape (10 TS)	64.05 $\pm$ 5.68	59.63 $\pm$ 2.20	68.05 $\pm$ 0.71	90.73 $\pm$ 1.25	91.14 $\pm$ 1.32	93.73 $\pm$ 0.60
Cotton buds (3 CB)	83.15 $\pm$ 3.15	80.10 $\pm$ 1.15	85.15 $\pm$ 1.82	98.56 $\pm$ 0.65	98.52 $\pm$ 1.20	98.56 $\pm$ 0.21
2-octyl cyanoacrylate glue	85.25 $\pm$ 4.51	76.03 $\pm$ 2.41	82.31 $\pm$ 0.49	90.12 $\pm$ 0.71	93.29 $\pm$ 2.01	95.33 $\pm$ 1.75
<b>Skin samples</b>						
Unabsorbed (3 CB + 2 TS)	55.20 $\pm$ 4.25	60.55 $\pm$ 1.51	55.20 $\pm$ 1.12	56.20 $\pm$ 1.05	63.80 $\pm$ 0.75	57.20 $\pm$ 0.90
Stratum corneum (10 TS)	8.25 $\pm$ 3.81	9.45 $\pm$ 2.65	10.25 $\pm$ 0.65	17.15 $\pm$ 1.35	15.42 $\pm$ 0.51	15.15 $\pm$ 0.71
Tape-stripped skin	20.64 $\pm$ 1.11	18.93 $\pm$ 1.63	24.64 $\pm$ 0.51	22.90 $\pm$ 0.35	19.25 $\pm$ 0.45	23.90 $\pm$ 0.62
Total recovery	84.09 $\pm$ 9.17	88.93 $\pm$ 5.79	90.09 $\pm$ 2.28	96.25 $\pm$ 2.75	98.47 $\pm$ 1.71	96.25 $\pm$ 2.23

Methanol (MeOH), Tape strips (TS) & Cotton buds (CB). Total recovery is the sum of unabsorbed, stratum corneum and tape-stripped skin % recovery values.

Skin extraction methods have been used to quantify various types of compounds in the whole skin or in a specific layer (Bronaugh & Maibach, 2005; Katrin Moser et al., 2001). These procedures usually employ a solvent to extract substances from skin samples in association with ultra-sonication or tissue homogenisation to facilitate its removal from skin samples (Bronaugh & Maibach, 2005). One example of a commonly used extraction solvent is methanol and is usually employed to extract lipophilic substances from skin (De Paula, Martins, & Bentley, 2008). In this study, the suitability of methanol: water (90:10 %v/v) and methanol as extraction solutions were investigated. The efficiency of extraction will vary with the solubility properties of the compound in the solvent (Surber, Schwarb, & Smith, 2005). Therefore, the solubility of all three drugs in the different extraction solutions was determined. This data is shown in Table 2-10, with all three drugs showing greater solubility in methanol (MCN 20.06 mg/mL, ITN 6.07 mg/mL and FNS 274.72 mg/mL).

Also, shown in Table 2-10 is the efficiency of the different extraction solutions to recover each drug from spiked control and skin samples. The control samples consisted of an empty vial, a vial containing adhesive tape (with the same area as the skin samples used in the penetration studies) a vial containing cotton buds and a vial containing a drop of 2-octyl cyanoacrylate glue. The skin samples consisted of full thickness abdominal skin with the same area of Franz diffusion cells employed. These samples were spiked with 100  $\mu$ L of methanol corresponding to 100  $\mu$ g of each drug for all three compounds. The samples were protected from light with foil and left to stand for 4 hr to allow the methanol to evaporate off. Then the extraction procedure was performed as described previously (in Section 2.2.2.3) using the two different extraction solutions.

Methanol: water (90:10 % v/v) yielded recovery values ranging from 59 % to 85 % for all three drugs in the control samples containing adhesive tape, cotton buds and a vial containing a drop of 2-octyl cyanoacrylate glue, whilst recovery values from the empty vials were  $94.70 \pm 2.52$  %,  $99.68 \pm 1.10$  % and  $98.70 \pm 0.51$  % for minocycline, isotretinoin and finasteride respectively. Also, total recovery

values for the skin samples ranged from 84 % to 90 % for all three drugs when methanol: water (90:10 % v/v) was used as the extraction solution.

Methanol yielded higher recovery values for each drug from the control samples containing adhesive tape, cotton buds and 2-octyl cyanoacrylate glue (> 90 %). Additionally, both extraction solutions produced similar recovery values from the empty vial for both isotretinoin and finasteride (> 98 %). However, using methanol alone as extraction solution produced higher recovery from the empty vial for minocycline ( $101.13 \pm 0.25$  %). This indicates that the absence of water to have improved minocycline stability. When it comes to drug extraction from skin a well conducted experiment should result in total drug recovery of over 90 % (Pendlington, 2008). However, the OECD guidelines permit a range of recovery 80 % to 120 % to be acceptable for regulatory purposes for volatile substances, unlabelled drugs and drugs with stability issues (OECD, 2004a). In this study, the total recovery from the skin samples ranged from 96 % to 98 % for all three drugs when methanol was used as the extraction solution. Therefore, methanol was the best option to extract all three drugs from adhesive tape, cotton buds and tape-stripped skin. It was also important to note that there was no interference in all three HPLC assays from contaminants leached out from cotton buds, adhesive tape and 2-octyl cyanoacrylate glue (data not shown).

### 2.3.2.4 Assay interference study

Franz cell diffusion experiments were performed using human abdominal skin to investigate if any endogenous skin components would affect the determination of minocycline, isotretinoin and finasteride. Each Franz cell was setup so that the donor chamber was left empty and the receptor chamber was filled with the appropriate receptor fluid for each drug. After 24 hr, the receptor fluid was removed and analysed via the appropriate HPLC method as described in Table 2-2. This analysis showed that skin extract contaminants eluted between 1 and 5 min along with the solvent front for all three methods (as shown in Figure 2-14). Therefore, no interfering peaks were noted at any of the elution times corresponding to minocycline ( $t_R = 9.8$ ), isotretinoin ( $t_R = 10.2$ ) and finasteride ( $t_R = 10.3$ ).

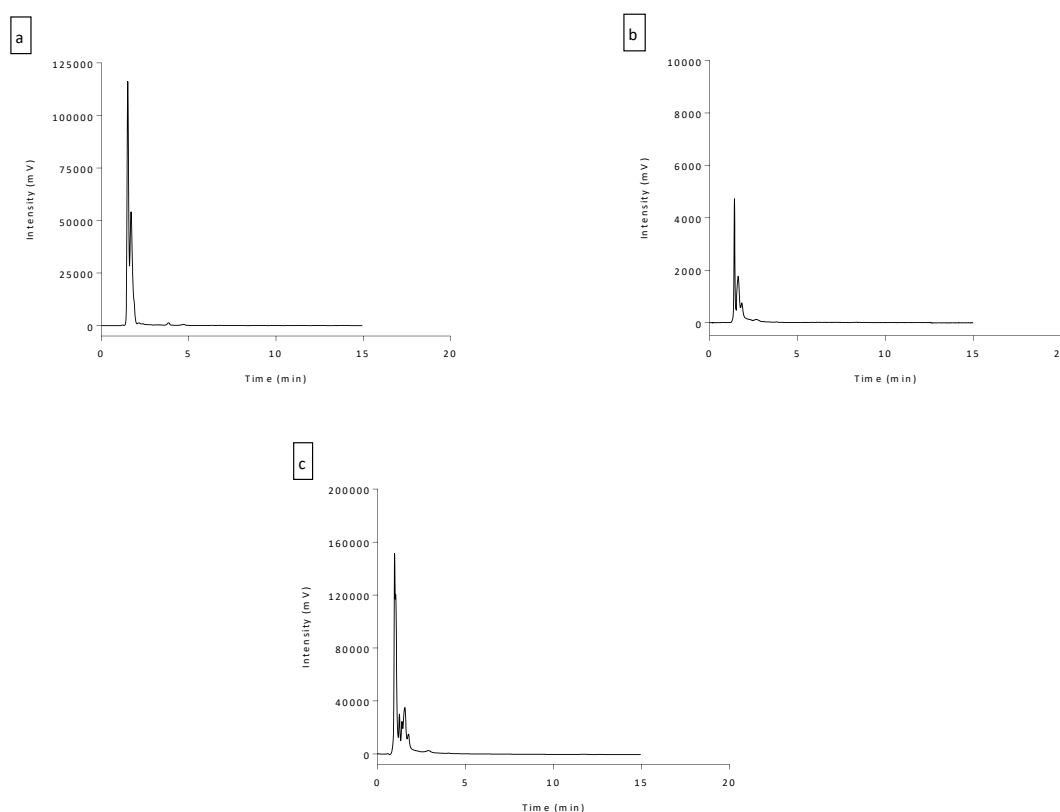


**Figure 2-14: HPLC chromatograms showing skin extract contaminants in the relevant receptor fluid selected for each drug after *in vitro* permeation study where the donor chamber was left blank (a) 0.5 % EDTA in 0.5M acetate buffer pH 4.5 analysed under chromatographic conditions for minocycline, (b) EtOH: PBS pH 7.4 (50:50 % v/v) analysed under chromatographic conditions for isotretinoin and (c) EtOH: PBS pH 7.4 (30:70 % v/v) analysed under chromatographic conditions for finasteride.**

## 2.4 Conclusion

HPLC methods for the quantification of minocycline, isotretinoin and finasteride in skin samples after *in vitro* permeation and penetration studies have been developed and shown to be 'fit for purpose'. All three analytical methods employed showed good linearity, accuracy, precision, reproducibility and sensitivity. Also, initial pre-formulation work was conducted to determine the saturated solubility and short-term stability of each drug in a range of vehicles and media. Both isotretinoin and finasteride were found to be stable under the conditions employed in the *in vitro* permeation and penetration studies, whilst minocycline was found to be less stable in the more hydrophilic vehicles. However, it was discovered that magnesium chloride improved the stability of minocycline in these vehicles, agreeing with what has been reported in the literature (Hasegawa et al., 1987; Melvin et al., 1962). Additionally, appropriate receptor and extraction fluids were developed for each drug and *in vitro* penetration studies were validated by determining the extraction efficiency of each solution and saturated solubility of each drug in the extraction fluid. As such, the *in vitro* permeation, penetration and analytical procedures developed were used to examine and quantify the effect of heat (45°C) on the skin permeation, distribution and follicular absorption of minocycline, isotretinoin and finasteride as described in Chapters 3, 4 and 5 respectively.

### **3 Effect of heat, CPEs and magnesium chloride on the skin permeation and distribution of minocycline**

### 3.1 Introduction

Minocycline is a tetracycline antibiotic that is effective in the treatment of acne (Hubbell, Hobbs, Rist, & White, 1982; Ochsendorf, 2010). Currently, only oral preparations of minocycline are available for the treatment of moderate-severe acne. However, oral delivery of minocycline is associated with systemic side effects such as dizziness, vertigo, nausea and systemic lupus erythematosus-like syndrome (Elewski et al., 2011; Good & Hussey, 2003). Therefore, there is a need to reduce these systemic side effects, possibly by developing optimised, stable topical minocycline formulations which can deliver high drug concentrations into the skin tissues and promote local drug targeting to the pilosebaceous unit (hair follicle and sebaceous gland). However, a major challenge in the development of topical formulations of minocycline relates to its sensitivity to moisture, temperature, light and its poor chemical stability in solution (Chow, Chan, & Heng, 2008; Wu & Fassihi, 2005).

In Chapter two, an attempt was made to stabilise minocycline in hydrophilic and non-hydrophilic dermatological vehicles under the conditions employed in the *in vitro* skin permeation experiments (37 °C and 50 °C to achieve skin surface temperatures of 32 °C and 45 °C, respectively). In this work, magnesium chloride (henceforth referred to as magnesium) was shown to contribute to the stabilisation of minocycline in various hydrophilic CPEs such as ethanol (EtOH), isopropyl alcohol (IPA), propylene glycol (PG) and Transcutol® P (TP). In contrast minocycline is more stable in hydrophobic solvents. What is now needed is an understanding of how these vehicles affect skin permeation and distribution and how increasing the skin temperature to 45 °C affects the three-potential rate-controlling steps of the percutaneous absorption process (formulation release, partitioning and diffusivity of the drug through the SC) to gain a better understanding of the effect of heat ( $\leq 45$  °C) and CPEs (with and without magnesium) on percutaneous absorption with an aim to optimise any effects observed.

Reports from the literature suggest that magnesium ( $Mg^{2+}$ ) can stabilise tetracyclines through complexation (Piccariello, 2013; Sauwaluxana Tongaree, Flanagan, & Poust, 1999; Wessels et al.,

1998), however, the exact stoichiometry of the complexes formed are unknown as different magnesium and minocycline stoichiometries have been reported. The method of continuous variation (Job plot) can be used to determine the stoichiometry of complex chemical entities (Renny, Tomasevich, Tallmadge, & Collum, 2013) and may therefore help improve our understanding of the interaction between magnesium and minocycline in the vehicles used here. In these experiments, the change in some physical property which in relation to the concentrations of the constituents of the complex (i.e. absorbance) is measured (Gil & Oliveira, 1990).

Furthermore, as minocycline is fluorescent, confocal laser scanning microscopy (CLSM) can be used to visualise drug distribution across skin tissue and therefore provide information about minocycline permeation across skin. Therefore, the effect of heat, CPEs and magnesium on the distribution of minocycline across full thickness human abdominal skin can be explored using this technique.

In this study, CLSM will be used to support the skin penetration studies by visualising the minocycline distribution across the different layers of skin. At the same time, the CLSM studies may provide crucial information on the drug transport pathways across skin and potentially identify the mechanisms which account for heat and CPEs enhancement of skin permeation. It may also highlight the influence of magnesium on the drug transport across skin. Thus, the aims of this study were as follows:

- To examine the effect of magnesium on the solubility of minocycline in selected hydrophilic dermatological vehicles and determine the stoichiometry of magnesium-minocycline complex.
- To study the effect of heat (45 °C) on the skin transport of minocycline from selected hydrophilic vehicles (with and without  $Mg^{2+}$ ) and hydrophobic vehicles using *in vitro* skin permeation and distribution methodologies developed in Chapter 2.
- To use methodologies such as CLSM, rheology and *in vitro* Franz diffusion cells with cellulose acetate to help provide understanding of the effects of vehicle and temperature on the delivery of minocycline to skin.

## 3.2 Materials and Methods

Minocycline HCl (99.9 %) was purchased from Sequoia Research Products (Pangbourne, UK). Acetonitrile HPLC grade (99.9 %), ethanol HPLC grade (99.9 %), methanol HPLC grade (99.9 %), propan-2-ol (isopropyl alcohol) (>99.5 %), propylene glycol (>99.0 %), Dura Seal™ (Diversified Biotech, USA), Spectra/Por™ regenerated cellulose membrane with molecular weight cut-off (MWCO) 2000 Da (Spectrum™ Laboratories Inc., USA), Hamilton GASTIGHT® syringes (Hamilton®, Switzerland), Parafilm M® laboratory film (Bemis® Flexible packaging, USA) were acquired from Fisher Scientific (Loughborough, UK). Ethylenediaminetetraacetic acid (EDTA, 99.0-101.0 %), was supplied by Sigma Aldrich (Gillingham, UK). Acetic acid (>99.0 %), isopropyl myristate (>96 %), magnesium chloride hexahydrate (>99.0) and Sodium thiosulfate pentahydrate (99.5%) were bought from Acros Organics (New Jersey, USA). Deionised water (18.2 M $\Omega$ •cm) was from Millipore Milli-Q® water system.

### 3.2.1 Quantitative analysis of minocycline

Quantitative analysis of minocycline was conducted using HPLC as described previously in Chapter 2, Section 2.2.1.1.

### 3.2.2 Effect of magnesium on the saturated solubility of minocycline

The effect of magnesium on the solubility of minocycline in various dermatological vehicles (EtOH, PG and TP) was assessed at room temperature (20 °C). An excess quantity of minocycline was added to 5.0 mL of each vehicle containing increasing amounts of magnesium (ranging from 0 to 1.0 M). The suspensions were stirred for 24 hr at 800 rpm in order to reach equilibrium, subsequently filtered through 0.45  $\mu$ m PTFE syringe filters, diluted with methanol, and then analysed using the HPLC method for minocycline described in Chapter 2, Section 2.2.1.1.

### **3.2.3 *In vitro* skin permeation experiments**

#### **3.2.3.1 Skin preparation**

Human abdominal skin supplied from ZenBio (USA) was prepared as described in Chapter 2, Section 2.2.2.6. Prior to commencing the permeation studies, the skin was removed from the freezer, thawed and cut to the appropriate size using a scalpel.

#### **3.2.3.2 Preparation of donor suspensions**

For the preparation of minocycline suspensions in the vehicles investigated refer to Chapter 2, Section 2.2.2.5.

#### **3.2.3.3 Franz cells set up**

##### **3.2.3.3.1 Infinite dose *in vitro* skin permeation studies**

The skin samples were placed on the individually calibrated unjacketed upright Franz diffusion cells (diameter 1.0 cm<sup>2</sup>: volume 3.0 mL) (Soham Scientific, UK), with the SC facing the donor compartment and the dermis facing the receptor. Both chambers were then wrapped together using Parafilm® (at 37 °C) or Dura Seal™ (50 °C) before being clamped together. The receiver fluid was 0.5 % EDTA in 0.5 M acetate buffer (pH 4.5) and stirred with a magnetic bar to ensure adequate mixing (600 rpm). The water bath temperature was maintained at either 37 °C and 50 °C to keep the skin surface at approximately 32 ± 1 °C and 45 ± 1 °C respectively. Prior to dosing, the Franz cells were equilibrated and the surface temperature was measured from the donor compartment using a Fisher Scientific Traceable Digital Thermometer with a type-K probe. Air bubbles were removed through the sampling arm by carefully tilting or inverting the diffusion cell and checks for leaks were made at the same time. A saturated suspension (0.5 mL) of minocycline was then introduced into the donor chamber. Following this, an aliquot of the receiver fluid (200 µL) was removed from receptor compartment via the sampling arm after 1, 2, 3, 4, 6, 18, 19, 20, 21, 22, 23 and 24 h and analysed via HPLC. An equal volume of pre-warmed receiver fluid was immediately added to replace the sampled volume. Six repetitions (n=6) of each experiment were performed.

### 3.2.4 Drug skin distribution studies

To determine the distribution of minocycline across the different skin layers the extraction procedure described in Chapter 2, Section 2.2.2.3 was followed with minor changes. These were: dry patting the skin samples with tissue paper and discarding the buds and tape strips used to remove excess formulation. For clarity, the full method is provided below.

After the completion of the diffusion experiments, the skin was removed from the Franz cell and carefully dried by patting with tissue paper. The residual formulation was removed following three separate cleaning phases. The first cleaning phase was conducted by carefully rolling a dry cotton bud over the skin upwards three times, then downwards three times, then clockwise and anticlockwise along the edges once. For the second cleaning phase, the first cleaning phase was repeated using a wet cotton bud soaked in methanol. For the third cleaning phase, the first cleaning step was repeated using a dry cotton bud. All three buds were then discarded. To remove any remaining surface formulation two tape strips were taken and discarded. To remove the SC, a further ten tape strips were taken and placed into an amber glass vial (Raber et al., 2014). Following SC removal, the skin was placed at 60 °C using a benchtop oven (Binder, Binder GmbH, Germany) for 2 min which allowed the epidermis to be separated from the dermis more easily. Epidermal and dermal samples were transferred into individual glass vials, to which 2.0 mL of methanol (the extraction fluid) was added. Each vial was then sonicated for 20 min before being transferred to a Stuart roller mixer SRT9 (Cole-Parmer, UK) overnight (16-18 hr). All samples were then filtered using 0.2 µm PTFE syringe filter before being analysed by HPLC as described in Chapter 2, Section 2.2.1.1. The extraction procedure was repeated until the drug content in the extracted samples were no longer detectable or below the LOQ.

### **3.2.5 Penetration of minocycline and magnesium-minocycline complex into skin: confocal laser scanning microscopy studies**

An aliquot (0.5 mL) of saturated suspension of minocycline and magnesium: minocycline (1:1 ratio by weight) was applied to the skin surface of each donor chamber for 24 hr at 37 °C and 50 °C (to achieve skin surface temperature of 32 °C and 45 °C respectively). Excess formulation was removed from the skin surface of each diffusion cell using the method described in Chapter 2, Section 2.2.2.3 (briefly, by consecutively employing a single dry cotton bud, a methanol soaked cotton bud then a dry cotton buds followed by two tape strips) and discarded.

After this, skin samples were held in a vertical orientation at the bottom of the embedding cassette with a drop of Optimal Cutting Temperature compound (OCT) embedding media. Once the orientation was satisfactory the cassette was filled to level with care taken to avoid the formation of large bubbles. The cassette was then carefully labelled to indicate the location of the SC. Then, working in a fume hood, a small steel bowl filled with acetone was placed in a Styrofoam container after which the surrounding space in the beaker was filled with dry ice pellet. Small amounts of dry ice pellets were slowly added to the bowl with acetone until the mixture stopped bubbling to produce a temperature of -78 °C. Using tongs, the filled embedding cassette with the correctly oriented tissue was immersed in the acetone to freeze it.

Then vertical sections (30 µm) were cut using a Bright Cryostat (OTF5000-003/D) (Bright Instruments Ltd, UK) with the cabinet temperature set to -24 °C. Tissues sections were immediately transferred on to polysine coated microscope slides. After this, each slide was submerged in a petri dish containing 1 M magnesium in ethanol for 5 min. Then slides were placed in a fume hood for approximately 1 hr to allow the ethanol to evaporate off. Once completely dry the coverslips were placed on top to protect the tissue and the samples were viewed under the confocal microscope (C1 confocal laser scanner connected to an Eclipse TE 2000 U inverted fluorescence microscope) with a 10x (0.3 NA) Plan Fluor DIC L/N1 objective (Nikon, Japan). An Argon-Ion laser was used to excite minocycline at 408 nm with emission fluorescence detected at ≥ 500 nm. The images obtained from the confocal microscope were

recorded and edited with EZ-C1 3.90 Viewer (Nikon, Japan). Gain settings for both the red and green channel were set at 100 units. Transmitted light was used to obtain skin structure details. The transmitted light channel gain was set at 37 units. Images were captured using the Nikon EZ-C1 software (Gold version 3.90). Images were chosen at 1024-pixel resolution with each image consisting of an average of 4 laser scans.

### 3.2.6 Determination of magnesium and minocycline stoichiometry

The stoichiometry of magnesium and minocycline in ethanol was determined by continuous variation method (Job's plot method) (Hirose, 2001). Briefly, equimolar ( $3 \times 10^{-4}$  M) magnesium and minocycline were mixed to a fixed volume (10 mL) by varying the molar ratio from 0.1 to 0.9, keeping the total molar concentration of each final solution constant. A summary of the dilutions prepared (minocycline with equimolar magnesium and their corresponding mole ratios) is shown in Table 3-1. After stirring for 1 hr, the absorbance (Abs) of each solution was measured by UV-Vis spectroscopy at 380 nm (using an Agilent Cary 60 UV-Vis spectrophotometer) and the change in absorbance ( $\Delta$ Abs) was determined as the difference between Abs with and without magnesium. Then  $\Delta$ Abs was plotted as a function of the  $Mg^{2+}$  molar fraction,  $\frac{[Mg^{2+}]}{[Mg^{2+}]+[MCN]}$  to yield the Job Plot. The molar fraction corresponding to the peak on the Job's plot was used to determine the binding stoichiometry for magnesium and minocycline.

**Table 3-1: Summary of the dilutions of minocycline (MCN) with equimolar magnesium ( $Mg^{2+}$ ) and their corresponding mole ratios.**

Solution number	Volume of $Mg^{2+}$ [ $3 \times 10^{-4}$ M] in EtOH (mL)	Volume of MCN [ $3 \times 10^{-4}$ M] in EtOH (mL)	Mole ratio ( $Mg^{2+}$ : MCN)	Mole fraction of $Mg^{2+}$
1	1.00	9.00	1:9	0.10
2	2.00	8.00	1:4	0.20
3	2.50	7.50	1:3	0.25
4	3.34	6.66	1:2	0.33
5	4.00	6.00	1:1.5	0.40
6	5.00	5.00	1:1	0.50
7	6.00	4.00	1.5:1	0.60
8	6.66	3.34	2:1	0.66
9	7.50	2.50	3:1	0.75
10	8.00	2.00	4:1	0.80
11	9.00	1.00	9:1	0.90

### 3.2.7 Viscosity measurements of minocycline formulations with and without magnesium at 32 °C and 45 °C

Saturated suspensions of minocycline in EtOH, PG, IPA: DPA and IPA: TP with and without magnesium were prepared as described in Chapter 2, Section 2.2.2.5. The equilibrated suspensions were filtered using a 0.45 µm PTFE syringe filter. The viscosity of these formulations was then measured using an AR1500ex Rheometer (TA Instruments, USA), fitted with a stainless steel parallel plate geometry (4 cm diameter) with a gap setting of 600 µm. Experiments were conducted at 32 °C and 45 °C with 2 min equilibration time for each temperature. These temperatures were selected to mimic the temperatures employed in the *in vitro* drug permeation and release studies. Each formulation was analysed by configuring the instrument on a continuous ramp mode with an increasing shear rate from 0 to 1000 (1/s) and the corresponding shear stress was measured. Triplicate measurements were made for each formulation and the mean viscosity was calculated directly from the stress/shear rate relationship from 0 to 1000 (1/s).

### 3.2.8 *In vitro* release rate study using cellulose membrane

The effect of temperature on the *in vitro* release properties of minocycline and magnesium: minocycline (1:1 ratio by weight) from different dermatological vehicles (EtOH, PG, TP, IPA: DPA & TP: DPA) was assessed using cellulose membrane. The ratio of the vehicles in the binary systems was 1:1. Diffusion experiments were carried out using individually calibrated unjacketed upright Franz diffusion (diameter 1.0 cm<sup>2</sup>: volume 3.0 mL) (Soham, Scientific, UK). The regenerated cellulose membrane was cut to the appropriate size and placed between the donor and receptor compartments of the Franz cell. A small PTFE coated magnetic bar was included in the receptor compartment such that stirring occurred throughout the duration of the experiment. The receptor compartment was filled with 0.5 % EDTA in 0.5 M acetate buffer (pH 4.5) and the Franz cell placed on a stirring plate submerged in a water bath maintained at the appropriate temperature (37 °C or 50 °C to achieve a membrane surface temperature of 32 °C and 45 °C respectively). After allowing the membrane to equilibrate with the receptor fluid, 0.5 mL of the formulation (saturated suspension at 37 °C or 50 °C for without and with

heat respectively) was then introduced into the donor chamber. The experimental duration was 6 hr and at appropriate time intervals (every 30 min), the entire receiver fluid was removed for sampling and replaced with an equal volume of fresh pre-warmed receiver fluid to maintain sink conditions throughout the duration of the experiment. Samples were then analysed using the HPLC assay for minocycline described in Chapter 2, Section 2.2.1.1. Six repetitions (n=6) of each experiment were performed.

The transport of minocycline across cellulose membrane was treated according to the Higuchi diffusion model (Equation 3-1). Although the Higuchi equation was originally derived to describe the release behaviour of drugs dispersed uniformly in an ointment matrix (Higuchi, 1960), it was later found to be applicable for many other pharmaceutical dosage forms including suspensions (Costa & Sousa Lobo, 2001; Higuchi, 1961).

$$Q = [DC_s(2C_v - C_s)t]^{1/2} \quad \text{Equation 3-1}$$

Where Q is, the cumulative amount released per unit area at time t, D is the diffusion coefficient,  $C_v$  is the original concentration of drug in the applied vehicle, and  $C_s$  is the saturated solubility of the drug in the applied vehicle. The amount permeating the membrane per unit surface area (Q) was plotted against the square root of time ( $t^{1/2}$ ). The gradient of this plot, which is equal to the release rate constant ( $\text{mg}/\text{cm}^2/\text{min}^{1/2}$ ) and the correlation coefficient were calculated by linear regression using the Higuchi equation (Equation 3-1).

### 3.2.9 *In vitro* release rate of minocycline and magnesium-minocycline complex across cellulose membrane: complete system heating vs heat applied from top

The effect of externally applied heat using sodium thiosulfate solution (ST) ( $\leq 45\text{ }^{\circ}\text{C}$  for 15 min and 25 min) on the *in vitro* release of minocycline and magnesium-minocycline (1:1 ratio in terms of weight) from PG was compared to no additional heat ( $32\text{ }^{\circ}\text{C}$ ) and complete system heating (water bath at  $45\text{ }^{\circ}\text{C}$  for the duration of the experiment). The use of sodium thiosulfate as potential energy source for heat facilitated drug transport was discussed in Chapter 1, Section 1.7.2.4. The release characteristics were evaluated using cellulose membrane and six repetitions were performed for each formulation at each condition. The method for the *in vitro* release studies described in Section 3.2.8 was employed with the following changes:

- 1) The Franz diffusion cells were dosed with  $100\text{ }\mu\text{L}$  of filtered saturated solution of each formulation equilibrated at the appropriate temperature.
- 2) After applying the formulation,  $2.5\text{ mL}$  or  $5\text{ mL}$  of sodium thiosulfate solution (chemical heating system) was introduced to the system to produce a membrane surface temperature of approximately  $45\text{ }^{\circ}\text{C}$  for 15 min and 25 min respectively. Aluminium foil was used to separate the heating system from the formulation. These experiments were conducted in a water bath at  $37\text{ }^{\circ}\text{C}$  to achieve a membrane surface temperature of  $32\text{ }^{\circ}\text{C}$ . Also, the control experiments (no additional heat ( $32\text{ }^{\circ}\text{C}$ ) and complete system heat ( $45\text{ }^{\circ}\text{C}$ )) were conducted in a water bath at  $37\text{ }^{\circ}\text{C}$  and  $50\text{ }^{\circ}\text{C}$  to achieve a membrane surface temperature of  $32\text{ }^{\circ}\text{C}$  and  $45\text{ }^{\circ}\text{C}$  respectively. In all cases, the experimental duration was 6 hr.

All samples produced were analysed via HPLC to determine the minocycline concentration using the HPLC assay described in Chapter 2, Section 2.2.1.1.

### 3.2.10 Data treatment and statistics

Statistical analysis of all the data was performed using GraphPad Prism version 7.00 for Windows, (GraphPad Software, La Jolla California, USA). The *in vitro* skin permeation and penetration data was initially analysed for normality using the Shapiro-Wilk test to determine if the data was either parametric or non-parametric, where the determined p value was either  $p > 0.05$  or  $p \leq 0.05$ , respectively. The statistical comparison was then performed using a one-way ANOVA with post hoc Tukey's HSD for parametric data (i.e. normally distributed,  $p > 0.05$  determined using the Shapiro-Wilk test) and Kruskal-Wallis test, with post-hoc comparison made using the Dunn's multiple comparison test for non-parametric data (i.e. unequal variances  $p \leq 0.05$  determined using the Shapiro-Wilk test). Statistically significant differences were assumed at 95% confidence level, i.e., when  $p < 0.05$ .

The enhancement ratios ( $E_R$ ) were determined using Equation 3-2 below:

$$E_R = \frac{Q(E)}{Q(C)} \quad \text{Equation 3-2}$$

Where Q (E) and Q (C) are the amount of the drug permeated into and across the skin when using enhancement strategies (i.e. heat and CPEs) and control (no additional heat and CPEs) respectively. The permeation parameters obtained at different temperature (J, Kh,  $D/h^2$  and  $T_L$ ) were then compared to the control (32 °C) using the student t-test or Mann-Whitney U test (when data were found to be not normally distributed). The chosen level of significance was  $p \leq 0.05$ .

### 3.3 Results and Discussion

#### 3.3.1 The effect of magnesium on the saturated solubility of minocycline

The effect of magnesium on the saturated solubility of minocycline in ethanol, propylene glycol and Transcutol® P is shown in Figure 3-1. The saturated solubility of minocycline without magnesium (control, shown as 0 M in Figure 3-1) in the vehicles investigated was in the order of PG > EtOH > TP, with values ranging from  $7.32 \pm 2.16$  mg/mL to  $83.29 \pm 6.45$  mg/mL.

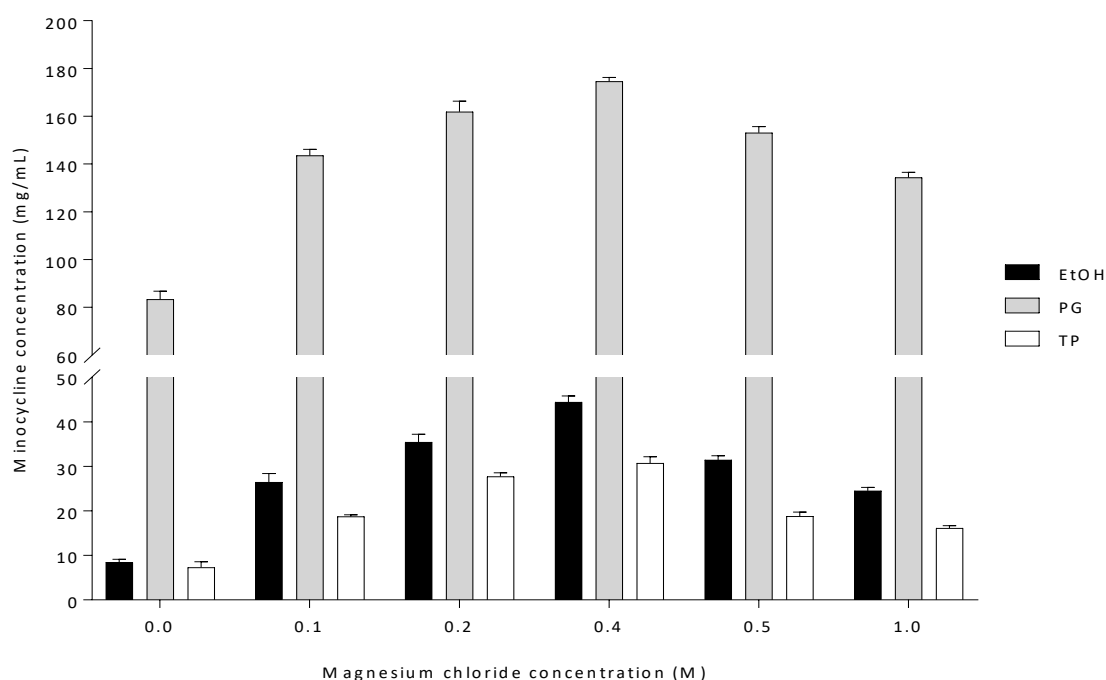


**Figure 3-1: The effect of magnesium chloride concentration on the saturated solubility of minocycline in the dermatological vehicles ethanol (EtOH), propylene glycol (PG) and Transcutol® P (TP) at room temperature. Data represent mean + range (n=3).**

The presence of magnesium increased the saturated solubility of minocycline in all three vehicles (EtOH, PG and TP) across the range of magnesium concentrations (0.1 to 1.0 M) investigated; the increase in solubility was greater in ethanol compared to the other two vehicles. At lower magnesium concentrations “salting in” effect was observed where the solubility of minocycline is enhanced. The optimal enhancement in solubility occurred at 0.4 M magnesium in all three vehicles, which corresponded to a 5.26-fold, 2.10-fold and 4.20-fold increase in solubility in EtOH, PG and TP respectively. At higher magnesium concentrations (> 0.4 M), the solubilities begin to decline but

remained above the saturated solubility of minocycline alone for all three vehicles. A possible explanation for this is that above 0.4 M magnesium “salting out” effect is observed causing minocycline to precipitate out of the solution leading to reduced solubility.

### 3.3.2 *In vitro* skin permeation and distribution across full thickness abdominal skin

The influence of temperature (32 °C and 45 °C) on the skin permeation and distribution of minocycline from different hydrophilic and hydrophobic dermatological vehicles was investigated. Hydrophilic vehicles studied were EtOH, IPA, PG, and TP all containing magnesium (to improve chemical stability of minocycline in these vehicles) and EtOH and PG without magnesium (to determine the influence of magnesium on minocycline permeation). The hydrophobic vehicles examined included DPA, GTCC and IPM. Additionally, the binary systems (1:1) IPA: DPA and TP: DPA with magnesium were tested to investigate synergy between the vehicles and synergy with heat. These binary systems were selected based on solvent compatibility tests which showed them to be miscible with each other and magnesium. The permeation profiles and skin distribution of minocycline from the different vehicles across full thickness human abdominal skin at 32 °C and 45 °C are depicted in Figure 3-2(a-b) and Figure 3-3(a-b) respectively.

At normal physiological skin temperature (32 °C), minocycline was seen in the receiver fluid at early time points when delivered from all the vehicles except for EtOH (Mg<sup>2+</sup>), PG (Mg<sup>2+</sup>) and TP (Mg<sup>2+</sup>), for which no minocycline was detected in the receiver fluid for the duration of the experiment [Figure 3-2(a)]. The cumulative amount of minocycline delivered at 24 hr ( $Q_{24}$ ), from both EtOH and PG was much larger in comparison to the other vehicles studied. However, delivery from IPA (Mg<sup>2+</sup>), IPA: DPA (Mg<sup>2+</sup>), TP: DPA (Mg<sup>2+</sup>) and the hydrophobic vehicles (DPA, IPM, and GTCC) were similar. The average fluxes (Table 3-2) were in the order of EtOH > PG > IPA: DPA (Mg<sup>2+</sup>) > TP: DPA (Mg<sup>2+</sup>) > IPA (Mg<sup>2+</sup>) > DPA > IPM > GTCC, with flux values ranging from  $0.08 \pm 0.01 \mu\text{g}/\text{cm}^2/\text{hr}$  to  $2.31 \pm 0.17 \mu\text{g}/\text{cm}^2/\text{hr}$ . The average flux could not be calculated for EtOH (Mg<sup>2+</sup>), PG (Mg<sup>2+</sup>) and TP (Mg<sup>2+</sup>) as minocycline was not detected in the receiver fluid when delivered from these vehicles.

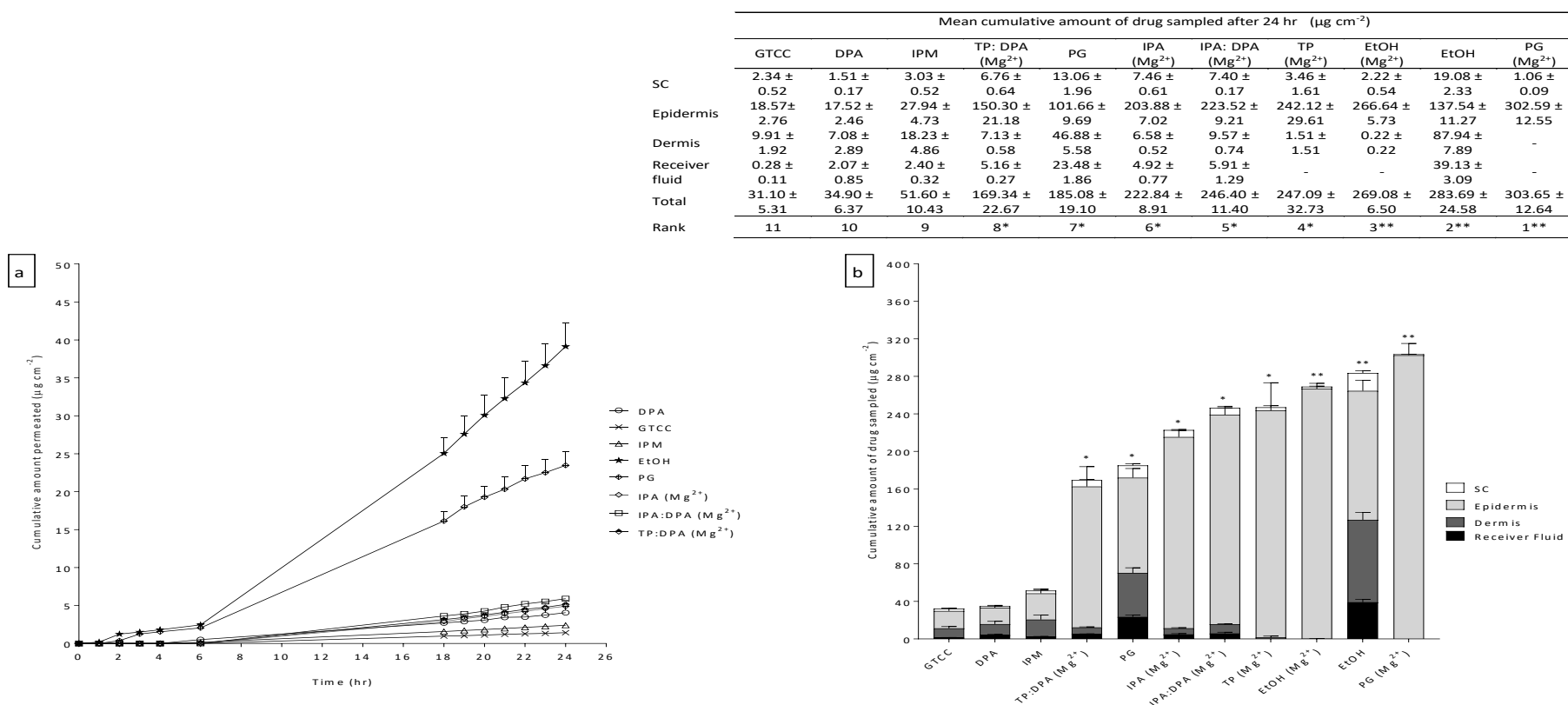


**Figure 3-2: Mean cumulative amount of minocycline (a) permeated across human abdominal skin at 32 °C over 24 hr from various vehicles (b) recovered from the stratum corneum (SC), epidermis and dermis at the end of the permeation study.** Minocycline was applied at a dose of 0.5 mL  $\text{cm}^{-2}$  to the skin surface in an equilibrated saturated suspension for each vehicle. Hydrophobic vehicles tested were Diisopropyl adipate (DPA), Crodamol GTCC (GTCC), Isopropyl myristate (IPM). Hydrophilic vehicles tested were Ethanol (EtOH), Isopropyl alcohol (IPA), Propylene glycol (PG) and Transcutol® P (TP) all containing magnesium ( $\text{Mg}^{2+}$ ): minocycline in a 1:1 ratio by weight. For comparative purposes EtOH and PG without magnesium were tested. The binary systems (1:1) IPA: DPA and TP: DPA were also investigated and contained the same 1:1 ratio of minocycline and magnesium. All points are mean + SEM of n=6 diffusion cells. Minocycline was not detected in the receiver fluid when delivered from EtOH ( $\text{Mg}^{2+}$ ), PG ( $\text{Mg}^{2+}$ ) and TP ( $\text{Mg}^{2+}$ ) (LOD: 0.21  $\mu\text{g/mL}$  and LOQ: 0.64  $\mu\text{g/mL}$ ). \*\* denotes a significant difference in total amount recovered compared to vehicles ranked 9<sup>th</sup> and higher. \* denotes a significant difference in total amount recovered compared to vehicles ranked 9<sup>th</sup> and higher.

A possible explanation for the greater delivery into the receiver from EtOH and PG without magnesium compared to the hydrophobic vehicles (DPA, GTCC and IPM) could be due to the difference in minocycline solubility in these vehicles (See Chapter 2 Section 2.3.2.2 for solubility data). Solvents can enhance drug fluxes of permeants by increasing; the solubilities of the permeants in the applied solvents, the absorption of the solvents into the SC and the solubilities and diffusivities of the permeants in the SC (Cross, Pugh, Hadgraft, & Roberts, 2001; Q. Zhang, Li, Liu, & Roberts, 2013; Q. Zhang, Li, & Roberts, 2011).

Minocycline has been reported to form a complex with magnesium (Piccariello, 2013; Wessels et al., 1998), which may significantly increase the molecular weight (size) of the complex to more than 500 Da. Therefore, for EtOH ( $Mg^{2+}$ ), PG ( $Mg^{2+}$ ) and TP ( $Mg^{2+}$ ), the increase in the size of the complex compared to the free drug could potentially decrease its transport across skin. A molecular weight less than 500 Da is ideal for a drug to be delivered passively across the SC (Bos & Meinardi, 2000).

However, this retarded delivery was absent when minocycline was delivered from IPA ( $Mg^{2+}$ ), as minocycline ( $4.92 \pm 0.77 \mu\text{g}/\text{cm}^2$ ) was detected in the receiver fluid. Possible explanations for these findings are: (i) the affinity of magnesium for minocycline is reduced in IPA compared to EtOH, PG and TP, or (ii) the stoichiometry of magnesium and minocycline is different in IPA compared to the other vehicles, resulting in the production of a smaller complex which is capable of diffusing and partitioning into the skin tissue more easily (iii) IPA is a better enhancer for delivering minocycline. Additionally, delivery from the binary systems IPA: DPA ( $Mg^{2+}$ ) and TP: DPA ( $Mg^{2+}$ ) lead to the detection of minocycline in the receiver fluid. The combination of DPA with IPA and TP was tested to examine if they acted synergistically to modify the SC barrier producing an enhanced penetration effect compared to DPA alone. However, in this study the no synergy was found between the IPA: DPA and TP: DPA in comparison to neat DPA.

With regards to minocycline skin tissue concentrations [Figure 3-2(b)], the vehicles investigated delivered different amounts of drug into the skin. The hydrophilic vehicles produced significantly higher tissue concentrations (sum of drug recovered from the SC, epidermis and dermis) compared to the hydrophobic vehicles, with values ranging between 303 and 30  $\mu\text{g}/\text{cm}^2$ . The hydrophilic vehicles produced between 3.3 to 9.9-fold increases in the amount of minocycline recovered from the skin tissue compared to the hydrophobic vehicles. Also, at 32 °C most of the drug was recovered from the epidermis for all the vehicles investigated, with this difference in tissue concentration between the epidermis and dermis being considerably more noticeable for the vehicles containing magnesium (EtOH and PG). This suggests that the presence of magnesium may have enhanced localisation of minocycline in the epidermis. This increased drug accumulation in the epidermis unlikely to be beneficial for the treatment of acne as delivery into the dermis/pilosebaceous units is more advantageous.

Additionally, the presence of magnesium significantly reduced the amount of minocycline recovered from the dermis for ethanol, with recovery values of  $87.94 \pm 7.88 \mu\text{g}/\text{cm}^2$  and  $0.22 \pm 0.22 \mu\text{g}/\text{cm}^2$  for EtOH and EtOH ( $\text{Mg}^{2+}$ ) respectively. Likewise, delivery from PG ( $\text{Mg}^{2+}$ ) resulted in no minocycline being recovered from the dermis, whilst delivery from PG resulted in a recovery value of  $46.88 \pm 5.58 \mu\text{g}/\text{cm}^2$ . Due to the polar nature of minocycline, there is a potential for hydrogen bonding to occur with either the keratin in the keratinocytes or even to the ceramide groups of the intercellular lipids. Such localised bonding with the skin lipids might lead to minocycline partitioning into and retention within the epidermis. The ability of doxycycline (a tetracycline antibiotic and polar compound) to undergo hydrogen bonding with skin has been previously reported by Banning & Heard (2002). The presence of hydrogen bonding groups on a penetrant is known to dramatically retard its permeation across the SC *in vitro* (Roberts, Pugh, & Hadgraft, 1996).

With heat (45 °C), minocycline was detected in the receiver fluid from all the vehicles investigated, although when delivered from EtOH (Mg<sup>2+</sup>), PG (Mg<sup>2+</sup>) and TP (Mg<sup>2+</sup>) minocycline was only detected in the receiver fluid from 20 hr onwards. Thus, the average flux could not be calculated for these vehicles. This result was similar to the experiments at 32 °C, where minocycline was not detected in the receiver fluid when delivered from these dermatological vehicles containing magnesium. This suggests that enhanced penetrant interaction with skin tissue due to the presence of magnesium also occurs at the higher temperature (45 °C).

At the higher temperature (45 °C) the rank of the average fluxes (Table 3-6) for each of the vehicles remained the same for experiments at the physiological skin temperature (32 °C), although the average flux values were significantly increased between 1.8 to 5.5-fold. The greatest enhancement in flux with heat (45 °C) was achieved for IPA: DPA (Mg<sup>2+</sup>) and the lowest for EtOH. The effect of increased membrane temperature (37 °C to 45 °C) on the diffusion of three model penetrants, methyl paraben, butyl paraben and caffeine delivered from aqueous suspensions was shown to induce a maximum of 3-fold enhancement (Akomeah et al., 2004). This was similar to the magnitude of enhancement seen in this study.

Additionally, at the higher temperature, significantly greater minocycline concentrations were recovered from the skin tissues compared to experiments at 32 °C when delivered from hydrophilic vehicles, with recovery values ranging between 438 to 7531 µg/cm<sup>2</sup>. This corresponded to between 2.1 to 45.9-fold rise in the total skin tissue concentrations compared to experiments at 32 °C. This is different to previous reports on the effect of elevated temperature (from 32 °C to 45 °C) on skin retention of hydrophilic drugs such as caffeine, where the increase in temperature failed to enhance drug uptake into the skin tissue significantly (Akomeah et al., 2004). However, a reason for this difference could be due to the fact that caffeine was delivered using PBS as the vehicle, whereas in this study various dermatological vehicles used as CPEs (EtOH, PG, IPA and TP) were employed, which further enhanced minocycline delivery with heat.

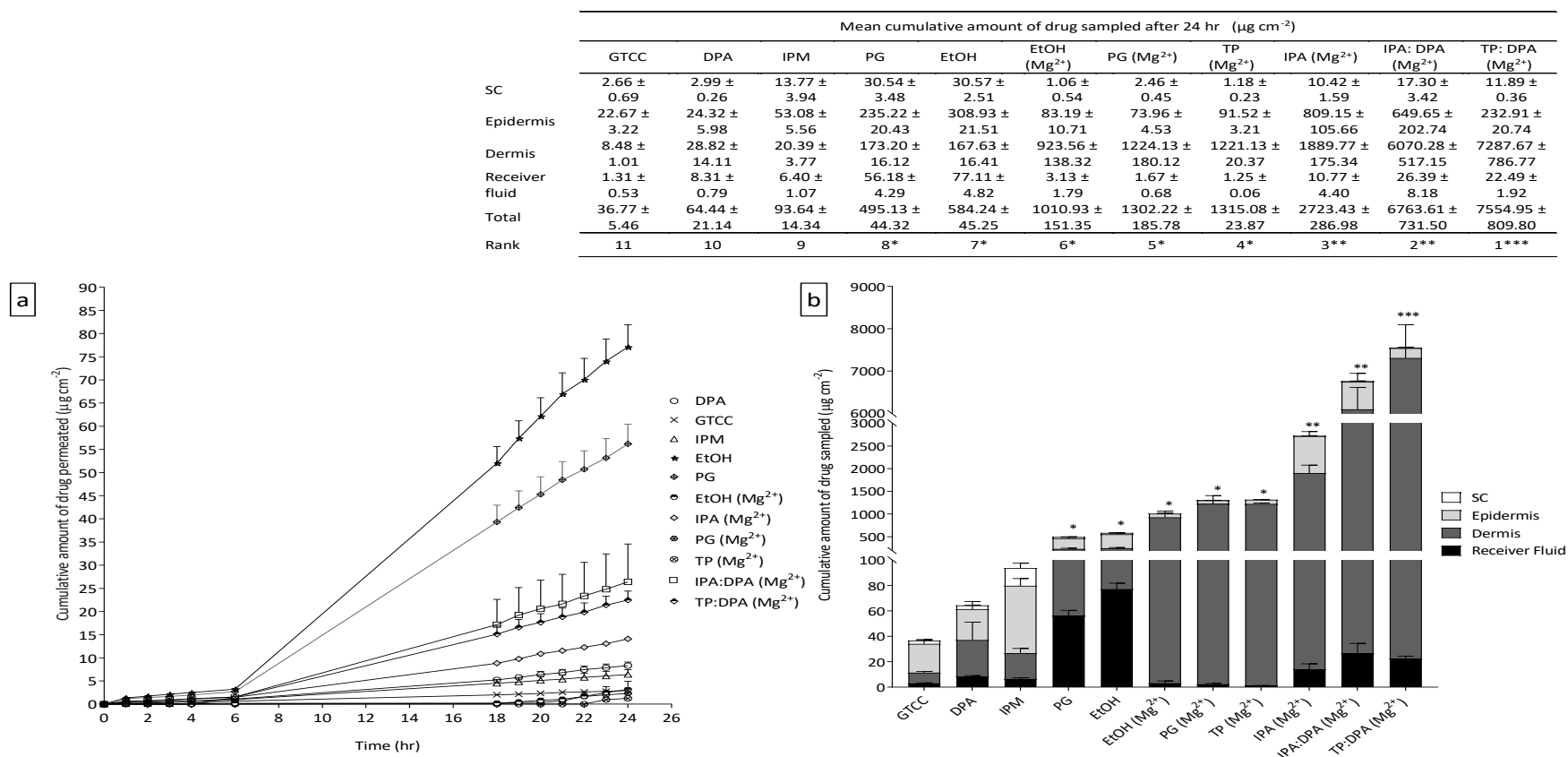


**Figure 3-3: Mean cumulative amount of minocycline (a) permeated across full thickness human abdominal skin at 45 °C over 24 hr from various vehicles (b) recovered from the stratum corneum (SC), epidermis and dermis at the end of the permeation study.** Minocycline was applied at a dose of 0.5 mL cm<sup>-2</sup> to the skin surface in an equilibrated saturated suspension for each vehicle. Hydrophobic vehicles tested were Diisopropyl adipate (DPA), Crodamol GTCC (GTCC), Isopropyl myristate (IPM). Hydrophilic vehicles tested were Ethanol (EtOH), Isopropyl alcohol (IPA), Propylene glycol (PG) and Transcutol P (TP) all containing magnesium ( $\text{Mg}^{2+}$ ): minocycline in a 1:1 ratio by weight. For comparative purposes EtOH and PG without magnesium were tested. The binary systems (1:1) IPA: DPA and TP: DPA were also investigated and contained the same 1:1 ratio of minocycline and magnesium. All points are mean + SEM of n=6 diffusion cells. \*\*\* denotes a significant difference in total amount recovered compared to vehicles ranked 8<sup>th</sup> and higher. \*\* denotes a significant difference in total amount recovered compared to vehicles ranked 9<sup>th</sup> and higher. \* denotes a significant difference in total amount recovered compared to vehicle ranked 9<sup>th</sup> and higher.

The greatest and lowest enhancement was achieved when delivered from TP: DPA ( $Mg^{2+}$ ) and EtOH respectively. Also, the hydrophilic vehicles and the binary systems produced 86 to 222-fold increases in the total skin tissue concentrations compared to the hydrophobic vehicles. Again, the poor minocycline solubility in these hydrophobic vehicles may be a possible explanation for this trend. The rank of the vehicles in terms of total delivery of minocycline into the skin tissue was TP: DPA ( $Mg^{2+}$ ) > IPA: DPA ( $Mg^{2+}$ ) > IPA ( $Mg^{2+}$ ), TP ( $Mg^{2+}$ ) > PG ( $Mg^{2+}$ ) > EtOH ( $Mg^{2+}$ ) > EtOH > PG > IPM > DPA > GTCC. Moreover, for EtOH ( $Mg^{2+}$ ), PG ( $Mg^{2+}$ ) and TP ( $Mg^{2+}$ ) the distribution of minocycline across the epidermis and dermis was altered significantly with heat (45 °C) as larger amounts of drug was recovered from the dermis compared to the experiments at 32 °C where little or no drug was recovered when delivered from these vehicles.

The higher amounts of minocycline (with magnesium or alone) delivered from the hydrophilic vehicles and binary systems relative to the hydrophobic vehicles, may reflect possible differences in the permeation pathway and/or mechanism by which minocycline is transported across skin. To provide a mechanistic insight into the role of heat and CPEs in enhancing percutaneous absorption, the experimental permeation data was modelled using Fick's first law (Chapter 1, Equation 1-4). According to this equation the flux of a drug across the membrane under steady state conditions ( $J$ ) is directly proportional to the partition ( $K$ ) and diffusion ( $D$ ) coefficient of the solute. Since the  $J$  and the lag time,  $T_L$  (defined as time taken to reach steady state, Equation 1-7) can be readily determined from the diffusion profile (plot of the cumulative amount permeated per unit area ( $Q$ ) vs time ( $t$ )), as the gradient and x-intercept of the linear portion of the graph respectively,  $D$  and  $K$  can then theoretically be obtained as illustrated in Equations 3-3 and 3-4 respectively. Since the diffusional pathlength across the SC ( $h$ ) is unknown (Williams, 2003),  $K$  and  $D$  cannot be directly calculated, but can be calculated as pathlength normalised values ( $Kh$  and  $D/h^2$ ). Conducting *in vitro* experiments for less than this period is known to result in errors of  $J$  and  $T_L$  estimates. For example, Shah (1993) demonstrated that the percentage error for  $J$  and  $T_L$  was about -60% from their theoretical values when these parameters were calculated over a period equal to one lag time.

$$\frac{D}{h^2} = \frac{1}{6T_L} \quad \text{Equation 3-3}$$

$$K \times h = 6 \times \left( \frac{J}{C_V} \right) \times T_L \quad \text{Equation 3-4}$$

To avoid inaccuracies in the determination of  $Kh$  and  $D/h^2$ , steady state drug flux must be attained during the duration of the experiment. Steady state flux for permeants is achieved after approximately three lag times ( $2.7 T_L$ ) (Crank, 1975).

The use of vehicle concentration ( $C_V$ ) in calculating the  $Kh$  was expected to lead to under estimation of the  $Kh$  values, due to significant differences in minocycline solubility in the hydrophilic and hydrophobic vehicles. Therefore,  $C_V$  in Equation 3-4 was replaced with the thermodynamic activity ( $\alpha$ ) instead. It is well established that the rate of permeation through the skin is driven by the thermodynamic activity and it is not necessarily directly linked to drug concentration in the vehicle (Higuchi, 1960). This implies that the use of saturated suspensions of the permeant in different vehicles (i.e. with the permeant at its maximum thermodynamic activity,  $\alpha = 1$ ) would provide identical flux irrespective of the concentration applied (when vehicle components do not interact with the membrane) as previously demonstrated experimentally by Twist & Zatz, (1988). Based on these previous findings, it was decided to use in the present work the thermodynamic activity of minocycline rather than its specific solubility in the vehicle, to model the experimental data obtained at both temperatures (32 °C and 45 °C).

For EtOH ( $Mg^{2+}$ ), PG ( $Mg^{2+}$ ) and TP ( $Mg^{2+}$ ) at both 32 °C and 45 °C, steady-state conditions were not achieved over the duration of the study (24 hr), thus making the use of Fick's first law inappropriate to analyse this permeation data. The permeation parameters calculated for the delivery of minocycline through human abdominal skin from the different dermatological vehicles (where steady state was achieved) at 32 °C and 45 °C are listed in Table 3-2.

**Table 3-2: Skin permeation parameters measured for minocycline in various dermatological vehicles (some of which contain magnesium to stabilise minocycline). Cumulative amount permeated ( $Q_{24}$ ), average flux ( $J$ ), pathlength normalised partition coefficient ( $Kh$ ), pathlength normalised diffusion coefficient ( $D/h^2$ ) and lag time ( $T_L$ ) were measured for both physiological skin temperature (32 °C) and elevated skin temperature (45 °C) using Fick's first law (mean  $\pm$  SEM, n=6). \* denotes significant difference in the parameter at 45 °C for each vehicle compared to the same vehicle at 32 °C.**

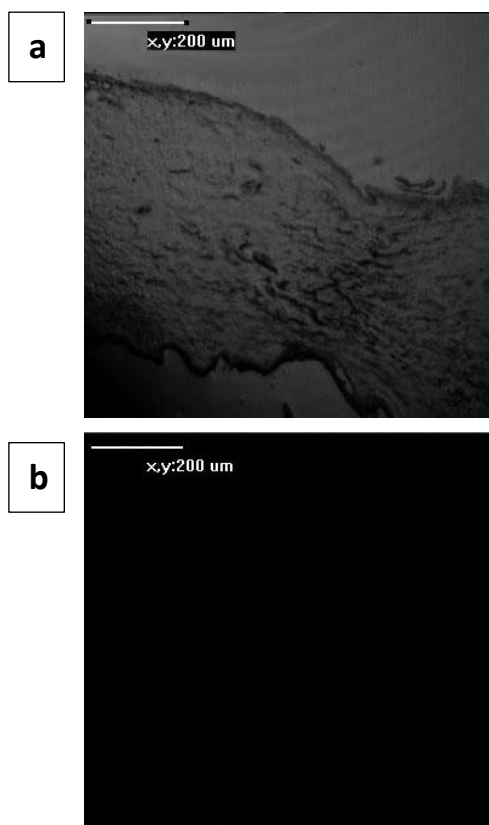
Vehicle	Membrane temperature (°C)	$J$ ( $\mu\text{g}/\text{cm}^2/\text{hr}$ )	$E_R$	$Q_{24}$	$E_R$	$T_L$ (hr)	$D/h^2$ ( $\times 10^{-2}\text{hr}^{-1}$ )	$E_R$	$Kh$ (cm)	$E_R$
DPA	32 °C	0.25 $\pm$ 0.05	2.04	4.06 $\pm$ 0.85	2.04	7.87 $\pm$ 0.24	2.12 $\pm$ 0.69	1.27	11.81 $\pm$ 0.36	1.60
	45 °C	0.51 $\pm$ 0.05*		8.31 $\pm$ 0.79*		6.19 $\pm$ 0.14*	2.69 $\pm$ 1.19		18.94 $\pm$ 0.43*	
GTCC	32 °C	0.08 $\pm$ 0.01	2.25	1.42 $\pm$ 0.11	2.08	4.66 $\pm$ 0.97	3.58 $\pm$ 0.17	1.00	2.24 $\pm$ 0.47	2.25
	45 °C	0.18 $\pm$ 0.02*		2.96 $\pm$ 0.53*		4.67 $\pm$ 0.67	3.57 $\pm$ 0.25		5.04 $\pm$ 0.72*	
IPM	32 °C	0.14 $\pm$ 0.02	2.29	2.40 $\pm$ 0.32	2.67	6.94 $\pm$ 0.84	2.40 $\pm$ 0.20	1.84	5.83 $\pm$ 0.71	1.25
	45 °C	0.32 $\pm$ 0.05*		6.40 $\pm$ 1.07*		3.78 $\pm$ 0.39*	4.41 $\pm$ 0.43*		7.26 $\pm$ 0.75	
EtOH	32 °C	2.31 $\pm$ 0.17	1.80	39.13 $\pm$ 3.09	1.97	6.92 $\pm$ 0.55	2.41 $\pm$ 0.30	1.19	95.91 $\pm$ 7.62	1.51
	45 °C	4.16 $\pm$ 0.25*		77.11 $\pm$ 4.82*		5.82 $\pm$ 0.65	2.86 $\pm$ 0.26		120.06 $\pm$ 16.22	
PG	32 °C	1.19 $\pm$ 0.16	2.30	23.48 $\pm$ 1.86	2.40	4.52 $\pm$ 0.69	3.69 $\pm$ 0.24	1.22	32.27 $\pm$ 4.93	1.88
	45 °C	2.74 $\pm$ 0.15*		56.18 $\pm$ 4.29*		3.69 $\pm$ 0.96	4.52 $\pm$ 0.17		60.66 $\pm$ 15.78	
IPA(Mg <sup>2+</sup> )	32 °C	0.33 $\pm$ 0.07	3.42	4.92 $\pm$ 0.77	2.86	8.33 $\pm$ 1.03	2.00 $\pm$ 0.16	1.21	16.49 $\pm$ 2.04	2.83
	45 °C	1.13 $\pm$ 0.14*		14.09 $\pm$ 2.40*		6.88 $\pm$ 0.77	2.42 $\pm$ 0.22		46.65 $\pm$ 5.22*	
IPA: DPA(Mg <sup>2+</sup> )	32 °C	0.39 $\pm$ 0.10	5.59	5.91 $\pm$ 1.29	4.47	8.83 $\pm$ 0.30	1.89 $\pm$ 0.56	1.48	20.66 $\pm$ 0.70	3.78
	45 °C	2.18 $\pm$ 0.37*		26.39 $\pm$ 8.18*		5.97 $\pm$ 0.67*	2.79 $\pm$ 0.25*		78.09 $\pm$ 8.76*	
TP: DPA(Mg <sup>2+</sup> )	32 °C	0.34 $\pm$ 0.02	3.35	5.16 $\pm$ 0.27	4.03	8.73 $\pm$ 1.21	1.91 $\pm$ 0.14	1.70	17.81 $\pm$ 2.47	1.98
	45 °C	1.14 $\pm$ 0.09*		20.82 $\pm$ 1.71*		5.15 $\pm$ 0.55*	3.24 $\pm$ 0.30*		35.23 $\pm$ 3.76*	

At physiological skin temperature (32 °C), the pathlength normalised partition coefficient ( $Kh$ , Table 3-2) for minocycline was found to be different between the different dermatological vehicles investigated. It is conceivable that the physicochemical properties for each vehicle (i.e. log  $P$  and molecular weight) contributed to differences in membrane partition coefficients (Cross et al., 2001), with the more hydrophilic and smaller vehicles showing greater partitioning into the skin compared to the hydrophobic and larger vehicles (e.g. ethanol and propylene glycol compared to GTCC and IPM). The application of a moderate level of heat to human abdominal skin significantly increased the pathlength normalised partition coefficient ( $Kh$ ) for all the vehicles except IPM. The increase in  $Kh$  ranged between 1.25 cm to 3.78 cm for all the vehicles investigated when the temperature was increased from 32 °C to 45 °C. The greatest enhancement was seen with IPA: DPA ( $Mg^{2+}$ ) and lowest with IPM.

In these studies, the pathlength normalised diffusion coefficient ( $D/h^2$ ) for minocycline was found to be similar for both the hydrophilic and hydrophobic vehicles. The increase in temperature to 45 °C was found to significantly increase the normalised diffusion coefficient of minocycline when delivered from DPA, IPM, IPA: DPA ( $Mg^{2+}$ ) and TP: DPA ( $Mg^{2+}$ ). The presence of DPA/IPM may be responsible for the increase in  $D/h^2$  as the hydrophilic vehicles (alone) at 45 °C did not significantly increase the diffusivity of minocycline. In these vehicles, improvement in  $D/h^2$  was associated with a significant reduction in the lag time. One possible explanation is that both DPA and IPM in conjunction with heat ( $\leq 45$  °C) increased SC lipid disorder and reduced the resistance encountered by the drug as it travels across the SC. This is in accordance with the literature as both DPA and IPM have been shown to increase drug flux by improving its diffusivity across the SC, which is usually accompanied by reduced lag times (Brinkmann & Müller-Goymann, 2005; Takahashi, Sakano, Numata, Kuroda, & Mizuno, 2002a; Tuntiyasawadikul, Limpongsa, Jaipakdee, & Sripanidkulchai, 2014). In general, the normalised diffusion coefficient was improved between 1.21 to 1.84-fold from all the vehicles investigated. The largest and lowest enhancements were observed for IPM and IPA ( $Mg^{2+}$ ) respectively. Whereas, for GTCC no improvements in  $D/h^2$  was observed. Overall, the effect on  $Kh$  seems to be greater than  $D/h^2$ .

### **3.3.3 Distribution of minocycline and magnesium-minocycline complex across full thickness human abdominal skin: confocal laser scanning microscopy studies**

The penetration of minocycline delivered from hydrophilic dermatological vehicles (ethanol and propylene glycol with and without magnesium) into full thickness human abdominal skin was visualised by CLSM. It was ensured that there was no auto fluorescence of human skin at the selected wavelength as demonstrated in Figure 3-4(a-b), which shows both the transmission and fluorescence micrographs of untreated skin sections. Figure 3-5(a) shows the skin distribution of minocycline in ethanol at physiological and elevated skin temperatures, 32 °C and 45 °C respectively. At physiological skin (32 °C) temperature Fickian diffusion was observed as more drug accumulation in the uppermost regions of the skin was observed, with less drug seen in the lower regions. At the elevated skin temperature of 45 °C the distribution of the drug within the skin was altered, so that more drug was delivered to the deeper regions in comparison to the lower skin temperature. In Figure 3-5(b), brighter fluorescence images were produced with EtOH (Mg<sup>2+</sup>) at both 32 °C and 45 °C compared to EtOH at the same temperature, which indicates that the presence of magnesium produced greater drug accumulation in the skin tissue. A similar trend was observed for both PG and PG (Mg<sup>2+</sup>) at both temperatures as shown in Figure 3-5 (c-d). In general, images with higher fluorescence intensity were produced at 45 °C compared to 32 °C. This is an indication of the delivery of higher drug tissue concentrations with the elevated temperature. The high fluorescent intensity combined with the skin permeation and distribution data suggests that drug tissue binding may be occurring. Doxycycline (a tetracycline antibiotic) has been shown to bind to both isolated human SC and epidermal tissue (Banning & Heard, 2002). Therefore, given the structural similarity of minocycline to doxycycline it is likely that minocycline will act in a comparable manner. Additionally, the higher fluorescence intensity observed with magnesium is indicative of the potential of local tissue targeting with magnesium containing formulations, which could be extremely beneficial for acne treatment.

**Control- Untreated Skin**

**Figure 3-4: Untreated (control) human abdominal skin sections (a) Transmitted light image (b) fluorescence image. Representative sections were selected. All skin sections were cut to 30 μm and visualised using a confocal laser scanning microscope with a laser line of 408 nm and an emission wavelength of  $\geq 500$  nm. No formulation was applied to the skin and the Franz cell was placed in water bath at 37 °C. Images taken from n=1 diffusion cell. Scale bars indicate 200 μm.**

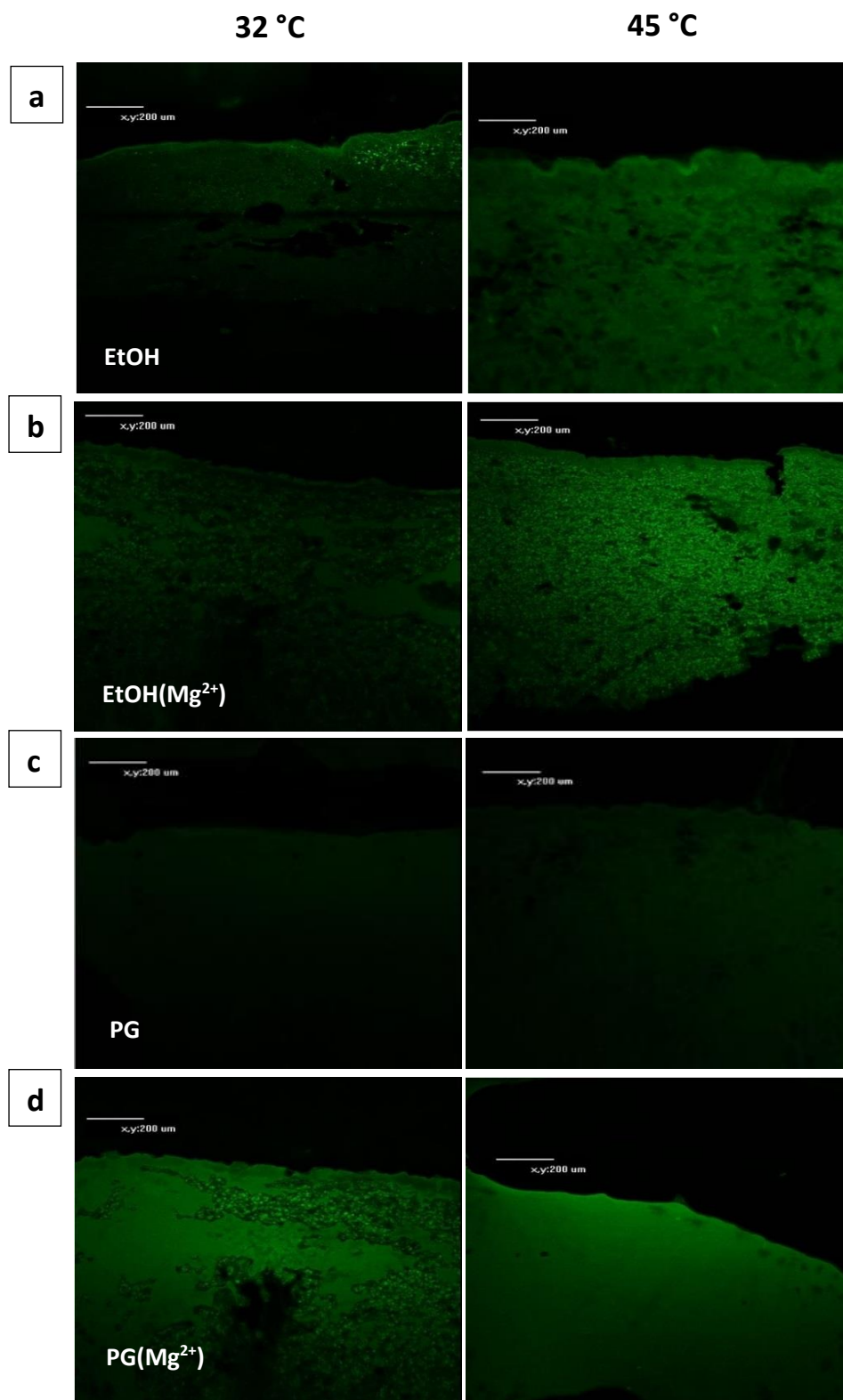


**Figure 3-5:** Human abdominal skin sections treated with minocycline in different dermatological vehicles (with and without magnesium) at 32 °C and 45 °C (a) EtOH (b) EtOH(Mg<sup>2+</sup>) (c) PG (d) PG(Mg<sup>2+</sup>). Representative sections for each group were selected. All skin sections were cut to 30  $\mu\text{m}$  and visualised using a confocal laser scanning microscope with a laser line of 408 nm and an emission wavelength of  $\geq 500$  nm. Formulations were applied to the skin at 0.5 mL cm<sup>-2</sup> for 24 hr. All treatment groups consisted of n=1 diffusion cell. Scale bars indicate 200  $\mu\text{m}$ .

### 3.3.4 Determination of magnesium and minocycline stoichiometry

To gain a better understanding of the interaction between magnesium and minocycline the method of continuous variations (Job's plot method) was employed. Ethanol was chosen as the vehicle to be investigated because the presence of magnesium enhanced the solubility of minocycline to the greatest extent in this dermatologically relevant vehicle. The stoichiometry of the magnesium-minocycline complex was determined using UV-Vis absorbance measurements. To use the Job's method to determine binding stoichiometry for a metal ion and ligand interaction, the free and the metal-ion-bound ligand should have significantly different absorbance at a chosen wavelength at which the metal ion has no absorbance. In this case 380 nm was selected for this reason as shown in the UV-Vis spectra obtained for minocycline and magnesium-minocycline complex (1:1 molar ratio) in Figure 3-6.

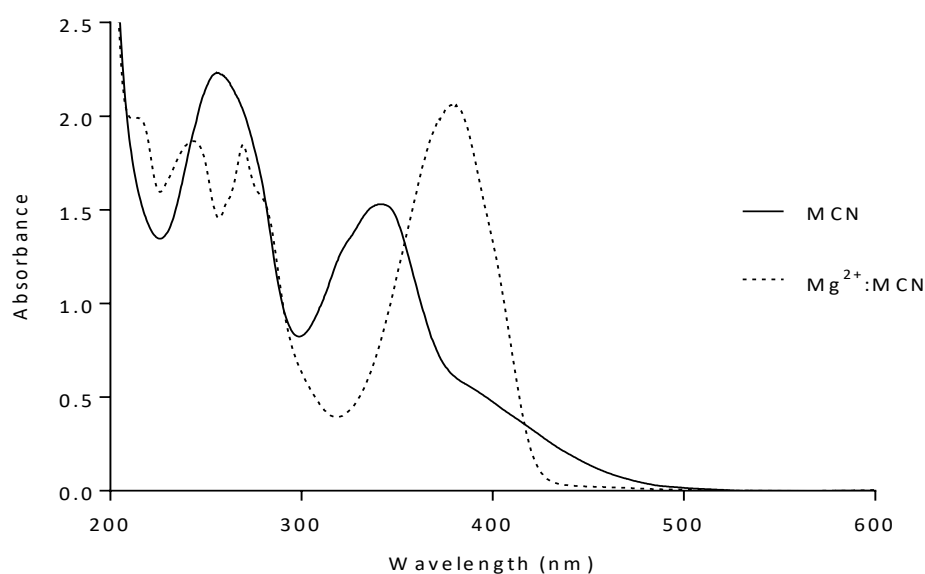


**Figure 3-6: UV-Vis spectra of minocycline (MCN) and the complex magnesium-minocycline (1:1 molar ratio) in ethanol from 200 to 600 nm, indicating the greatest difference in absorbance between free and complexed minocycline occurs at 380 nm.**

Absorbance readings at 380 nm were determined for a series of magnesium and minocycline mixtures with increasing magnesium molar fraction but a constant total magnesium and minocycline concentration. A corresponding series of mixtures of minocycline without magnesium were prepared

to determine the change in absorbance brought about by the formation of the magnesium-minocycline complex. The change in absorbance was plotted as a function of the magnesium molar fraction. The Job's Plot for magnesium binding to minocycline is shown in Figure 3-7.

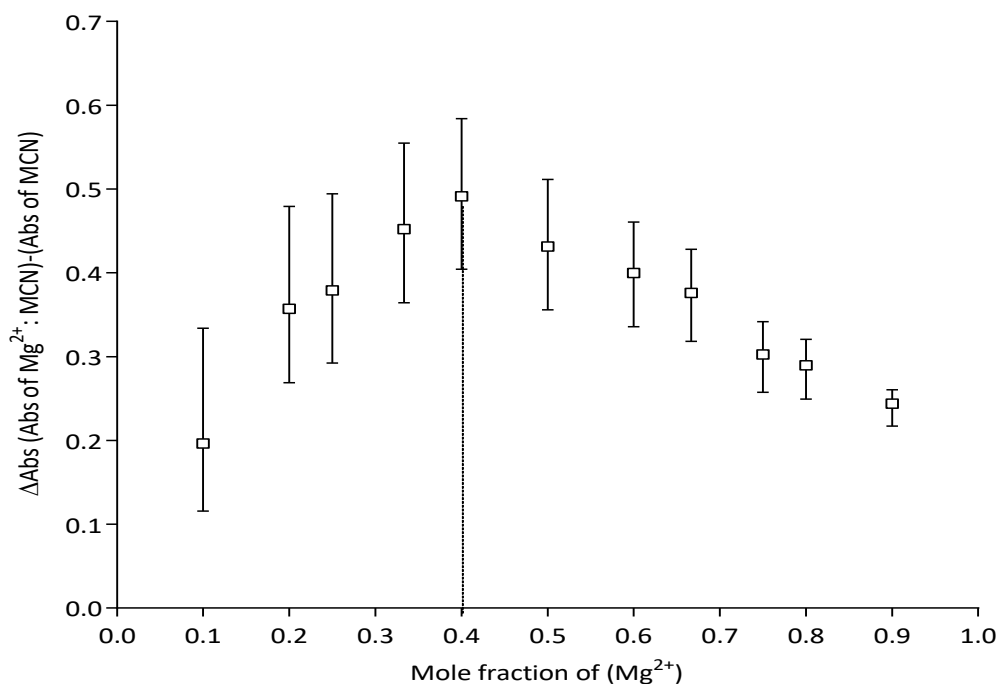


**Figure 3-7: Continuous variation plot (Job Plot) for the complexation of magnesium ( $Mg^{2+}$ ) and minocycline (MCN) in ethanol from UV-Vis absorbance measurements at room temperature ( $\lambda = 380$  nm). The total concentration of  $Mg^{2+}$  and MCN was  $3.0 \times 10^{-4}$  M. Data represent mean  $\pm$  range ( $n=3$ ).**

A 0.4 mole fraction of  $Mg^{2+}$  produced the maximum  $\Delta Abs$  (peak on the Job Plot), which suggests that magnesium formed a 2:3 complex with minocycline within the range of concentrations investigated. However, the Kruskal Wallis test (with Dunn's multiple comparisons test) revealed there was no statistically significant differences between the  $\Delta Abs$  produced at magnesium mole fractions of 0.33, 0.40 and 0.50, which correspond to a 1:2, 2:3 and 1:1 magnesium-minocycline stoichiometry respectively. Therefore, it is uncertain whether a 2:3 magnesium-minocycline complex is formed instead of 1:2 / 1:1 magnesium-minocycline complex. Additionally, it is possible that more than one complex type can exist simultaneously, as tetracyclines have been reported from both 1:2 and 1:1 metal-tetracycline complexes (Doluisio & Martin, 1963; Piccariello, 2013; Wessels et al., 1998). Unfortunately, the Job's method is unable to reveal if more than one complex is present (Brynn

Hibbert & Thordarson, 2016). Nevertheless, it can help identify the predominant complex in a solution (Gil & Oliveira, 1990). The determination of the exact structure (and stoichiometry) of the complex are beyond the scope of the current study.

### 3.3.5 Viscosity measurements of minocycline formulations with and without magnesium at 32 °C and 45 °C

The dynamic viscosities of filtered saturated solutions containing magnesium and minocycline (1:1 ratio by weight) and minocycline alone was measured using AR1500ex Rheometer 32 °C and 45 °C, this data is shown below in Table 3-3. All the vehicles with and without magnesium at both 32 °C and 45 °C displayed Newtonian flow (flow curves not shown). All the formulations employed in the viscosity studies were prepared in the same way and the formulations used in the *in vitro* release and permeation studies and contained the same ratio of magnesium and minocycline where appropriate.

**Table 3-3: Viscosities of filtered saturated solutions containing magnesium chloride and minocycline (1:1 ratio by weight) and minocycline alone at 32 °C and 45 °C. The ratio of the binary vehicles is 1:1.**

Formulation	Temperature (°C)	Dynamic viscosity (mPa.S)
EtOH	32	4.82
	45	4.76
EtOH(Mg <sup>2+</sup> )	32	39.04
	45	27.75
PG	32	36.42
	45	22.25
PG(Mg <sup>2+</sup> )	32	156.67
	45	80.57
TP: DPA	32	5.36
	45	5.18
TP: DPA (Mg <sup>2+</sup> )	32	715.83
	45	325.83
IPA: DPA	32	4.71
	45	4.51
IPA: DPA (Mg <sup>2+</sup> )	32	346.23
	45	196.73

Magnesium chloride was observed to increase the viscosity of the formulations evaluated. At 32 °C, this increase in viscosity with magnesium ranged from 4.30 (PG) to 133.55-fold (TP: DPA). Whereas, at 45 °C the rise in viscosity with magnesium was less compared to the lower temperature and ranged

from 3.62 (PG) to 62.90-fold (TP: DPA). Afzal et al. (1989) reported that magnesium chloride increased the viscosity of aqueous solutions, with higher magnesium concentrations increasing viscosity further. When more magnesium is added, the number of molecules in per unit volume increase, which lead to the Van Der Waals Force between different magnesium ions and the vehicle to become stronger. As more magnesium chloride is added a network between the groups are formed leading to increased solvent system viscosity. The effect of temperature on the viscosity of these solutions was also investigated and found to reduce (up to 2.4-fold) with increasing temperature (20 °C to 50 °C) (Afzal, Saleem, & Mahmood, 1989).

From the Stokes Einstein equation (Equation 1-9, Chapter 1 Section 1.7.2.4), viscosity is inversely proportional to temperature. As would be expected, in this experiment increasing the temperature reduced the viscosity of all the formulations investigated. However, the magnitude in the decline in viscosity was observed to be dissimilar for the different formulations tested. For formulations without magnesium the drop-in viscosity ranged from 1.01 to 1.64-fold, with EtOH and PG producing the lowest and greatest fall in viscosity respectively. In contrast, the decline in viscosity ranged from 1.40 to 2.19-fold for the magnesium containing formulations, with EtOH ( $Mg^{2+}$ ) and TP: DPA ( $Mg^{2+}$ ) generating the minimum and maximum drop in viscosity with increased temperature.

### 3.3.6 *In vitro* release studies using cellulose membrane

The incorporation of magnesium chloride into the dermatological vehicles investigated for reasons of improving minocycline stability was shown to alter drug permeation and penetration into the skin (Section 3.3.2). The observed changes in drug permeation and distribution could be due to the increase in vehicle viscosity (with the addition of magnesium chloride) and/or the increase in the size of diffusing species due to the formation of magnesium-minocycline complexes in the vehicles studied, especially if magnesium-minocycline complexes with 2:3 and 1:2 stoichiometries are formed compared to the unbound minocycline. Thus, *in vitro* release studies were conducted to determine the difference in drug release when minocycline is delivered as the complex or the free drug using regenerated cellulose membrane with MWCO of 2000 Da. Whilst, the use of artificial membranes cannot be used to predict solute permeation across the skin barrier as a result of their inability to mimic the structural complexity associated with the SC, it may be used to provide an indication of how easily the drug is released from the vehicle during the development of a dermal or transdermal formulation to aid in the selection process or alternatively as a quality control tool (Flynn et al., 1999). Therefore, in this study cellulose membrane was employed to provide insight into how magnesium (through its effects on size of the diffusing species and viscosity of the formulations) and temperature may affect the skin permeation of minocycline.

The *in vitro* release experiments were performed using saturated systems to ensure equal drug thermodynamic activity (leaving potential of the drug) in the chosen vehicles. This allows the influence of the vehicle, size of the penetrant (magnesium-minocycline complex vs free drug) and heat on drug release to be determined (Al-Khamis, Davis, & Hadgraft, 1986). Higuchi plots at 32 °C and 45 °C were constructed and the gradients equated to release rate constants. A linear relationship ( $R^2 \geq 0.92$ ) was obtained when the cumulative amount of minocycline released from all the vehicles (with and without magnesium at both 32 °C and 45 °C) were plotted against the square root of time. The release rates were thus found to obey the Higuchi equation (root-time kinetics).

The release profiles of minocycline from the different vehicles with and without magnesium at 32 °C and 45 °C are depicted in Figure 3-8(a-b) and the *in vitro* release parameters derived (release rate constants and correlation coefficients) are shown in Tables 3-3 (for the 32 °C data) and 3-4 (for the 45 °C data).

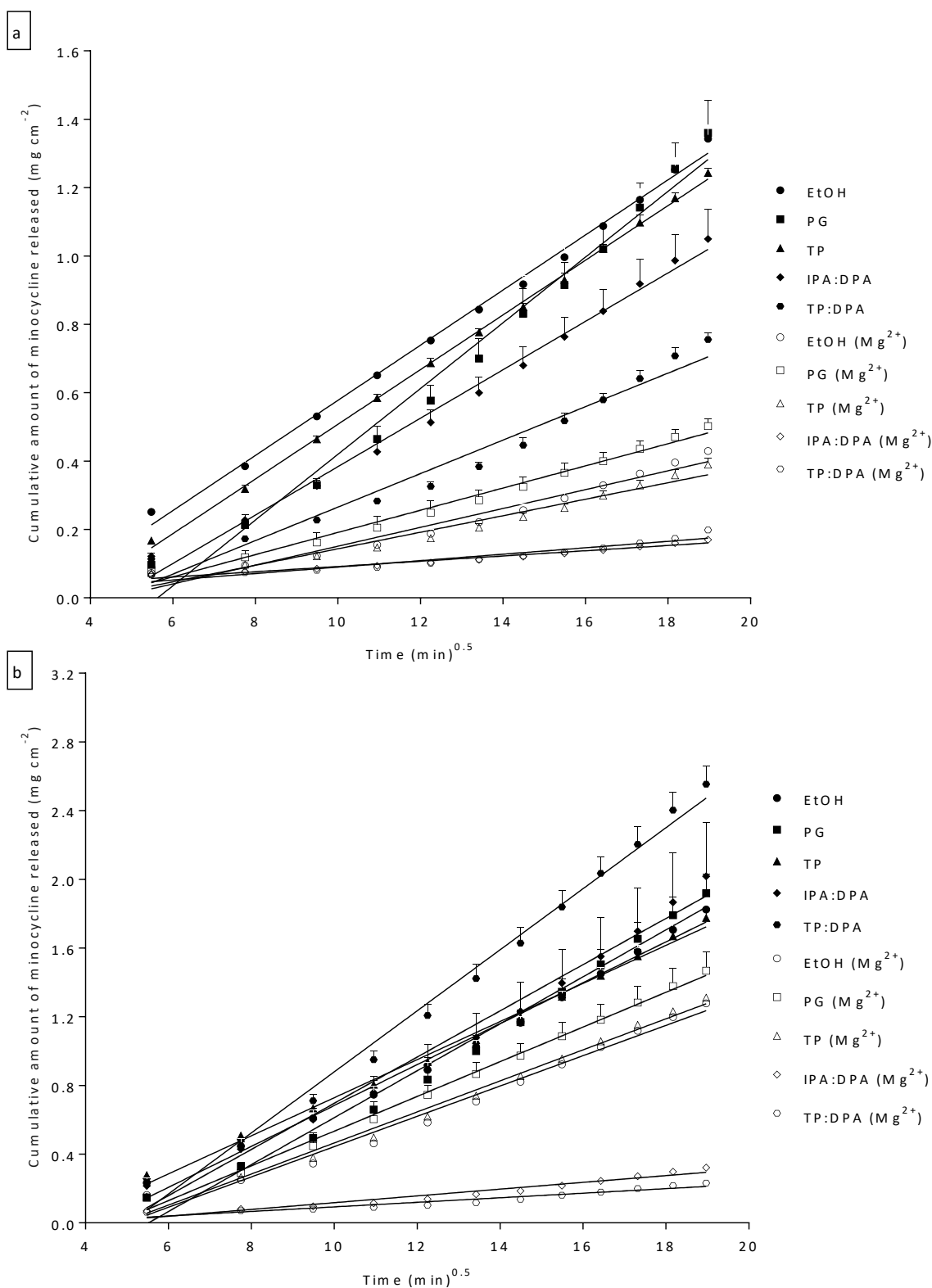


**Figure 3-8:** *In vitro* release profiles (Higuchi plots) of minocycline (a) 32°C and (b) 45 °C across cellulose membrane. Minocycline with and without magnesium was delivered from equilibrated saturated suspensions in various dermatological vehicles. Data represent mean + SEM (n=6).

The release rate of minocycline from all the vehicles investigated at 32 °C were in the order of PG > EtOH > TP > IPA: DPA > TP: IPA > PG(Mg<sup>2+</sup>) > EtOH(Mg<sup>2+</sup>) > TP(Mg<sup>2+</sup>) > TP: DPA(Mg<sup>2+</sup>) > IPA: DPA(Mg<sup>2+</sup>), with release rates ranging from  $9.61 \times 10^{-2} \pm 0.40 \times 10^{-2}$  to  $0.76 \times 10^{-2} \pm 0.03 \times 10^{-2}$  mg/cm<sup>2</sup>/min<sup>1/2</sup>. The release of minocycline from vehicles containing magnesium was significantly slower than from the respective vehicle without magnesium. This suggests that the size of the magnesium – minocycline complex compared to the unbound minocycline maybe an important factor affecting drug release across the cellulose membrane.

In the neat vehicles (EtOH, PG and TP), the presence of magnesium in the system reduced the release rate of minocycline 2.93, 2.96 and 3.32-fold for EtOH, PG and TP respectively. Reduced minocycline release rates were also observed in the binary systems (IPA: DPA and TP: DPA) with magnesium. However, in these systems the effect of magnesium was more pronounced with the release rates reduced by 5.20 and 9.32-fold for TP: DPA and IPA: DPA respectively. In all cases, the differences between the same respective vehicle with and without magnesium were statistically significant.

**Table 3-4: Cumulative amount released after 6hr (Q<sub>6</sub>) and release rate constants of minocycline from different vehicles with and without magnesium at 32 °C using cellulose membrane. Data represent mean ± SEM (n=6). \* denotes significantly reduced minocycline release for each vehicle compared to the same respective vehicle without magnesium.**

Vehicles	Parameters			
	Q <sub>6</sub> (mg/cm <sup>2</sup> )	Release rate constant (10 <sup>-2</sup> mg/cm <sup>2</sup> /min <sup>1/2</sup> )	Fold decrease	R <sup>2</sup>
EtOH	1.28 ± 0.04	8.06 ± 0.15		0.99
EtOH(Mg <sup>2+</sup> )	0.36 ± 0.03	2.75 ± 0.17*	2.93	0.96
PG	1.30 ± 0.10	9.61 ± 0.40		0.98
PG(Mg <sup>2+</sup> )	0.44 ± 0.02	3.24 ± 0.18*	2.96	0.98
TP	1.18 ± 0.02	7.99 ± 0.10		0.99
TP(Mg <sup>2+</sup> )	0.33 ± 0.02	2.41 ± 0.10*	3.32	0.96
IPA: DPA	0.98 ± 0.08	7.08 ± 0.35		0.99
IPA: DPA (Mg <sup>2+</sup> )	0.11 ± 0.01	0.76 ± 0.03*	9.32	0.96
TP: DPA	0.69 ± 0.02	4.89 ± 0.15		0.96
TP: DPA (Mg <sup>2+</sup> )	0.13 ± 0.01	0.94 ± 0.04*	5.20	0.92

The release of a drug from a vehicle can be affected by numerous factors such as formulation viscosity, the size of the diffusing molecules and temperature. Therefore, a plausible explanation for the differences observed in minocycline release rates from the various vehicles with and without magnesium, is the difference in viscosity between magnesium containing vehicle and the corresponding vehicle without magnesium. Drug release from topical formulations have been shown to decline due to increased vehicle viscosity (Bregni et al., 2008; Rafiee-Tehrani & Mehramizi, 2000). In this study, magnesium was found to increase the viscosity of all the systems investigated, especially the binary systems (IPA: DPA and TP: DPA) (data shown in Section 3.3.5). These findings are in accordance with the research of Afzal, Saleem, & Mahmood (1989), who reported increased viscosity of aqueous solutions with increased magnesium chloride concentrations.

At the higher temperature (45 °C), the order of the drug release rate from the vehicles changed. The release rate constants of minocycline were in the order of TP: DPA > PG > IPA: DPA > EtOH > TP > PG ( $Mg^{2+}$ ) > TP ( $Mg^{2+}$ ) > EtOH ( $Mg^{2+}$ ) > IPA: DPA ( $Mg^{2+}$ ) > TP: DPA ( $Mg^{2+}$ ), with release rates ranging from  $17.77 \times 10^{-2} \pm 0.60 \times 10^{-2}$  to  $1.33 \times 10^{-2} \pm 0.12 \times 10^{-2}$  mg/cm<sup>2</sup>/min<sup>1/2</sup> (Table 3-5). Increasing the receptor temperature by 7-8 °C was shown to be effective at improving drug release from topical formulations containing model drugs caffeine, methyl paraben and butyl paraben by a factor of 1.53 to 1.66 (Akomeah et al., 2004). The increase in penetrant transfer was attributed to an increase in molecular motion due to a rise in temperature. In this study, the increase in membrane temperature (32 °C to 45 °C) enhanced minocycline release by a factor of 1.4 to 3.8. The increase in drug release with raised temperature was greater for the more viscous vehicles (those containing magnesium). This is believed to be due to the greater reduction in vehicle viscosity of these formulations with the elevated temperature.

**Table 3-5: Cumulative amount released after 6hr ( $Q_6$ ) and release rate constants of minocycline from different vehicles with and without magnesium ( $Mg^{2+}$ ) at 45 °C using cellulose membrane. Data represent mean  $\pm$  SEM (n=6). \* denotes significantly reduced minocycline release for each vehicle compared to the same respective vehicle without magnesium.**

Vehicles	Parameters			
	$Q_6$ (mg/cm <sup>2</sup> )	Release rate constant (10 <sup>-2</sup> mg/cm <sup>2</sup> /min <sup>1/2</sup> )	Fold decrease	R <sup>2</sup>
EtOH	1.76 $\pm$ 0.05	11.91 $\pm$ 0.39		0.99
EtOH( $Mg^{2+}$ )	1.21 $\pm$ 0.01	8.82 $\pm$ 0.39	1.35	0.98
PG	1.85 $\pm$ 0.11	13.67 $\pm$ 0.56		0.98
PG( $Mg^{2+}$ )	1.40 $\pm$ 0.11	10.10 $\pm$ 0.21	1.35	0.99
TP	1.71 $\pm$ 0.05	11.09 $\pm$ 0.26		0.99
TP( $Mg^{2+}$ )	1.25 $\pm$ 0.02	9.04 $\pm$ 0.32	1.23	0.99
IPA: DPA	1.95 $\pm$ 0.31	13.45 $\pm$ 0.54		0.98
IPA: DPA ( $Mg^{2+}$ )	0.26 $\pm$ 0.02	1.97 $\pm$ 0.16	6.83	0.94
TP: DPA	2.49 $\pm$ 0.11	17.77 $\pm$ 0.60		0.99
TP: DPA ( $Mg^{2+}$ )	0.17 $\pm$ 0.004	1.33 $\pm$ 0.12	13.36	0.92

The previous trend at 32 °C where the release of minocycline from vehicles containing magnesium was slower than the respective vehicle without magnesium was also noted at 45 °C. However, the difference in minocycline release rates from vehicles containing magnesium compared to the corresponding vehicle without magnesium were less pronounced compared to the experiments at 32 °C, except for TP: DPA where the presence of magnesium reduced the release rate by 13.36-fold (compared to 5.20-fold at 32 °C).

Overall, no clear correlation was observed between bulk formulation viscosity and the drug release rate within each experimental temperature investigated (32 °C and 45 °C) as shown below in Figure 3-9.

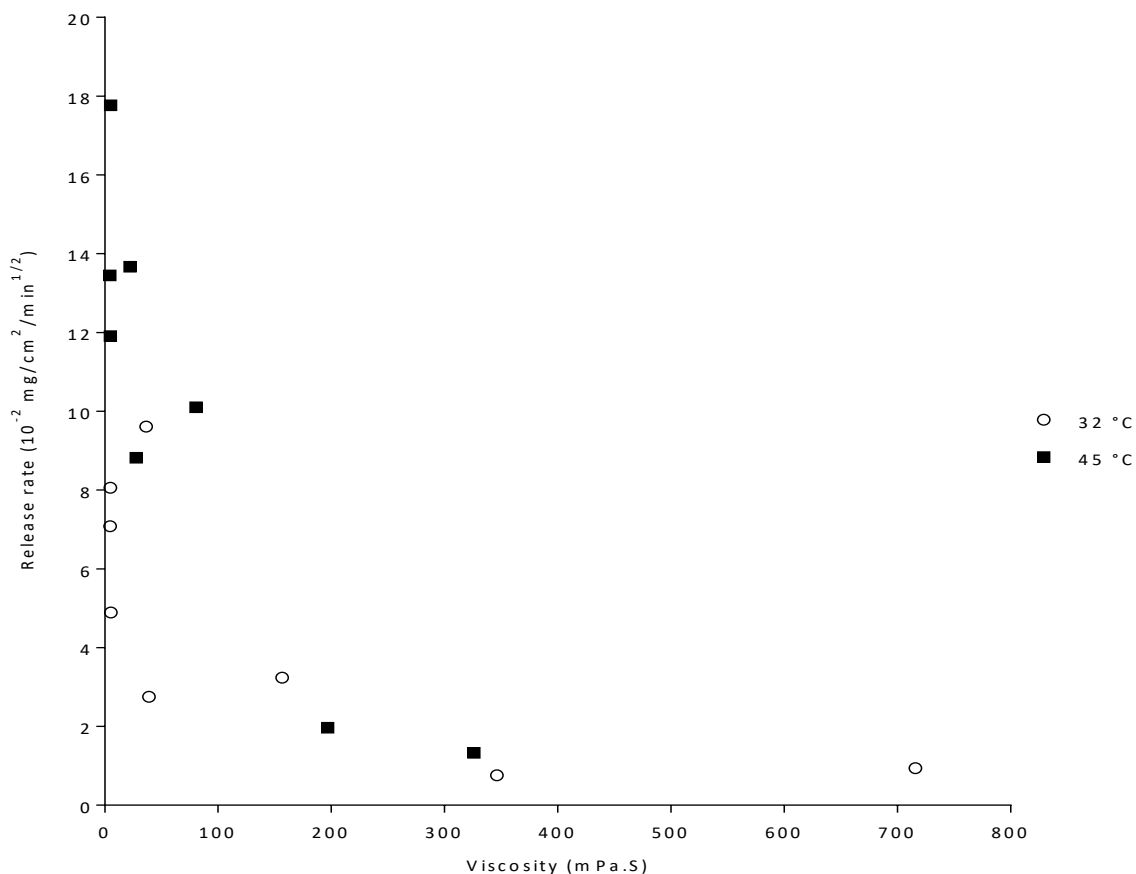


**Figure 3-9: Relationship between vehicle viscosity and the release rate of minocycline for all the vehicles investigated at 32 °C and 45 °C.**

It is possible that the micro-viscosity of the formulations (especially those containing magnesium) maybe more important for explaining the relationship between formulation viscosity and drug release. Micro-viscosity represents the viscosity of the drugs diffusional pathway rather than that of the bulk formulation (Al-Khamis et al., 1986). Previous studies have reported a decrease in drug release rate due to an increase in the viscosity of the microenvironment in the matrix structure of polymer based formulations, resulting in slower drug diffusion through channels/pores in the microenvironment within the formulation (Pongjanyakul & Puttipatkhachorn, 2007). Within individual formulations a trend where higher drug release was associated with reduced viscosity may support this or suggests that vehicle specific effects also impact on the relationship between drug release and formulation viscosity. This relationship is depicted in Figure 3-10 below for IPA: DPA with and without magnesium and is representative of the trend observed for all the other vehicles

investigated. Also, Figure 3-10 highlights the influence of temperature on vehicle viscosity and drug release from the formulation.

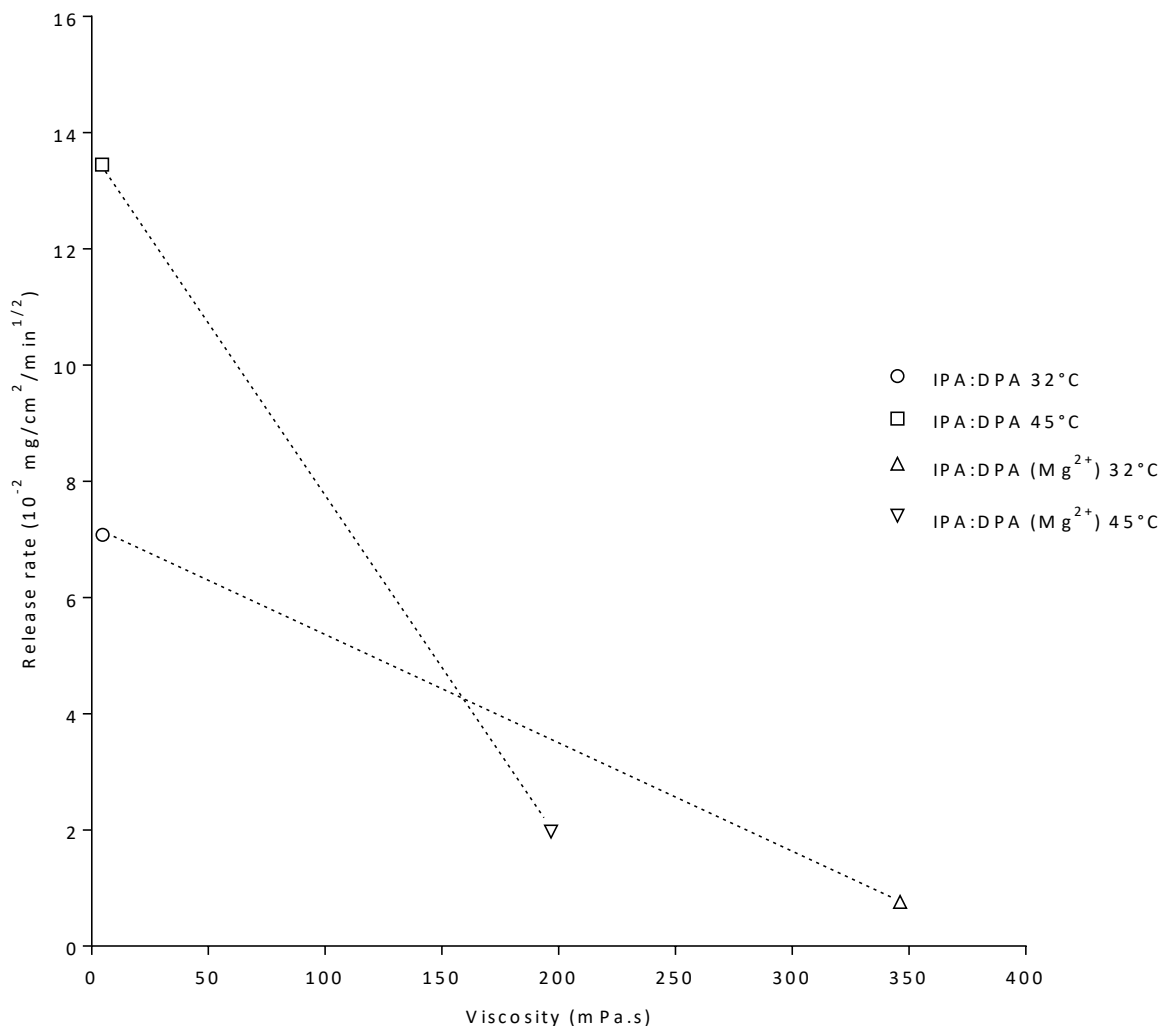


**Figure 3-10: Influence of temperature (32 °C and 45 °C) on minocycline release from IPA: DPA with and without magnesium chloride (Mg<sup>2+</sup>) and vehicle viscosity.**

Increasing the temperature from 32 °C to 45 °C had a greater impact on drug release at the higher viscosities [i.e. for IPA: DPA(Mg<sup>2+</sup>)], with larger reductions in viscosity resulting in greater increase in drug release from the formulation. As previously discussed in Section 1.7.2.4, the increase in diffusivity with elevated temperature is thought to be mainly through the reduction in vehicle viscosity rather than the kinetic energy changes (Longworth, 1954). Also, the impact of viscosity change was reduced with increased temperature.

Another contributing factor for the differences detected in minocycline release from the vehicles with magnesium compared to the respective vehicle without magnesium at both temperatures could be the difference in the size of the magnesium-minocycline complex compared to the free minocycline molecule. The impact of molecular size on diffusion across a membrane can be explained using the Stokes Einstein equation. The Stokes Einstein equation (Equation 1-9, Chapter 1 Section 1.7.2.4) describes the relationship between temperature (T), viscosity ( $\eta$ ) and size (r, radius) of a spherical particle to its diffusion under Brownian motion. From the Stokes Einstein equation, diffusion coefficient (D) is inversely proportional to r (the radius of a spherical particle).

The volume of a spherical particle can be determined using Equation 3-5 below:

$$V = \frac{4}{3}\pi r^3 \quad \text{Equation 3-5}$$

Where V is the molecular volume and r is the radius. Assuming that the molecular volume is proportional to molecular weight of a molecule, and then referring back to the Stokes Einstein equation, the diffusion coefficient is inversely proportional to the cube root of the molecular weight (MW) as shown below in Equation 3-6.

$$D \propto \frac{1}{\sqrt[3]{MW}} \quad \text{Equation 3-6}$$

Using this relationship, the influence of the size of the magnesium-minocycline complex on diffusion across the membrane can be predicted. In the literature, 1:1, 1:2 and 2:1 magnesium-minocycline stoichiometries have been reported in various aqueous solutions (Jin et al., 2007; Piccariello, 2013; Wessels et al., 1998). However, in this work a stoichiometry of 2:3 (magnesium-minocycline) was determined in EtOH using Job's method. The variation in the stoichiometries of magnesium-minocycline reported is not entirely surprising as factors such as the nature of the solvent employed, the presence of impurities, the concentrations (of both magnesium and minocycline), temperature and pH may all influence the stoichiometry of the complex formed (Tongaree, Goldberg, Flanagan, &

Poust, 2000). Furthermore, it is possible that more than one complex type can exist simultaneously. The potential impact of increasing the number of minocycline molecules (and therefore the size of the complex) from 1 to 4 on the drug diffusion coefficient (which is proportional to flux or release rate constant) was calculated using Equation 3-6. This data is presented in Table 3-6.

**Table 3-6: The predicted impact of increasing the number of minocycline molecules (size of complex) on the diffusion of minocycline.**

Number of minocycline molecules	Molecular weight (MW)	$\frac{1}{\sqrt[3]{MW}}$	Fold decrease
1	493.94	0.127	-
2	987.88	0.100	1.27
3	1481.82	0.088	1.44
4	1975.70	0.079	1.61

Doubling the size of the complex (by introducing a second minocycline molecule) has the greatest impact on drug flux, with the consecutive addition of a minocycline molecule reducing flux to a lesser extent compared to the addition of the preceding molecule. Therefore, increasing the number of minocycline molecules (and hence the size of the complex) is predicted to reduce the release rate by 1.27, 1.44 and 1.61-fold, when the number of minocycline molecules that coordinate with magnesium to form the complex were increased to 2, 3 and 4 molecules respectively. Thus, comparing the fold change in the release rate of minocycline to those generated experimentally (i.e. at 32 °C and 45 °C) may allow estimation of the stoichiometry of the magnesium-minocycline complex by using the number of minocycline molecules (MW) if a good correlation is attained.

No direct correlation was apparent between the potential molecular weight of the diffusing species (the size of the magnesium-minocycline complex) and release rate when comparing the predicted and experimental fold change values obtained at 32 °C. The decrease in the release rate was considerably greater than that would be expected from changes in the size of the diffusing species, suggesting that the increase in size alone is unlikely to explain the differences in release rates.

Similarly, at 45 °C the decrease in release rates from the binary systems was too great to be explained by the increase in size complex size. In contrast, for the neat systems, the decrease in the release rates were smaller and therefore closer to what might be expected by the changes in the size of the diffusing species. Overall, it is unclear to what extent each of these factors (viscosity and size of diffusing species) impact drug release.

The use of cellulose membrane provided an insight into the effect of temperature on drug release. Thus, increasing the temperature from 32 °C to 45 °C was found to enhance the drug release rate from 1.40 to 3.7-fold for all the vehicles investigated. For the vehicles without magnesium the order of release from the vehicles was TP: DPA > IPA: DPA > EtOH > PG > TP. Whereas, the rank of the drug release from the vehicles containing magnesium chloride was TP (Mg<sup>2+</sup>) > EtOH (Mg<sup>2+</sup>) > PG (Mg<sup>2+</sup>) > IPA: DPA (Mg<sup>2+</sup>) > TP: DPA (Mg<sup>2+</sup>). Including magnesium chloride in the vehicles reduced release rate 1.23 to 13.36-fold. The differences in release profiles observed at the different temperatures are believed to be as a result of the increase in penetrant molecular motion and reduced vehicle viscosity (especially the magnesium containing vehicles) due to the 13 °C rise in temperature.

### **3.3.7 *In vitro* release of minocycline and magnesium-minocycline complex: complete system heating vs heat applied from top**

The use of heat as an enhancement strategy (as part of a topical preparation) in a clinical setting will require a method of generating heat in-situ for short periods after the application of the formulation. Phase change materials such as sodium thiosulphate (capable of heating up to 45 °C) possess this ability and have been investigated as a potential source of heat to enhance solute skin permeation (Wood et al., 2011). Therefore, the effect of short bursts of heat (45 °C for 15 and 25 min) generated by sodium thiosulfate (ST) on drug release from propylene glycol (PG) with and without magnesium (Mg<sup>2+</sup>) was investigated and compared to experiments at 32 °C (control) and 45 °C (whole system heating). PG was selected because it was effective with heat at producing high minocycline tissue concentrations and reduced delivery into the receiver fluid when combined with magnesium in the infinite studies (data shown in Section 3.3.2). This effect may be useful in reducing systemic side

effects of minocycline which can be severe. Also, minocycline demonstrated good stability in PG with magnesium (data in Chapter 2, Section 2.3.2.1). Additionally, minocycline was sufficiently stable in PG alone over the six-hr study (>95% at both temperatures, data not shown), so release from both PG and PG: Mg<sup>2+</sup> can be reliably compared. The release of minocycline from PG and PG: Mg<sup>2+</sup> is shown in Figures 3-11(a) and 3-11(b) respectively.

Drug release from PG [Figure 3-11(a)] was significantly greater when the entire system was kept at 45 °C for the duration of the experiment (1.98 to 2.46-fold more). The cumulative amount released ranged from 655.23 ± 94.13 to 1611.24 ± 154.80 µg/cm<sup>2</sup>, with PG (ST-15 min) and PG 45°C producing the minimum and maximum release. Also, the difference in the cumulative amount delivered at 6 hr for the control and those employing ST were not found to be significant.

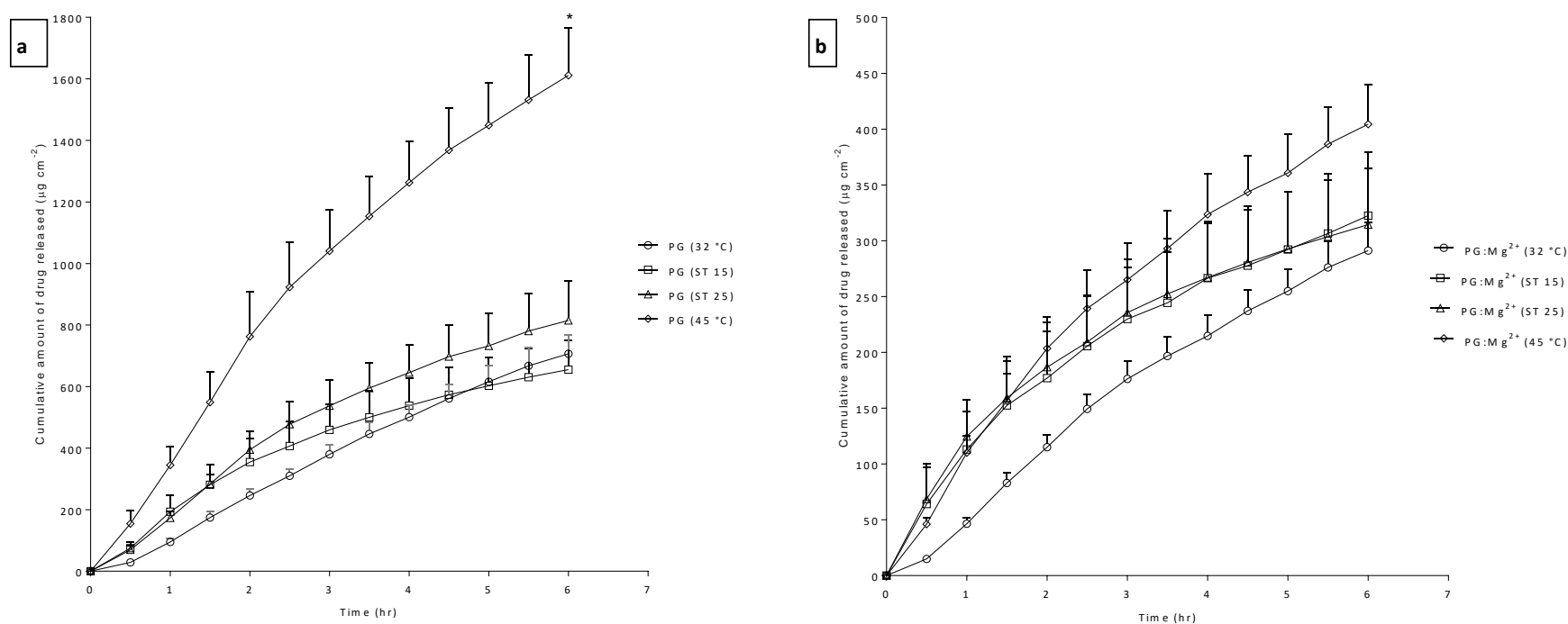


**Figure 3-11: Mean cumulative amount of minocycline released across cellulose membrane (a) from propylene glycol (PG) (b) propylene glycol containing magnesium (PG: Mg<sup>2+</sup>). Filtered saturated solution of minocycline 100  $\mu\text{L}$  was applied to the membrane surface. Experiments were conducted in a water bath at 32 °C for 6 hr with and without sodium thiosulfate solution (ST) producing heat (45°C) for 15 & 25 min (ST 15 & ST 25 respectively) and also in a water bath 45°C. All points are mean + SEM of n=6 diffusion cells. \* denotes significant difference in the amount released from PG at 45 °C for 6 hr compared to other conditions employed at the 6 hr time point. No statistical differences were found between the different heating conditions in the amount released from PG: Mg<sup>2+</sup> at the 6 hr time point.**

The cumulative amount released from PG: Mg<sup>2+</sup> ranged from 291.20 ± 25.33 µg/cm<sup>2</sup> to 404.40 ± 35.63 µg/cm<sup>2</sup>. The lowest and highest amounts of drug was released from PG: Mg<sup>2+</sup> (32 °C) and PG: Mg<sup>2+</sup> (45 °C) respectively. The level of enhancement observed with complete system heating (45 °C) was from 1.25 and 1.40-fold at 6 hr compared to the other conditions. Additionally, drug release was much slower for PG: Mg<sup>2+</sup> in comparison to PG, this effect of magnesium on drug release was previously observed in the Section 3.3.6.

Using ST as a heating system was more beneficial at early time points compared to the control (32 °C), as drug release was more significant from both PG and PG (Mg<sup>2+</sup>) at 0.5 hr and 1.0 hr. A comparison of the cumulative amount released from each vehicle at 0.5 hr and 1.0 hr is shown in Figure 3-12(a-b).

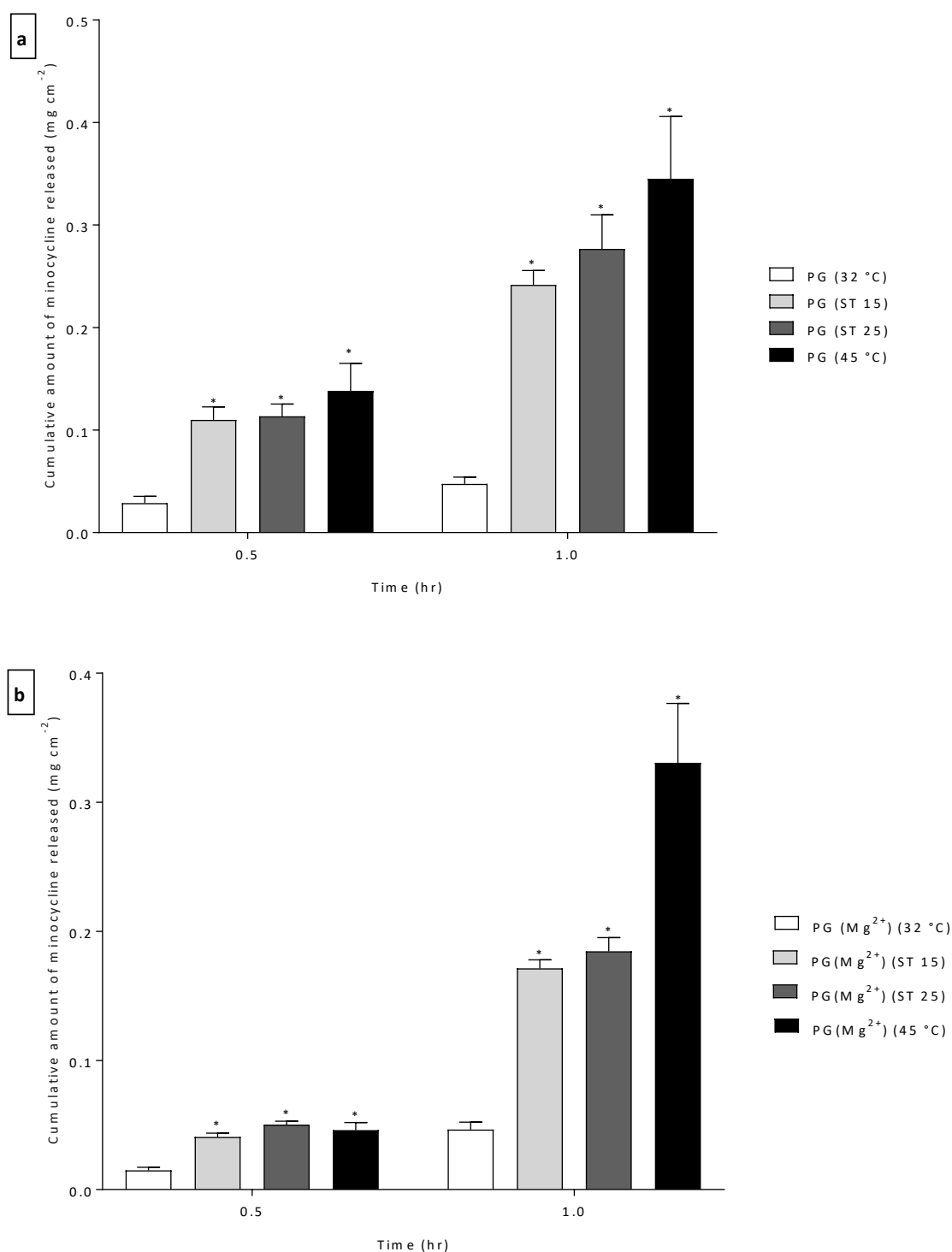


**Figure 3-12: Cumulative amount released after 0.5 and 1.0 hr from (a) propylene glycol (PG) (b) propylene glycol with magnesium (PG: Mg<sup>2+</sup>) using cellulose membrane. Heat (45 °C) on top was produce using sodium thiosulphate for 15 and 25 min (ST 15 & ST 25 respectively), a water bath at 45 °C for the duration of the study (whole system heating) and a water bath at 32 °C (control). Data represent mean + SEM (n=6). \* denotes significant drug release compared to control (32 °C).**

Also, at these early time points using ST is as effective as complete system heating, as drug release was not significantly different when using ST and complete system heating at early times (0.5h) for both PG and PG: Mg<sup>2+</sup>. Using the ST heating system is associated with the presence of a thermal gradient (which mimics the likely clinical situation more) between the formulation (elevated temperature) and the membrane surface (low temperature). Under such conditions the formulation components attain drift mobility (as described in Section 1.7.2.4) which brings about a thermophoretic driving force. This thermophoretic driving force in addition to Brownian diffusion both enhance diffusion, as diffusion occurs down the temperature and concentration gradients (McAuley & Caserta, 2015).

For PG [Figure 3-10(a)], using ST for both 15 and 25 min generated a 3.79-fold increase in the cumulative amount released at 0.5 h compared to the control (32 °C). At 1 h, using the chemical heating system for 15 and 25 min also lead to a 5.0 and 5.8-fold increase in the cumulative amount released respectively, compared to the control. For PG (Mg<sup>2+</sup>) [Figure 3-10(b)], a similar trend was observed, as the use of ST increased the cumulative amount released by approximately 3.0 and 3.7-fold at 0.5 h and 1.0 h respectively compared to the control.

### 3.4 Conclusion

This Chapter evaluated the effect of heat and CPEs on the permeation and skin distribution of minocycline across full thickness human abdominal skin. Increasing the temperature from 32 °C to 45 °C was observed to increase drug flux 1.80 to 5.59-fold across full thickness human abdominal skin. This indicates that the combination of heat and CPEs is an effective strategy for enhancing minocycline transport across skin. Investigation into the mechanism of heat, suggest that the increased transport of minocycline across skin is due to the simultaneous improvements in diffusion and partition coefficients. For IPM and heat, the increased minocycline delivery was mainly attributed to improvements in diffusion coefficient, whereas for all the enhancers (including the binary systems) improvements in partitioning were greater (often 2-fold higher than diffusion coefficient).

Using the hydrophilic vehicles produced both greater drug delivery into the receiver fluid and higher drug tissue concentrations compared to the hydrophobic vehicles. This was attributed to the greater improvements in partitioning with hydrophilic vehicles with the application of heat. Additionally, the incorporation of magnesium into the hydrophilic vehicles and the binary systems (IPA: DPA and TP: DPA) further enhanced skin uptake of minocycline.

In particular, drug delivery from both EtOH and PG was altered by the presence of magnesium. In these vehicles, the presence of magnesium produced higher drug tissue concentrations and slower drug permeation. It was postulated that magnesium possibly enhanced minocycline interaction with the endogenous skin components (possibly through H-bonding). The CLSM studies supported the data from the *in vitro* skin distribution studies. A similar trend was observed across cellulose membrane, where the release of minocycline from the dermatological vehicles containing magnesium was slower than the respective vehicle without magnesium at both temperatures. However, employing the elevated temperature was found to increase the drug release rate for all the vehicles investigated possibly by increasing penetrant molecular motion and by reducing vehicle viscosity. The increased size of the magnesium-minocycline complex compared to the unbound drug and the increased vehicle

viscosity with magnesium are believed to be some of the factors contributing to this observed reduction in drug release rate.

Finally, sodium thiosulfate (ST) was found to be significantly better at improving drug release compared to experiments at 32 °C (no additional heat) and equally as effective as whole system heating (45 °C) at early time points (0.5 hr and 1.0 hr), which highlights the potential usefulness of using ST in topical formulations as a source for generating heat in-situ.

**4 Effect of heat and CPEs on the *in vitro*  
percutaneous absorption of isotretinoin**

## 4.1 Introduction

Following on from the delivery of minocycline described in the previous Chapter, another drug of interest in the management of acne is isotretinoin. Oral administration of isotretinoin has been shown to be the most effective treatment for severe acne (Hodgkiss-Harlow, Eichenfield, & Dohil, 2011; Layton, 2009). However, systemic delivery of isotretinoin is associated with significant side-effects, such as hypertriglyceridemia, severe drying of mucus membranes/skin, corneal opacities and is highly teratogenic (Brzezinski, Borowska, Chiriac, & Smigielski, 2017). Topical formulations of isotretinoin have been developed to minimise systemic side-effects and toxicity. Yet, the topical application of isotretinoin has not been as effective as systemic delivery and is also associated with side-effects although not as severe in comparison to oral administration (Kaymak, Taner, & Taner, 2009; Tschan, Steffen, & Supersaxo, 1997). Currently, topical isotretinoin is indicated for mild-moderate acne only. Therefore, improved uptake of isotretinoin into the hair follicles and skin to enable the treatment of more severe acne using topical formulations would be beneficial. This may potentially be achieved by combining CPEs with physiologically tolerable heat ( $\leq 45\text{ }^{\circ}\text{C}$ ), which is an underutilised and under investigated penetration enhancement strategy. Although, the use of heat as an enhancement strategy is likely to be practical only for short durations; it may still be sufficient to improve drug delivery into the skin and increase drug concentrations in the hair follicles and pilosebaceous units.

Therefore, the aim of this Chapter was to investigate the effect of heat ( $\leq 45\text{ }^{\circ}\text{C}$ ) and CPEs on the follicular absorption, skin distribution and receiver fluid concentrations of isotretinoin following topical application from selected dermatological vehicles (EtOH, DPA, PG, PGML 90 and TP). These vehicles were selected because they demonstrated appropriate solubility and stability for isotretinoin (from the initial pre-formulation studies presented in Chapter 2). Additionally, the marketed product Isotrex<sup>®</sup> gel containing 0.05% w/w isotretinoin was tested and used as a comparator in all the *in vitro* experiments conducted in this Chapter. To achieve this aim, a series of objectives were set as detailed below:

- Investigate the influence of heat ( $\leq 45\text{ }^{\circ}\text{C}$ ) on the uptake of isotretinoin into the receptor compartment of Franz diffusion cells and skin tissue, from a series of saturated solutions of the drug in neat CPEs detailed above and the marketed product Isotrex<sup>®</sup> gel 0.05% w/w.
- Conduct finite dose skin permeation and distribution experiments comparing the effect of heat ( $\leq 45\text{ }^{\circ}\text{C}$ ) on the delivery of isotretinoin 0.05% w/w into the receptor of Franz diffusion cell and skin tissue from 50:50 binary prototype formulations (EtOH: DPA, EtOH: IPM, EtOH: PG and EtOH: PGML 90) to that from neat EtOH and the marketed product Isotrex<sup>®</sup> gel 0.05% w/w.
- Compare the impact of sodium thiosulfate (ST) generated heat (45 °C for 15 min and 25 min) and complete system heating (water bath at 45 °C for the whole duration of experiment) on the follicular absorption of topically applied isotretinoin from a selected 50:50 binary system and Isotrex<sup>®</sup> gel 0.05% w/w using differential tape stripping.

## 4.2 Materials and Methods

Isotretinoin (99.9 %) was purchased from Sequoia Research Products (Pangbourne, UK). Acetonitrile HPLC grade (99.9 %), ethanol HPLC grade (99.9 %), formic acid (98.0-100.0 %), methanol HPLC grade (99.9 %), propylene glycol (>99.0 %), phosphate buffer solution (PBS) tablets, Dura Seal™ (Diversified Biotech, USA), Hamilton GASTIGHT® syringes (Hamilton®, Switzerland) and Parafilm M® laboratory film (Bemis® Flexible packaging, USA) were acquired from Fisher Scientific (Loughborough, UK). Isopropyl myristate (>96 %) and Sodium thiosulfate pentahydrate (99.5 %) were bought from Acros Organics (New Jersey, USA). Diisopropyl adipate (> 99.8 %) was supplied by Croda (Barcelona, Spain). Propylene glycol monolaurate 90 (> 99.8 %) and Transcutol® P (>99.8%) were purchased from Gattefosse (France). Cotton buds (Johnson & Johnson Ltd, Maidenhead, UK), Isotrex® Gel 0.05% w/w and Scotch® Magic™ Invisible Tape (3M, USA) were procured from UH campus pharmacy (Hatfield, UK). Polytetrafluoroethylene (PTFE) syringe filters 25mm 0.22µm were purchased from dot-red® analytical (Cambridgeshire, UK). Deionised water (18.2 MΩ•cm) was obtained from a Millipore Milli-Q® water system.

### 4.2.1 Quantitative analysis of isotretinoin

Quantitative analysis of isotretinoin was conducted using HPLC as described previously in Chapter 2, Section 2.2.1.1.

## **4.2.2 *In vitro* experiments**

### **4.2.2.1 Skin preparation**

Human abdominal skin was supplied by ZenBio (USA) and prepared as described in Chapter 2 Section 2.2.2.6. Prior to commencing the permeation studies, the skin was removed from the freezer, thawed and cut to the appropriate size using a scalpel.

### **4.2.2.2 Preparation of donor suspensions**

For the preparation of isotretinoin suspensions in the vehicles investigated refer to Chapter 2, Section 2.2.2.5. For the finite dose permeation studies, isotretinoin 0.05% w/v in the following 50: 50 binary systems (EtOH: DPA, EtOH: IPM, EtOH: PG and EtOH: PGML 90) and in neat EtOH were prepared in amber glass vials (batch size 10 mL). This concentration was chosen to match the marketed product Isotrex<sup>®</sup> gel 0.05 % w/w.

### **4.2.2.3 Franz cells set up**

#### **4.2.2.3.1 Infinite dose skin permeation studies**

The skin samples were placed on the individually calibrated unjacketed upright Franz diffusion cells (diameter 1.0 cm<sup>2</sup>: volume 3.0 mL) (Soham Scientific, UK), with the SC facing the donor compartment and the dermis facing the receptor. Both chambers were then wrapped together using Parafilm<sup>®</sup> (at 37 °C) or Dura Seal™ (at 50 °C) before being clamped together. The receiver fluid was EtOH: PBS pH 7.4 (50:50 % v/v) and stirred with a magnetic bar to ensure adequate mixing (600 rpm). The water bath temperature was maintained at 37 °C and 50 °C to keep the skin surface at approximately 32 ± 1 °C and 45 ± 1 °C respectively. Prior to dosing, the Franz cells were equilibrated at the appropriate temperature and then the membrane surface temperature was measured from the donor compartment using a Fisher Scientific Traceable Digital Thermometer with a type-K probe. Air bubbles were removed through the sampling arm by carefully tilting or inverting the diffusion cell and checks for leaks were made at the same time. A saturated suspension (0.5 mL) of isotretinoin was then introduced into the donor chamber. Following this the receiver fluid (200 µL) was removed from

receptor compartment via the sampling arm after 1, 2, 3, 4, 6, 8, 18, 19, 20, 21, 22, 23 and 24 hr and analysed via HPLC. An equal volume of pre-warmed receiver fluid was immediately added to replace the sampled volume. Six repetitions (n=6) of each experiment were performed. Franz cells were covered with aluminium foil to protect isotretinoin from light.

#### 4.2.2.3.2 Finite dose skin permeation studies

Following on from the infinite dose experiments four prototype formulations: EtOH: DPA, EtOH: IPM, EtOH: PG and EtOH: PGML 90 (50: 50 ratios) were chosen to investigate whether synergistic enhancement occurred with mixed solvents. The drug transport from these formulations was tested and compared to that from neat EtOH and the marketed product Isotrex<sup>®</sup> gel 0.05% w/w. The latter is a topical gel containing isotretinoin (0.05% w/w), butylated hydroxytoluene, hydroxypropyl-cellulose and EtOH (Medicines.org.uk, 2017). All the prototype formulations and the neat EtOH (employed as a secondary control) were prepared to contain isotretinoin 0.05% w/v to match the marked product Isotrex<sup>®</sup> gel. The Franz cells were dosed with finite doses of 10  $\mu\text{L cm}^{-2}$  or 10  $\text{mg cm}^{-2}$  for topical solutions (selected 50: 50 binary systems) and semi-solid (Isotrex<sup>®</sup> gel) respectively. This dose mimics as closely as possible the *in vivo* application of topical products. Apart from dosing the Franz cells with a smaller amount of formulation the procedure described in Section 4.2.2.3.1 was followed to conduct the finite dose experiments.

#### **4.2.2.3.3 The effect of a short burst of heat on follicular absorption and skin distribution of isotretinoin: 1 hr vs 24 hr duration experiments**

To determine the effect of short bursts of heat on follicular absorption and skin distribution of isotretinoin delivered from Isotrex® gel 0.05% w/w and a filtered saturated solution (1.38% w/v, prepared at 32 °C) of EtOH: PGML 90 (50:50) over short and extended periods of time, finite dose experiments using the procedure described above in Section 4.2.2.3.2 were conducted for 1 hr and 24 hr respectively. After applying the formulation, 2.5 mL or 5 mL of sodium thiosulfate (ST) solution was added to produce a membrane surface temperature of approximately 45 °C for 15 and 25 min respectively. Aluminium foil was used to separate the heating system from the formulation. These experiments were conducted in a water bath at 37 °C. Control experiments were conducted in a water bath at 37 °C and 50 °C to produce membrane surface temperatures of 32 °C and 45 °C respectively. Aluminium foil was placed in the donor chamber of each Franz diffusion cell to mimic experiments using the ST chemical heating system. The receiver fluid was sampled only at the end of each experiment (1 hr and 24 hr). Six repetitions (n=6) were performed for each formulation under each treatment group.

At the end of the permeation studies, the skin samples were removed from Franz diffusion cells. Then the residual formulation was removed from the aluminium foil, donor chamber and skin surface using the cleaning procedure with the cotton buds described above Chapter 2, Section 2.2.2.3. To remove any remaining skin surface formulation two tape strips were taken. Then the differential tape stripping was performed to determine the follicular penetration and skin distribution of isotretinoin following the method described in Section 4.2.2.5.

#### **4.2.2.4 Drug skin distribution studies**

To determine the distribution of isotretinoin across the different skin layers (SC, epidermis and dermis) after the completion of the infinite and finite dose skin permeation experiments, the extraction procedure described in Chapter 2, Section 2.2.2.3 was followed.

#### **4.2.2.5 Localisation of isotretinoin in the hair follicles: cyanoacrylate biopsy (differential tape stripping)**

Differential stripping involves using a combination of tape stripping and cyanoacrylate skin surface biopsies. Briefly, 10 tape strips were taken to remove the SC and transferred into an amber glass vial. After the SC removal, a drop of cyanoacrylate superglue was applied onto the tape stripped skin and was covered with a glass slide under slight pressure. After 5 min, the cyanoacrylate superglue polymerised, and the glass slide was removed with one quick movement leaving the follicular casts and corneocytes on the slide. The cast was transferred into amber glass vial using forceps. The remaining skin was heat separated as described above in Chapter 2, Section 2.2.2.3, where the epidermis and dermis were placed in separate amber glass vials. Subsequently, 2.0 mL of methanol (the extraction fluid) was added to each vial. Each vial was then sonicated for 20 min before being transferred to a Stuart roller mixer SRT9 (Cole-Parmer, UK) overnight (16-18 hr). All samples were then filtered using 0.2 µm PTFE syringe filters before being analysed by HPLC as described in Chapter 2, Section 2.2.1.1. The extraction procedure was repeated until the drug content in the extracted samples were no longer detectable or below the LOQ.

#### **4.2.3 Data treatment and statistics**

The data were analysed as described previously (Chapter 3, Section 3.2.10).

### 4.3 Results and Discussion

#### 4.3.1 Infinite dose *in vitro* skin permeation and distribution studies

The permeation profiles and skin distribution data for the infinite dose experiments at 32 °C and 45 °C are shown in Figures 4-1 (a-b) and 4-2 (a-b) respectively. Parameters including average flux ( $J$ ), lag time ( $T_L$ ), pathlength normalised diffusion ( $D/h^2$ ) and partition coefficients ( $k/h$ ) were determined as described in Chapter 3 Section 3.3.5 to gain an insight into the possible mechanisms of enhancement with heat. This data is presented in Table 4-1.

At physiological skin temperature (32 °C) isotretinoin was delivered into the receiver fluid at early time points from all the formulations investigated. Permeation profiles at 32 °C are presented in Figure 4-1(a). The cumulative amount of isotretinoin recovered from the receiver fluid at 24 hr ( $Q_{24}$ ) ranged from  $0.79 \pm 0.03$  to  $2.06 \pm 0.81 \mu\text{g}/\text{cm}^2$ , with the lowest and highest recovery for Isotrex<sup>®</sup> gel and PG respectively. Thus, in terms of average drug flux (calculated between 18-24 hr) the rank of the formulations was in the following order: PG > EtOH > IPM > PGML 90 > TP > DPA > Isotrex<sup>®</sup> gel. The fluxes of other highly lipophilic solutes have been reported to increase when delivered from neat PG (Hilton et al., 1994) or neat EtOH (Friend, Catz, Heller, Reid, & Baker, 1988). Additionally, Lehman and co-workers, observed short chain alcohols such as PG and isopropyl alcohol (IPA) were better at delivering retinoids compared to other vehicles such as mineral oil, DPA and polyethylene glycol 400 (Lehman, Slattery, & Franz, 1988). Both PG and EtOH (short-chain alcohols) are thought to enhance percutaneous absorption via extraction of SC lipids and/or improvements in drug partitioning into the SC (Roberts & Cross, 2002).

Mean cumulative amount of drug sampled after 24 hr ( $\mu\text{g cm}^{-2}$ )							
	Isotrex <sup>®</sup>	IPM	TP	EtOH	PG	PGML 90	DPA
SC	0.86 ± 0.14	11.30 ± 2.87	21.57 ± 6.07	23.29 ± 8.67	20.19 ± 4.35	24.45 ± 4.38	25.61 ± 5.12
Epidermis	0.48 ± 0.06	44.99 ± 5.98	62.91 ± 17.45	57.83 ± 19.60	72.72 ± 15.00	51.86 ± 10.35	73.82 ± 15.49
Dermis	0.46 ± 0.01	20.86 ± 2.57	17.31 ± 2.91	32.76 ± 7.30	31.60 ± 15.02	56.83 ± 18.16	43.07 ± 6.63
Receiver fluid	0.79 ± 0.03	1.29 ± 0.30	0.80 ± 0.09	1.80 ± 0.30	2.06 ± 0.81	0.99 ± 0.22	0.83 ± 0.03
Total	2.59 ± 0.24	78.35 ± 11.72	101.79 ± 26.42	115.67 ± 35.87	126.57 ± 35.17	134.13 ± 33.11	143.33 ± 27.26
Rank	7	6*	5*	4*	3*	2*	1**

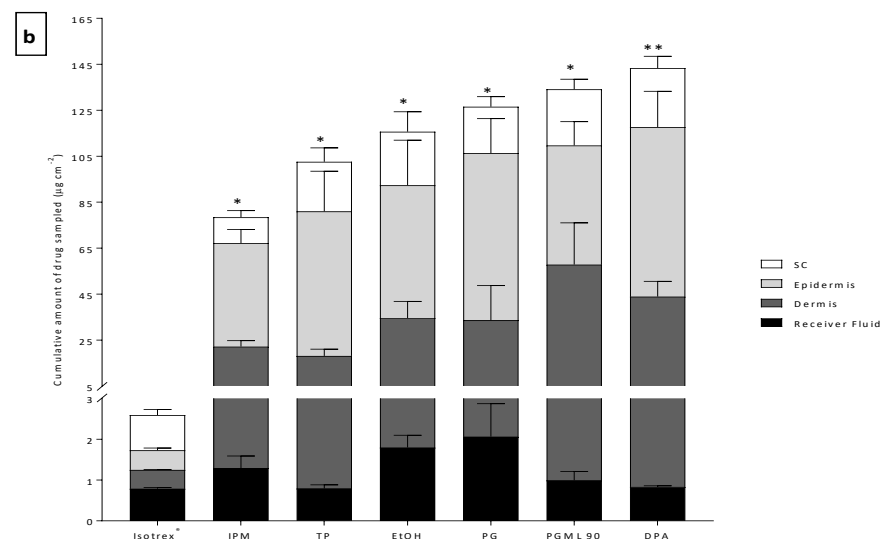
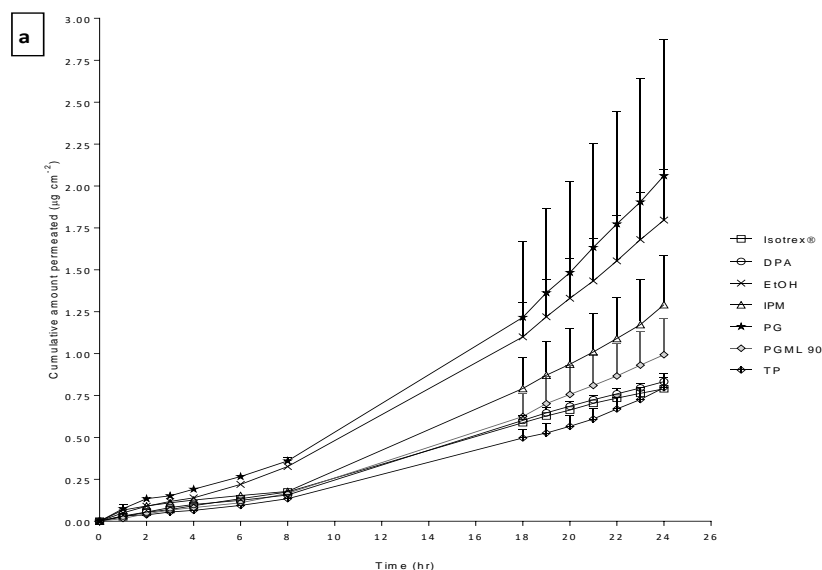


**Figure 4-1: Mean cumulative amount isotretinoin (a) permeated through human abdominal skin at 32 °C over 24 hr from various vehicles (b) recovered from the stratum corneum (SC), epidermis, dermis and receiver fluid at the end of the infinite dose permeation study.** Isotretinoin was applied  $0.5 \text{ mL cm}^{-2}$  to the skin surface in a previously equilibrated saturated suspension for each vehicle. Vehicles tested were Diisopropyl adipate (DPA), Ethanol (EtOH), Isopropyl myristate (IPM), Propylene glycol (PG), Propylene glycol monolaurate 90 (PGML 90), Transcutol P<sup>®</sup> (TP) and the marketed product Isotrex<sup>®</sup> gel 0.05 % w/w was used as control and  $0.5 \text{ g cm}^{-2}$  was applied to the skin surface. All points are mean + SEM of  $n=6$  diffusion cells. \*\* denotes significant difference in the total amount of isotretinoin delivered compared to vehicles ranked 6<sup>th</sup> and higher. \* denotes significant difference in the total amount of isotretinoin delivered compared to vehicles ranked 7<sup>th</sup>.

With regards to drug tissue concentrations [sum of SC, epidermis and dermis] at 32 °C [Figure 4-1(b)], some differences in the vehicles were observed, as PGML 90 and DPA delivered more drug into the dermis than PG and EtOH which delivered more into the receiver fluid.

In terms of the total amount of drug delivered [sum of drug recovered from SC, epidermis, dermis and receiver fluid], all the vehicles investigated delivered significantly greater amount of drug in comparison to Isotrex<sup>®</sup> gel. The increase in total amount delivered ranged from 30.25 to 55.34-fold, with IPM and DPA producing the lowest and greatest enhancement respectively. The rank of the formulations with respect to the total amount of drug delivered was in the following order: DPA > PGML 90 > PG > EtOH > TP > IPM > Isotrex<sup>®</sup> gel, with the total amount delivered ranging from  $2.59 \pm 0.24$  to  $143.533 \pm 27.26$   $\mu\text{g}/\text{cm}^2$  at the end of the study.

With the application of heat (45 °C), greater levels of isotretinoin were delivered into the receiver fluid from all the formulations investigated as shown in Figure 4-2(a). Therefore, the cumulative amount ( $Q_{24}$ ) of isotretinoin recovered from the receiver fluid at 24 hr increased significantly ( $p \leq 0.05$ ) compared to the 32 °C experiments (Table 4-1). Drug receiver fluid concentrations at 24 hr ranged from  $3.27 \pm 0.76$  to  $56.54 \pm 13.95$   $\mu\text{g}/\text{cm}^2$  with the lowest and highest recovery for PG and EtOH respectively. This corresponded to a 1.59 to 31.41-fold increase in the amount of isotretinoin recovered from the receiver fluid compared to each respective formulation at 32 °C. Overall, the rank of the formulations/vehicles in terms of drug flux (J) at 45 °C was in the following order: EtOH > IPM > TP > DPA > Isotrex<sup>®</sup> gel > PGML 90 > PG, with flux values ranging from  $0.185 \pm 0.039$  to  $3.141 \pm 0.557$   $\mu\text{g}/\text{cm}^2/\text{hr}$ .

Also, at this higher temperature (45 °C) the total amount of isotretinoin delivered into the skin tissue for all the vehicles/formulations investigated increased. Improved accumulation of different drugs in the membrane with the application of moderate level of heat (up to 45 °C) has been observed in other studies, in which human skin was employed (maximum enhancement effect 2-fold) (Akomeah et al., 2004; Wood, Brown, et al., 2012). However, in this study the improvement in the total amount of drug

recovered from the skin tissue with heat ranged from 1.71 to 6.23-fold, with TP and Isotrex<sup>®</sup> gel producing the smallest and largest enhancements respectively. This enhanced delivery from Isotrex<sup>®</sup> gel is believed to be due to improved drug release from the gel. The application of heat (40 °C) was previously shown to significantly increase drug release from transdermal patches of diclofenac sodium and lidocaine HCl (Otto & Villiers, 2013).

As previously seen in the 32 °C experiment, the vehicle with the highest flux (EtOH) did not produce the greatest drug skin deposition, instead PGML 90 (second to last in rank in terms of flux) produced the maximum drug tissue concentrations. This indicates that the enhancing effects of PGML 90 were also improved with the elevated temperature, and further suggests that the vehicles investigated interact differently with the skin and therefore potentially employ different mechanism to improve drug uptake into and across skin. Overall, the rank of the formulations in terms of total amount drug delivered was in the following order: PGML 90 > EtOH > DPA > IPM > PG > TP > Isotrex<sup>®</sup> gel, with the total amount delivered ranging from  $17.87 \pm 1.88$  to  $382.24 \pm 91.67$   $\mu\text{g}/\text{cm}^2$ .

	Mean cumulative amount of drug sampled after 24 hr ( $\mu\text{g cm}^{-2}$ )						
	Isotrex®	TP	PG	IPM	DPA	EtOH	PGML 90
SC	$0.78 \pm 0.05$	$17.38 \pm 5.15$	$20.85 \pm 6.36$	$18.61 \pm 7.32$	$8.92 \pm 2.35$	$12.63 \pm 1.87$	$60.54 \pm 21.67$
Epidermis	$1.84 \pm 0.21$	$82.53 \pm 9.19$	$120.07 \pm 21.88$	$106.65 \pm 23.74$	$119.90 \pm 23.21$	$60.64 \pm 4.15$	$170.96 \pm 44.97$
Dermis	$8.59 \pm 1.01$	$72.85 \pm 12.04$	$63.96 \pm 13.79$	$84.46 \pm 11.58$	$131.23 \pm 9.85$	$149.64 \pm 46.28$	$145.99 \pm 23.28$
Receiver fluid	$6.66 \pm 0.62$	$9.39 \pm 1.45$	$3.27 \pm 0.76$	$17.27 \pm 4.86$	$11.70 \pm 2.02$	$56.54 \pm 13.95$	$4.75 \pm 1.74$
Total	$17.87 \pm 1.88$	$182.14 \pm 27.83$	$208.15 \pm 42.03$	$226.99 \pm 47.50$	$271.75 \pm 37.43$	$279.45 \pm 66.25$	$382.24 \pm 91.67$
Rank	7	6*	5*	4*	3*	2*	1*

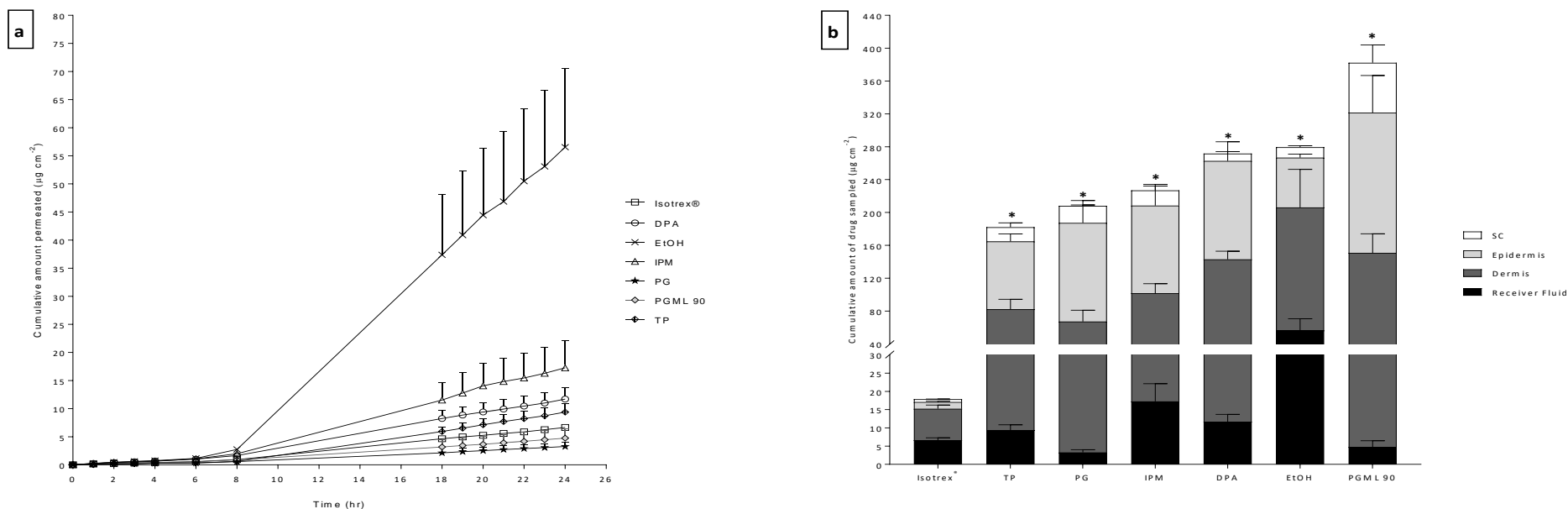


**Figure 4-2: Mean cumulative amount isotretinoin (a) permeated through human abdominal skin at 45 °C over 24 hr from various vehicles (b) recovered from the stratum corneum (SC), epidermis, dermis and receiver fluid at the end of the infinite dose permeation study.** Isotretinoin was applied  $0.5 \text{ mL cm}^{-2}$  to the skin surface in a previously equilibrated saturated suspension for each vehicle. Vehicles tested were Diisopropyl adipate (DPA), Ethanol (EtOH), Isopropyl myristate (IPM), Propylene glycol (PG), Propylene glycol monolaurate 90 (PGML 90), Transcutol P® (TP) and the marketed product Isotrex® gel 0.05 % w/w was used as a control and  $0.5 \text{ g cm}^{-2}$  was applied to the skin surface. All points are mean + SEM of  $n=6$  diffusion cells. \* denotes a significant difference in the total amount of isotretinoin delivered compared to the vehicle ranked 7<sup>th</sup>.

In an attempt to gain a mechanistic understanding of how these strategies (CPEs plus heat) influenced isotretinoin transport across skin, the pathlength normalised values of partition ( $Kh$ ) and diffusion coefficients ( $D/h^2$ ) were calculated using thermodynamic activity instead of solubility in the vehicle ( $C_v$ ) as described in Chapter 3, Section 3.3.5. The calculated  $Kh$  and  $D/h^2$  for the delivery of isotretinoin through human abdominal skin from different dermatological vehicles and Isotrex<sup>®</sup> gel at 32 °C and 45 °C are listed in Table 4-1.

Within the 32 °C data, the pathlength normalised partition coefficient ( $Kh$ ) for isotretinoin was found to be different between the different formulations/vehicles investigated. There was a significant ( $p \leq 0.05$ ) increase in the  $Kh$  of isotretinoin into the skin tissue from all the formulations investigated compared to the control Isotrex<sup>®</sup> gel. The increase in  $Kh$  ranged from 1.14 to 7.81-fold with DPA and PG producing the lowest and greatest enhancement respectively. Within the 32 °C data the  $D/h^2$  of isotretinoin was very similar for all the formulations investigated and no significant statistical differences were observed between them ( $p \geq 0.05$ ).

The introduction of heat (45 °C) increased  $Kh$  of isotretinoin into the skin for all the formulations investigated as shown in Table 4-1. This increase in  $Kh$  with heat was significant ( $p \leq 0.05$ ) for all formulations except for PG. The enhancement in  $Kh$  compared to each respective formulation ranged from 1.08 to 25.05-fold (Table 4-1), with the PG and EtOH showing the smallest and greatest increases respectively. With regards to the pathlength normalised diffusion coefficient ( $D/h^2$ ) the increase in temperature to 45 °C produced minimal increases in the  $D/h^2$  for isotretinoin when delivered from all the vehicles investigated, any apparent increases were not statistically significant ( $p \geq 0.05$ ).

**Table 4-1: Skin permeation parameters measured for isotretinoin in different dermatological formulations. Cumulative amount permeated ( $Q_{24}$ ), average flux ( $J$ ), pathlength normalised partition coefficient ( $Kh$ ), pathlength normalised diffusion coefficient ( $D/h^2$ ) and lag time ( $T_L$ ) were measured for both physiological skin temperature (32 °C) and elevated skin temperature (45 °C) using Fick's first law (mean  $\pm$  SEM, n=6). \* denotes significant difference in the parameter at 45 °C for each vehicle compared to the same respective vehicle at 32 °C.**

Vehicle	Membrane temperature (°C)	$J$ ( $\mu\text{g}/\text{cm}^2/\text{hr}$ )	$E_R$	$Q_{24}$ ( $\mu\text{g}/\text{cm}^2$ )	$E_R$	$T_L$ (hr)	$D/h^2$ ( $\times 10^{-2}\text{hr}^{-1}$ )	$E_R$	$Kh$ (cm)	$E_R$
Isotrex® gel	32	$0.034 \pm 0.002$	9.24	$0.79 \pm 0.03$	8.43	$4.91 \pm 0.52$	$3.39 \pm 0.32$	1.28	$1.00 \pm 0.11$	7.44
	45	$0.314 \pm 0.033^*$		$6.66 \pm 0.62^*$		$3.95 \pm 0.61$	$4.22 \pm 0.27$		$7.44 \pm 1.15^*$	
DPA	32	$0.038 \pm 0.001$	16.11	$0.83 \pm 0.03$	14.10	$3.98 \pm 0.35$	$3.35 \pm 0.48$	1.18	$1.14 \pm 0.08$	13.56
	45	$0.612 \pm 0.106^*$		$11.70 \pm 2.02^*$		$4.21 \pm 0.58$	$3.96 \pm 0.29$		$15.46 \pm 2.13^*$	
EtOH	32	$0.115 \pm 0.020$	27.31	$1.80 \pm 0.30$	31.41	$8.10 \pm 1.32$	$2.06 \pm 0.13$	1.09	$5.59 \pm 0.91$	25.05
	45	$3.141 \pm 0.557^*$		$56.54 \pm 13.95^*$		$7.43 \pm 1.70$	$2.24 \pm 0.10$		$140.03 \pm 32.04^*$	
IPM	32	$0.081 \pm 0.018$	11.28	$1.29 \pm 0.30$	13.39	$8.59 \pm 0.32$	$1.94 \pm 0.52$	1.65	$4.17 \pm 0.16$	6.84
	45	$0.914 \pm 0.267^*$		$17.27 \pm 4.86^*$		$5.20 \pm 0.54^*$	$3.21 \pm 0.31$		$28.52 \pm 2.96^*$	
PG	32	$0.140 \pm 0.060$	1.32	$2.06 \pm 0.81$	1.59	$9.30 \pm 0.81$	$1.79 \pm 0.21$	1.22	$7.81 \pm 0.68$	1.08
	45	$0.185 \pm 0.039$		$3.27 \pm 0.76$		$7.63 \pm 0.92$	$2.18 \pm 0.18$		$8.47 \pm 1.01^*$	
PGML 90	32	$0.060 \pm 0.013$	4.32	$0.99 \pm 0.22$	4.80	$8.15 \pm 0.91$	$2.05 \pm 0.18$	1.20	$2.93 \pm 0.33$	3.58
	45	$0.259 \pm 0.078^*$		$4.75 \pm 1.74^*$		$6.75 \pm 1.44$	$2.47 \pm 0.12$		$10.49 \pm 2.24^*$	
TP	32	$0.050 \pm 0.008$	11.36	$0.80 \pm 0.09$	11.74	$8.16 \pm 1.43$	$2.04 \pm 0.12$	1.18	$2.45 \pm 0.43$	9.64
	45	$0.568 \pm 0.100^*$		$9.39 \pm 1.45^*$		$6.93 \pm 1.04$	$2.41 \pm 0.16$		$23.62 \pm 3.54^*$	

### 4.3.2 Finite dose *in vitro* skin permeation and distribution studies

The transport and retention of isotretinoin across human abdominal skin was investigated by conducting finite dose studies at 32 °C and 45 °C to simulate "in use" conditions. Isotretinoin was delivered from 50:50 solvent systems (EtOH: DPA, EtOH: IPM, EtOH: PG and EtOH: PGML 90) to look for synergy between the vehicles and synergy with heat (45 °C). Delivery from these vehicles was compared to that from neat EtOH and the marketed product Isotrex® gel. All the formulations investigated contained 0.05% w/v of isotretinoin to match the marketed product Isotrex® gel, which contains 0.05% w/w isotretinoin. DPA, IPM, PG and PGML 90 were selected for inclusion into the 50:50 solvent systems because they were found to promote the uptake of isotretinoin into the skin tissue with the application of heat (as shown in the infinite dose studies). Additionally, EtOH was included as a volatile co-solvent to increase the thermodynamic activity as it evaporates, therefore, increasing the escaping tendency of the drug from the vehicle into the skin including the hair follicles (Oliveira, Hadgraft, & Lane, 2012). For all the formulations/vehicles investigated the mass balance ranged from approximately 85.00 % to 90.82 % at both temperatures investigated (Table 4-2). This level of recovery was deemed acceptable as the OECD guidelines recommend recoveries over 80 % for drugs with stability issues (OECD, 2004a). As with the infinite dose experiments, precautions were taken to protect the isotretinoin from light during this study i.e. covering with aluminium foil, however, drug degradation still occurred. Tschan and co-workers previously highlighted the sensitivity of isotretinoin to light, where up to 60% of isotretinoin in the donor chamber was lost to degradation when exposed to light over 24 hr (Tschan et al., 1997). The skin permeation profiles and distribution data are shown in Figure 4-3(a-b) and Figure 4-4(a-b) for 32 °C and 45 °C respectively.

At 32 °C, isotretinoin was delivered into the receiver fluid from 1 hr onwards when applied from Isotrex<sup>®</sup> gel, EtOH, EtOH: IPM and EtOH: PG, with these formulations producing an initial increase in permeation which slowed but continued through the duration of the experiment (finite dose permeation profiles) [Figure 4-3(a)]. However, for both EtOH: DPA and EtOH: PGML 90, isotretinoin was first detected in the receiver fluid at later times (18 hr onwards). The amount of isotretinoin delivered into the receiver fluid ranged from  $0.20 \pm 0.04$  to  $0.66 \pm 0.10 \mu\text{g}/\text{cm}^2$ , with EtOH: PGML 90 and EtOH: PG producing the lowest and highest delivery respectively. These corresponded to 4.00 % and 13.20 % of the applied dose respectively.

The differences observed with the amount of drug recovered from the receiver fluid could be due to the varying degrees of thermodynamic activity (drug saturation level) in the residual formulation. Assuming the total loss of EtOH from the binary systems, the drug saturation level in the residual formulation was 5 %, 6 %, 10 % and 70 % for PGML 90, DPA, IPM and PG respectively. Therefore, the increased thermodynamic activity in PG in comparison to the other vehicles could be a possible explanation for the greater delivery achieved with PG compared to the other vehicles. This finding fits well with other studies that showed the level of saturation was proportional to drug flux (Iervolino, Cappello, Raghavan, & Hadgraft, 2001). Similarly, with Isotrex<sup>®</sup> gel the evaporation of EtOH is believed to result in supersaturation of isotretinoin (solubility of isotretinoin in hydroxypropyl cellulose is unknown/not determined), with the hydrophilic polymer acting as anti-nucleating agent and preventing the crystallisation of the drug. The use of polymers as anti-nucleating agents to slow/prevent drug crystallisation is well documented (Reid, Benaouda, Khengar, Jones, & Brown, 2013).

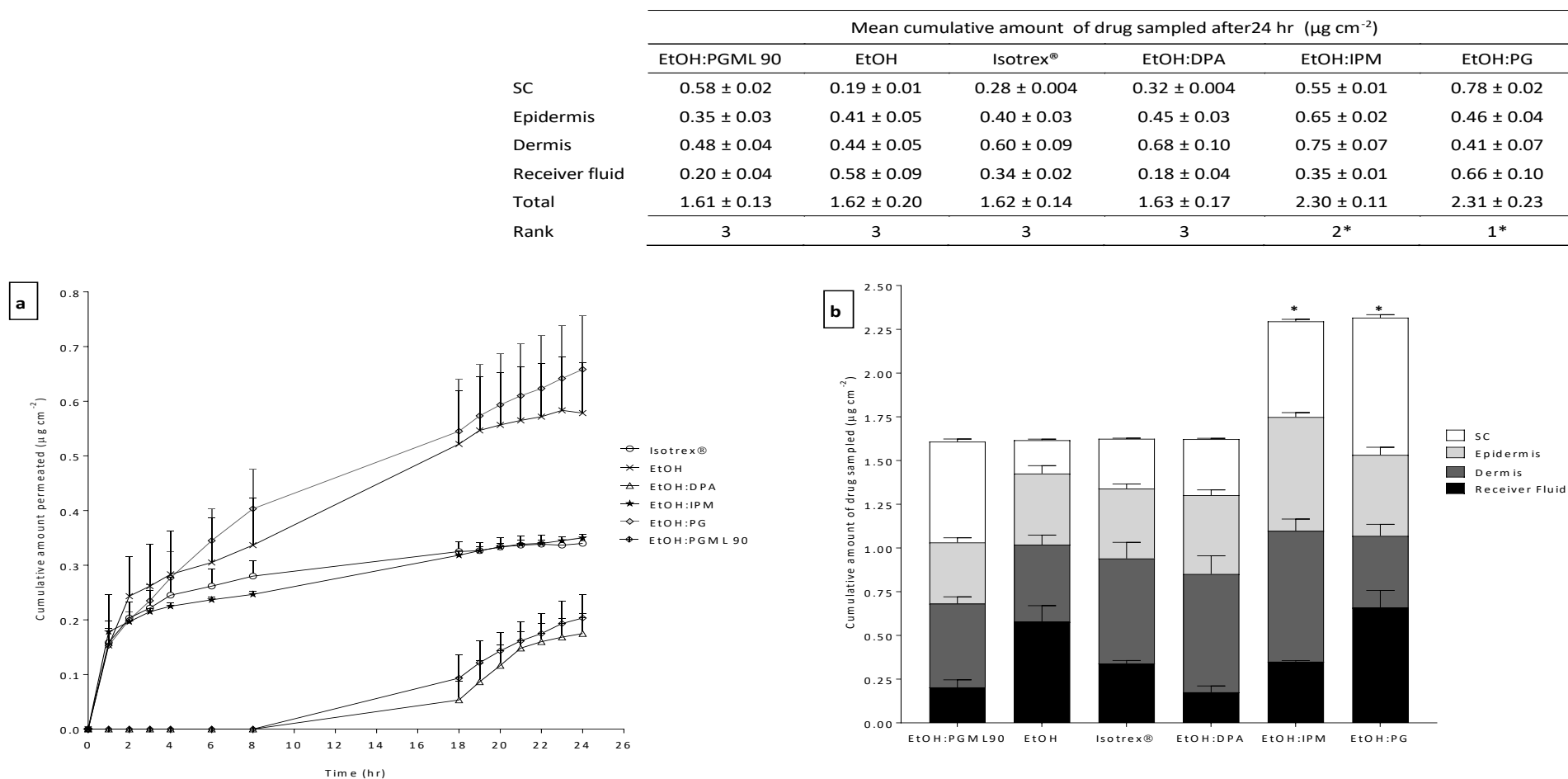


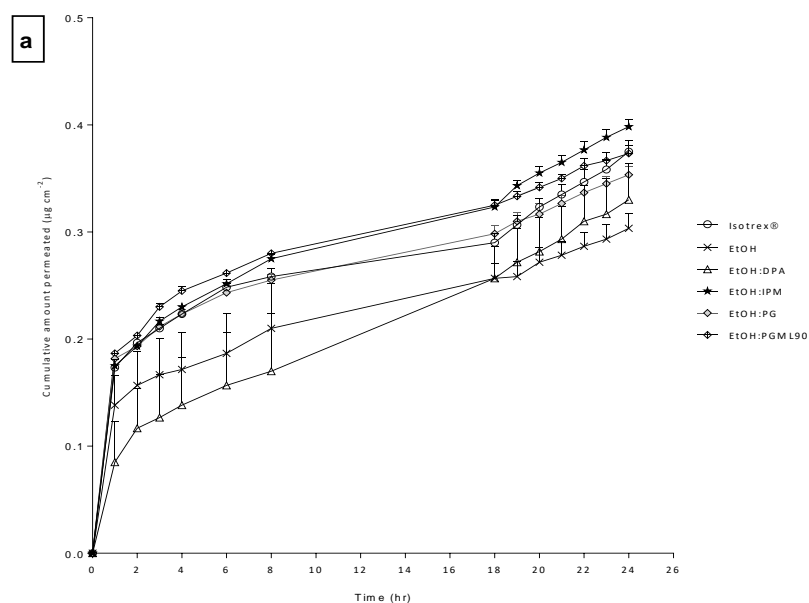
**Figure 4-3: Mean cumulative amount of isotretinoin (a) permeation through human abdominal skin at 32°C over 24 hr from various vehicles (b) recovered from the skin surface, stratum corneum (SC), epidermis, dermis and receiver fluid at the end of the finite dose permeation study.** Isotretinoin 0.05 % w/v was applied 10  $\mu\text{L cm}^{-2}$  to the skin surface in 50:50 binary systems. Binary systems tested were Ethanol: Diisopropyl adipate (EtOH: DPA), Ethanol: Isopropyl myristate (EtOH: IPM), Ethanol: Propylene glycol (EtOH: PG), Ethanol: Propylene glycol monolaurate 90 (EtOH: PGML 90). The marketed product Isotrex<sup>®</sup> gel 0.05 % w/w and neat Ethanol (EtOH) were used as controls and 10 mg  $\text{cm}^{-2}$  and 10  $\mu\text{L cm}^{-2}$  was applied to the skin surface respectively. All points are mean + SEM of n=6 diffusion cells. \* denotes significant difference in the total amount of isotretinoin delivered compared to the vehicles ranked 3<sup>rd</sup>.

Also, at 32 °C varying amounts of isotretinoin was recovered from the different skin layers [Figure 4-3(b)], with the total amount of drug recovered from the skin tissue (SC + epidermis + dermis) ranging from  $1.04 \pm 0.11$  to  $1.95 \pm 0.10$   $\mu\text{g}/\text{cm}^2$ , with EtOH and EtOH: IPM generating the minimum and maximum delivery. No correlation was observed between the amount of drug recovered from the receiver fluid and skin tissue, which highlights the complex nature of percutaneous absorption, especially under finite dose conditions.

With regards to the total amount of isotretinoin recovered (SC + epidermis + dermis + receiver fluid), both EtOH: PG and EtOH: IPM delivered greater amounts of drug, which was statistically significant in comparison to all the other formulations investigated. There was no statistical difference in the total amount of isotretinoin delivered between the other formulations tested. Thus, in terms of total drug delivery the rank of the formulations was in the following order: EtOH: PG > EtOH: IPM > EtOH: DPA > Isotrex<sup>®</sup> > EtOH > EtOH: PGML 90, with the amount of isotretinoin delivered ranging from  $1.61 \pm 0.13$   $\mu\text{g}/\text{cm}^2$  to  $2.31 \pm 0.23$   $\mu\text{g}/\text{cm}^2$ . This was equivalent to 32.20 % and 46.20 % of the applied dose respectively.

At 45 °C, isotretinoin was detected in the receiver fluid at early time points (1 hr onwards) for all the formulations tested. The permeation profiles at this higher temperature are shown in Figure 4-4(a). With the application of heat, all the formulations produced finite dose profiles as was seen with some of formulations at 32 °C. Also, compared to the experiments at 32 °C, the application of heat altered the amount of isotretinoin delivered into the receiver fluid differently from all the formulations investigated. For Isotrex<sup>®</sup>, EtOH: IPM, EtOH: DPA and EtOH: PGML 90, the higher temperature increased the amount of isotretinoin delivery into the receiver fluid. Within these formulations, Isotrex<sup>®</sup> and EtOH: PGML 90 produced the minimum and maximum enhancement, which corresponded to 1.12 to 1.85-fold increase in comparison to the same respective vehicle at 32 °C, respectively.

However, from EtOH and EtOH: PG the amount of isotretinoin delivered into the receiver fluid decreased compared to each respective formulation at 32 °C. A possible explanation for the decline in the amount of drug delivered into the receiver fluid from these two preparations could be due to the quicker uptake of EtOH and PG into the skin compared to the drug and therefore lead to loss of EtOH and PG from the donor chamber causing the drug to crystallise out due to solvent/vehicle loss. Also, the evaporation of both EtOH and PG from the donor chamber could have contributed to solvent loss from the donor chamber leading to increased rate of drug crystallisation. Previous permeation studies have shown that approximately 40 % to 60 % of PG is lost from the donor chamber to evaporation, especially under finite dose conditions where the dose loaded is very small (Trottet, Merly, Mirza, Hadgraft, & Davis, 2004; Tsai et al., 1992). At the higher temperature (45 °C), the rank of the formulations in terms of delivery into the receiver fluid was in the following order: EtOH: IPM > Isotrex<sup>®</sup> gel > EtOH: PGML 90 > EtOH: PG > EtOH: DPA > EtOH, with the quantity of drug delivered ranging from  $0.30 \pm 0.01 \mu\text{g}/\text{cm}^2$  to  $0.40 \pm 0.01 \mu\text{g}/\text{cm}^2$ , which is equivalent to 6 % to 8 % of the applied dose respectively.



	Mean cumulative amount of drug sampled after 24 hr ( $\mu\text{g cm}^{-2}$ )					
	EtOH	Isotrex®	EtOH:PG	EtOH:DPA	EtOH:PGML 90	EtOH:IPM
SC	1.07 $\pm$ 0.08	0.50 $\pm$ 0.06	0.82 $\pm$ 0.03	0.42 $\pm$ 0.02	0.33 $\pm$ 0.02	0.40 $\pm$ 0.04
Epidermis	0.40 $\pm$ 0.05	0.52 $\pm$ 0.08	0.92 $\pm$ 0.19	1.05 $\pm$ 0.20	0.81 $\pm$ 0.20	0.94 $\pm$ 0.17
Dermis	0.74 $\pm$ 0.10	1.38 $\pm$ 0.24	0.82 $\pm$ 0.05	1.28 $\pm$ 0.23	1.76 $\pm$ 0.39	1.59 $\pm$ 0.24
Receiver fluid	0.30 $\pm$ 0.01	0.38 $\pm$ 0.01	0.35 $\pm$ 0.01	0.33 $\pm$ 0.03	0.37 $\pm$ 0.01	0.40 $\pm$ 0.01
Total	2.51 $\pm$ 0.24	2.78 $\pm$ 0.39	2.91 $\pm$ 0.28	3.08 $\pm$ 0.48	3.27 $\pm$ 0.62	3.33 $\pm$ 0.46
Rank	6	5	4	3	2	1

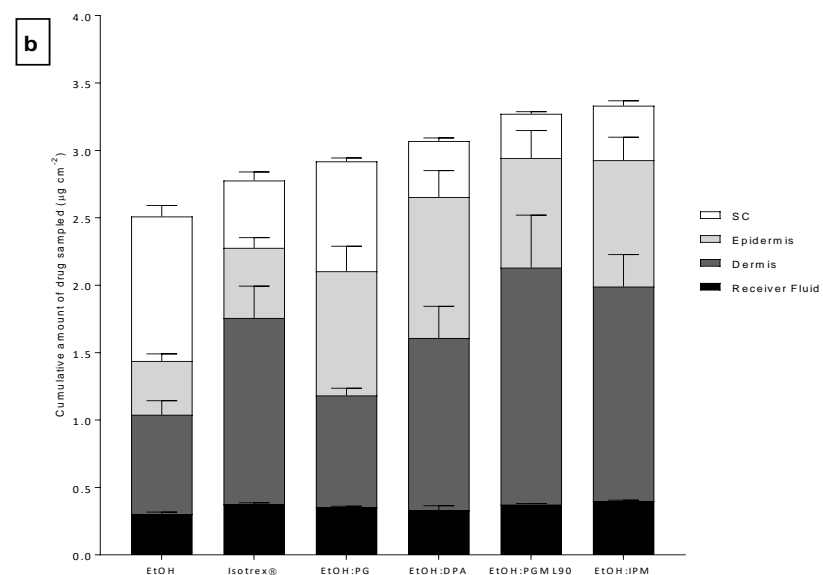


**Figure 4-4: Mean cumulative amount of isotretinoin (a) permeation through human abdominal skin at 45 °C over 24 hr from various vehicles (b) recovered from the skin surface, stratum corneum (SC), epidermis, dermis and receiver fluid at the end of the finite dose permeation study.** Isotretinoin 0.05 % w/v was applied 10  $\mu\text{L cm}^{-2}$  to the skin surface in 50:50 binary systems. Binary systems tested were Ethanol: Diisopropyl adipate (EtOH: DPA), Ethanol: Isopropyl myristate (EtOH: IPM), Ethanol: Propylene glycol (EtOH: PG), Ethanol: Propylene glycol monolaurate 90 (EtOH: PGML 90). The marketed product Isotrex® gel 0.05 % w/w and neat Ethanol (EtOH) were used as controls and 10  $\text{mg cm}^{-2}$  and 10  $\mu\text{L cm}^{-2}$  was applied to the skin surface respectively. All points are mean + SEM of n=6 diffusion cells. Differences in the total amount of isotretinoin delivered from all the formulations were not statistically significant.

**Table 4-2: Percentage of isotretinoin recovered from skin surface, stratum corneum (SC), epidermis, dermis and receiver fluid at the end of the 24 hr finite dose permeation studies (Mean  $\pm$  SEM, n=6).**

CPEs	Membrane surface temperature	Percentage (%) of applied dose recovered					Receiver fluid	Total recovery
		Skin surface	SC	Epidermis	Dermis			
Isotrex	32 °C	54.00 $\pm$ 4.60	5.60 $\pm$ 0.08	8.00 $\pm$ 0.60	12.00 $\pm$ 1.80	6.80 $\pm$ 0.40	86.40 $\pm$ 7.48	
	45 °C	31.80 $\pm$ 4.40	10.00 $\pm$ 1.20	10.40 $\pm$ 1.60	27.60 $\pm$ 4.80	7.60 $\pm$ 0.20	87.40 $\pm$ 12.20	
EtOH	32 °C	54.60 $\pm$ 1.80	3.80 $\pm$ 0.20	8.20 $\pm$ 1.00	8.80 $\pm$ 1.00	11.60 $\pm$ 2.00	87.00 $\pm$ 6.00	
	45 °C	35.60 $\pm$ 4.20	21.40 $\pm$ 1.60	8.00 $\pm$ 1.00	14.80 $\pm$ 2.00	6.00 $\pm$ 0.02	85.80 $\pm$ 8.82	
EtOH: DPA (1:1)	32 °C	52.40 $\pm$ 1.40	6.40 $\pm$ 0.08	9.00 $\pm$ 0.60	13.60 $\pm$ 2.00	3.60 $\pm$ 0.80	85.00 $\pm$ 4.88	
	45 °C	29.20 $\pm$ 3.00	8.42 $\pm$ 0.40	21.00 $\pm$ 4.00	25.60 $\pm$ 4.60	6.60 $\pm$ 0.60	90.82 $\pm$ 12.60	
EtOH: IPM (1:1)	32 °C	40.00 $\pm$ 2.80	11.00 $\pm$ 0.20	13.00 $\pm$ 0.40	15.00 $\pm$ 1.40	7.00 $\pm$ 0.02	86.00 $\pm$ 4.82	
	45 °C	22.20 $\pm$ 2.60	6.60 $\pm$ 0.60	18.80 $\pm$ 3.40	31.80 $\pm$ 4.80	8.00 $\pm$ 0.20	87.40 $\pm$ 11.60	
EtOH: PG (1:1)	32 °C	42.00 $\pm$ 5.40	15.60 $\pm$ 0.40	9.20 $\pm$ 0.80	8.20 $\pm$ 1.40	13.20 $\pm$ 2.00	88.20 $\pm$ 10.00	
	45 °C	32.40 $\pm$ 1.20	16.40 $\pm$ 0.80	18.40 $\pm$ 3.80	16.40 $\pm$ 1.00	7.00 $\pm$ 0.20	90.60 $\pm$ 7.00	
EtOH: PGML 90 (1:1)	32 °C	56.80 $\pm$ 6.80	11.60 $\pm$ 0.40	7.00 $\pm$ 0.60	9.60 $\pm$ 0.80	4.00 $\pm$ 0.80	89.00 $\pm$ 9.40	
	45 °C	24.20 $\pm$ 3.20	6.60 $\pm$ 0.40	16.20 $\pm$ 4.00	35.20 $\pm$ 7.80	7.40 $\pm$ 0.20	89.60 $\pm$ 15.60	

With the application of heat (45 °C), higher quantities of drug were recovered from the skin tissue in relation to the experiments at 32 °C. For Isotrex<sup>®</sup> gel, EtOH: DPA, EtOH: PGML 90 and EtOH: IPM the highest amount of drug was recovered from the dermis as shown in Figure 4-4(b), delivery into the dermis was increased up to 3.6-fold. For EtOH: PG similar quantities of drug were recovered from the different skin layers, whereas for neat EtOH, the largest quantity was recovered from the SC. Overall, the enhancement in drug tissue (SC + epidermis + dermis) concentrations ranged from 1.50 to 2.13-fold, with EtOH: IPM and neat EtOH producing the minimum and maximum increase in drug tissue concentration respectively.

The rank of the formulations in terms of the total amount of isotretinoin delivered was in the following order: EtOH: IPM > EtOH: PGML 90 > EtOH: DPA > EtOH: PG > Isotrex<sup>®</sup> gel > EtOH, with the total amount of isotretinoin delivered ranging from  $2.51 \pm 0.24 \mu\text{g}/\text{cm}^2$  to  $3.33 \pm 0.46 \mu\text{g}/\text{cm}^2$ . This was equivalent to 50.2 % and 66.6 % of the applied dose respectively. Thus, the application of heat enhanced the total quantity of isotretinoin delivered (SC + epidermis + dermis + receiver fluid) 1.3 to 2.0-fold, with EtOH: PG and EtOH: PGML 90 producing the lowest and highest enhancement. Statistical differences were not found between the different formulations investigated in terms of the total amount of drug delivered.

### 4.3.3 The effects of heat applied from top on drug delivery into the hair follicles, skin tissue and receiver fluid over 24 hr

When administering isotretinoin via the skin for the treatment of acne, increased follicular and skin tissue concentrations is highly sought (such that targeted delivery is achieved, and therefore potentially reducing adverse effects). Therefore, modulating the interplay of non-follicular permeation and follicular uptake via the application of short bursts of heat (45 °C) from top in combination with certain CPEs could be a new, revolutionising strategy to treat many different skin and/or scalp diseases in the future.

Thus, in this section the effect of a short application of heat from top on the delivery of isotretinoin into the hair follicles, skin tissue and receiver fluid from Isotrex® gel and EtOH: PGML 90 was investigated. Short periods of heating were investigated because it is more realistic and practical, especially in clinical setting. Furthermore, the use of a short burst of heat could also offer other advantages over current treatments including reduction of *Propionibacterium acnes* colonisation of the appendages (considered to be a fundamental factor contributing to acne formation). Elevated temperature can trigger the synthesis of heat shock proteins, which are involved in regulating the immune response (Colaco, Bailey, Walker, & Keeble, 2013; van Eden, van der Zee, & Prakken, 2005). The importance of such an effect has been reported in the work of Joo et al (2012), in which attempts were made to develop a device combining light (maximum peak intensity: 468 nm) and thermal (49.1 °C for 3 min) methods to treat acne lesions. This device (with no active included) was found to cause a marked reduction in the size of pustules after 48 hr; the efficacy of the thermal treatment was attributed to production of heat shock proteins (Joo, Kang, Choi, Nelson, & Jung, 2012).

From the finite dose studies EtOH: PGML 90 worked best with heat (2-fold enhancement), thus it was selected for further investigation to gain a better understanding of how it works with heat. In this experiment The EtOH: PGML 90 formulation was optimised for thermodynamic activity by using a filtered saturated solution (prepared at 32 °C). Isotrex® gel was again used as a control. The dose

distribution of isotretinoin in hair follicles, skin tissue (SC, epidermis and dermis) and receiver fluid delivered from Isotrex<sup>®</sup> gel and ETOH: PGML 90 are shown in Figure 4-5 and Figure 4-6 respectively as the percent dose applied recovered. These experiments were conducted for 24 hr at 32 °C with and without sodium thiosulfate (ST) solution producing heat ( $\leq 45$  °C) for 15 & 25 min (ST 15 & ST 25 respectively) and also at 45 °C (water bath, whole system heating). The total mass balance for both formulations was above 80 %.

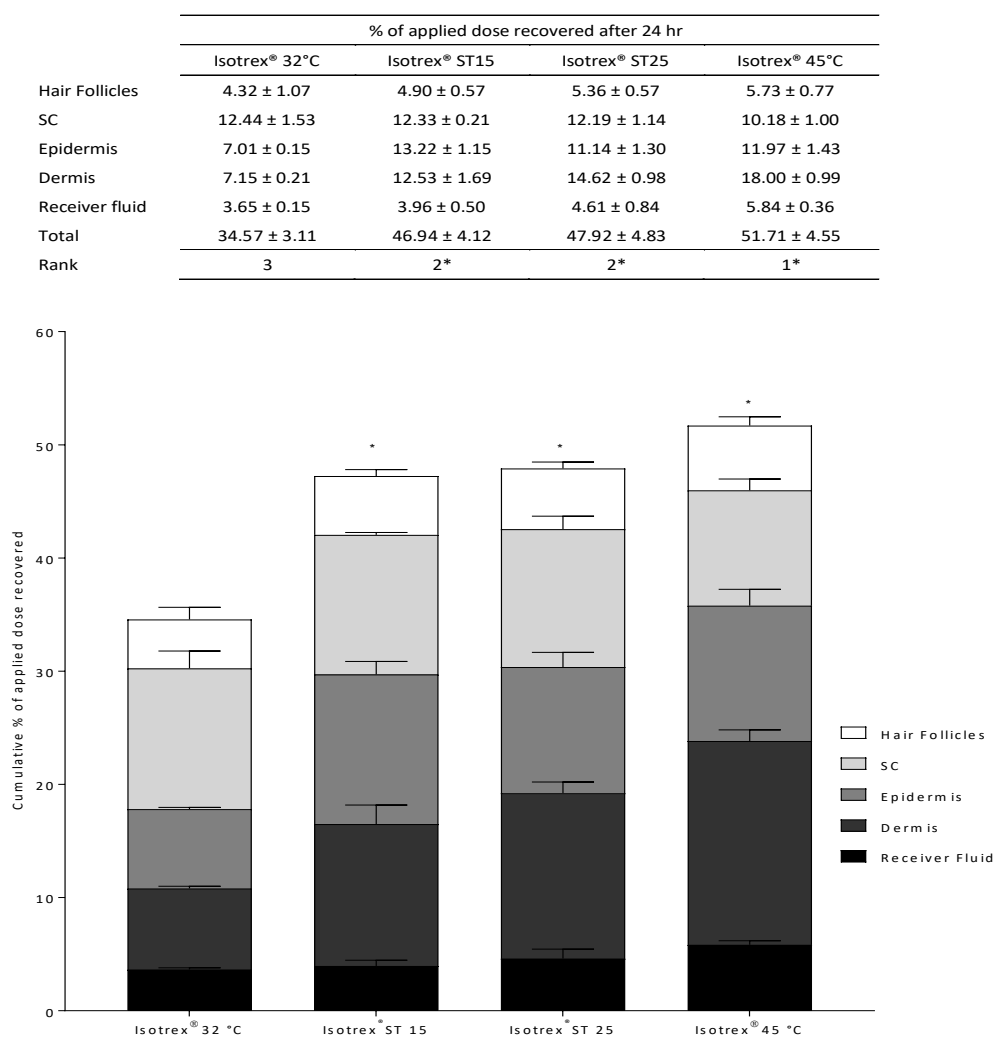


**Figure 4-5: Dose distribution of isotretinoin in human abdominal skin and receiver fluid delivered from Isotrex<sup>®</sup> gel.** Experiments were conducted for 24 hr at 32 °C with and without sodium thiosulfate (ST) solution producing heat for 15 & 25 min (ST 15 & ST 25 respectively) and also at 45 °C. Each bar indicates the amount of isotretinoin that was recovered from the skin surface (unabsorbed), hair follicles, in the skin (SC + epidermis + dermis) or receiver fluid. The marketed product Isotrex<sup>®</sup> gel 0.05% w/w 10 mg cm<sup>-2</sup> was applied to the skin surface. All bars are mean + SEM of n=6 diffusion cells. \* denotes a significant difference in total amount recovered compared to formulations ranked 3<sup>rd</sup>.

For Isotrex<sup>®</sup> gel, whole system heating (using water bath to give membrane temperature of 45 °C for the whole duration of the experiment), ST 15 and ST 25 (the application of heat from top for both 15 and 25 min) significantly increased the total percentage of isotretinoin recovered compared to the control (32 °C). In terms of drug uptake into the hair follicles, whole system heating, ST 25 and ST 15 increased the fraction of isotretinoin recovered from the hair follicles 1.33-fold, 1.24-fold 1.13-fold respectively in comparison to the control (32 °C). The fraction of isotretinoin recovered from the SC did not increase with the application of heat. However, this was not the case for the epidermis and dermis, as the fraction of isotretinoin recovered was enhanced 1.59 to 1.89-fold and 1.75 to 2.51-fold respectively, with whole system heating producing the maximum enhancement followed by ST 25 and ST 15. Similarly, receiver fluid concentrations were increased 1.08 to 1.60-fold with the application of heat, with the order of enhancement following this trend: whole system heating > ST 25 > ST 15.

For the binary system EtOH: PGML 90, only whole system heating (45 °C) was statistically significant but there appeared to be a trend on increasing drug delivery with increased duration of heating.

	% of applied dose recovered after 24 hr			
	EtOH:PGML 90 32°C	EtOH:PGML 90 ST15	EtOH:PGML 90 ST25	EtOH:PGML 90 45°C
Hair Follicles	4.67 ± 0.34	6.23 ± 0.43	6.71 ± 0.62	5.64 ± 0.41
SC	5.72 ± 0.49	6.15 ± 0.67	6.45 ± 1.10	7.99 ± 0.96
Epidermis	17.18 ± 1.17	10.85 ± 0.97	10.59 ± 0.80	17.29 ± 1.10
Dermis	11.46 ± 1.69	17.72 ± 0.66	23.05 ± 1.46	42.03 ± 1.14
Receiver Fluid	0.63 ± 0.04	1.92 ± 0.19	5.27 ± 0.60	2.05 ± 0.07
Total	39.66 ± 3.73	42.87 ± 2.92	52.07 ± 4.58	75.00 ± 3.68
Rank	4	3	2	1*

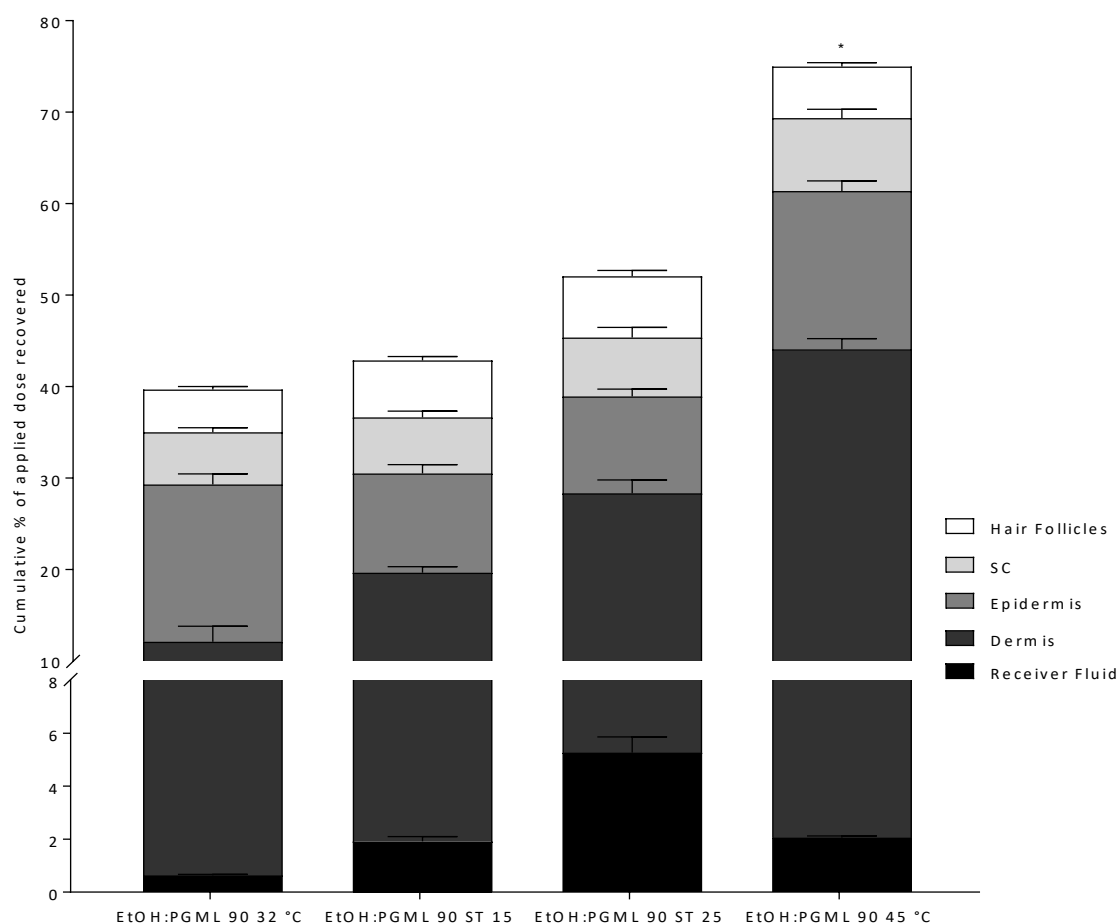


**Figure 4-6: Dose distribution of isotretinoin in human abdominal skin and receiver fluid delivered from EtOH: PGML 90 binary system.** Experiments were conducted for 24 hr at 32 °C with and without sodium thiosulfate (ST) solution producing heat for 15 & 25 min (ST15 & ST25 respectively) and at 45 °C. Each bar indicates the amount of isotretinoin that was recovered from the hair follicles, in the skin (SC + epidermis + dermis) or receiver fluid. Isotretinoin filtered saturated solution (1.38 % w/v) 10  $\mu\text{L cm}^{-2}$  in EtOH: PGML 90 (1:1) binary system was applied to the skin surface. All bars are mean + SEM of n=6 diffusion cells. \* denotes a significant difference in total amount recovered compared to formulations ranked 2<sup>nd</sup> and higher.

With respect to EtOH: PGML 90, drug recovery from the hair follicles was enhanced by 1.21, 1.33 and 1.44-fold with whole system heating, ST 15 and ST 25 respectively compared to the control (32 °C). Whereas, the fraction of drug recovered from the SC and dermis was enhanced 1.08 to 1.40-fold and 1.55 to 3.67-fold respectively, with whole system heating producing the greatest enhancement, followed by ST 25 and ST 15. In contrast, the application of heat was found not to increase the amount of isotretinoin delivered into the epidermis from EtOH: PGML 90. The receiver fluid concentrations were enhanced 3.25, 3.00 and 8.37-fold with ST 15, whole system heating and ST 25 respectively. Thus, for EtOH: PGML 90 greater increases in isotretinoin uptake into the receiver fluid were observed with any application of heat compared to the control (same formulation at 32 °C). This suggests that EtOH: PGML 90 works better with heat at delivering isotretinoin compared to the marketed product Isotrex<sup>®</sup> gel.

The enhancement effect of heat on percutaneous absorption is highly complex and depends on a combination of different mechanisms of action (Shahzad et al., 2015). Based on the findings from the infinite dose studies (Section 4.3.1), the ability of heat to increase the partitioning and uptake of the drug into the membrane was found to be the main reason for the improved transport of isotretinoin across the skin at high temperature (45 °C). Therefore, the application of heat ( $\leq 45$  °C) from top for short periods (15 and 25 min) was expected to further enhance drug partitioning into the hair follicles and skin tissue by increasing the kinetic energy of drug molecules. In addition, the presence of a temperature gradient with the application of heat from top could further act as driving force for diffusion into the hair follicles and skin tissues (McAuley & Caserta, 2015).

#### **4.3.4 The effects of heat from top on drug delivery into the hair follicles, skin tissue and receiver fluid over 1 hr**

It was postulated that running the same experiments for 1 hr instead of 24 hr might provide improved understanding of the effect of heat on follicular absorption, since this route is thought to be important in the early stages of drug transport (Otberg et al., 2008). Thus, experiments lasting 1 hr were conducted for both formulations (Isotrex<sup>®</sup> gel and EtOH: PGML 90) with no heat (32 °C) and 25 min of heat from top. The distribution of isotretinoin in hair follicles, skin (SC, epidermis and dermis) and receiver fluid, with and without the application of sodium thiosulfate solution (ST) is depicted in Figure 4-7 as percentage of the dose applied to make comparisons between the two formulations easier (since the two formulations differ greatly in terms of isotretinoin concentration). For all experiments, the mass balance was above 80 %. Without ST, the total average amount of isotretinoin absorbed ranged from 19-22 % of the dose applied for both formulations, with the application of ST resulting in a 1.3-fold and 2.2-fold increase in total drug absorption from Isotrex<sup>®</sup> gel and EtOH: PGML 90 respectively. With the application of heat (ST 25), the increase in the total amount of isotretinoin recovered was significantly increased for EtOH: PGML 90 only.

	% of applied dose recovered after 1 hr			
	Isotrex®	Isotrex® ST 25	EtOH:PGML 90	EtOH:PGML 90 ST 25
Hair Follicles	3.31 ± 0.24	4.76 ± 0.26	4.44 ± 0.38	9.41 ± 0.50
SC	9.87 ± 1.50	15.68 ± 1.88	6.26 ± 1.07	6.99 ± 0.42
Epidermis	5.38 ± 2.91	3.45 ± 0.31	1.60 ± 0.60	3.64 ± 0.24
Dermis	2.39 ± 0.15	2.85 ± 0.14	6.12 ± 2.55	19.31 ± 1.36
Receiver Fluid	1.49 ± 0.67	2.12 ± 0.68	0.73 ± 0.11	3.06 ± 0.08
Total	22.44 ± 5.47	28.86 ± 3.27	19.15 ± 4.71	42.41 ± 2.60

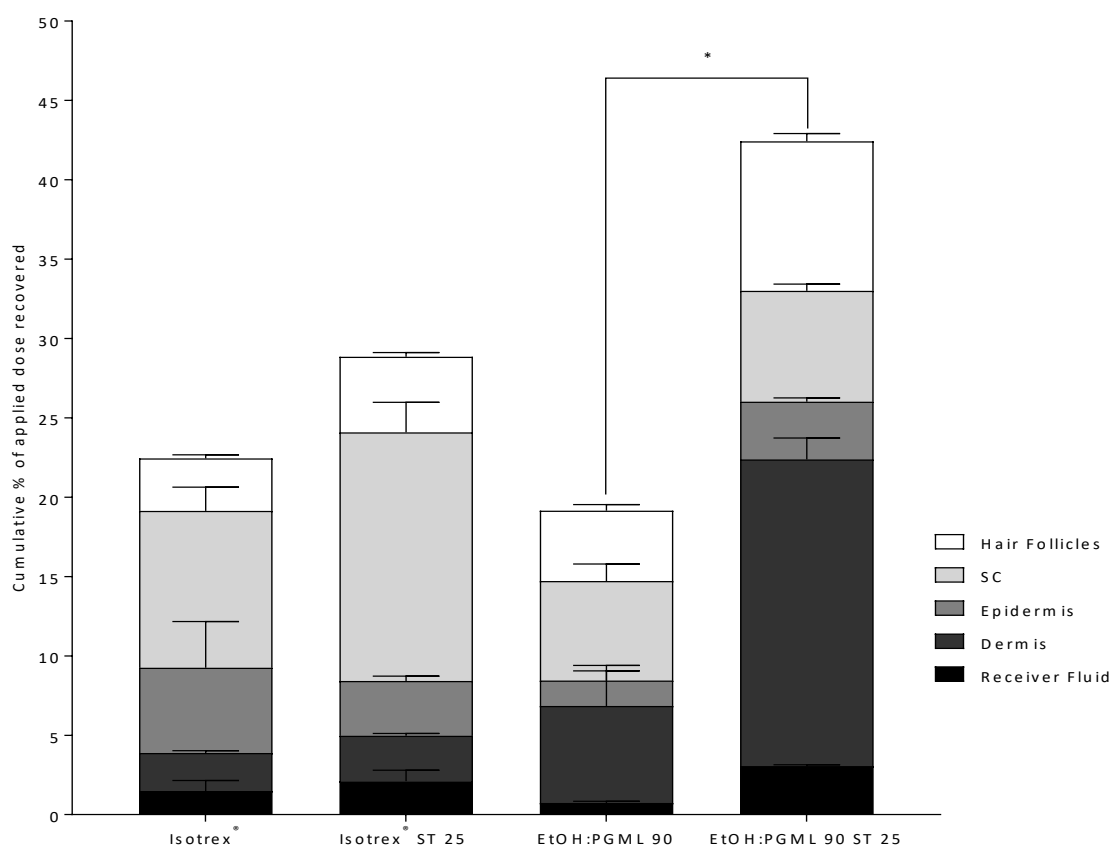


**Figure 4-7: Dose distribution of isotretinoin in human abdominal skin and receiver fluid delivered from various formulations.** Experiment was conducted for 1 hr at 32°C with and without sodium thiosulfate (ST) solution producing heat for 25 min (ST 25). Each bar indicates the amount of isotretinoin that was recovered from hair follicles, in the skin (SC + epidermis + dermis) or receiver fluid. The marketed product Isotrex® gel 0.05% w/w 10 mg cm<sup>-2</sup> and isotretinoin filtered saturated solution 1.38% w/v 10 μL cm<sup>-2</sup> in EtOH: PGML 90 (1:1) binary system was applied to the skin surface respectively. All bars are mean + SEM of n=6 diffusion cells.

For the control (32 °C) EtOH: PGML 90, the fraction of isotretinoin recovered from the hair follicles and SC in the 1 hr study were similar to the fraction recovered in the 24 hr study. Whereas, the fraction of drug recovered from the epidermis, dermis and receiver fluid were less in the 1 hr study. However,

with the application of localised heat for 25 min (ST 25) greater amounts of isotretinoin were recovered from the hair follicles in the 1 hr study in comparison to all the different heating conditions employed in the 24 hr study. The fraction of isotretinoin recovered from the hair follicles after 1 hr was similar to the fraction recovered after 24 hr of no heat (32 °C) and localised heating for 15 min (ST 15) for Isotrex<sup>®</sup> gel, indicating the more prominent role the hair follicles play in the transports of drugs at early time points.

With the application of localised heat (ST 25) for EtOH: PGML 90 in the 1 hr experiment, the increase in the fraction of isotretinoin recovered from the hair follicles (2.12-fold), epidermis (2.28-fold), dermis (3.16-fold) and receiver fluid (4.19-fold) was greater than the SC (1.12-fold) suggesting follicular targeting. This trend of drug transport was not observed with Isotrex<sup>®</sup> gel as the increase in fraction of drug recovered from the SC (1.59-fold) was more than the follicles (1.44-fold), dermis (1.19) and receiver fluid (1.42-fold) with ST 25.

Although the application of heat improved isotretinoin delivery from both formulations, this was not to the same extent. The binary system EtOH: PGML 90 provided significantly greater increases in drug delivery in combination with heat ( $P < 0.05$ ). In addition, the amount of isotretinoin delivered to the hair follicle was considerably greater from the EtOH: PGML 90 formulation. Also, the greater increase in isotretinoin dermal concentration with localised heating in comparison to the SC and epidermis, suggests that the main route of drug transport into the dermis may have been the hair follicles especially at early time points ( $\leq 1$  hr), which is indicative of potential follicular targeting. It appears, therefore, that CPEs and heat can act synergistically to enhance topical drug delivery to the skin tissue (especially the dermis) and hair follicles. This suggests that formulation components (e.g. CPEs) are likely to play an important role in influencing the effect of heat on drug transport across skin because of potential synergistic effects. Therefore, in a clinical setting it may be possible to further optimise delivery into the hair follicles (targeted follicular delivery) by combining EtOH: PGML 90 with heat for

very short periods i.e. 5 to 10 min and then wiping away any remaining formulation to prevent/reduce system delivery.

Also, it important to keep in mind that in human skin *ex vivo* skin, the follicular reservoir is diminished to 9.5% of the *in vivo* hair follicle reservoir as a result of the contraction of the elastic fibers surrounding the hair follicles during excision from the donor, as well as the sudden absence of blood flow and loss of hydration (Patzelt *et al* 2008). Therefore, results obtained under these conditions would be expected to underestimate follicular penetration, meaning that it is possible that much higher follicular concentrations are achieved *in vivo*.

#### 4.4 Conclusion

The effect of heat on the delivery of isotretinoin from a range of dermatological vehicles across full thickness abdominal skin was investigated. With the application of heat, isotretinoin flux was enhanced for all the formulations investigated, with EtOH producing the greatest increase in isotretinoin flux (27-fold). These enhancements were large compared to the same respective formulation at 32 °C due to improvements in partitioning (up to 25-fold increase), whilst improvements in diffusivity were considerably smaller (up to 1.7-fold). With respect to isotretinoin skin uptake, PGML 90 produced the greatest delivery into the skin tissue with heating, whilst delivering the least amount of isotretinoin into the receiver fluid.

The results obtained in this study demonstrated that the differential stripping technique is able to quantify the enhanced contribution of hair follicles in the transport of isotretinoin across skin with the application of heat at both 1 hr and 24 hr time points. For EtOH: PGML 90, a higher recovery of the drug was seen from the hair follicles with localised heating for 25 min at 1 hr and 24 hr time points compared to heating the skin for 24 hr (whole system heating), indicating a greater positive impact of localised heating on follicular transport compared to whole system heating. This data also showed that the absorption into the hair follicles is rapid as greater amounts of drug was recovered from the

hair follicles at early time points. Furthermore, the results obtained with Isotrex® gel and EtOH: PGML 90 showed distinct differences in the localisation of isotretinoin in the hair follicles, skin tissue and receiver fluid depending on the formulation components and the length of application of heat.

The data obtained from the follicular uptake and skin permeation studies confirmed that it is possible, depending on the type of vehicle used in combination with heat, one can maximise follicular and dermal uptake. This could help improve the effectiveness of topical treatments of various conditions like acne and androgenetic alopecia.

**5 Influence of CPEs and heat on the skin permeation, distribution  
and follicular absorption of finasteride**

## 5.1 Introduction

Androgenetic alopecia (AGA) is associated with increased levels of dihydrotestosterone (DHT) and 5-alpha reductase enzyme activity in the scalp follicles. The enzyme 5-alpha reductase is responsible for the conversion of testosterone to DHT. The pathogenesis and prevalence of AGA was covered in Chapter 1 Section 1.3.2.2. There are two types of 5-alpha reductase enzymes that contribute to AGA, the type I isoenzyme is present in the skin (including the scalp) and the type II isoenzyme is found in the hair follicles and prostate. Finasteride, a 4-azasteroid inhibitor of 5-alpha reductase is known to inhibit the type II isoenzyme and does this more effectively than with the type I isoenzyme (Wood & Rittmaster, 1994). Consequently, long-term oral administration of finasteride was found to decrease the level of DHT in bald scalps leading to the reversal of the progressive miniaturisation of the scalp follicles and shortening the different phases of the hair growth cycle (Dallob et al., 1994; Diani et al., 1992). However, the systemic administration of finasteride causes several unwanted side-effects, such as reduced libido and impairment of spermatogenesis in men and feminising male foetuses in pregnant women (Amory, 2007; Chiriaco, Cauci, Mazzon, & Trombetta, 2016). Therefore, topical application of finasteride would be more preferable in the treatment of AGA to minimise the side effects associated with systemic delivery. Moreover, topical administration of finasteride in an ethanol/propylene glycol vehicle has been shown to cause local inhibition of androgen-controlled sebaceous gland growth in an animal model, indicating the potential efficacy of topical finasteride in AGA (Chen et al., 1995). Similarly, Sintov, Serafimovich, & Gilhar (2000) reported topical application of finasteride stimulated hair growth in human bald scalp grafted onto mice, further demonstrating the efficacy of topical finasteride.

In recent years, many attempts have been made to produce topical finasteride formulations that enhance drug uptake into the skin and/or the PSU using delivery systems such as microemulsions (Biruss, Kählig, & Valenta, 2007), lipid nanoparticles (Gomes, Martins, Ferreira, Segundo, & Reis, 2014), liquid crystalline nanoparticles (Madheswaran, Baskaran, Yong, & Yoo, 2014), liposomes (Biruss &

Valenta, 2006; Kumar, Singh, Bakshi, & Katare, 2007; Tabbakhian, Tavakoli, Jaafari, & Daneshamouz, 2006) and niosomes (Vimal, Sankar, Srinivas, & Kumaresan, 2012). Whilst, some of these nanoparticulate based formulations have been able to enhance drug delivery into the PSU, the overall concentrations of finasteride delivered were low. Also, some of these studies employed animal skin models such as hamster flank skin, abdominal mice skin and abdominal porcine skin, which are less suitable in comparison to human scalp skin as models for investigating the topical delivery of finasteride into the hair follicles and skin tissue for the treatment of AGA. In addition, these types of delivery systems often suffer from poor stability and are associated with high production costs. Thus, there is a need to develop drug delivery systems with high patient acceptability that can improve the uptake of finasteride into both the hair follicles and skin tissue. The use of physical enhancement strategies such as physiologically tolerable heat ( $\leq 45\text{ }^{\circ}\text{C}$ ) in combination with CPEs holds great promise for enhancing skin permeation through the SC and for targeting hair follicles as demonstrated with the delivery of isotretinoin as described in Chapter 4. Thus, to further improve our understanding of the effects of heat and CPEs on follicular drug delivery, human scalp skin was used as a model membrane in this Chapter. Human scalp skin has greater follicular density in comparison to human abdominal skin and therefore is the best possible model for investigating the effect of heat and CPEs on the topical delivery of finasteride into the hair follicles for the treatment of AGA.

To date, the combined influence of physiologically tolerable heat ( $\leq 45\text{ }^{\circ}\text{C}$ ) and CPEs on the delivery of finasteride into skin tissue and hair follicles has not been investigated. Therefore, the aim of this Chapter was to study, the influence of physiological tolerable heat ( $\leq 45\text{ }^{\circ}\text{C}$ ) on the uptake of finasteride into the hair follicles, its distribution within the different skin layers (SC, viable epidermis, dermis) and its permeation through human scalp skin, under the influence of different dermatological vehicles commonly employed as CPEs. Furthermore, the feasibility of using shorter durations of externally applied physiologically tolerable heat to enhance finasteride transport across the skin was examined to gain a more detailed understanding of the influence of heat with different vehicles on drug absorption into the skin and deposition into the hair follicles.

## 5.2 Materials and Methods

Finasteride (99.9 %) was purchased from Sequoia Research Products (Pangbourne, UK). Acetonitrile HPLC grade (99.9 %), propan-2-ol (>99.5 %), methanol HPLC grade (99.9 %), propylene glycol (>99.0 %), phosphate buffer solution (PBS) tablets, Dura Seal™ (Diversified Biotech, USA), Hamilton GASTIGHT® syringes (Hamilton®, Switzerland) and Parafilm M® laboratory film (Bemis® Flexible packaging, USA) and Sodium thiosulfate pentahydrate (99.5%) (Acros Organic, USA) were acquired from Fisher Scientific (Loughborough, UK). Diisopropyl adipate (> 99.8 %) and Dimethyl isosorbide (> 99.8 %) were supplied by Croda (Barcelona, Spain). Transcutol® P (>99.8%) was purchased from Gattefosse (France). Cotton buds (Johnson & Johnson Ltd, Maidenhead, UK) and Scotch® Magic™ Invisible Tape (3M, USA) were acquired from UH campus pharmacy (Hatfield, UK). Polytetrafluoroethylene (PTFE) syringe filters 25mm 0.22µm was purchased from dot-red® analytical (Cambridgeshire, UK). Individually calibrated unjacketed upright Franz diffusion cells (volume 3.0 mL: diameter 1.0 cm<sup>2</sup>) were acquired from Soham Scientific (UK). Deionised water (18.2 MΩ•cm) was from Millipore Milli-Q® water system.

### 5.2.1 HPLC analysis of finasteride

Chromatographic analysis of finasteride was conducted as described previously in Chapter 2, Section 2.2.1.1.

## 5.2.2 In vitro experiments

### 5.2.2.1 Skin preparation

Human scalp skin supplied from ZenBio (USA) was prepared as described in Chapter 2, Section 2.2.2.6. Prior to commencing the permeation studies, the skin was removed from the freezer, thawed and cut to the appropriate size using a scalpel.

### 5.2.2.2 Preparation of donor suspensions

For the preparation of finasteride suspensions in the vehicles investigated refer to Chapter 2, Section 2.2.2.5.

### 5.2.2.3 Franz Cells set up

#### 5.2.2.3.1 Infinite dose skin permeation studies

The skin samples were placed on the Franz cells, with the SC facing the donor compartment and the dermis facing the receptor. Both chambers were then wrapped together using Parafilm® (at 37 °C) or Dura Seal™ (50 °C) before being clamped together. The receiver fluid was EtOH: PBS pH 7.4 (30:70 % v/v) and stirred with a magnetic bar to ensure adequate mixing (600 rpm). Prior to dosing, the Franz cells were equilibrated in the water bath for approximately 30 min. Air bubbles were removed through the sampling arm by carefully tilting or inverting the diffusion cell and checks for leaks were made at the same time. The water bath temperature was maintained at 37 °C and 50 °C to keep the skin surface at approximately  $32 \pm 1$  °C and  $45 \pm 1$  °C respectively. The skin surface temperature was measured from the donor compartment using a Fisher Scientific Traceable Digital Thermometer with a type-K probe. A saturated suspension (0.5 mL) of finasteride was then introduced into the donor chamber. Following this, the receiver fluid (200 µL) was removed from receptor compartment via the sampling arm after 1, 2, 3, 4, 5, 6, 8, 18, 19, 20, 21, 22, 23 and 24 hr and analysed via HPLC. An equal volume of pre-warmed receiver fluid was immediately added to replace the sampled volume. Six repetitions (n=6) of each experiment were again performed.

### 5.2.2.3.2 Finite dose skin permeation studies

In this study, the effect of externally applied heat using sodium thiosulfate solution (ST) ( $\leq 45\text{ }^{\circ}\text{C}$  at 15 min and 25 min) on the transport of finasteride across full thickness human scalp skin was compared to no additional heat ( $32\text{ }^{\circ}\text{C}$ ) and complete system heating (water bath at  $45\text{ }^{\circ}\text{C}$  for the duration of the experiment). Finasteride was delivered from two prototype formulations: IPA: PG and IPA: TP in 50:50 ratios. The Franz cells were dosed with  $10\text{ }\mu\text{L}$  of filtered saturated solutions. To investigate the effect of externally applied heat, 2.5 mL or 5 mL of ST solution (chemical heating system) was added to produce a membrane surface temperature of approximately  $45\text{ }^{\circ}\text{C}$  for 15 min and 25 min respectively, after applying the formulation. Aluminium foil was used to separate the heating system from the formulation. These experiments were conducted in water bath at  $37\text{ }^{\circ}\text{C}$ . Control experiments were conducted in a water bath at  $37\text{ }^{\circ}\text{C}$  and  $50\text{ }^{\circ}\text{C}$  to produce membrane surface temperature of  $32\text{ }^{\circ}\text{C} \pm 1\text{ }^{\circ}\text{C}$  and  $45\text{ }^{\circ}\text{C} \pm 1\text{ }^{\circ}\text{C}$  respectively. Aluminium foil was placed in the donor chamber of each Franz diffusion cell to mimic experiments using the ST chemical heating system. The receiver fluid ( $200\text{ }\mu\text{L}$ ) was removed from receptor compartment via the sampling arm after 1, 2, 3, 4, 5, 6, 8, 18, 19, 20, 21, 22, 23 and 24 hr and analysed via HPLC. Equal volume of pre-warmed receiver fluid immediately replaced the sampled volume. Six repetitions ( $n=6$ ) were performed.

After the finite dose permeation studies, the skin samples were removed from Franz diffusion cells. Then the residual formulation was removed from the aluminium foil, donor chamber and skin surface using the cleaning procedure with the cotton buds described in Chapter 2, Section 2.2.2.3. To remove any remaining skin surface formulation two tape strips were taken. Then differential tape stripping was performed to determine the follicular penetration and skin distribution of finasteride following the method described in Section 5.2.2.5.

#### **5.2.2.3.3 The effect of a short burst of heat on follicular absorption and skin distribution of finasteride: 1-hr vs 24-hr duration experiments**

To determine the effect of short bursts of heat on follicular absorption and skin distribution of finasteride delivered from IPA: PG and IPA: TP over short and extended periods of time, finite dose experiments using the same procedure described above in Section 5.2.2.3.2 were conducted for 1 hr and 24 hr respectively. The receiver fluid was sampled only at the end of each experiment (1 hr and 24 hr). Four repetitions (n=4) were performed for each formulation under each treatment group to maximise the usage of the scalp skin.

#### **5.2.2.4 Drug skin distribution studies**

To determine the distribution of finasteride across the different skin layers after the completion of the infinite and finite dose skin permeation experiments, the extraction procedure described in Chapter 2, Section 2.2.2.3 was followed.

#### **5.2.2.5 Localisation of finasteride in the hair follicles: cyanoacrylate biopsy (differential tape stripping)**

Differential tape stripping (tape stripping and cyanoacrylate skin surface biopsies) was conducted to establish the extent of follicular transport using the method described in Chapter 4, Section 4.2.2.5. Following this, the distribution of finasteride across the epidermis and dermis was determined as described in Chapter 2, Section 2.2.2.3.

#### **5.2.3 Data treatment and statistics**

The data were analysed as described previously (Chapter 3, Section 3.2.10).

## 5.3 Results and Discussion

### 5.3.1 Infinite dose in vitro skin permeation and distribution studies

Infinite dose permeation studies using human scalp skin and saturated suspensions of finasteride in DPA, DMI, IPA, PG and TP were conducted at 32 °C and 45 °C over 24 hr to determine the effects of physiologically tolerable heat (produced in a water bath) and CPEs on drug permeation. This was followed by analysis of the influence of heat and CPEs on the drug uptake and distribution within the different skin layers (SC, epidermis and dermis). The permeation profiles and skin penetration (distribution) data at 32 °C and 45°C are shown in Figures 5-1 (a-b) and 5-2 (a-b) respectively.

At 32 °C finasteride was detected in the receiver fluid at early time points (from 1 h onwards) for all the vehicles investigated [Figure 5-1(a)], with IPA delivering the highest concentrations at early time points (1-6 hr). The cumulative amount of finasteride permeated at 24 hr ( $Q_{24}$ ) ranged from  $17.82 \pm 1.36 \mu\text{g}/\text{cm}^2$  to  $80.58 \pm 7.30 \mu\text{g}/\text{cm}^2$ , with DMI and PG producing the lowest and highest receiver fluid concentrations respectively. At  $Q_{24}$  finasteride permeation from PG and IPA (which showed the highest permeation) was statistically the same, but delivery from both vehicles was significantly greater ( $p < 0.05$ ) than that from DPA, DMI and TP. No significant differences were found between finasteride permeation from DPA, DMI and TP at  $Q_{24}$ .

The average fluxes (J) were calculated from the linear portion of the permeation profiles (18-24h) and are shown in Table 5-1. At 32°C the drug fluxes ranged from  $1.089 \pm 0.01 \mu\text{g}/\text{cm}^2/\text{hr}$  to  $4.626 \pm 0.41 \mu\text{g}/\text{cm}^2/\text{hr}$  and the rank of the vehicles in terms of J was in the following order: PG > IPA > TP > DMI > DPA.

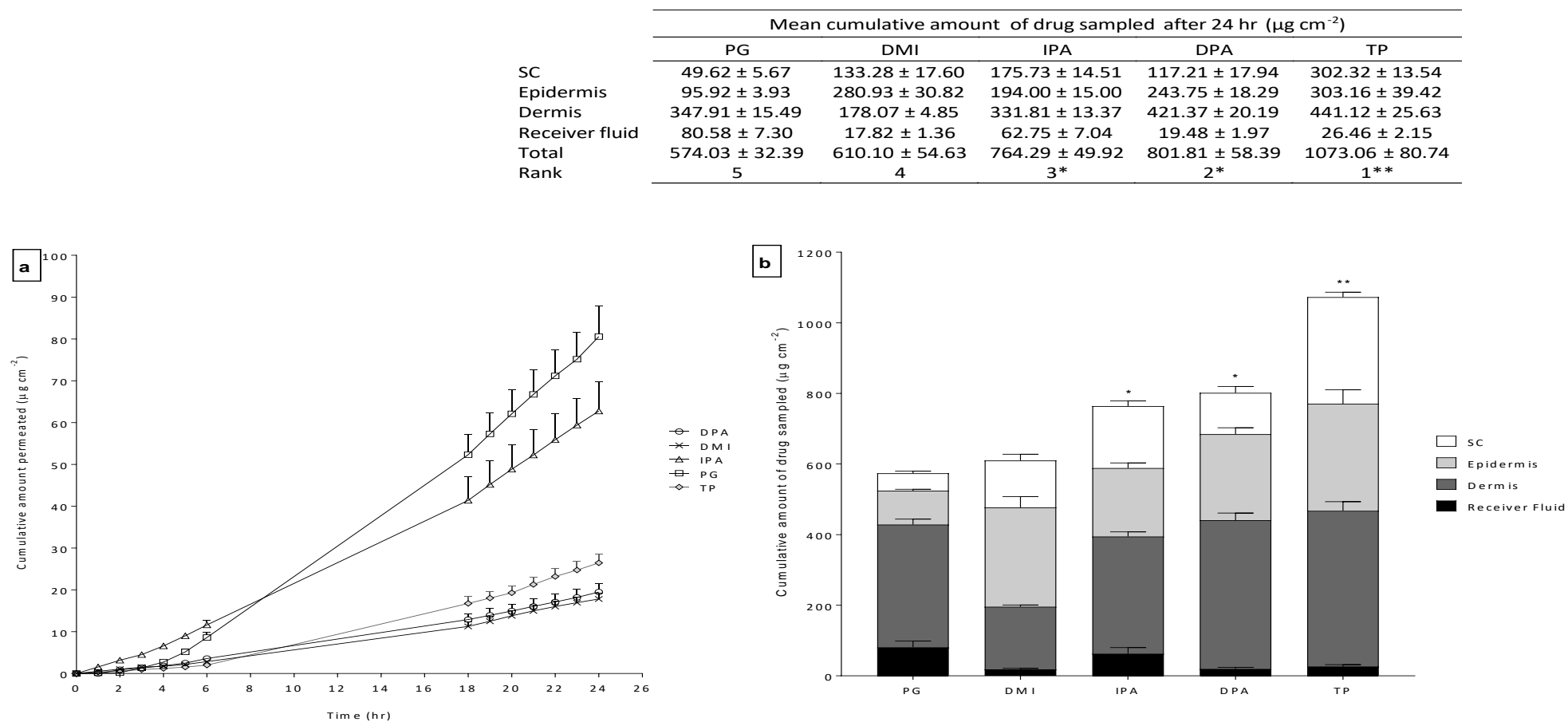


**Figure 5-1: Mean cumulative amount finasteride (a) permeated through human scalp skin at 32 °C over 24 hr from various vehicles (b) recovered from the stratum corneum (SC), epidermis, dermis and receiver fluid at the end of the infinite dose permeation study.** Finasteride was applied 0.5 mL cm<sup>-2</sup> to the skin surface in a saturated, equilibrated un-filtered solution for each vehicle. Vehicles tested were Diisopropyl adipate (DPA), Dimethyl isosorbide (DMI), Isopropyl alcohol (IPA), Propylene glycol (PG) and Transcutol® P (TP). All points are mean + SEM of n=6 diffusion cells. \*\* denotes a significant difference in total amount delivered compared to vehicles ranked 2<sup>nd</sup> and higher. \* denotes a significant difference in total amount delivered compared to vehicles ranked 4<sup>th</sup> and higher.

With regards to the skin distribution of finasteride at 32 °C, varying amounts of drug was recovered from the different skin layers for the vehicles investigated as shown in Figure 5-1(b). The greatest amount of drug was recovered from the dermis for all the vehicles tested apart from DMI, for which most of the drug was recovered from the epidermis. Overall, the total drug delivered [SC + Epidermis + Dermis + Receiver fluid] ranged from  $574.03 \pm 32.39 \mu\text{g}/\text{cm}^2$  to  $1073.06 \pm 80.74 \mu\text{g}/\text{cm}^2$ , with PG and TP producing the minimum and maximum drug tissue concentrations respectively. Thus, the rank of the vehicles in terms of total drug delivery was: TP > DPA > IPA > DMI > PG as shown in Figure 5-1(b). Also, total delivery from TP was significantly greater than all the other vehicles, whilst delivery from both DPA and IPA was significantly greater than DMI and PG.

At the higher temperature (45 °C), increased drug delivery into the receiver fluid from all the vehicles investigated was observed. The cumulative amount of drug detected in the receiver at 24 hr ( $Q_{24}$ ) ranged from  $45.64 \pm 3.00 \mu\text{g}/\text{cm}^2$  to  $342.62 \pm 27.84 \mu\text{g}/\text{cm}^2$  with DPA and IPA producing the lowest and highest drug delivery into the receiver fluid respectively [Figure 5-2(a)]. This corresponded to a 2.34 and 5.46-fold increase in drug receiver fluid concentrations for each of these solvents compared to the permeation experiments at 32 °C. Comparing the amount of drug in the receiver fluid at 24 hr ( $Q_{24}$ ), delivery from IPA and PG was found to be significantly greater than delivery from TP, DPA and DMI. Significant differences were not found in finasteride permeation between IPA and PG. Equally no differences were observed between TP, DPA and DMI.

With the application of heat the ranking of the vehicles in terms of average drug flux ( $J$ ) between 18 and 24 hr was in the following order: IPA > PG > TP > DMI > DPA, with drug flux ranging from  $2.352 \pm 0.13 \mu\text{g}/\text{cm}^2/\text{hr}$  to  $20.138 \pm 1.57 \mu\text{g}/\text{cm}^2/\text{hr}$ . Compared with the experiments at 32 °C, this corresponded to a 2.16 to 5.67-fold increase in flux for the same solvents. Moreover, the increase drug flux with heat was found to be statistically significant for all the vehicles investigated ( $p < 0.05$ ).

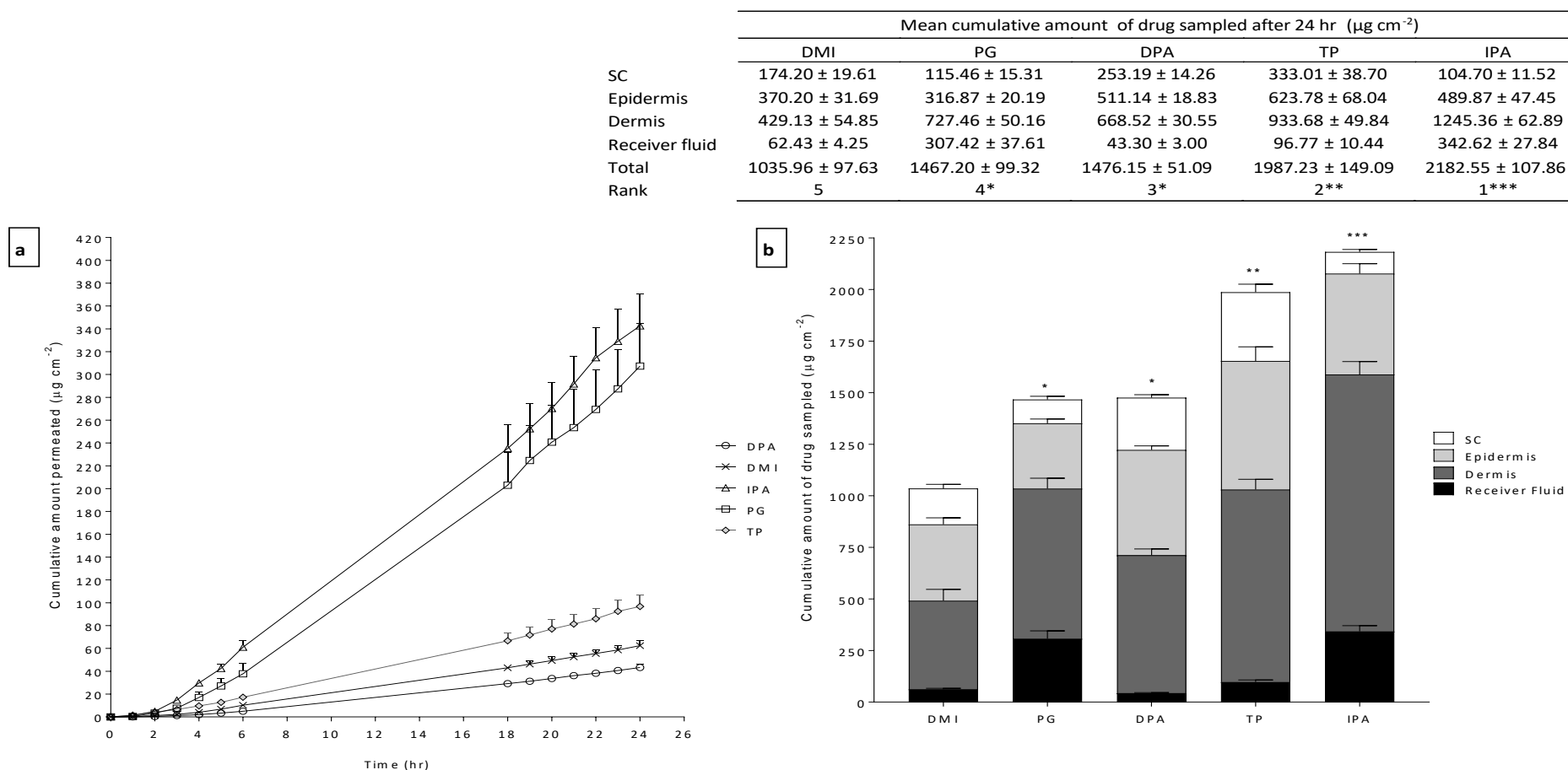


**Figure 5-2: Mean cumulative amount finasteride (a) permeated through human scalp skin at 45 °C over 24 hr from various vehicles (b) recovered from the stratum corneum (SC), epidermis and dermis at the end of the infinite dose permeation study.** Finasteride was applied 0.5 mL cm<sup>-2</sup> to the skin surface in a saturated, equilibrated un-filtered solution for each vehicle. Vehicles tested were Diisopropyl adipate (DPA), Dimethyl isosorbide (DMI), Isopropyl alcohol (IPA), Propylene glycol (PG) and Transcutol® P (TP). All points are mean + SEM of n=6 diffusion cells. \*\*\* denotes a significant difference in total amount recovered compared to vehicles ranked 2<sup>nd</sup> and higher. \*\* denotes a significant difference in total amount recovered compared to vehicles ranked 3<sup>rd</sup> and higher. \* denotes a significant difference in total amount delivered compared to the vehicle ranked 5<sup>th</sup>.

At 45 °C a similar trend was observed in terms of the amount of drug recovered from the different skin layers with respect to the 32 °C penetration experiments, as the greatest amount of drug was recovered from the dermis for all the vehicles tested [Figure 5-2(b)]. The total amount of drug recovered from the dermis for all the vehicles tested [Figure 5-2(b)]. The total amount of drug delivered at 45 °C ranged from  $1035.96 \pm 97.63 \mu\text{g}/\text{cm}^2$  to  $2182.54 \pm 107.86 \mu\text{g}/\text{cm}^2$ , with DMI and IPA respectively producing the lowest and greatest delivery into the skin tissue and receiver fluid. Thus, the ranking of the vehicles in terms of total amount of drug delivered at 45 °C was in the following order: IPA > TP > PG > DPA > DMI. Compared to the experiments at 32 °C, the application of heat increased the total amount of finasteride recovered from the skin tissue, with this enhancement ranging from 1.64 to 2.61-fold for DMI and IPA respectively. Overall, TP and IPA produced significantly greater total skin tissue and receiver fluid concentrations (total delivery) compared to DPA, PG and DMI (vehicles ranked 3 and higher), whereas, delivery from DPA was significantly more compared to PG and DMI (vehicles ranked 4 and higher).

An interesting observation at both 32 °C and 45 °C was the poor correlation between the drug receiver fluid concentrations and drug tissue concentrations. For example, PG delivered the drug into the receiver fluid at a much faster rate compared to the other vehicles, whilst producing the lowest drug tissue concentrations. In comparison, TP delivered lower concentrations into the receiver whilst producing the highest drug tissue concentrations. This suggests that different vehicles can influence the way a drug interacts with the skin, indicating the complexity of the drug transport process across human skin.

To gain a better understanding of the mechanisms involved in the improvement of drug transport across human skin, the pathlength normalised partition coefficient ( $Kh$ ) and pathlength normalised diffusion coefficients ( $D/h^2$ ) were measured for both physiological skin temperature (32 °C) and elevated skin temperature (45 °C) using Fick's first law as described in Section 1.6. As before, thermodynamic activity (unity of 1) was employed instead of  $C_v$  in calculating  $Kh$  as saturated suspensions were used in this study.

At the elevated temperature, a rise in  $Kh$  and  $D/h^2$  was observed for finasteride in all of the vehicles investigated. However, the magnitude of the ER of  $Kh$  and  $D/h^2$  varied considerably for the different vehicles investigated as shown in Table 5-1. The ER of  $D/h^2$  with heat was between 1.00 and 1.73-fold, with DPA and TP producing the smallest and largest improvement. More substantively, the increase in  $Kh$  ranged from 1.75 to 5.56-fold, with TP and IPA producing the minimum and maximum enhancement respectively with the enhancement in  $Kh$  being greater in comparison to  $D/h^2$  for all of the vehicles tested. Consequently, this data suggests that heat increases drug transport across human skin mainly via improvements in drug-vehicle partitioning into the skin. This is in contrast to most of the current literature which suggests heat is likely to enhance diffusivity (Akomeah et al., 2004; Chang & Riviere, 1991; Park et al., 2008), although they did not separate the influence of diffusivity and partitioning to gain a full mechanistic understanding. In reality, the simultaneous improvements in diffusivity and partitioning are likely to contribute significantly to the overall increases in drug transport seen with heat.

**Table 5-1: Skin permeation parameters measured for saturated suspension of finasteride in different dermatological vehicles. Cumulative amount permeated ( $Q_{24}$ ), average flux ( $J$ ), pathlength normalised partition coefficient ( $Kh$ ), pathlength normalised diffusion coefficient ( $D/h^2$ ) and lag time ( $T_L$ ) were measured for both physiological skin temperature (32 °C) and elevated skin temperature (45 °C) using Fick's first law (mean  $\pm$  SEM, n=6). \* denotes significant difference in the parameter at 45 °C for each vehicle compared to the same vehicle at 32 °C.**

Vehicle	Membrane temperature (°C)	$J$ ( $\mu\text{g}/\text{cm}^2/\text{hr}$ )	$E_R$	$Q_{24}$ ( $\mu\text{g}/\text{cm}^2$ )	$E_R$	$T_L$ (hr)	$D/h^2(\times 10^{-2}\text{hr}^{-1})$	$E_R$	$Kh$ (cm)	$E_R$
DPA	32	1.089 $\pm$ 0.01	2.16	19.48 $\pm$ 1.97	2.34	6.99 $\pm$ 0.38	2.38 $\pm$ 0.44	1.00	45.67 $\pm$ 2.48	2.16
	45	2.352 $\pm$ 0.13*		45.64 $\pm$ 3.00*		7.00 $\pm$ 0.37	2.38 $\pm$ 0.45		98.78 $\pm$ 5.22*	
DMI	32	1.098 $\pm$ 0.06	2.90	17.82 $\pm$ 1.36	3.50	6.60 $\pm$ 0.45	2.52 $\pm$ 0.37	1.46	43.48 $\pm$ 2.96	1.98
	45	3.184 $\pm$ 0.26*		62.43 $\pm$ 4.25*		4.52 $\pm$ 0.60*	3.69 $\pm$ 0.28*		86.35 $\pm$ 11.46*	
IPA	32	3.555 $\pm$ 0.28	5.67	62.75 $\pm$ 7.04	5.46	6.31 $\pm$ 0.49	2.64 $\pm$ 0.34	1.02	177.68 $\pm$ 10.45	5.56
	45	20.138 $\pm$ 1.57*		342.62 $\pm$ 27.84*		6.18 $\pm$ 0.30	2.70 $\pm$ 0.56		746.72 $\pm$ 36.25*	
PG	32	4.626 $\pm$ 0.41	3.61	80.58 $\pm$ 7.30	3.82	6.63 $\pm$ 0.56	2.51 $\pm$ 0.30	1.06	184.02 $\pm$ 15.54	3.42
	45	16.696 $\pm$ 1.50*		307.42 $\pm$ 37.61*		6.29 $\pm$ 0.30	2.65 $\pm$ 0.56		630.11 $\pm$ 30.54*	
TP	32	1.656 $\pm$ 0.11	3.04	26.46 $\pm$ 2.15	3.66	7.25 $\pm$ 0.49	2.30 $\pm$ 0.34	1.73	72.04 $\pm$ 4.87	1.75
	45	5.028 $\pm$ 0.74*		96.77 $\pm$ 10.44*		4.20 $\pm$ 0.53*	3.97 $\pm$ 0.31*		126.71 $\pm$ 15.99*	

### 5.3.2 The effect of heat applied from top on drug delivery into the hair follicles, skin tissue and receiver fluid over 24 hr: *in vitro* finite dose studies

*In vitro* finite dose permeation studies using human scalp skin were conducted to more closely mimic in use conditions. Finasteride was delivered from filtered saturated solutions in 50: 50 solvent systems (IPA: PG and IPA: TP) to investigate whether synergy in penetration enhancement occurred when mixed solvent systems were used. IPA was included as a volatile co-solvent to increase the thermodynamic activity as it evaporates, therefore, increasing the escaping tendency of the drug from the vehicle into the skin including the hair follicles. TP was selected for inclusion into the 50: 50 prototype solvent systems employed in this study because it produced the second highest total delivery at 45 °C and highest total delivery at 32 °C. Additionally, TP was found to promote the localisation of finasteride into the skin tissue with the application of heat, whilst also delivering lower amounts of drug into the receiver fluid compared to the other vehicles investigated in the infinite dose studies. PG was chosen it showed good overall delivery, but in particular better permeation than TP therefore offering comparison. Also, PG was selected because it has been reported to facilitate/promote follicular accumulation of lipophilic permeants in human scalp skin (Grams & Bouwstra, 2002), which would be advantageous in a topical product containing finasteride for the treatment of AGA.

In this study, the influence of short periods (15 and 25 min) of externally applied heat on drug deposition into the hair follicles, different skin layers and permeation through human scalp skin was investigated by comparing this data to no additional heat (32 °C) and complete system heating (45 °C produced in a water bath for 24 hr). The short durations (15 and 25 min) of heat (45 °C) were produced using ST. In contrast to the isotretinoin study, finasteride showed larger differences in solubility at these temperatures (32 °C and 45 °C). In order to remove the influence of temperature on saturation/driving force saturated solutions were prepared at both 32 °C and 45 °C. In this Franz cell study 10 µL of the formulations (filtered saturated solutions) were applied on the surface of the skin corresponding to a dose equivalent to 1629.6 µg and 900.7 µg for IPA: PG and IPA: TP respectively at

32 °C. At the higher temperature 45 °C, this dose was equal to 1727.6 µg and 1038.9 µg for IPA: PG and IPA: TP respectively. For both experiments, the mass balance ranged from approximately 91-96 % for all the different treatment groups (Table 5-2). This level of recovery was deemed acceptable as the OECD guidelines recommend recoveries over 90 % for drugs without stability issues (OECD, 2004a). The permeation profiles and skin and follicular deposition data is shown in Figures 5-3(a-b) and 5-4(a-b) for IPA: PG and IPA: TP respectively.

**Table 5-2: Percentage of finasteride recovered from skin surface, hair follicles, in skin (SC + epidermis + dermis) and receiver fluid (mean ± SEM, n=6).**

CPEs	Treatment condition	Percentage (%) of applied dose recovered				
		skin surface	Hair follicles	In skin	Receiver fluid	Total recovery
IPA:PG	32 °C	82.85 ± 2.50	1.95 ± 0.23	9.78 ± 0.94	0.33 ± 0.02	94.91 ± 3.69
	ST 15	77.60 ± 1.47	2.66 ± 0.27	13.25 ± 0.96	0.45 ± 0.03	93.96 ± 2.73
	ST 25	74.89 ± 1.34	3.11 ± 0.29	14.86 ± 0.83	0.59 ± 0.03	93.45 ± 2.49
	45 °C	65.26 ± 1.46	4.27 ± 0.34	21.19 ± 1.59	2.13 ± 0.06	92.85 ± 3.45
IPA:TP	32 °C	72.47 ± 1.50	2.00 ± 0.24	20.27 ± 1.58	0.60 ± 0.38	95.34 ± 3.70
	ST 15	68.75 ± 1.38	3.11 ± 0.30	18.35 ± 1.28	0.63 ± 0.04	90.94 ± 3.00
	ST 25	64.23 ± 1.34	4.48 ± 0.35	22.70 ± 1.41	0.97 ± 0.05	92.53 ± 3.15
	45 °C	60.66 ± 1.50	4.85 ± 0.37	27.91 ± 2.24	2.88 ± 0.09	96.30 ± 4.20

Delivery from IPA: PG (50: 50) led to the detection of finasteride in the receiver at early time points (from 1 hr onwards) from all the different treatment groups investigated as shown in Figure 5-4(a). Also, all the IPA: PG permeation profiles follow a finite dose. After 6 hr the rate of drug delivery into the receiver fluid starts to decrease. From 2 hr onwards, IPA: PG 45 °C (complete system heating) delivers much higher quantities of finasteride into the receiver fluid compared to all the other treatment conditions. Similarly, at early time points (2-6 hr) delivery from IPA: PG ST 25 (heating from top for 25 min) was superior compared to IPA: PG ST 15 and IPA: PG 32 °C. Thus, the cumulative amount permeated at 24 hr may be ranked as follows: IPA: PG 45 °C > IPA: PG ST 25 > IPA: PG ST 15 > IPA: PG 32 °C, with the minimum and maximum cumulative amount permeated ranging from  $5.39 \pm 0.81 \mu\text{g}/\text{cm}^2$  to  $36.79 \pm 2.74 \mu\text{g}/\text{cm}^2$ . Therefore, the application of heat enhanced the amount of finasteride delivered into the receiver fluid, with this enhancement ranging from 1.44 to 6.83-fold for IPA: PG ST 15 and IPA: PG 45 °C respectively. This suggests that the amount of finasteride delivered

into the receiver fluid from IPA: PG can be tailored by controlling the length of time heat is applied to the skin. In terms of the percentage of the applied dose that permeated, IPA: PG 32 °C (0.33%) and IPA: PG 45 °C (2.13%) produced the minimum and maximum delivery into the receiver fluid.

The results for finasteride recovery from the hair follicles and the different skin layers (SC, epidermis and dermis) following the differential tape stripping and the skin distribution study respectively, for IPA: PG are shown in Figure 5-3(b). For IPA: PG 32 °C (no heat) the amount of finasteride recovered from the hair follicles was  $31.79 \pm 2.12 \mu\text{g}/\text{cm}^2$ . The application of heat led to a 1.69 to 2.31-fold increase in the amount of finasteride recovered from the hair follicles, with IPA: TP ST 15 and IPA: TP 45 °C (entire system heating) producing the lowest and highest enhancement respectively. Thus, the amount of finasteride recovered from the hair follicles was in the following order: IPA: PG 45 °C > IPA: PG ST 25 > IPA: PG ST 15 > IPA: PG 32 °C.

With regards to drug distribution across the different skin layers, the highest amount of finasteride was consistently recovered from the epidermis for all the different treatment groups except for IPA: PG 45 °C, where the greatest amount of finasteride was recovered from the dermis. A possible explanation for this is the greater duration of heating time (24 hr) compared to the other treatment groups which enhanced its drug uptake capacity by increasing drug solubility within the skin tissue. In terms of the total amount of drug retained inside the skin (SC + epidermis + dermis) the highest quantities of finasteride were recovered for IPA: PG 45 °C compared to all the other treatment groups. Overall, the rank of the different treatment groups in terms of the total amount of finasteride recovered from skin tissue was in the following order: IPA: PG 45 °C > IPA: PG ST 25 > IPA: PG ST 15 > IPA: PG 32 °C, with the total of amount of finasteride recovered from inside the skin ranging from  $159.58 \pm 15.24 \mu\text{g}/\text{cm}^2$  to  $366.09 \pm 27.44 \mu\text{g}/\text{cm}^2$ . The percentage of the applied dose retained within the skin tissue ranged from 9.79 % to 21.19 % with IPA: PG 32 °C and IPA: PG 45 °C generating the lowest and highest retention respectively.

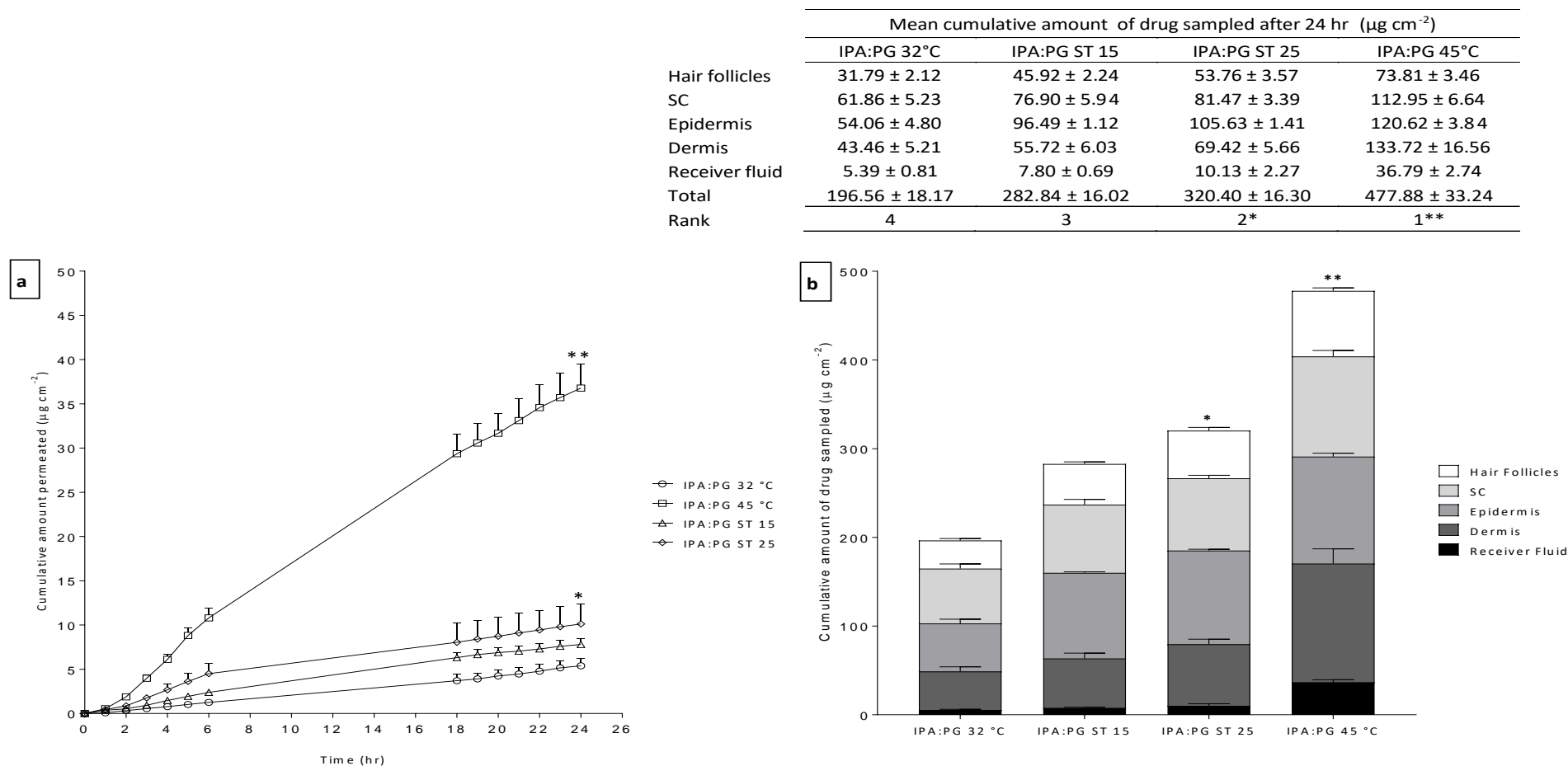
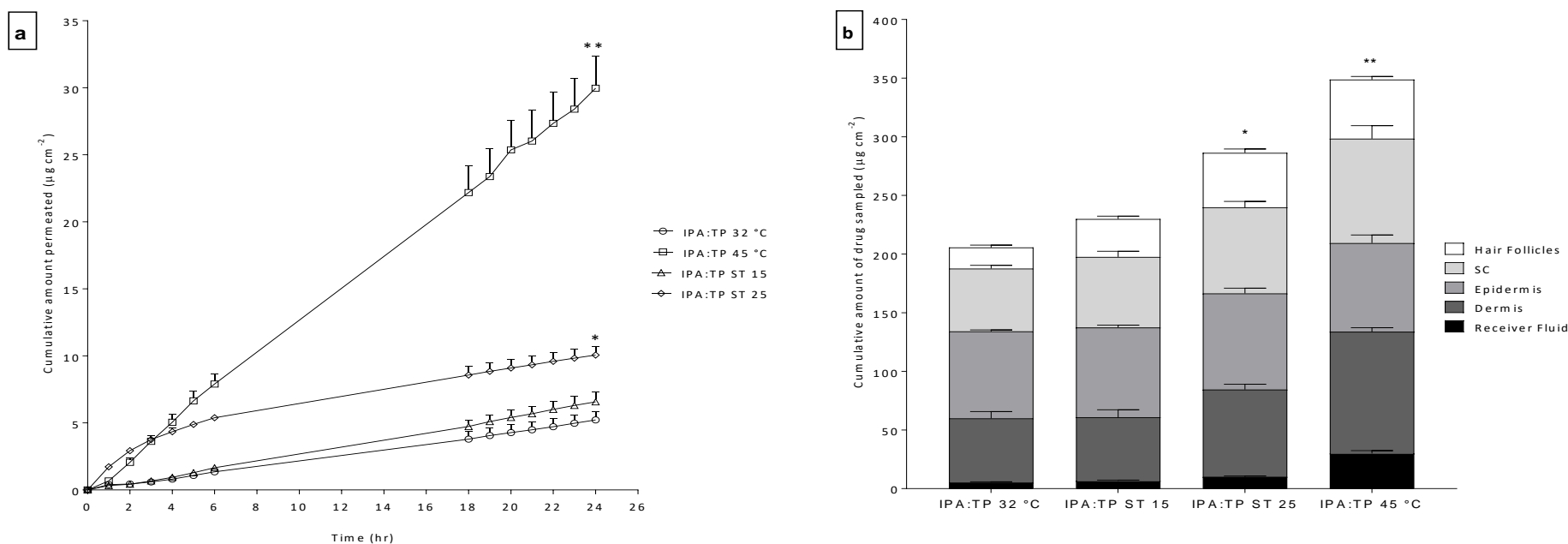


**Figure 5-3: Mean cumulative amount of finasteride (a) permeated through human scalp skin (b) recovered from the hair follicles, stratum corneum (SC), epidermis, dermis and receiver fluid at the end of the finite dose permeation study.** Experiments were conducted in a water bath at 32 °C for 24 hr with and without sodium thiosulfate (ST) solution producing heat for 15 & 25 min (ST 15 & ST 25 respectively) and also in a water bath at 45 °C. Finasteride 10  $\mu\text{L cm}^{-2}$  was applied to the skin surface in 50:50 Isopropyl alcohol: Propylene glycol (IPA: PG). All points are mean + SEM of n=6 diffusion cells. The total mass balance was above 92 % and the total percentage of applied dose delivered ranged from 12 to 27 %. \*\* denotes a significant difference in total amount recovered compared vehicles ranked 2<sup>nd</sup> and higher. \* denotes a significant difference in total amount recovered compared vehicles ranked 3<sup>rd</sup> and higher.

Using IPA: TP (50: 50) as the vehicles, permeation of finasteride into the receiver fluid was observed for the same conditions as IPA: PG (50:50) for no heat (32 °C for 24 hr), ST 15 (15 min of heat from top), ST 25 (25 min of heat from top) and complete system heating (45 °C for 24hr). These permeation profiles are shown in Figure 5-4(a) as the cumulative amount permeated as a function time. Finasteride was detected in the receiver at early time points (from 1 hr onwards) for all the different treatment groups investigated. Over the first 2 hr of the study, IPA: TP ST 25 delivered more drug into the receiver fluid compared to IPA: TP 45 °C (entire system heating), IPA: TP ST 15 and IPA: TP 32 °C (no heat). However, after 3 hr, delivery from IPA: TP 45 °C catches up to the IPA: TP ST 25 and eventually starts to surpass IPA: TP ST 25 after 4 hr, with IPA: TP 45 °C continuing to outperform IPA: TP ST 25 to the end of the study. Figure 5-4(a) shows that, at 24 hr, the highest amount of finasteride permeated for IPA: TP 45 °C (29.97  $\mu\text{g}/\text{cm}^2$ ) followed by IPA: TP ST 25 (10.06  $\mu\text{g}/\text{cm}^2$ ), IPA: TP ST 15 (6.5  $\mu\text{g}/\text{cm}^2$ ) and IPA: TP 32 °C (5.22  $\mu\text{g}/\text{cm}^2$ ). Therefore, employing ST (for both 15 and 25 min) and complete system heating increased finasteride permeation 1.26 to 5.74-fold, with IPA: TP ST 15 and IPA: TP 45 °C producing the lowest and highest enhancement. The inability of ST to enhance finasteride transport across skin to the same extent as complete system heating is most likely due to the difference in the extent of heating time (15 or 25 min vs 24 hr, respectively). Additionally, the percentage of the applied dose that permeated into the receiver fluid ranged from 0.60 % to 2.88 % for IPA: TP, with IPA: TP 32 °C and IPA: TP 45 °C producing the lowest and highest delivery respectively.



	Mean cumulative amount of drug sampled after 24 hr (µg cm <sup>-2</sup> )			
	IPA:TP 32°C	IPA:TP ST 15	IPA:TP ST 25	IPA:TP 45°C
Hair follicles	18.08 ± 1.90	32.30 ± 2.41	46.58 ± 3.26	50.35 ± 2.56
SC	53.52 ± 2.80	60.16 ± 4.77	73.26 ± 5.19	89.10 ± 10.96
Epidermis	74.17 ± 1.18	76.56 ± 1.97	82.02 ± 4.44	103.87 ± 3.34
Dermis	54.73 ± 5.75	54.30 ± 6.37	74.42 ± 4.49	96.83 ± 4.31
Receiver fluid	5.22 ± 0.64	6.58 ± 0.72	10.06 ± 0.66	29.97 ± 2.42
Total	205.71 ± 12.27	229.89 ± 16.18	286.33 ± 18.04	370.13 ± 23.58
Rank	4	3	2*	1**

**Figure 5-4: Mean cumulative amount of finasteride (a) permeated through human scalp skin (b) recovered from the hair follicles, stratum corneum (SC), epidermis, dermis and receiver fluid at the end of the finite dose permeation study.** Experiments were conducted in a water bath at 32°C for 24 hr with and without sodium thiosulphate (ST) solution producing heat for 15 & 25 min (ST 15 & ST 25 respectively) and also in water bath at 45 °C. Finasteride 10 µL cm<sup>-2</sup> was applied to the skin surface in 50:50 Isopropyl alcohol: Transcutol® P (IPA: TP). All points are mean + SEM of n=6 diffusion cells. The total mass balance was above 90 % and the total percentage of applied dose delivered ranged from 22 to 35 %. \*\* denotes a significant difference in total amount recovered compared vehicles ranked 2<sup>nd</sup> and higher. \* denotes a significant difference in total amount recovered compared vehicles ranked 3<sup>rd</sup> and higher.

The results for finasteride recovery from the hair follicles and the different skin layers (SC, epidermis and dermis) following the differential tape stripping and the penetration study respectively, for IPA: TP are shown in Figure 5-4(b). For IPA: TP 32 °C (no heat) the amount of finasteride recovered from the hair follicles was  $18.08 \pm 1.90 \mu\text{g}/\text{cm}^2$ . The application of heat led to a 1.78 to 2.78-fold increase in the amount of finasteride recovered from the hair follicles, with IPA: TP ST 15 and IPA: TP 45 °C (entire system heating) producing the lowest and highest enhancement respectively. Thus, the amount of finasteride recovered from the hair follicles was in the following order: IPA: TP 45 °C > IPA: TP ST 25 > IPA: TP ST 15 > IPA: TP 32 °C. Similarly, the percentage of the applied dose recovered from the hair follicles followed the same order, with the percentage recovery ranging from 2.00 to 4.85 %.

With regards to drug distribution across the different skin layers, the highest amount of finasteride was consistently recovered from the epidermis for all the different treatment groups. In terms of the total amount of drug retained inside the skin (SC + epidermis + dermis) the highest quantities of finasteride were recovered for IPA: TP 45 °C compared to all the other treatment groups. Overall, the rank of the different treatment groups in terms of the total amount of finasteride recovered from skin tissue was in the following order: IPA: TP 45 °C > IPA: TP ST 25 > IPA: TP ST 15 > IPA: TP 32 °C, with the total amount of finasteride recovered from inside the skin ranging from  $182.62 \pm 14.22 \mu\text{g}/\text{cm}^2$  to  $289.97 \pm 23.31 \mu\text{g}/\text{cm}^2$ . However, when comparing the percentage of the applied dose retained within the skin tissue, only IPA: TP 15 produced lower retention (18.35 %) compared to IPA: TP 32 °C (20.27 %) because of the comparatively higher dose applied. Both IPA: TP ST 25 and IPA: TP 45 °C retained 22.70 % and 27.91 % of the applied dose inside the skin respectively. Delivery into the skin from IPA: PG was greater than that from IPA: TP. This possibly relates to the higher dose applied rather than another specific enhancement mechanism. The finite dose studies showed that complete system heating was superior in comparison to ST and the control (no heat) after 24 hr with respect to increasing finasteride transport and uptake in the skin and hair follicles. However, at early time points delivery of finasteride into the receiver fluid from ST aided formulations were comparable to those heated at 45 °C in a water bath.

### 5.3.3 The effect of heat applied from top on drug delivery into the hair follicles, skin tissue and receiver fluid over 1 hr: *in vitro* finite dose studies

Heat generated using ST is more likely to be beneficial at early time points, with short periods of heating being more advantageous and realistic option in a clinical setting. Thus, the finite dose experiments were repeated and stopped after 1 hr to investigate the effect of shorter periods of heating (generated using ST) on the amount of finasteride retained in the skin, hair follicles and the amount permeated into the receiver fluid. This will help improve our understanding of how heat improve drug absorption into the skin. These results are presented in Figures 5-5 and 5-6 for IPA: PG and IPA: TP respectively.

The amount of finasteride recovered from the receiver fluid after 1 hr with IPA: PG systems ranged from 0.25  $\mu\text{g}/\text{cm}^2$  to 0.53  $\mu\text{g}/\text{cm}^2$ , with IPA: PG 32 °C and IPA: PG ST 25 producing the lowest and highest delivery respectively. This trend was also observed in the 24 hr studies where very similar levels of finasteride were delivered into the receiver fluid 1 hr into the study. With regards to finasteride deposition into the hair follicles, comparatively lower retention was evident for IPA: PG 32 °C (30.41  $\mu\text{g}/\text{cm}^2$ ) and IPA: PG ST 15 (55.24  $\mu\text{g}/\text{cm}^2$ ) compared with IPA: PG ST 25 (60.25  $\mu\text{g}/\text{cm}^2$ ). In the 1 hr study, the amount of finasteride recovered from the hair follicles was 3.40-fold greater than the amount of drug recovered from the SC for IPA: PG 32 °C. This trend was also observed with IPA: PG ST 15 and IPA: PG ST 25 as more drug was recovered from the hair follicles (2.3 to 2.6-fold) compared to the SC for both conditions. A similar trend was also observed for IPA: TP where the amount of finasteride recovered from the hair follicles was approximately 12 to 15-fold greater in comparison to the amount of finasteride recovered from the SC after 1 hr under all the treatments conditions investigated (32 °C, ST 15 and ST 25). This possibly suggests that the hair follicles contribute more to the absorption of finasteride into the skin compared to the SC at early time points when comparing within each condition.

	Mean cumulative amount recovered after 1hr ( $\mu\text{g cm}^{-2}$ )		
	IPA:PG 32°C	IPA:PG ST 15	IPA:PG ST 25
Hair follicles	30.41 $\pm$ 3.99	55.24 $\pm$ 6.10	60.25 $\pm$ 8.61
SC	8.98 $\pm$ 1.21	21.58 $\pm$ 1.93	26.28 $\pm$ 1.42
Epidermis	18.78 $\pm$ 1.89	40.35 $\pm$ 1.20	41.97 $\pm$ 1.28
Dermis	22.78 $\pm$ 1.64	64.10 $\pm$ 1.53	67.67 $\pm$ 1.21
Receiver fluid	0.25 $\pm$ 0.08	0.46 $\pm$ 0.07	0.53 $\pm$ 0.04
Total	81.20 $\pm$ 9.01	181.73 $\pm$ 10.83	196.70 $\pm$ 12.56
Rank	3	2*	1**

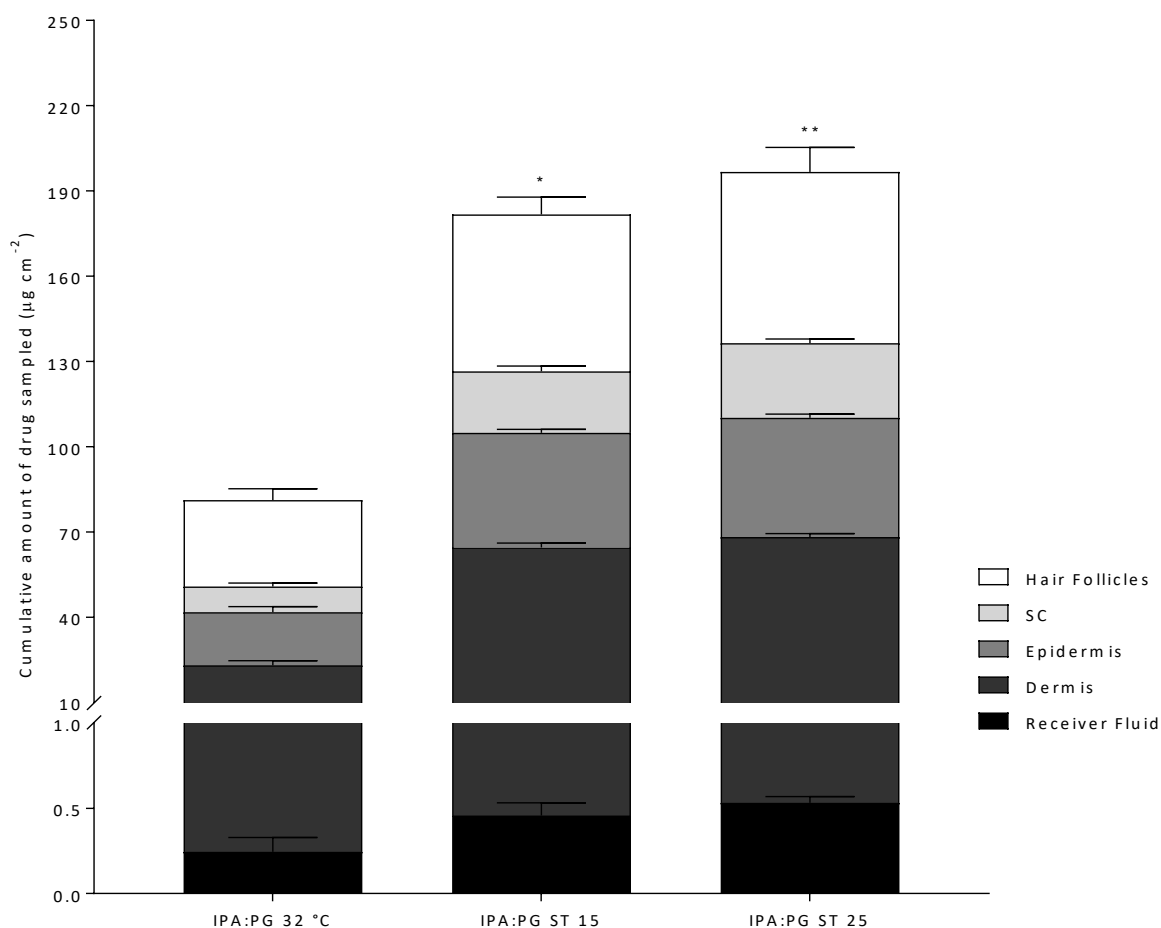


**Figure 5-5: Dose distribution of finasteride in human scalp skin and receiver fluid delivered from IPA: PG binary system (50:50). Filtered saturated solution of finasteride  $10 \mu\text{L cm}^{-2}$  was applied to the skin surface.** Experiments were conducted for 1 hr at 32 °C with and without sodium thiosulfate solution (ST) producing heat for 15 & 25 min (ST 15 & ST 25 respectively). Each bar indicates the amount of finasteride that was recovered from the hair follicles, in the skin (SC + epidermis + dermis) or receiver fluid. All bars are mean + SEM of n=4 diffusion cells. \*\* denotes significant difference in the total amount delivered compared vehicles ranked 2<sup>nd</sup> and higher. \* denotes significant difference in the total amount recovered compared to the vehicle ranked 3<sup>rd</sup>.

With the application of localised heat (ST 15 and ST 25), the increase in the amount of finasteride recovered from the SC (2.4 to 2.9-fold) was greater than that observed for the hair follicles (1.8 to 2.0-fold), suggesting that targeted follicular delivery is not achieved when heat is combined with IPA: PG. Overall, the amount of finasteride recovered from the hair follicles after 1 hr for IPA: PG 32 °C was equal to the amount recovered after 24 hr. In contrast, for both IPA: PG ST 15 and IPA: PG ST 25 the amount of finasteride recovered after 1 hr was greater than the amount recovered after 24 hr. These findings further highlight the importance of hair follicles in the transport of finasteride at early time points as well as emphasising the potential benefits of using heat to enhance drug follicular delivery at early time points. In terms of finasteride uptake into the skin tissue after 1 hr, the largest amount of finasteride was recovered from the dermis with IPA: PG ST 25, followed by IPA: PG ST 15 and IPA: PG 32 °C, with the amount of finasteride recovered ranging from 22.78  $\mu\text{g}/\text{cm}^2$  to 67.67  $\mu\text{g}/\text{cm}^2$ . This was the same trend observed in the 24-hr studies. The amount of finasteride deposited in the skin (SC, epidermis and dermis) after 1 hr corresponds to approximately 50% of the amount delivered after 24 hr from IPA: PG, suggesting that the uptake of finasteride into the skin from IPA: PG is relatively quick.

For IPA: TP, the amount of finasteride recovered from the receiver fluid ranged from 0.35  $\mu\text{g}/\text{cm}^2$  to 2.26  $\mu\text{g}/\text{cm}^2$ , with IPA: TP 32 °C and IPA: TP ST 25 producing the minimum and maximum delivery respectively (Figure 5-6). This order of drug delivery into the receiver fluid followed the same trend as the 24 hr studies where similar amounts of finasteride were detected in the receiver fluid 1 hr into the study. The deposition of finasteride into the hair follicles was lower for IPA: TP 32 °C (23.76  $\mu\text{g}/\text{cm}^2$ ) and IPA: TP ST 15 (31.26  $\mu\text{g}/\text{cm}^2$ ) compared with IPA: TP ST 25 (45.63  $\mu\text{g}/\text{cm}^2$ ). This trend where longer durations of heating produced greater delivery into the skin/hair follicles was previously observed.

	Mean cumulative amount recovered after 1 hr ( $\mu\text{g cm}^{-2}$ )		
	IPA:TP 32°C	IPA:TP ST 15	IPA:TP ST 25
Hair follicles	23.76 $\pm$ 6.82	31.26 $\pm$ 5.52	45.63 $\pm$ 4.71
SC	1.59 $\pm$ 0.38	2.21 $\pm$ 0.21	3.77 $\pm$ 0.29
Epidermis	3.37 $\pm$ 0.63	4.51 $\pm$ 0.59	6.97 $\pm$ 0.63
Dermis	6.92 $\pm$ 0.49	8.91 $\pm$ 0.95	22.10 $\pm$ 2.68
Receiver fluid	0.35 $\pm$ 0.02	0.47 $\pm$ 0.01	2.26 $\pm$ 0.33
Total	35.99 $\pm$ 8.34	47.36 $\pm$ 7.28	80.73 $\pm$ 8.64
Rank	3	2	1*

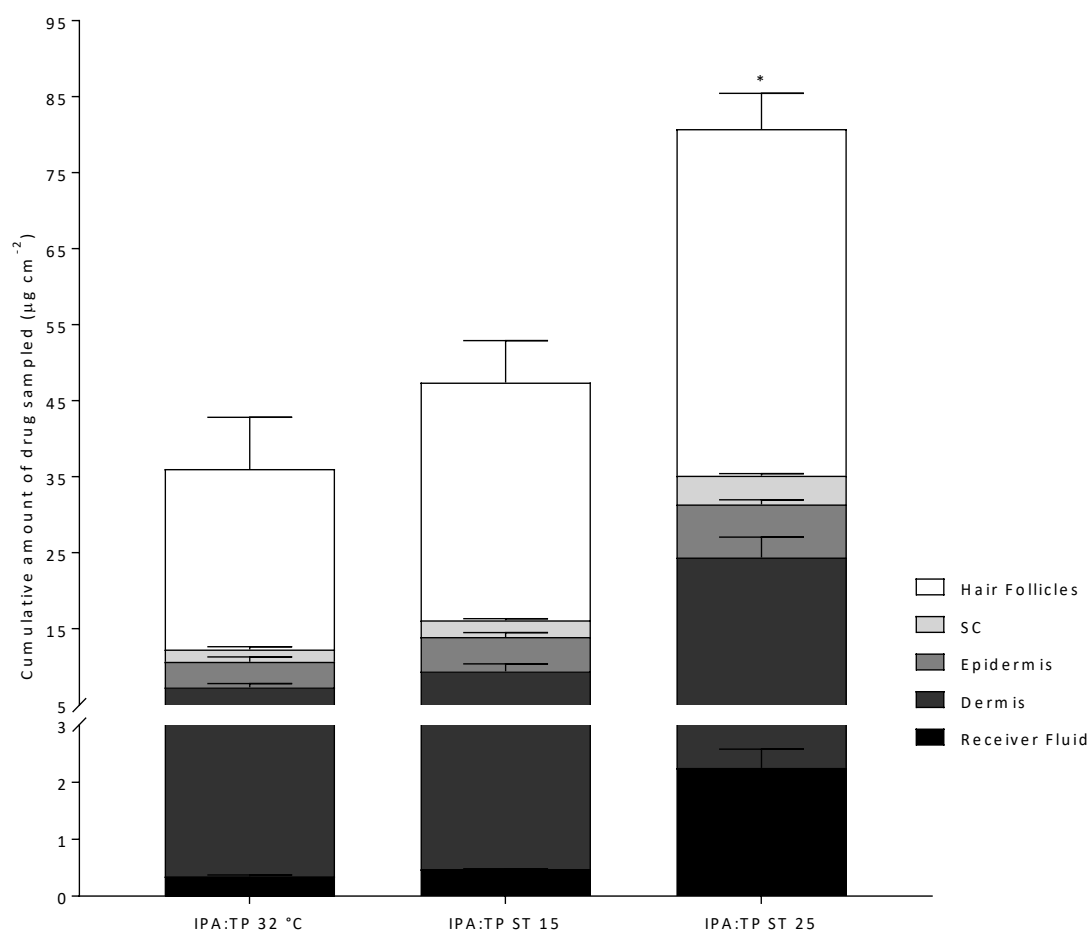


**Figure 5-6: Dose distribution of finasteride in human scalp skin and receiver fluid delivered from IPA: TP binary system (50:50). Filtered saturated solution of finasteride  $10 \mu\text{L cm}^{-2}$  was applied to the skin surface.** Experiments were conducted for 1 hr at 32 °C with and without sodium thiosulfate solution (ST) producing heat for 15 & 25 min (ST 15 & ST 25 respectively). Each bar indicates the amount of finasteride that was recovered from the hair follicles, in the skin (SC + epidermis + dermis) or receiver fluid. All bars are mean + SEM of n=4 diffusion cells. \* denotes significant difference in the total amount recovered compared to vehicles ranked 2<sup>nd</sup> and higher.

With the application of heat (ST 15 and ST 25) the amount of finasteride recovered from the hair follicles (1.3 to 1.9-fold) and SC (1.3 to 2.3-fold) were increased to a similar extent, which possibly indicates that targeted follicular delivery is not achieved when heat is combined with IPA: TP. For IPA:

TP, the amount of finasteride deposited in the skin (SC, epidermis and dermis) after 1 hr corresponds to approximately 6 % to 14 % of the amount delivered after 24 hr from IPA: TP, suggesting that the uptake of finasteride into the skin from IPA: TP is relatively slower compared to IPA: PG. Overall, finasteride delivery from IPA: PG was much better than IPA: TP, which possibly means it would be more effective in the real world.

#### 5.4 Conclusion

The delivery of finasteride from a range of neat dermatological vehicles (with penetration enhancing properties) with and without the application of heat across human scalp skin was investigated. With the application of heat IPA and PG delivered higher amounts of finasteride into the receiver fluid compared with the other vehicles. Also, in comparison with the same respective vehicle at 32 °C, PG and IPA enhanced drug flux 3.6 and 5.6-fold at the elevated temperature (45 °C). With respect to finasteride skin uptake, TP and IPA produced greater finasteride retention in the skin compared with the other vehicles. This suggests that formulation components (CPEs) are likely to play a key role in influencing the effect of heat on drug transport across skin. For all the enhancers investigated, the data suggests partitioning was more important. However, in reality the combination of heat and CPEs can enhance finasteride transport by simultaneously improving drug-vehicle partitioning and diffusion into the skin. It appears, therefore, that vehicles and heat can act synergistically to enhance topical delivery to the skin tissue.

For the finite dose studies, heated water bath (entire system heating) produced increased permeation; however, the magnitude was greater than what is seen with a more clinically relevant heating system (externally applied heat for short periods). Nonetheless, the relevant systems showed increased drug uptake into the skin and hair follicles compared to no heat (32 °C) for both IPA: PG and IPA: TP. However, at early time points (approximately 1hr) external heat for short periods was equivalent or even better in some case when compared with entire system heating. Overall, IPA: PG produced greater deposition of finasteride in the skin and hair follicles, yet, similar amounts of finasteride was

delivered into the receiver fluid for both IPA: PG and IPA: TP after 24 hr. The 1 hr finite dose studies suggest that hair follicles play a crucial role in the uptake of finasteride at early time points, as higher amounts of finasteride were recovered from the hair follicles after 1 hr compared with 24 hr. Also, heating from top led to greater finasteride delivery into the skin compared with no heat, with 25 min of heat localised performing the best for both solvent systems. This is advantageous for the topical treatment of AGA as the active needs to target both the hair follicles and dermal tissues. Also, sodium thiosulfate has been shown to be a useful source of generating heat for enhancing topical drug uptake into both the hair follicles and in skin tissue. The duration (15 and 25 min) of heating investigated in this study may not be suitable/convenient in the real world/clinical setting. Therefore, shorter periods of heating (1 to 10 min) from on top should be investigated along with more complex binary and ternary solvent systems to offer more efficient finasteride delivery to the skin tissue/hair follicles and to further highlight the benefits of using sodium thiosulfate as source of generating heat to facilitate drug transport.

## **6 General Discussion**

## 6.1 General Discussion

Topical drug delivery (using conventional topical formulations) is generally associated with low bioavailability, with only a small percentage (1-3 %) of the dose applied being delivered into the skin (Hadgraft & Lane, 2016). This poor absorption is attributable to the excellent barrier properties of the SC which poses a challenge to the delivery of many drugs into the skin from topical formulations. Therefore, there is a need to develop optimised formulations that improve drug uptake and transport across skin. Over the years, many enhancement strategies have been developed to overcome the barrier properties of the SC and these can be categorised into active and passive methods. The passive approach involves the optimisation of the formulation or drug carrying vehicle in order to increase the permeability of the skin to the drug. Examples of this strategy include the use of CPEs, prodrugs and supersaturated systems. In contrast, active strategies normally involve providing additional energy or mechanical methods of enhancing delivery. Examples of this enhancement method include iontophoresis, sonophoresis and micro-needles, with these approaches capable of delivering molecules with higher molecular weight such as peptides, proteins and oligonucleotides or achieving much faster onset of action (Schoellhammer, Blankschtein, & Langer, 2014).

Another active enhancement strategy which is relatively less investigated is physiologically tolerable heat ( $\leq 45$  °C), a strategy which was the focus of this thesis. It is generally accepted that local or systemic exposure to heat improves drug skin permeation by increasing diffusivity, partitioning and the solubility of the drug in the SC at the elevated temperature (Shahzad et al., 2015). The higher temperature can also affect drug release from the formulation, drug solubility/thermodynamic activity in the formulation and increase dermal clearance of the drug from the application site (Shahzad et al., 2015). Moreover, at higher temperatures (40-45 °C), phase transitions in skin lipids from an orthorhombic (gel like structure) to a more hexagonal phase (liquid crystalline) occur, which is expected to result in increased skin permeability due to the higher degree of disorder in the lipid packing in the later phase (Lawson, Anigbogu, Williams, Barry, & Edwards, 1998).

This approach can be further exploited by combining with CPEs to produce synergy in enhancing drug transport across skin. In this thesis, the influence of increasing skin temperature from 32 °C to 45 °C on transdermal flux and dermal retention was studied using three active pharmaceutical ingredients; minocycline, isotretinoin and finasteride. The selected drugs were delivered as saturated suspensions from various dermatological vehicles commonly used as CPEs. These three drugs have very different lipophilicities; minocycline (Log P = -0.61, (Di Stefano et al., 2008)), isotretinoin (Log P = 6.6, (Nankervis et al., 1995)) and finasteride (Log P= 3.2, (Thorsteinn Loftsson et al., 2005)) but similar molecular weights. Therefore, the ability of heat to enhance the transport of drugs exhibiting a range of lipophilic properties was examined. Two of the major parameters influencing percutaneous absorption, the diffusion and partition coefficients (as pathlength normalised) were determined with a view to gain insight into the mechanisms through which heat can enhance drug delivery to the skin.

It should be noted that not all the same vehicles/CPEs were investigated for all three penetrants, as vehicles were specifically selected for each compound based on their solubility and stability data (presented in Chapter 2). However, the delivery of all three compounds was investigated using propylene glycol (PG) and diisopropyl adipate (DPA) under infinite dose conditions and therefore, it is possible to make comparisons on the influence of heat on drug flux when delivery from PG and DPA for the three permeants. One caveat is that human scalp skin was used in the finasteride experiments which is more permeable than the human abdominal skin which was used for minocycline and isotretinoin experiments possibly due to the greater follicular density (Feldmann & Maibach, 1967), and therefore care must be taken when extrapolating the findings of enhanced drug delivery of minocycline and isotretinoin delivered from PG and DPA formulations with that of finasteride delivered from the same vehicles.

Figures 6-1 and 6-2 depict the enhancement in permeation parameters such as flux, normalised partition and diffusion coefficients for minocycline, isotretinoin and finasteride, when delivered from PG and DPA with the application of heat (45 °C).

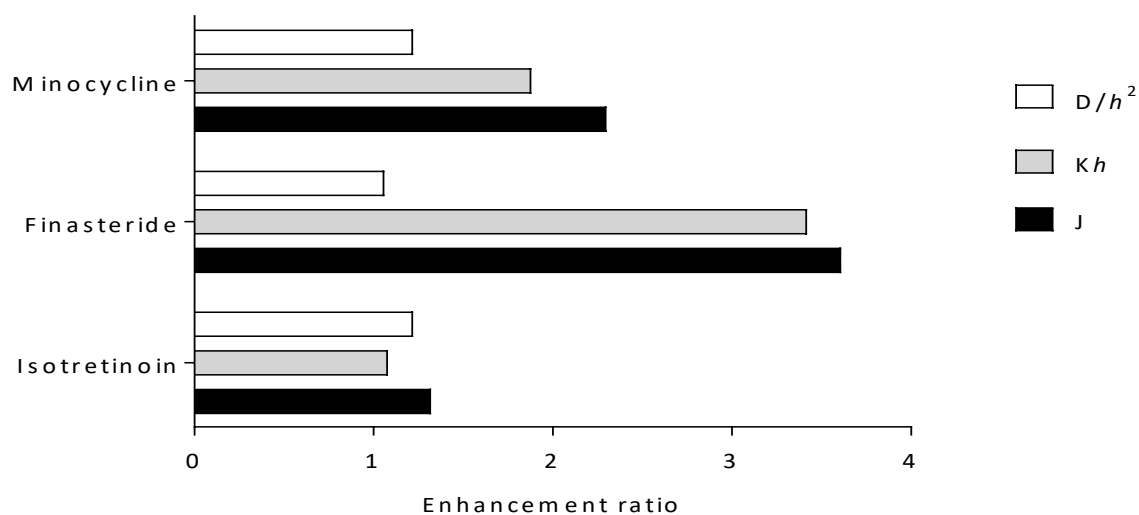


**Figure 6-1: Enhancement in drug flux ( $J$ ) and normalised partition ( $Kh$ ) and diffusion ( $D/h^2$ ) coefficient of minocycline, isotretinoin and finasteride with the application of heat (45 °C) delivered from propylene glycol (PG).**

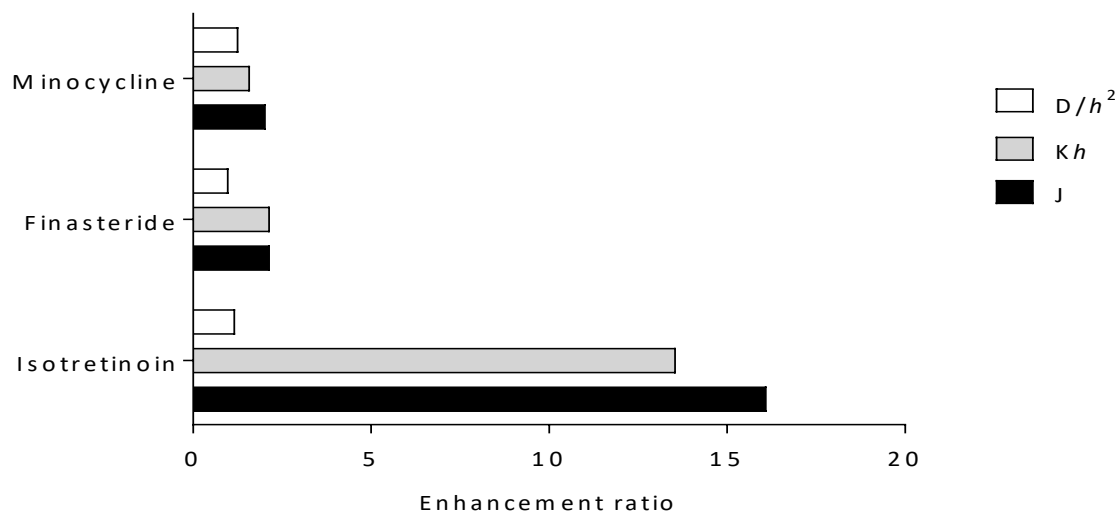


**Figure 6-2: Enhancement in drug flux ( $J$ ) and normalised partition ( $Kh$ ) and diffusion ( $D/h^2$ ) coefficient of minocycline, isotretinoin and finasteride with the application of heat (45 °C) delivered from diisopropyl adipate (DPA).**

When combined with heat, PG enhanced drug flux 2.3, 1.3 and 3.6-fold for minocycline, isotretinoin and finasteride respectively. This suggests, PG maybe more suited in heated systems to improving the transport of solutes with low to moderate lipophilicity across skin. For minocycline and finasteride, the enhancement in flux with heat was attributed to improvements in partitioning, which was increased 1.9 and 3.4-fold for minocycline and finasteride respectively. With the application of heat, no significant increase in diffusivity was observed for both minocycline and finasteride when delivered from PG (up to 1.1-fold increase). For isotretinoin, delivery from PG with heat produced very little improvement in either diffusivity (1.2-fold increase) or partitioning (1.1-fold increase).

Delivery from DPA plus heat increased drug flux 2.0, 16.1 and 2.2-fold for minocycline, isotretinoin and finasteride respectively. This suggests that the drug, vehicle and temperature interaction has a greater potential for improving delivery in the case of isotretinoin, the most lipophilic of the drugs investigated when a relatively lipophilic vehicle is also used. For all three compounds, improvements in diffusivity with heat were very minimal (up to 1.3-fold increases), therefore, the increase in flux with heat was attributed to enhanced partitioning (1.6, 13.6 and 2.2-fold for minocycline, isotretinoin and finasteride respectively). Fatty acid diesters such as DPA have been reported to improve the permeability of hydrophilic solutes more than hydrophobic solutes, possibly by extracting lipids from the SC resulting in increased skin permeability (Takahashi, Sakano, Numata, Kuroda, & Mizuno, 2002b). However, the data presented indicates that DPA with heat may be more suited at enhancing the percutaneous absorption of highly lipophilic drugs. In an attempt to confirm this hypothesis, future work investigating the influence of heat with DPA on the transport of highly lipophilic molecules is required.

For DPA the enhancement in drug flux with heat was in the following order isotretinoin > finasteride > minocycline, which implies that elevated temperature (45 °C) is more effective at enhancing transport of lipophilic compounds when delivered from DPA. Whereas for PG with heat the enhancement in flux was limited for highly lipophilic drugs. To date, there has been only one study

investigating the influence of temperature on permeation of solutes (delivered as aqueous suspensions) with different lipophilicities across skin (caffeine, methyl paraben and butyl paraben) (Akomeah et al., 2004). When using a similar skin temperature range to that employed in this study (30 to 45 °C) these authors observed that heat increased the epidermal flux of the more lipophilic permeants to a greater extent (Akomeah et al., 2004). In particular, their data showed that the flux of caffeine, methyl paraben and butyl paraben, which have Log P values of -0.07, 1.96 and 3.57 respectively, increased significantly by 2.0, 2.1 and 3.0-fold respectively, when increasing the skin temperature from 37 °C to 45 °C. However, an improvement in diffusion coefficient of the solutes was assumed to be responsible for the observed enhancement in solute flux across skin. The findings of this study showed that improvements in partitioning were significantly greater and therefore had more of an effect on the transport of permeants across skin than diffusivity. It is possible that improved partitioning, could be achieved through an improvement in solvent uptake into the SC (Twist & Zatz, 1988). Consequently, in the presence of heat increased solvent uptake into the SC may occur, enabling more drug to be transferred into the skin.

Overall, the enhancement in solute flux with the application of heat from the various vehicles was different for each molecule. For minocycline, improvements in flux ranged from 1.8 to 5.6-fold, for isotretinoin flux was increased 1.3 to 27.3-fold and for finasteride, flux was enhanced by 2.2 to 5.7-fold. Therefore, the extent to which temperature affects skin absorption is likely to be dependent on both the physicochemical properties of the compound and formulation components (CPEs in particular).

The instability of minocycline in hydrophilic vehicles/solutions was a difficulty that needed to be overcome when formulating the drug, designing the receiver fluid for *ex vivo* Franz cell experiments and ensuring the accurate quantification of drug in samples. Improving the chemical stability of minocycline was particularly necessary when conducting studies at elevated temperatures. Thus, the stabilising agent magnesium chloride was incorporated into the hydrophilic vehicles (PG and EtOH),

which provided improved minocycline stability in these vehicles at 50 °C over 24 hr (from 71 % to > 94 %) (data shown in Chapter 2). The stability of minocycline (Chow et al., 2008) and oxytetracycline (Tongaree et al., 2000) in non-aqueous hydrophilic vehicles has been previously reported to be improved by magnesium chloride. The tetracyclines are believed to form a complex with magnesium, which stabilises the molecule against degradation (Wessels et al., 1998). Using the continuous method of variation (Job Plot with UV-Vis absorbance), an attempt was made to determine the stoichiometry of magnesium and minocycline in EtOH to improve our understanding of how these molecules interact. The data generated suggested magnesium – minocycline stoichiometry of 2:3, which has not been previously reported for magnesium and minocycline. The majority of data reported in the literature suggest 1:2 and 1:1 metal-tetracycline complexes (Doluisio & Martin, 1963; Piccariello, 2013; Wessels et al., 1998). Potentially however both could exist simultaneously. Additionally, a well-known limitation of the Job's plot is the inability to determine if more than one complex is present in the solution (Brynn Hibbert & Thordarson, 2016). Whilst, it was outside the scope of this study to determine the exact stoichiometry of magnesium and minocycline, it would be beneficial to determine this to help in the optimisation of potential future topical minocycline formulations, with respect to both stability of the complex and the understanding of enhanced skin permeation. Other methods that could help determine metal-ligand stoichiometry/interaction include; nuclear magnetic resonance (NMR) (Hirose, 2001) and isothermal titration calorimetry (ITC) (Saboury, 2006). Therefore, further studies using these techniques should be conducted to help elucidate the magnesium - minocycline stoichiometry.

The addition of magnesium to EtOH and PG was observed to significantly reduce minocycline skin permeation whilst causing a small increase in the skin uptake of minocycline at 32 °C. This reduced permeation of minocycline when combined with magnesium chloride in EtOH or PG was attributed to increased vehicle viscosity with magnesium (Table 3-3) and possibly the complexation of magnesium with minocycline, leading to an increase in the size of penetrant which further slows its diffusion across skin. Additionally, doxycycline (a tetracycline antibiotic) has been reported to have a high affinity for

human skin (through binding to keratin, epidermal lipids and melanin through H-bonding) (Banning & Heard, 2002). Thus, minocycline would be expected to behave in a similar manner given its structural similarity to doxycycline. At 32 °C, the presence of magnesium chloride in EtOH and PG resulted in greater minocycline delivery into the epidermis only.

However, in the presence of magnesium, minocycline skin uptake (total amount of drug recovered from skin) was enhanced 4.1-fold and 8.1-fold for EtOH and PG respectively at the higher temperature (45 °C), whilst delivery into the receiver fluid was relatively slow. Increased delivery of minocycline to the skin tissue (especially the dermis) with heat with low systemic delivery (possibly simulated by receiver fluid concentration) could be advantageous in the treatment of acne. The dermis is the location of the pilosebaceous units, which would be the target site of minocycline. Thus, the efficacy of topical minocycline could potentially be improved using this strategy, reducing the need for oral administration of minocycline and its associated systemic side-effects. Additionally, a short-term low-dose magnesium diet has been used to effectively treat autoimmune arthritis (Brenner, Laragione, & Gulko, 2017), whilst nebulised magnesium has been shown to be a potential treatment for acute severe asthma (Turner, Ford, Kidd, Broadley, & Powell, 2017) because of its anti-inflammatory properties. Therefore, incorporation of magnesium into potential topical minocycline formulation may further improve its efficacy, since inflammation is a major contributing factor in the pathophysiology of acne. Additional studies are required using the clinically relevant heating system for short periods (up to 25 min of localised heat) to determine if the same trend of drug transport is observed particularly under finite dose conditions. Additionally, the effect of changing the ratio of magnesium: minocycline in the vehicle on drug permeation and release could be investigated to potentially optimise minocycline delivery into the skin.

Delivery of the drugs in the present research into the pilosebaceous units is highly desirable in the treatment of acne and alopecia. To date, no studies have been published investigating the effect of heat on the follicular absorption of topically applied drugs. To address this, the influence of heat on

follicular delivery of isotretinoin and finasteride was studied. Heat was generated using a water bath to produce a membrane surface temperature of 45 °C (complete system heating). Whilst, this model is useful for investigating the mechanism involved with the enhancement in percutaneous absorption with heat, it is less clinically relevant because of the long durations of heat (24 hr). Skin exposure to a temperature of 40 °C for extended period of time may result in thermal injury, cause pain or lead to blister formation (Hutchinson & Hutchinson, 2008; Lindeque, Shuler, & Bates, 2013; Moritz & Henriques, 1947). Also, in a clinical setting the application of heat to the skin surface may result in a temperature gradient across the SC from the outside to the inside, a scenario not replicated with water bath heating. This thermal gradient could provide an additional driving force for diffusion (Soret effect) (McAuley & Caserta, 2015). Therefore, a more clinically relevant heating system, with a temperature of approx. 45 °C for relatively shorter durations (15 and 25 min) applied to the donor chamber was also investigated. This model employed heat from the crystallisation of sodium thiosulfate (ST) (exothermic process). The use of ST as heat source in topical delivery systems has been previously reported (Wood et al., 2011; Wood, Jones, et al., 2012).

The analysis of the data generated from this work shows that both complete system heating and localised heating produced by ST were effective at increasing delivery of both isotretinoin and finasteride, with the level of enhancement ranging from (1.1-fold to 2.4-fold). Employing heat increased the amount of drug that was recovered from the hair follicles, skin tissue and receiver fluid, with complete system heating producing the greatest enhancements followed by 25 min and 15 min of localised heat. Generally, whole system heating was much better at increasing the total amount of drug delivered. The vehicles that worked well with whole system heating were also shown to work well with the more relevant heating system. This suggests that whole system heating is a good model for identifying vehicles that can work well with heat to improve drug absorption into the skin.

It was difficult to fully characterise the effect of heat on follicular absorption from this data, since drug transport through the hair follicles is thought to be a rapid process (Blume-Peytavi et al., 2010) with

hair follicles significantly contributing to the transport process at early times (e.g. only after 5 min) (Otberg et al., 2008). Additionally, the impact of local heat on drug permeation is lost upon removal of heat source (Shomaker, Zhang, & Ashburn, 2000). Consequently, experiments were conducted for 1 hr to determine the influence of localised heat (43 °C for 15 and 25 min) on follicular transport of isotretinoin and finasteride. For isotretinoin, since 25 min of localised heat appeared to work better with both the binary system (EtOH: PGML 90) and Isotrex® gel, it was decided to explore the effectiveness of such a combination over 1 hr.

Locally heating the skin surface for 25 min was enough to significantly increase the delivery of isotretinoin from EtOH: PGML 90 into the hair follicles 2.1-fold. Under the same heating conditions, delivery of isotretinoin from Isotrex® gel into the hair follicles was increased 1.4-fold compared to no additional heat (32 °C). For finasteride, the analysis of the data showed that localised heating for periods as short as 15 and 25 min was sufficient to significantly increase the transport of finasteride from IPA: PG and IPA: TP into the hair follicles after 1 hr, to a similar extent (ca. 2-fold). It is also possible that follicular transport may have contributed to the increased dermal uptake (up to 2.8-fold) when heat was applied from the top. Thus, it is possible that short-term application of heat may facilitate targeted delivery of drugs into the appendages.

In this research the increased drug delivery into the hair follicles from EtOH: PGML 90, IPA: PG and IPA: TP could be due to increased vehicle (PGML 90, PG and TP) miscibility with sebum. Motwani and co-workers assessed the melting point shifts of model sebum in the presence of a series of polar and non-polar organic solvents using differential scanning calorimetry (DSC). This worked demonstrated that solvents, which are commonly used as CPEs, such as IPM, DMI and TP were effective at lowering the melting points of sebum (Motwani, Rhein, & Zatz, 2002). In a follow up study, the same authors demonstrated that the deposition of salicylic acid into the hair follicles increased when the drug was applied in vehicles/CPEs that interacted with sebum, thus altering its solubility parameter in such a way that the uptake of the active into the hair follicles is favoured (Motwani, Rhein, & Zatz, 2004).

Additionally, the higher level of delivery into the hair follicles achieved with localised heating could be due to the effects of heat on sebum viscosity. The application of a moderate level of heat ( $\leq 45$  °C) may be able to reduce sebum viscosity and increase the kinetic energy of drug molecules so that diffusivity through the hair follicles can be improved (according to the Stokes-Einstein, Equation 1-9). Changes in sebum viscosity with increasing temperature was observed in the work of Butcher and Coonin (1949). These authors reported that the viscosity of human sebum collected from the forehead, decreased from 0.098 to 0.055 Pa.S within the temperature range of 26.5 °C to 38 °C (Butcher & Coonin, 1949). A further fundamental effect of heat is that it may improve the uptake of formulation ingredients e.g., CPEs into sebum, which in turn can promote drug partitioning into the hair follicles; as such the combined use of heat and CPEs could result in having either a synergistic or additive effect on follicular transport.

In this present study, direct contact between heat generating solution (ST) and the formulation/skin was prevented using aluminium foil (to keep them apart). Previous studies have reported using ST to enlarge aqueous pathways created by electroporation, which in turn enhanced the transdermal flux of macromolecules compared to when electroporation alone was used (Ilic, Gowrishankar, Vaughan, Herndon, & Weaver, 1999; Zewert, Pliquett, Vanbever, Langer, & Weaver, 1999). Thus, further studies are required to determine whether allowing the ST solution to interact with the skin would have any penetration enhancing capabilities. Another important factor to consider is that human skin was used a model membrane for investigating the effect of heat on follicular delivery. A limitation in using human skin *in vitro*, is that the follicular reservoir is reduced to about 10 % of the follicular reservoir *in vivo* due to the contraction of elastic fibre after skin specimen excision (Patzelt, Richter, et al., 2008). Thus, increased follicular delivery would be expected *in vivo*. Additionally, the existing *in vitro* models (Franz diffusion cells) are not well suited to study the effect of dermal clearance on percutaneous absorption *in vivo*. However, shorter durations of heat are likely to limit any losses caused by clearance.

In conclusion, the work described in this thesis has shown that the application of heat ( $\leq 45\text{ }^{\circ}\text{C}$ ) can significantly enhance skin permeation of hydrophilic and hydrophobic drugs (up to 27-fold when isotretinoin was delivered from EtOH in water bath at  $45\text{ }^{\circ}\text{C}$ ) mainly through improvements in partitioning of the drug from the formulation into the SC. Heat was found to enhance the flux of hydrophobic drugs more when delivered from DPA and PG. Therefore, the level of enhancement achieved was found to be dependent on both the physicochemical properties of the solutes and formulation components (CPEs). In the presence of magnesium chloride, the majority of minocycline was recovered from the epidermis. However, the application of heat was found to alter the skin distribution of minocycline (in the presence of magnesium chloride) so that the majority of the drug was recovered from the dermis (the target site for minocycline), potentially improving its efficacy. Also, localised heating for short periods (15-25 min) in combination with fatty acid esters and alcohols and their derivatives demonstrated the positive impact heat and CPEs can have on follicular transport (up to 2-fold increase). This strategy potentially allows for targeted delivery through hair follicles which is likely to be a significant advance for drugs like isotretinoin, with significant side effect profiles. Therefore, this work has demonstrated that the novel strategy employing the customised use of physiologically tolerable heat ( $\leq 45\text{ }^{\circ}\text{C}$ ) to target the follicular structures and enhance drug delivery is a highly promising approach which, following further investigations will be highly beneficial in the optimisation of current topical formulations and development of new drug delivery systems.

## 7 References

- Afzal, M., Saleem, M., & Mahmood, M. T. (1989). Temperature and concentration dependence of viscosity of aqueous electrolytes from 20°C to 50°C chlorides of (sodium(1+), potassium(1+), magnesium(2+), calcium(2+), barium(2+), strontium(2+), cobalt(2+), nickel(2+), copper(2+) and chromium(3+). *Journal of Chemical & Engineering Data*, 34(3), 339–346.
- Agarwal, R., Katare, O. P., & Vyas, S. P. (2000). The pilosebaceous unit: A pivotal route for topical drug delivery. *Methods and Findings in Experimental and Clinical Pharmacology*, 22(2), 129–133.
- Akomeah, F., Nazir, T., Martin, G. P., & Brown, M. B. (2004). Effect of heat on the percutaneous absorption and skin retention of three model penetrants. *European Journal of Pharmaceutical Sciences*, 21(2–3), 337–345.
- Al-Khamis, K. I., Davis, S. S., & Hadgraft, J. (1986). Microviscosity and drug release from topical gel formulations. *Pharmaceutical Research*, 3(4), 214–217.
- Albery, W. J., & Hadgraft, J. (1979). Percutaneous absorption: in vivo experiments. *The Journal of Pharmacy and Pharmacology*, 31(3), 140–7.
- Alexander, A., Dwivedi, S., Ajazuddin, Giri, T. K., Saraf, S., Saraf, S., & Tripathi, D. K. (2012). Approaches for breaking the barriers of drug permeation through transdermal drug delivery. *Journal of Controlled Release*, 164(1), 26–40.
- Alexeev, V., Igoucheva, O., Domashenko, A., Cotsarelis, G., & Yoon, K. (2000). Localized in vivo genotypic and phenotypic correction of the albino mutation in skin by RNA-DNA oligonucleotide. *Nature Biotechnology*, 18(1), 43–7.
- Amory, J. K. (2007). Drug effects on spermatogenesis. *Drugs of Today*, 43(10), 717–724.
- Anigbogu, A. N. C., Williams, A. C., Barry, B. W., & Edwards, H. G. M. (1995). Fourier transform raman

- spectroscopy of interactions between the penetration enhancer dimethyl sulfoxide and human stratum corneum. *International Journal of Pharmaceutics*, 125(2), 265–282.
- Arias, K., Robinson, S. G., Lyngaas, S. S., Cherala, S. S., Hartzell, M., Mei, S., ... Jin, L. (2016). Minocycline and tigecycline form higher-order Ca<sup>2+</sup> complexes of stronger affinity than tetracycline. *Inorganica Chimica Acta*, 441, 181–191.
- Aronson, J. K. (Ed.). (2014). *Meyler's Side Effects of Drugs: The International Encyclopedia of Adverse Drug Reactions and Interactions*. *Meyler's Side Effects of Drugs: The International Encyclopedia of Adverse Drug Reactions and Interactions* (15th ed.). Oxford, United Kingdom: Elsevier B.V.
- Arora, A., Kisak, E., Karande, P., Newsam, J., & Mitragotri, S. (2010). Multicomponent chemical enhancer formulations for transdermal drug delivery: More is not always better. *Journal of Controlled Release*, 144(2), 175–180.
- Aslam, I., Fleischer, A., & Feldman, S. (2015). Emerging drugs for the treatment of acne. *Expert Opinion on Emerging Drugs*, 20(1), 91–101.
- Aungst, B. J., Rogers, J. N., & Shefter, E. (1986). Enhancement of naloxone penetration through human skin in vitro using fatty acids, fatty alcohols, surfactants, sulfoxides and amides. *International Journal of Pharmaceutics*, 33(1–3), 225–234.
- Banga, A. K. (2011). Iontophoretic Intradermal and Transdermal Drug Delivery. In *Transdermal and Intradermal Delivery of Therapeutic Agents : Application of Physical Technologies* (pp. 81–129). Boca Raton: CRC Press.
- Banning, T. P., & Heard, C. M. (2002). Binding of doxycycline to keratin, melanin and human epidermal tissue. *International Journal of Pharmaceutics*, 235(1–2), 219–227.
- Barry, B. W. (1983). Skin transport. In B. W. Barry (Ed.), *Dermatological Formulations: Percutaneous Absorption* (pp. 95–126). New York: Marcel Dekker.

- Barry, B. W. (2001). Novel mechanisms and devices to enable successful transdermal drug delivery. *European Journal of Pharmaceutical Sciences*, 14(2), 101–114.
- Barry, B. W. (2002). Drug delivery routes in skin: a novel approach. *Advanced Drug Delivery Reviews*, 54(Supplement), S31–S40.
- Barry, B. W. (2004). Breaching the skin's barrier to drugs. *Nature Biotechnology*, 22(2), 165–167.
- Barry, B. W. (2005). Penetration Enhancer Classification. In E. W. Smith & H. I. Maibach (Eds.), *Percutaneous Penetration Enhancers* (2nd ed., pp. 3–16). CRC Press.
- Basra, M. K. A., & Finlay, A. Y. (2007). The family impact of skin diseases: the Greater Patient concept. *The British Journal of Dermatology*, 156(5), 929–37.
- Benaouda, F., Brown, M. B., Shah, B., Martin, G. P., & Jones, S. A. (2012). The influence of self-assembling supramolecular structures on the passive membrane transport of ion-paired molecules. *International Journal of Pharmaceutics*, 439(1–2), 334–341.
- Benson, H. (2005). Transdermal drug delivery: penetration enhancement techniques. *Current Drug Delivery*, 2(1), 23–33.
- Benson, H. A. E. (2012). Skin Structure, Function, and Permeation. In H. A. E. Benson & A. Watkinson (Eds.), *Topical and Transdermal Drug Delivery: Principles and Practice* (pp. 3–22). Singapore: John Wiley & Sons Inc.
- Benson, H. a E. (2005). Transdermal drug delivery: penetration enhancement techniques. *Current Drug Delivery*, 2(1), 23–33.
- Biruss, B., Kählig, H., & Valenta, C. (2007). Evaluation of an eucalyptus oil containing topical drug delivery system for selected steroid hormones. *International Journal of Pharmaceutics*, 328(2), 142–151.

- Biruss, B., & Valenta, C. (2006). Skin permeation of different steroid hormones from polymeric coated liposomal formulations. *European Journal of Pharmaceutics and Biopharmaceutics*, 62(2), 210–9.
- Blank, I. H. (1953). Further Observations on Factors Which Influence the Water Content of the Stratum Corneum<sup>1</sup>. *The Journal of Investigative Dermatology*, 21(4), 259–271.
- Blank, I. H., Scheuplein, R. J., & Macfarlane, D. J. (1967). Mechanism of Percutaneous Absorption. *The Journal of Investigative Dermatology*, 49(6), 582–589.
- Blume-Peytavi, U., Massoudy, L., Patzelt, A., Lademann, J., Dietz, E., Rasulev, U., & Garcia Bartels, N. (2010). Follicular and percutaneous penetration pathways of topically applied minoxidil foam. *European Journal of Pharmaceutics and Biopharmaceutics*, 76(3), 450–453.
- BNF 66. (2013). *British National Formulary* (66th ed.). London: Pharmaceutical Press.
- Boddé, H. E., van den Brink, I., Koerten, H. K., & de Haan, F. H. N. (1991). Visualization of in vitro percutaneous penetration of mercuric chloride; transport through intercellular space versus cellular uptake through desmosomes. *Journal of Controlled Release*, 15(3), 227–236.
- Bos, J. D., & Meinardi, M. M. (2000). The 500 Dalton rule for the skin penetration of chemical compounds and drugs. *Experimental Dermatology*, 9(3), 165–9.
- Bregni, C., Chiappetta, D., Faiden, N., Carlucci, A., García, R., & Pasquali, R. (2008). Release study of diclofenac from new carbomer gels. *Pakistan Journal of Pharmaceutical Sciences*, 21(1), 12–6.
- Brenner, M., Laragione, T., & Gulko, P. S. (2017). Short-term low-magnesium diet reduces autoimmune arthritis severity and synovial tissue gene expression. *Physiological Genomics*, 49(4), 238–242.
- Brinkmann, I., & Müller-Goymann, C. C. (2005). An attempt to clarify the influence of glycerol, propylene glycol, isopropyl myristate and a combination of propylene glycol and isopropyl myristate on human stratum corneum. *Die Pharmazie*, 60(3), 215–20.

- Bronaugh, R. L., & Maibach, H. I. (2005). *Percutaneous absorption : drugs, cosmetics, mechanisms, methodology*. New York: Informa Healthcare.
- Brynn Hibbert, D., & Thordarson, P. (2016). The death of the Job plot, transparency, open science and online tools, uncertainty estimation methods and other developments in supramolecular chemistry data analysis. *Chemical Communications*, 52(87), 12792–12805.
- Brzezinski, P., Borowska, K., Chiriac, A., & Smigielski, J. (2017). Adverse effects of isotretinoin: A large, retrospective review. *Dermatologic Therapy*, 30(4), e12483.
- Burton, J. L., Cunliffe, W. J., Stafford, I., & Shuster, S. (1971). The Prevalence of Acne Vulgaris in Adolescence. *British Journal of Dermatology*, 85(2), 119–126.
- Butcher, E. O., & Coonin, A. (1949). The physical properties of human sebum. *The Journal of Investigative Dermatology*, 12(4), 249–54.
- Cash, T. F. (1992). The psychological effects of androgenetic alopecia in men. *Journal of the American Academy of Dermatology*, 26(6), 926–31.
- Cash, T. F., Price, V. H., & Savin, R. C. (1993). Psychological effects of androgenetic alopecia on women: comparisons with balding men and with female control subjects. *Journal of the American Academy of Dermatology*, 29(4), 568–75.
- Cash, T. F., Santos, M. T., & Williams, E. F. (2005). Coping with body-image threats and challenges: validation of the Body Image Coping Strategies Inventory. *Journal of Psychosomatic Research*, 58(2), 190–9.
- Chan, S. Y., & Li Wan Po, A. (1989). Prodrugs for dermal delivery. *International Journal of Pharmaceutics*, 55(1), 1–16.
- Chang, S., & Riviere, J. E. (1991). Percutaneous absorption of parathion in vitro in porcine skin: Effects of dose, temperature, humidity, and perfusate composition on absorptive flux. *Fundamental and*

- Applied Toxicology*, 17(3), 494–504.
- Chen, C., Puy, L. A., Simard, J., Li, X., Singh, S. M., & Labrie, F. (1995). Local and systemic reduction by topical finasteride or flutamide of hamster flank organ size and enzyme activity. *The Journal of Investigative Dermatology*, 105(5), 678–82.
- Chi, S. C., Park, E. S., & Kim, H. (1995). Effect of penetration enhancers on flurbiprofen permeation through rat skin. *International Journal of Pharmaceutics*, 126(1), 267–274.
- Chiriaco, G., Cauci, S., Mazzon, G., & Trombetta, C. (2016). An observational retrospective evaluation of 79 young men with long-term adverse effects after use of finasteride against androgenetic alopecia. *Andrology*, 4(2), 245–50.
- Chow, K. T., Chan, L. W., & Heng, P. W. S. (2008). Formulation of hydrophilic non-aqueous gel: drug stability in different solvents and rheological behavior of gel matrices. *Pharmaceutical Research*, 25(1), 207–17.
- Christophers, E., & Kilgman, A. M. (1965). Percutaneous absorption in aged skin. In W. Montagna (Ed.), *Advances in Biology of Skin* (Volume 6, pp. 163–175). Oxford: Pergamon Press.
- Clarys, P., Alewaeters, K., Jadoul, A., Barel, A., Manadas, R. O., & Pr at, V. (1998). In vitro percutaneous penetration through hairless rat skin: influence of temperature, vehicle and penetration enhancers. *European Journal of Pharmaceutics and Biopharmaceutics*, 46(3), 279–83.
- Clarys, P., & Barel, A. (1995). Quantitative evaluation of skin surface lipids. *Clinics in Dermatology*, 13(4), 307–21.
- Coenye, T., Peeters, E., & Nelis, H. J. (2007). Biofilm formation by *Propionibacterium acnes* is associated with increased resistance to antimicrobial agents and increased production of putative virulence factors. *Research in Microbiology*, 158(4), 386–92.
- Colaco, C. A., Bailey, C. R., Walker, K. B., & Keeble, J. (2013). Heat Shock Proteins: Stimulators of Innate

- and Acquired Immunity. *BioMed Research International*, 1–11.
- Colin Long, C. (2002). Common Skin Disorders and Their Topical Treatment. In K. A. Walters (Ed.), *Dermatological and Transdermal Formulations : Dermatological and Transdermal Formulations* (pp. 41–60). New York: Marcel Dekker Inc.
- Cooper, E. R., Merritt, E. W., & Smith, R. L. (1985). Effect of fatty acids and alcohols on the penetration of acyclovir across human skin in vitro. *Journal of Pharmaceutical Sciences*, 74(6), 688–9.
- Costa, P., & Sousa Lobo, J. M. (2001). Modeling and comparison of dissolution profiles. *European Journal of Pharmaceutical Sciences*, 13(2), 123–133.
- Cotsarelis, G. (2006). Epithelial stem cells: a folliculocentric view. *The Journal of Investigative Dermatology*, 126(7), 1459–68.
- Cross, S. E., Pugh, W. J., Hadgraft, J., & Roberts, M. S. (2001). Probing the Effect of Vehicles on Topical Delivery: Understanding the Basic Relationship Between Solvent and Solute Penetration Using Silicone Membranes. *Pharmaceutical Research*, 18(7), 999–1005.
- Cummings, E. G. (1969). Temperature and Concentration Effects on Penetration of N-Octylamine through Human Skin In Situ. *The Journal of Investigative Dermatology*, 53(1), 64–70.
- Cunliffe, W. J., & Shuster, S. (1969). The rate of sebum excretion in man. *British Journal of Dermatology*, 81(9), 697–704.
- Curran, J. N., McGuigan, K. G., & O’Broin, E. (2013). A case of deep burns, while diving the Lusitania. *Diving and Hyperbaric Medicine*, 43(2), 113.
- Cutts, J., Lee, G., Berarducci, M., Thomas, C., Dempsey, P., & Kadish, S. (2002). Goosebumps. *The Lancet*, 360(9334), 690.
- Dallob, A. L., Sadick, N. S., Unger, W., Lipert, S., Geissler, L. A., Gregoire, S. L., ... Tanaka, W. K. (1994).

- The effect of finasteride, a 5 alpha-reductase inhibitor, on scalp skin testosterone and dihydrotestosterone concentrations in patients with male pattern baldness. *The Journal of Clinical Endocrinology & Metabolism*, 79(3), 703–706.
- Dancik, Y., Thompson, C., Krishnan, G., & Roberts, M. S. (2010). Cutaneous Metabolism and Active Transport in Transdermal Drug Delivery. In N. A. Monteiro-Riviere (Ed.), *Toxicology of the Skin* (pp. 69–82). New York: Informa Healthcare.
- Davis, A. F., & Hadgraft, J. (1991). Effect of supersaturation on membrane transport: 1. Hydrocortisone acetate. *International Journal of Pharmaceutics*, 76(1–2), 1–8.
- De Paula, D., Martins, C. A., & Bentley, M. V. L. B. (2008). Development and validation of HPLC method for imiquimod determination in skin penetration studies. *Biomedical Chromatography*, 22(12), 1416–1423.
- Dessinioti, C., & Katsambas, A. D. (2010). The role of *Propionibacterium acnes* in acne pathogenesis: facts and controversies. *Clinics in Dermatology*, 28(1), 2–7.
- Diani, A. R., Mulholland, M. J., Shull, K. L., Kubicek, M. F., Johnson, G. A., Schostarez, H. J., ... Buhl, A. E. (1992). Hair growth effects of oral administration of finasteride, a steroid 5 alpha-reductase inhibitor, alone and in combination with topical minoxidil in the balding stump-tail macaque. *The Journal of Clinical Endocrinology & Metabolism*, 74(2), 345–350.
- Di Stefano, A., Sozio, P., Iannitelli, A., Cerasa, L. S., Fontana, A., Di Biase, G., Barbato, F. (2008). Characterization of alkanoyl-10-O-minocyclines in micellar dispersions as potential agents for treatment of human neurodegenerative disorders. *European Journal of Pharmaceutical Sciences*, 34(2–3), 118–128.
- Dokka, S., Cooper, S. R., Kelly, S., Hardee, G. E., & Karras, J. G. (2005). Dermal delivery of topically applied oligonucleotides via follicular transport in mouse skin. *The Journal of Investigative*

- Dermatology*, 124(5), 971–5.
- Doluisio, J. T., & Martin, A. N. (1963). Metal Complexation of the Tetracycline Hydrochlorides. *Journal of Medicinal Chemistry*, 6(1), 16–20.
- El-Nahas, H., Fakhry, G., El-Ghamry, H., Sabry, & Shereen. (2011). Effect of various penetration enhancers concentrations on diclafenac sodium release from cellulose acetate phthalate polymeric film. *Asian Journal of Pharmaceutics*, 5(1).
- Elewski, B. E., Draelos, Z., Dréno, B., Jansen, T., Layton, A., & Picardo, M. (2011). Rosacea - global diversity and optimized outcome: proposed international consensus from the Rosacea International Expert Group. *Journal of the European Academy of Dermatology and Venereology*, 25(2), 188–200.
- Elias, P. M. (2005). Stratum corneum defensive functions: an integrated view. *The Journal of Investigative Dermatology*, 125(2), 183–200.
- Escobar-Chávez, J. J., Bonilla-Martinez, D., & Villegas-González, M. A. (2010). Sonophoresis: A valuable Physical Enhancer to Increased Transdermal Drug Delivery. In J. J. Escobar-Chávez (Ed.), *Current Technologies to Increase the Transdermal Delivery of Drugs* (pp. 53–77). Sharjah: Bentham Science Publishers.
- Escobar-Chávez, J. J., Bonilla-Martínez, D., Villegas-González, M. A., Molina-Trinidad, E., Casas-Alancaster, N., & Revilla-Vázquez, A. L. (2011). Microneedles: a valuable physical enhancer to increase transdermal drug delivery. *Journal of Clinical Pharmacology*, 51(7), 964–77.
- FDA. (1994). *Reviewer Guidance: Validation of Chromatographic Methods*.
- Feldmann, R. J., & Maibach, H. I. (1967). Regional variation in percutaneous penetration of <sup>14</sup>C cortisol in man. *The Journal of Investigative Dermatology*, 48(2), 181–3.
- Finnin, B. C., & Morgan, T. M. (1999). Transdermal penetration enhancers: applications, limitations,

- and potential. *Journal of Pharmaceutical Sciences*, 88(10), 955–8.
- Flynn, G. L., Shah, V. P., Tenjarla, S. N., Corbo, M., DeMagistris, D., Feldman, T. G., ... Zatz, J. L. (1999). Assessment of value and applications of in vitro testing of topical dermatological drug products. *Pharmaceutical Research*, 16(9), 1325–30.
- Friend, D., Catz, P., Heller, J., Reid, J., & Baker, R. (1988). Transdermal delivery of levonorgestrel I: Alkanols as permeation enhancers in vitro. *Journal of Controlled Release*, 7(3), 243–250.
- Fritsch, W. C., Stoughton, R. B., & Stapelfeldt, A. (1963). The Effect of Temperature and Humidity on the Penetration of C14 Acetylsalicylic Acid in Excised Human Skin<sup>1</sup>. *The Journal of Investigative Dermatology*, 41(5), 307–311.
- Fuchs, E. (1990). Epidermal differentiation. *Current Opinion in Cell Biology*, 2(6), 1028–1035.
- Fuchs, E. (2007). Scratching the surface of skin development. *Nature*, 445(7130), 834–42.
- Furuishi, T., Fukami, T., Suzuki, T., Takayama, K., & Tomono, K. (2010). Synergistic effect of isopropyl myristate and glyceryl monocaprylate on the skin permeation of pentazocine. *Biological and Pharmaceutical Bulletin*, 33(2).
- Garrido-Mesa, N., Zarzuelo, A., & Gálvez, J. (2013). What is behind the non-antibiotic properties of minocycline? *Pharmacological Research: The Official Journal of the Italian Pharmacological Society*, 67(1), 18–30.
- Gay, C. L., Guy, R. H., Golden, G. M., Mak, V. H., & Francoeur, M. L. (1994). Characterization of low-temperature (i.e., < 65 degrees C) lipid transitions in human stratum corneum. *The Journal of Investigative Dermatology*, 103(2), 233–9.
- Gelfuso, G. M., Gratieri, T., Delgado-Charro, M. B., Guy, R. H., & Vianna Lopez, R. F. (2013). Iontophoresis-targeted, follicular delivery of minoxidil sulfate for the treatment of alopecia. *Journal of Pharmaceutical Sciences*, 102(5), 1488–94.

- Gil, V. M. S., & Oliveira, N. C. (1990). On the use of the method of continuous variations. *Journal of Chemical Education*, 67(6), 473.
- Gollnick, H. (2003). Current Concepts of the Pathogenesis of Acne Implications for Drug Treatment, 63(15), 1579–1596.
- Gomes, M. J., Martins, S., Ferreira, D., Segundo, M. A., & Reis, S. (2014). Lipid nanoparticles for topical and transdermal application for alopecia treatment: development, physicochemical characterization, and in vitro release and penetration studies. *International Journal of Nanomedicine*, 9(7), 1231–42.
- Good, M. L., & Hussey, D. L. (2003). Minocycline: stain devil? *The British Journal of Dermatology*, 149(2), 237–9.
- Goodman, M., & Barry, B. W. (1989). Lipid-protein-partitioning (LPP) theory of skin enhancer activity: finite dose technique. *International Journal of Pharmaceutics*, 57(1), 29–40.
- Grams, Y. Y., & Bouwstra, J. A. (2002). Penetration and distribution of three lipophilic probes in vitro in human skin focusing on the hair follicle. *Journal of Controlled Release*, 83(2), 253–262.
- Grams, Y. Y., & Bouwstra, J. (2005). Penetration and Distribution in Human Skin Focusing on the Hair Follicle. In R. L. Bronaugh & H. I. Maibach (Eds.), *Percutaneous Absorption : Drugs, Cosmetics, Mechanisms, Methods* (4th ed., pp. 177–192). Boca Raton: Taylor & Francis Group.
- Grams, Y. Y., Whitehead, L., Lamers, G., Sturmman, N., & Bouwstra, J. A. (2005). On-line diffusion profile of a lipophilic model dye in different depths of a hair follicle in human scalp skin. *The Journal of Investigative Dermatology*, 125(4), 775–82.
- Hadgraft, J. (1983). Percutaneous absorption: possibilities and problems. *International Journal of Pharmaceutics*, 16(3), 255–270.
- Hadgraft, J., & Lane, M. E. (2016). Advanced topical formulations (ATF). *International Journal of*

- Pharmaceutics*, 514(1), 52–57.
- Hadgraft, J., Peck, J., Williams, D. G., Pugh, W. J., & Allan, G. (1996). Mechanisms of action of skin penetration enhancers/retarders: Azone and analogues. *International Journal of Pharmaceutics*, 141(1–2), 17–25.
- Hadgraft, J., & Valenta, C. (2000). pH, pKa and dermal delivery. *International Journal of Pharmaceutics*, 200(2), 243–247.
- Hamilton, J. B. (1941). Male hormone substance: a prime factor in acne. *The Journal of Clinical Endocrinology & Metabolism*, 1(7), 570–592.
- Han, I., Kim, M., & Kim, J. (2004). Enhanced transfollicular delivery of adriamycin with a liposome and iontophoresis. *Experimental Dermatology*, 13(2), 86–92.
- Harada, K., Murakami, T., Yata, N., & Yamamoto, S. (1992). Role of intercellular lipids in stratum corneum in the percutaneous permeation of drugs. *The Journal of Investigative Dermatology*, 99(3), 278–82.
- Harding, C. R. (2004). The stratum corneum: structure and function in health and disease. *Dermatologic Therapy*, 17(s1), 6–15.
- Hasegawa, K. ., Takatsuki, N. ., Takatsuki, T. ., & Osaka, M. . (1987, October 20). Composition stably containing minocycline for treating periodontal diseases. Japan: United States Patent.
- Hay, R. J., Johns, N. E., Williams, H. C., Bolliger, I. W., Dellavalle, R. P., Margolis, D. J., ... Naghavi, M. (2014). The global burden of skin disease in 2010: an analysis of the prevalence and impact of skin conditions. *The Journal of Investigative Dermatology*, 134(6), 1527–34.
- Heard, C. M. (2015). Ethanol and other alcohols: Old enhancers, alternative perspectives. In N. Dragicevic & H. I. Maibach (Eds.), *Percutaneous Penetration Enhancers Chemical Methods in Penetration Enhancement: Modification of the Stratum Corneum* (pp. 151–172). Springer Berlin

Heidelberg.

Henzl, M. R., & Loomba, P. K. (2003). Transdermal delivery of sex steroids for hormone replacement therapy and contraception: A review of principles and practice. *Journal of Reproductive Medicine for the Obstetrician and Gynecologist*, *48*(7), 525–540.

Higuchi, T. (1960). Physical Chemical analysis of Percutaneous Absorption Process from Creams and Ointments. *J. Soc. Cosmet. Chem*, *11*, 70–82.

Higuchi, T. (1961). Rate of release of medicaments from ointment bases containing drugs in suspension. *Journal of Pharmaceutical Sciences*, *50*, 874–5.

Hilton, J., Woollen, B. H., Scott, R. C., Auton, T. R., Trebilcock, K. L., & Wilks, M. F. (1994). Vehicle effects on in vitro percutaneous absorption through rat and human skin. *Pharmaceutical Research*, *11*(10), 1396–400.

Hirata, K., Helal, F., Hadgraft, J., & Lane, M. E. (2013). Formulation of carbenoxolone for delivery to the skin. *International Journal of Pharmaceutics*, *448*(2), 360–5.

Hirose, K. (2001). A Practical Guide for the Determination of Binding Constants. *Journal of Inclusion Phenomena and Macrocyclic Chemistry*, *39*(3/4), 193–209.

Hodgkiss-Harlow, C. J., Eichenfield, L. F., & Dohil, M. A. (2011). Effective monitoring of isotretinoin safety in a pediatric dermatology population: A novel “patient symptom survey” approach. *Journal of the American Academy of Dermatology*, *65*(3), 517–524.

Hoelgaard, A., Møllgaard, B., & Baker, E. (1988). Vehicle effect on topical drug delivery. IV. Effect of N-methylpyrrolidone and polar lipids on percutaneous drug transport. *International Journal of Pharmaceutics*, *43*(3), 233–240.

Hollestein, L. M., & Nijsten, T. (2014). An insight into the global burden of skin diseases. *The Journal of Investigative Dermatology*, *134*(6), 1499–501.

- Holmes, R. L., Williams, M., & Cunliffe, W. J. (1972). Pilo-sebaceous duct obstruction and acne. *British Journal of Dermatology*, *87*(4), 327–332.
- Horne, R., Kelly, D., Kirchoffer, L., Koontz, R., & Young, J. (2011). Skincare Treatment. United States: United States Patent.
- Hotchkiss, S. A. M., Miller, J. M., & Caldwell, J. (1992). Percutaneous absorption of benzyl acetate through rat skin in vitro. 2. Effect of vehicle and occlusion. *Food and Chemical Toxicology*, *30*(2), 145–153.
- Hubbell, C. G., Hobbs, E. R., Rist, T., & White, J. W. (1982). Efficacy of minocycline compared with tetracycline in treatment of acne vulgaris. *Archives of Dermatology*, *118*(12), 989–92.
- Hutchinson, M. J., & Hutchinson, M. R. (2008). Factors contributing to the temperature beneath plaster or fiberglass cast material. *Journal of Orthopaedic Surgery and Research*, *3*(1), 10.
- ICH. (2003). *Stability Testing of New Drug Substances and Products Q1A(R2)*. Geneva. Retrieved from <http://www.ich.org/products/guidelines/quality/article/quality-guidelines.html>
- ICH. (2005). *Validation of Analytical Procedures: Text and Methodology Q2(R1)*. Geneva. Retrieved from <http://www.ich.org/products/guidelines/quality/article/quality-guidelines.html>
- Iervolino, M., Cappello, B., Raghavan, S. L., & Hadgraft, J. (2001). Penetration enhancement of ibuprofen from supersaturated solutions through human skin. *International Journal of Pharmaceutics*, *212*(1), 131–41.
- Ilic, L., Gowrishankar, T. R., Vaughan, T. E., Herndon, T. O., & Weaver, J. C. (1999). Spatially constrained skin electroporation with sodium thiosulfate and urea creates transdermal microconduits. *Journal of Controlled Release : Official Journal of the Controlled Release Society*, *61*(1–2), 185–202.
- Inui, S., & Itami, S. (2011). Molecular basis of androgenetic alopecia: From androgen to paracrine

- mediators through dermal papilla. *Journal of Dermatological Science*, 61(1), 1–6.
- Ioannides, D., & Lazaridou, E. (2015). Female pattern hair loss. *Current Problems in Dermatology*, 47, 45–54.
- Jacob, C. I., Dover, J. S., & Kaminer, M. S. (2001). Acne scarring: A classification system and review of treatment options. *Journal of the American Academy of Dermatology*, 45(1), 109–117.
- Jacobi, U., Toll, R., Sterry, W., & Lademann, J. (2005). Do follicles play a role as penetration pathways in in vitro studies on porcine skin? - : An optical study. *Laser Physics*, 15(11), 1594–1598.
- Jain, N., Jain, G. K., Ahmad, F. J., & Khar, R. K. (2007). Validated stability-indicating densitometric thin-layer chromatography: application to stress degradation studies of minocycline. *Analytica Chimica Acta*, 599(2), 302–9.
- Janssens, M., van Smeden, J., Gooris, G. S., Bras, W., Portale, G., Caspers, P. J., ... Bouwstra, J. A. (2012). Increase in short-chain ceramides correlates with an altered lipid organization and decreased barrier function in atopic eczema patients. *Journal of Lipid Research*, 53(12), 2755–66.
- Jin, L., Amaya-Mazo, X., Apel, M. E., Sankisa, S. S., Johnson, E., Zbyszynska, M. A., & Han, A. (2007). Ca<sup>2+</sup> and Mg<sup>2+</sup> bind tetracycline with distinct stoichiometries and linked deprotonation. *Biophysical Chemistry*, 128(2–3), 185–196.
- Johansen, M., Møllgaard, B., Wotton, P. K., Larsen, C., & Hoelgaard, A. (1986). In vitro evaluation of dermal prodrug delivery — transport and bioconversion of a series of aliphatic esters of metronidazole. *International Journal of Pharmaceutics*, 32(2–3), 199–206.
- Joo, Y., Kang, H., Choi, E. H., Nelson, J. S., & Jung, B. (2012). Characterization of a new acne vulgaris treatment device combining light and thermal treatment methods. *Skin Research and Technology*, 18(1), 15–21.
- Kanikkannan, N. (2002). Iontophoresis-based transdermal delivery systems. *BioDrugs*, 16(5), 339–47.

- Kanikkannan, N., & Singh, M. (2002). Skin permeation enhancement effect and skin irritation of saturated fatty alcohols. *International Journal of Pharmaceutics*, 248(1–2), 219–228.
- Karande, P., & Mitragotri, S. (2009). Enhancement of transdermal drug delivery via synergistic action of chemicals. *Biochimica et Biophysica Acta*, 1788(11), 2362–73.
- Kaufman, K. D. (2002). Androgens and alopecia. *Molecular and Cellular Endocrinology*, 198(1–2), 89–95.
- Kaymak, Y., Taner, E., & Taner, Y. (2009). Comparison of depression, anxiety and life quality in acne vulgaris patients who were treated with either isotretinoin or topical agents. *International Journal of Dermatology*, 48(1), 41–46.
- Keith, B. R., & Chilcott, R. P. (2008). Physicochemical factors affecting skin absorption. In R. P. Chilcott & P. Shirely (Eds.), *Principles and practice of skin toxicology* (pp. 83–92). Chichester, UK: John Wiley & Sons.
- Khan, M. W., ur-Rahman, N., Nawaz, A., & Khan, J. A. (2014). Formulation and in vitro evaluation of sumatriptane succinate transdermal patches. *Latin American Journal of Pharmacy*, 33(4).
- Kim, J., Ochoa, M.T., Krutzik, S. R., Takeuchi, O., Uematsu, S., Legaspi, A. J., Modlin, R. L. (2002). Activation of Toll-Like Receptor 2 in Acne Triggers Inflammatory Cytokine Responses. *The Journal of Immunology*, 169(3), 1535–1541.
- Kim, M. K., Lee, C. H., & Kim, D. D. (2000). Skin permeation of testosterone and its ester derivatives in rats. *The Journal of Pharmacy and Pharmacology*, 52(4), 369–75.
- Klemsdal, T. O., Gjesdal, K., & Bredesen, J. E. (1992, January). Heating and cooling of the nitroglycerin patch application area modify the plasma level of nitroglycerin. *European Journal of Clinical Pharmacology*.
- Kligman, A. M., & Katz, A. G. (1968). Pathogenesis of Acne Vulgaris. *Archives of Dermatology*, 98(1),

53.

- Komata, Y., Inaoka, M., Kaneko, A., & Fujie, T. (1992). In vitro percutaneous absorption of thiamine disulfide from a mixture of propylene glycol and fatty acid. *Journal of Pharmaceutical Sciences*, *81*(8), 744–6.
- Kornick, C. A., Santiago-Palma, J., Moryl, N., Payne, R., & Obbens, E. A. M. T. (2003). Benefit-Risk Assessment of Transdermal Fentanyl for the Treatment of Chronic Pain. *Drug Safety*, *26*(13), 951–973.
- Kubis, A., Dybek, K., & Krutul, H. (1987). Investigation of stability of tetracycline hydrochloride in methylcellulose gel. *Die Pharmazie*, *42*(8), 519–20.
- Kumar, R., Singh, B., Bakshi, G., & Katare, O. P. (2007). Development of liposomal systems of finasteride for topical applications: design, characterization, and in vitro evaluation. *Pharmaceutical Development and Technology*, *12*(6), 591–601.
- Lademann, J., Richter, H., Schaefer, U. F., Blume-Peytavi, U., Teichmann, A., Otberg, N., & Sterry, W. (2006). Hair follicles - a long-term reservoir for drug delivery. *Skin Pharmacology and Physiology*, *19*(4), 232–6.
- Lademann, J., Richter, H., Schanzer, S., Knorr, F., Meinke, M., Sterry, W., & Patzelt, A. (2011). Penetration and storage of particles in human skin: perspectives and safety aspects. *European Journal of Pharmaceutics and Biopharmaceutics*, *77*(3), 465–8.
- Lane, M. E., Santos, P., Watkinson, A. C., & Hadgraft, J. (2012). Passive Skin Permeation Enhancement. In H. A. E. Benson & A. C. Watkinson. (Eds.), *Topical and Transdermal Drug Delivery: Principles and Practice* (pp. 23–42). Singapore: John Wiley & Sons Inc.
- Lauer, A. C., Ramachandran, C., Lieb, L. M., Niemiec, S., & Weiner, N. D. (1996). Targeted delivery to the pilosebaceous unit via liposomes. *Advanced Drug Delivery Reviews*, *18*(3), 311–324.

- Lavker, R. M., Sun, T.-T., Oshima, H., Barrandon, Y., Akiyama, M., Ferraris, C., ... Christiano, A. M. (2003). Hair follicle stem cells. *The Journal of Investigative Dermatology. Symposium Proceedings*, 8(1), 28–38.
- Lavon, I., & Kost, J. (2004). Ultrasound and transdermal drug delivery. *Drug Discovery Today*, 9(15), 670–6.
- Lawson, E. E., Anigbogu, A. N., Williams, A. C., Barry, B. W., & Edwards, H. G. (1998). Thermally induced molecular disorder in human stratum corneum lipids compared with a model phospholipid system; FT-Raman spectroscopy. *Spectrochimica Acta. Part A, Molecular and Biomolecular Spectroscopy*, 54A(3), 543–58.
- Layton, A. (2009). The use of isotretinoin in acne. *Dermato-Endocrinology*, 1(3), 162–9.
- Lee, C. K., Uchida, T., Noguchi, E., Kim, N. S., Goto, S., Bener, B., ... Potts, R. O. (1993). Skin permeation enhancement of tegafur by ethanol/panasate 800 or ethanol/water binary vehicle and combined effect of fatty acids and fatty alcohols. *Journal of Pharmaceutical Sciences*, 82(11), 1155–9.
- Lee, F. W., Earl, L., & Williams, F. M. (2001). Interindividual variability in the percutaneous penetration of testosterone through human skin in vitro. *Toxicology*, 168(1), 63.
- Lee, W., Shen, S., Wang, K., Hu, C., & Fang, J. (2002). The Effect of Laser Treatment on Skin to Enhance and Control Transdermal Delivery of 5-Fluorouracil. *Journal of Pharmaceutical Sciences*, 91(7), 1613–1626.
- Lehman, P. A., Slattery, J. T., & Franz, T. J. (1988). Percutaneous absorption of retinoids: influence of vehicle, light exposure, and dose. *The Journal of Investigative Dermatology*, 91(1), 56–61.
- Leopold, C. S., & Maibach, H. I. (1996). Effect of lipophilic vehicles on in vivo skin penetration of methyl nicotinate in different races. *International Journal of Pharmaceutics*, 139(1–2), 161–167.
- Letawe, C., Boone, M., & Pierard, G. E. (1998). Digital image analysis of the effect of topically applied

- linoleic acid on acne microcomedones. *Clinical and Experimental Dermatology*, 23, 56–58.
- Liang, Y., Denton, M. B., & Bates, R. B. (1998). Stability studies of tetracycline in methanol solution. *Journal of Chromatography. A*, 827(1), 45–55.
- Lieb, L. M., Liimatta, A. P., Bryan, R. N., Brown, B. D., & Krueger, G. G. (1997). Description of the intrafollicular delivery of large molecular weight molecules to follicles of human scalp skin in vitro. *Journal of Pharmaceutical Sciences*, 86(9), 1022–9.
- Lindeque, B. G. P., Shuler, F. D., & Bates, C. M. (2013). Skin Temperatures Generated Following Plaster Splint Application. *Orthopedics*, 36(5), 364–367.
- Loftsson, T., Hreinsdóttir, D., & Másson, M. (2005). Evaluation of cyclodextrin solubilization of drugs. *International Journal of Pharmaceutics*, 302(1), 18–28.
- Loftsson, T., Somogyi, G., & Bodor, N. (1989). Effect of choline esters and oleic acid on the penetration of acyclovir, estradiol, hydrocortisone, nitroglycerin, retinoic acid and trifluorothymidine across hairless mouse skin in vitro. *Acta Pharmaceutica Nordica*, 1(5), 279–286.
- Longsworth, L. (1954). Temperature Dependence of Diffusion In Aqueous solutions. *Journal of Physical Chemistry*, 58(9), 770–773.
- Lopez-Castellano, A., & Merino, V. (2010). Chemical Enhancers. In J. J. Escobar-Chávez & V. Merino (Eds.), *Current Technologies to Increase the Transdermal Delivery of Drugs* (pp. 23–40). Mexico: Bentham e Books.
- Lotte, C., Wester, R. C., Rougier, A., & Maibach, H. I. (1993). Racial differences in the in vivo percutaneous absorption of some organic compounds: a comparison between black, Caucasian and Asian subjects. *Archives of Dermatological Research*, 284(8), 456–9.
- Lu, G. U., Ciotti, S. N., Valiveti, S., Grice, J. E., & Cross, S. E. (2008). Targeting the pilosebaceous gland. In K. A. Walters & M. S. Roberts (Eds.), *Dermatologic, Cosmeceutic, and Cosmetic Development*:

- Therapeutic and Novel Approaches* (pp. 169–188). New York: Informa Healthcare.
- Madheswaran, T., Baskaran, R., Yong, C. S., & Yoo, B. K. (2014). Enhanced topical delivery of finasteride using glyceryl monooleate-based liquid crystalline nanoparticles stabilized by cremophor surfactants. *AAPS PharmSciTech*, *15*(1), 44–51.
- Maghraby, G. M. M. El, Williams, A. C., & Barry, B. W. (2001). Skin hydration and possible shunt route penetration in controlled estradiol delivery from ultradeformable and standard liposomes. *Journal of Pharmacy and Pharmacology*, *53*(10), 1311–1322.
- Maibach, H. I., Feldman, R. J., Milby, T. H., & Serat, W. F. (1971). Regional variation in percutaneous penetration in man. Pesticides. *Archives of Environmental Health*, *23*(3), 208–11.
- Mancini, A. J. (2008). Incidence, prevalence, and pathophysiology of acne. *John Hopkins Advance Studies in Medicine*, *8*(4), 100–105.
- McAuley, W. J., & Caserta, F. (2015). Film-forming and Heated Systems. In R. F. Donnelly & T. R. R. Singh (Eds.), *Novel Delivery Systems for Transdermal and Intradermal Drug Delivery* (pp. 97–124). Chichester, UK: John Wiley & Sons, Ltd.
- McAuley, W. J., Oliveira, G., Mohammed, D., Beezer, A. E., Hadgraft, J., & Lane, M. E. (2010). Thermodynamic considerations of solvent/enhancer uptake into a model membrane. *International Journal of Pharmaceutics*, *396*(1–2), 134–9.
- Medicines.org.uk. (2017). Isotrex Gel - Summary of Product Characteristics (SPC) - (eMC). Retrieved from <https://www.medicines.org.uk/emc/medicine/7503>
- Megrab, N. A., Williams, A. C., & Barry, B. W. (1995). Oestradiol permeation across human skin, silastic and snake skin membranes: The effects of ethanol/water co-solvent systems. *International Journal of Pharmaceutics*, *116*(1), 101–112.
- Meidan, V. M., Bonner, M. C., & Michniak, B. B. (2005). Transfollicular drug delivery--is it a reality?

- International Journal of Pharmaceutics*, 306(1–2), 1–14.
- Meidan, V. M., Docker, M., Walmsley, A. D., & Irwin, W. J. (1998). Low Intensity Ultrasound as a Probe to Elucidate the Relative Follicular Contribution to Total Transdermal Absorption. *Pharmaceutical Research*, 15(1), 85–92.
- Melvin, M., Noseworthy, B., & Spiegel, J. . (1962, March 20). Thioglycerol and formaldehyde sulfoxylate stabilized tetracycline antibiotics in polyhydric alcohol solvents. United States of America: United States Patent.
- Menon, G. K. (2002). New insights into skin structure: scratching the surface. *Advanced Drug Delivery Reviews*, 54(Suppl 1), S3-17.
- Merino, V., & Lopez, A. (2010). Transdermal Iontophoresis. In J. J. Escobar-Chávez (Ed.), *Current Technologies to Increase the Transdermal Delivery of Drugs* (pp. 41–52). Sharjah: Bentham Science Publishers.
- Michel, C., Purmann, T., Mentrup, E., Seiller, E., & Kreuter, J. (1992). Effect of liposomes on percutaneous penetration of lipophilic materials. *International Journal of Pharmaceutics*, 84(2), 93–105.
- Millar, S. E. (2002). Molecular Mechanisms Regulating Hair Follicle Development. *Journal of Investigative Dermatology*, 118(2), 216–225.
- Milstone, L. M. (2004). Epidermal desquamation. *Journal of Dermatological Science*, 36(3), 131–140.
- Moldoveanu, Șerban., & David, V. (2013). *Essentials in modern HPLC separations*. New York: Elsevier.
- Møllgaard, B., & Hoelgaard, A. (1983). Vehicle effect on topical drug delivery. II. Concurrent skin transport of drugs and vehicle components. *Acta Pharmaceutica Suecica*, 20(6), 443–50.
- Monselise, A., Cohen, D. E., Wanser, R., & Shapiro, J. (2015). What ages hair? *International Journal of*

- Women's Dermatology*, 1(4), 161–166.
- Montagna, W., & Ellis, R. (1958). The Vascularity and Innervation of Human Hair Follicles. In W. Montagna & R. Ellis (Eds.), *The Biology of Hair Growth* (pp. 219–227). New York: Academic Press Inc.
- Moritz, A. R., & Henriques, F. C. (1947). Studies of Thermal Injury.II. The Relative Importance of Time and Surface Temperature in the Causation of Cutaneous Burns. *The American Journal of Pathology*, 23(5), 695–720.
- Moser, K., Kriwet, K., Kalia, Y. N., & Guy, R. H. (2001). Enhanced skin permeation of a lipophilic drug using supersaturated formulations. *Journal of Controlled Release*, 73(2–3), 245–53.
- Moser, K., Kriwet, K., Naik, A., Kalia, Y. N., & Guy, R. H. (2001). Passive skin penetration enhancement and its quantification in vitro. *European Journal of Pharmaceutics and Biopharmaceutics*, 52(2), 103–112.
- Motwani, M. R., Rhein, L. D., & Zatz, J. L. (2002). Influence of vehicles on the phase transitions of model sebum. *Journal of Cosmetic Science*, 53(1), 35–42.
- Motwani, M. R., Rhein, L. D., & Zatz, J. L. (2004). Deposition of salicylic acid into hamster sebaceous glands. *Journal of Cosmetic Science*, 55(6), 519–531.
- Nadler, S. F., Steiner, D. J., Erasala, G. N., Hengehold, D. a, Hinkle, R. T., Beth Goodale, M., ... Weingand, K. W. (2002). Continuous low-level heat wrap therapy provides more efficacy than Ibuprofen and acetaminophen for acute low back pain. *Spine*, 27(10), 1012–7.
- Nadler, S. F., Steiner, D. J., Petty, S. R., Erasala, G. N., Hengehold, D. a, & Weingand, K. W. (2003). Overnight use of continuous low-level heatwrap therapy for relief of low back pain. *Archives of Physical Medicine and Rehabilitation*, 84(3), 335–42.
- Nankervis, R., Davis, S. S., Day, N. H., & Shaw, P. N. (1995). Effect of lipid vehicle on the intestinal

- lymphatic transport of isotretinoin in the rat. *International Journal of Pharmaceutics*, 119(2), 173–181.
- Narayanasamy Kanikkannan, R. J. B., & Singh, M. (2005). Structure-Activity Relationship of Chemical Penetration Enhancers. In E. W. Smith & H. I. Maibach (Eds.), *Percutaneous Penetration Enhancers* (2nd ed., pp. 17–34). CRC Press.
- Nast, A., Dréno, B., Bettoli, V., Bukvic Mokos, Z., Degitz, K., Dressler, C., ... Gollnick, H. (2016). *S3-Guideline for the Treatment of Acne (Update 2016)*. Berlin.
- Nayak, A. K., Mohanty, B., & Sen, K. K. (2010). Comparative evaluation of in vitro diclofenac sodium permeability across excised mouse skin from different common pharmaceutical vehicles. *International Journal of PharmTech Research*, 2(1).
- Novák-Pékli, M., el-Hadi Mesbah, M., & Pethó, G. (1996). Equilibrium studies on tetracycline-metal ion systems. *Journal of Pharmaceutical and Biomedical Analysis*, 14(8–10), 1025–9.
- Ochsendorf, F. (2010). Minocycline in Acne Vulgaris: Benefits and Risks. *American Journal of Clinical Dermatology*, 11(5), 327–341.
- OECD. (2004a). *OECD Guidance Document for the Conduct of Skin Absorption Studies*. Organisation for Economic Co-operation and Development.
- OECD. (2004b). *OECD Guidelines for the Testing of Chemicals. Skin Absorption: In Vitro Method 428*. Organisation for Economic Co-operation and Development.
- Ogiso, T., & Shintani, M. (1990). Mechanism for the enhancement effect of fatty acids on the percutaneous absorption of propranolol. *Journal of Pharmaceutical Sciences*, 79(12), 1065–71.
- Ogiso, T., Shiraki, T., Okajima, K., Tanino, T., Iwaki, M., & Wada, T. (2002). Transfollicular drug delivery: penetration of drugs through human scalp skin and comparison of penetration between scalp and abdominal skins in vitro. *Journal of Drug Targeting*, 10(5), 369–78.

- Ogura, M., Paliwal, S., & Mitragotri, S. (2008). Low-frequency sonophoresis: current status and future prospects. *Advanced Drug Delivery Reviews*, *60*(10), 1218–23.
- Olatunji, O., Al-Qallaf, B., & Das, D. B. (2010). Transdermal Drug Delivery Using Microneedles. In J. J. Escobar-Chávez (Ed.), *Current Technologies to Increase the Transdermal Delivery of Drugs* (pp. 96–119). Sharjah: Bentham Science Publishers.
- Oliveira, G., Beezer, A. E., Hadgraft, J., & Lane, M. E. (2010). Alcohol enhanced permeation in model membranes. Part I. Thermodynamic and kinetic analyses of membrane permeation. *International Journal of Pharmaceutics*, *393*(1–2), 61–7.
- Oliveira, G., Hadgraft, J., & Lane, M. E. (2012). The influence of volatile solvents on transport across model membranes and human skin. *International Journal of Pharmaceutics*, *435*(1), 38–49.
- Oliveira, G., Leverett, J. C., Emamzadeh, M., & Lane, M. E. (2014). The effects of heat on skin barrier function and in vivo dermal absorption. *International Journal of Pharmaceutics*, *464*(1–2), 145–51.
- Orth, P., Saenger, W., & Hinrichs, W. (1999). Tetracycline-Chelated Mg<sup>2+</sup> Ion Initiates Helix Unwinding in Tet Repressor Induction. *Biochemistry*, *38*(1), 191–198.
- Otberg, N., Patzelt, A., Rasulev, U., Hagemeister, T., Linscheid, M., Sinkgraven, R., ... Lademann, J. (2008). The role of hair follicles in the percutaneous absorption of caffeine. *British Journal of Clinical Pharmacology*, *65*(4), 488–492.
- Otberg, N., Richter, H., Schaefer, H., Blume-Peytavi, U., Sterry, W., & Lademann, J. (2004). Variations of hair follicle size and distribution in different body sites. *The Journal of Investigative Dermatology*, *122*(1), 14–9.
- Otto, D., & Villiers, M. (2013). The Experimental Evaluation and Molecular Dynamics Simulation of a Heat-Enhanced Transdermal Delivery System. *AAPS PharmSciTech*, *14*(1), 111–120.

- Ousler III, G. ., Chapin, M. ., Abelson, M. ., & Shapiro, A. (2012, April 19). Ophthalmic Formulations, Methods Of Manufacture And Methods of Normalizing Meibomian Gland Secretions. United States of America: United States Patent.
- Park, J.-H., Lee, J.-W., Kim, Y.-C., & Prausnitz, M. R. (2008). The effect of heat on skin permeability. *International Journal of Pharmaceutics*, 359(1–2), 94–103.
- Parks, L., Balkrishnan, R., Hamel-Gariépy, L., & Feldman, S. R. (2003). The importance of skin disease as assessed by “willingness-to-pay”. *Journal of Cutaneous Medicine and Surgery*, 7(5), 369–71.
- Pattnaik, S., Swain, K., Rao, J. V., Varun, T., & Mallick, S. (2015). Temperature influencing permeation pattern of alfuzosin: An investigation using DoE. *Medicina*, 51(4), 253–261.
- Patzelt, A., Knorr, F., Blume-Peytavi, U., Sterry, W., & Lademann, J. (2008). Hair follicles, their disorders and their opportunities. *Drug Discovery Today: Disease Mechanisms*, 5(2), e173–e181.
- Patzelt, A., & Lademann, J. (2013). Drug delivery to hair follicles. *Expert Opinion on Drug Delivery*, 10(6), 787–97.
- Patzelt, A., Richter, H., Buettemeyer, R., Huber, H. J. R., Blume-Peytavi, U., Sterry, W., & Lademann, J. (2008). Differential stripping demonstrates a significant reduction of the hair follicle reservoir in vitro compared to in vivo. *European Journal of Pharmaceutics and Biopharmaceutics*, 70(1), 234–8.
- Patzelt, A., Richter, H., Knorr, F., Schäfer, U., Lehr, C.-M., Dähne, L., ... Lademann, J. (2011). Selective follicular targeting by modification of the particle sizes. *Journal of Controlled Release*, 150(1), 45–8.
- Pawelczyk, E., & Matlak, B. (1982). Kinetics of drug decomposition. Part 74. Kinetics of degradation of minocycline in aqueous solution. *Polish Journal of Pharmacology and Pharmacy*, 74(34), 409–421.

- Peck, K. D., Ghanem, A.-H., & Higuchi, W. I. (1995). The effect of temperature upon the permeation of polar and ionic solutes through human epidermal membrane. *Journal of Pharmaceutical Sciences*, *84*(8), 975–982.
- Pellett, M., Davis, A., & Hadgraft, J. (1994). Effect of supersaturation on membrane transport: 2. Piroxicam. *International Journal of Pharmaceutics*, *111*(1), 1–6.
- Pendlington, R. (2008). In Vitro Percutaneous Absorption Measurements. In R. P. Chilcott & S. Price (Eds.), *Principles and practice of skin toxicology* (pp. 129–148). Singapore: John Wiley & Sons.
- Perumal, O., Murthy, S. N., & Kalia, Y. N. (2013). Turning theory into practice: the development of modern transdermal drug delivery systems and future trends. *Skin Pharmacology and Physiology*, *26*(4–6), 331–42.
- Piccariello, T. (2013, July 18). Metal coordinated compositions. United States of America: United States Patent.
- Plewig, G. (1974). Acne vulgaris: proliferative cells in sebaceous glands. *British Journal of Dermatology*, *90*(6), 623–630.
- Poblet, E., Ortega, F., & Jiménez, F. (2002). The arrector pili muscle and the follicular unit of the scalp: a microscopic anatomy study. *Dermatologic Surgery*, *28*(9), 800–3.
- Pochi, P. E., & Strauss, J. S. (1964). Sebum Production, Casual Sebum Levels, Titratable Acidity of Sebum, and Urinary Fractional 17-Ketosteroid Excretion in Males With Acne. *The Journal of Investigative Dermatology*, *43*, 383–388.
- Pongjanyakul, T., & Puttipipatkachorn, S. (2007). Sodium alginate-magnesium aluminum silicate composite gels: Characterization of flow behavior, microviscosity, and drug diffusivity. *AAPS PharmSciTech*, *8*(3), E158–E165.
- Potts, R. O., & Francoeur, M. L. (1990). Lipid biophysics of water loss through the skin. *Proceedings of*

- the National Academy of Sciences of the United States of America*, 87(10), 3871–3.
- Potts, R. O., & Francoeur, M. L. (1991). The influence of stratum corneum morphology on water permeability. *The Journal of Investigative Dermatology*, 96(4), 495–9.
- Potts, R. O., & Guy, R. H. (1992). Predicting Skin Permeability. *Pharmaceutical Research*, 9(5), 663–669.
- Prausnitz, M. R., Mikszta, J. A., Cormier, M., & Andrianov, A. K. (2009). Microneedle-based vaccines. *Current Topics in Microbiology and Immunology*, 333, 369–93.
- Proksch, E., Fölster-Holst, R., & Jensen, J.-M. (2006). Skin barrier function, epidermal proliferation and differentiation in eczema. *Journal of Dermatological Science*, 43(3), 159–169.
- Pugh, W. J. (2001). Relationship between H-bonding of penetrants to stratum corneum lipids and diffusion. *Journal of Toxicology: Cutaneous and Ocular Toxicology*, 20(2–3), 303–317.
- Queille-Roussel, C., Poncet, M., Mesaros, S., Clucas, A., Baker, M., & Soloff, A.-M. (2001). Comparison of the cumulative irritation potential of adapalene gel and cream with that of erythromycin/tretinoin solution and gel and erythromycin/isotretinoin gel. *Clinical Therapeutics*, 23(2), 205–212.
- Quinn, H. L., Courtenay, A. J., Kearney, M.-C., & Donnelly, R. F. (2015). Microneedle Technology. In R. F. Donnelly & T. R. R. Singh (Eds.), *Novel Delivery Systems for Transdermal and Intradermal Drug Delivery* (pp. 179–208). Chichester, UK: John Wiley & Sons, Ltd.
- Raber, A. S., Mittal, A., Schäfer, J., Bakowsky, U., Reichrath, J., Vogt, T., ... Lehr, C.-M. (2014). Quantification of nanoparticle uptake into hair follicles in pig ear and human forearm. *Journal of Controlled Release*, 179, 25–32.
- Rafiee-Tehrani, M., & Mehramizi, A. (2000). In Vitro Release Studies of Piroxicam from Oil-in-Water Creams and Hydroalcoholic Gel Topical Formulations. *Drug Development and Industrial*

- Pharmacy*, 26(4), 409–414.
- Raleigh, G., Rivard, R., & Fabus, S. (2005). Air-activated chemical warming devices: effects of oxygen and pressure. *Undersea & Hyperbaric Medicine : Journal of the Undersea and Hyperbaric Medical Society, Inc*, 32(6), 445–9.
- Rapp, S. R., Feldman, S. R., Exum, M. L., Fleischer, A. B., & Reboussin, D. M. (1999). Psoriasis causes as much disability as other major medical diseases. *Journal of the American Academy of Dermatology*, 41(3 Pt 1), 401–7.
- Rastogi, R., Anand, S., Dinda, A. K., & Koul, V. (2010). Investigation on the synergistic effect of a combination of chemical enhancers and modulated iontophoresis for transdermal delivery of insulin. *Drug Development and Industrial Pharmacy*, 36(8), 993–1004.
- Rebora, A. (2004). Pathogenesis of androgenetic alopecia. *Journal of the American Academy of Dermatology*, 50(5), 777–9.
- Redasani, V. K., & Bari, S. B. (2015). Approaches for Prodrugs. In *Prodrug Design: Perspectives, Approaches and Applications in Medicinal Chemistry* (pp. 33–48). New York: Academic Press.
- Reid, M. L., Benaouda, F., Khengar, R., Jones, S. a, & Brown, M. B. (2013). Topical corticosteroid delivery into human skin using hydrofluoroalkane metered dose aerosol sprays. *International Journal of Pharmaceutics*, 452(1–2), 157–65.
- Reid, M. L., Jones, S. A., & Brown, M. B. (2009). Transient drug supersaturation kinetics of beclomethasone dipropionate in rapidly drying films. *International Journal of Pharmaceutics*, 371(1–2), 114–9.
- Renny, J. S., Tomasevich, L. L., Tallmadge, E. H., & Collum, D. B. (2013). Method of continuous variations: applications of job plots to the study of molecular associations in organometallic chemistry. *Angewandte Chemie (International Ed. in English)*, 52(46), 11998–2013.

- Ribaud, C., Garson, J. C., Doucet, J., & Lévêque, J. L. (1994). Organization of stratum corneum lipids in relation to permeability: influence of sodium lauryl sulfate and preheating. *Pharmaceutical Research*, *11*(10), 1414–8.
- Ritter, L., & Suffern, N. . (1992, June). Stable, cosmetically acceptable topical gel formulation and method of treatment for acne. United States of America: United States Patent.
- Riviere, J. E. (2011). Absorption. In J. E. Riviere (Ed.), *Comparative Pharmacokinetics* (pp. 39–71). Wiley-Blackwell.
- Roberts, M. S., & Cross, S. E. (2002). Dermatological and Transdermal Formulations. In K. A. Walters (Ed.), *Skin Transport* (pp. 89–195). New York: Marcel Dekker Inc.
- Roberts, M. S., Favretto, W. A., Meyer, A., Reckmann, M., & Wongseelashote, T. (1982). Topical Bioavailability of Mrthyl Salicylate. *Australian and New Zealand Journal of Medicine*, *12*(3), 303–304.
- Roberts, M. S., Pugh, W. J., & Hadgraft, J. (1996). Epidermal permeability: Penetrant structure relationships. 2. The effect of h-bonding groups in penetrants on their diffusion through the stratum corneum. *International Journal of Pharmaceutics*, *132*(1–2), 23–32.
- Roberts, M. S., & Walker, M. (1993). The Most Natural Penetration Enhancer. In K. A. Walters & J. Hadgraft (Eds.), *Pharmaceutical Skin Penetration Enhancement* (pp. 1–30). New York: Marcel Dekker.
- Roskos, K. V, Maibach, H. I., & Guy, R. H. (1989). The effect of aging on percutaneous absorption in man. *Journal of Pharmacokinetics and Biopharmaceutics*, *17*(6), 617–30.
- Rougier, A., Lotte, C., Corcuff, P., & Maibach, H. (1988). Relationship between skin permeability and corneocyte size according to anatomic site, age, and sex in man. *Journal of the Society of Cosmetic Chemists*, *39*(1), 15–26.

- Roy, S. D., & Flynn, G. L. (1990). Transdermal delivery of narcotic analgesics: pH, anatomical, and subject influences on cutaneous permeability of fentanyl and sufentanil. *Pharmaceutical Research*, 7(8), 842–7.
- Ryan, C. A., Gerberick, G. F., & Kern, P. S. (2010). Skin Sensitization. In N. A. Monteiro-Riviere (Ed.), *Toxicology of the Skin* (pp. 192–202). New York: Informa Healthcare.
- Saar, B. G., Contreras-Rojas, L. R., Xie, X. S., & Guy, R. H. (2011). Imaging drug delivery to skin with stimulated Raman scattering microscopy. *Molecular Pharmaceutics*, 8(3), 969–75.
- Saboury, A. A. (2006). A review on the ligand binding studies by isothermal titration calorimetry. *Journal of the Iranian Chemical Society*, 3(1), 1–21.
- Sakaguchi, T., Toma, M., Yoshida, T., Omura, H., & Takasu, H. (1958). Metal Chelate Compounds with Tetracycline Derivatives. VII. : The Structure of Tetracycline Chelates. *Chemical & Pharmaceutical Bulletin*, 6(1), 1–9.
- Salman, M., Angel, A., & Swaminathan, V. (2014, May 29). Tetracycline topical formulations, preparation and uses thereof. United States of America: United States Patent.
- Sampogna, F., Tabolli, S., & Abeni, D. (2013). Impact of different skin conditions on quality of life. *Giornale Italiano Di Dermatologia E Venereologia*, 148(3), 255–261.
- Sansone, G., & Reisner, R. M. (1971). Differential rates of conversion of testosterone to dihydrotestosterone in acne and in normal human skin. A possible pathogenic factor in acne. *The Journal of Investigative Dermatology*.
- Sarheed, O., & Frum, Y. (2012). Use of the skin sandwich technique to probe the role of the hair follicles in sonophoresis. *International Journal of Pharmaceutics*, 43(2), 179–183.
- Sato, K., Sugibayashi, K., & Morimoto, Y. (1988). Effect and mode of action of aliphatic esters on the in vitro skin permeation of nicorandil. *International Journal of Pharmaceutics*, 43(1), 31–40.

- Sawyer, J., Febraro, S., Masud, S., Ashburn, M. a., & Campbell, J. C. (2009). Heated lidocaine/tetracaine patch (Synera™, Rapydan™) compared with lidocaine/prilocaine cream (EMLA®) for topical anaesthesia before vascular access. *British Journal of Anaesthesia*, *102*(2), 210–215.
- Schaefer, H., & Lademann, J. (2001). The role of follicular penetration. A differential view. *Skin Pharmacology and Applied Skin Physiology*, *14 Suppl 1*, 23–7.
- Schaefer, H., & Redelmeier, T. E. (1996). *Skin barrier : principles of percutaneous absorption*. Karger.
- Scheuplein, R. J. (1967). Mechanism of Percutaneous Absorption. II. Transient diffusion and the relative importance of various routes of skin penetration. *Journal of Investigative Dermatology*, *48*(1), 79–88.
- Scheuplin, R., & Blank, I. H. (1971). Permeability of the skin. *Physiological Reviews*, *51*(4), 702–47.
- Schmitt, M. O., & Schneider, S. (2000). Spectroscopic investigation of complexation between various tetracyclines and Mg<sup>2+</sup> or Ca<sup>2+</sup>. *PhysChemComm*, *3*(9), 42–55.
- Schoellhammer, C. M., Blankschtein, D., & Langer, R. (2014). Skin permeabilization for transdermal drug delivery: recent advances and future prospects. *Expert Opinion on Drug Delivery*, *11*(3), 393–407.
- Schofield, J., Grindlay, D., & Williams, H. (2009). Skin conditions in the UK : a health care needs assessment. Centre of Evidence Based Dermatology, University of Nottingham.
- Scott, R. C., & Ramsey, J. D. (1987). Comparison of the In Vivo and In Vitro Percutaneous Absorption of a Lipophilic Molecule (Cypermethrin, a Pyrethroid Insecticide). *Journal of Investigative Dermatology*, *89*(2), 142–146.
- Seidler, A. M., Bayoumi, A. M., Goldstein, M. K., Cruz, P. D., & Chen, S. C. (2012). Willingness to pay in dermatology: assessment of the burden of skin diseases. *The Journal of Investigative*

- Dermatology*, 132(7), 1785–90.
- Shabir, G. A. (2003). Validation of high-performance liquid chromatography methods for pharmaceutical analysis Understanding the differences and similarities between validation requirements of the US Food and Drug Administration, the US Pharmacopeia and the International Confe. *Journal of Chromatography A*, 987(1–2), 57–66.
- Shahzad, Y., Louw, R., Gerber, M., & du Plessis, J. (2015). Breaching the skin barrier through temperature modulations. *Journal of Controlled Release*, 202, 1–13.
- Shinjita, D., & Reynolds, R. (2013). Acne Pathophysiology. In J. A. Zeichner (Ed.), *Acneiform Eruptions in Dermatology : A Differential Diagnosis* (pp. 3–12). New York: Springer Berlin Heidelberg.
- Shomaker, T. S., Zhang, J., & Ashburn, M. a. (2000). Assessing the impact of heat on the systemic delivery of fentanyl through the transdermal fentanyl delivery system. *Pain Medicine (Malden, Mass.)*, 1(3), 225–30.
- Singh, S., & Singh, J. (1993). Transdermal drug delivery by passive diffusion and iontophoresis: a review. *Medicinal Research Reviews*, 13(5), 569–621.
- Sintov, A., Serafimovich, S., & Gilhar, A. (2000). New topical antiandrogenic formulations can stimulate hair growth in human bald scalp grafted onto mice. *International Journal of Pharmaceutics*, 194(1), 125–34.
- Sloan, K. B. (1989). Prodrugs for dermal delivery. *Advanced Drug Delivery Reviews*, 3(1), 67–101.
- Smith, E. W., & Maibach, H. I. (Eds.). (2006). Percutaneous Penetration Enhancers. In *Percutaneous penetration enhancers* (2nd ed.). United States of America: CRC Press.
- Smith, N. B. (2007). Perspectives on transdermal ultrasound mediated drug delivery. *International Journal of Nanomedicine*, 2(4), 585–94.

- Southwell, D., & Barry, B. W. (1983). Penetration enhancers for human skin: mode of action of 2-pyrrolidone and dimethylformamide on partition and diffusion of model compounds water, n-alcohols, and caffeine. *The Journal of Investigative Dermatology*, *80*(6), 507–14.
- Southwell, D., Barry, B. W., & Woodford, R. (1984). Variations in permeability of human skin within and between specimens. *International Journal of Pharmaceutics*, *18*(3), 299–309.
- Sperling, L. C. (1991). Hair anatomy for the clinician. *Journal of the American Academy of Dermatology*, *25*(1 Pt 1), 1–17.
- Squier, C. A, Cox, P., & Wertz, P. W. (1991). Lipid content and water permeability of skin and oral mucosa. *The Journal of Investigative Dermatology*, *96*(1), 123–6.
- Stanely, T., Hull, W., & Rigby, L. (2001). Transdermal drug patch with attached pocket for controlled heating device. United States: United States Patent.
- Stathakis, V., Kilkenny, M., & Marks, R. (1997). Descriptive epidemiology of acne vulgaris in the community. *The Australasian Journal of Dermatology*, *38*(3), 115–123.
- Surber, C., Schwarb, F. P., & Smith, E. (2005). Tape-Stripping Technique. In H. I. Bronaugh, Robert L; Maibach (Ed.), *Percutaneous absorption: drugs, cosmetics, mechanisms, methods* (pp. 395–410). New York: Marcel Dekker, Inc.
- Swarbrick, J., Lee, G., Brom, J., & Gensmantel, N. P. (1984). Drug permeation through human skin II: Permeability of ionizable compounds. *Journal of Pharmaceutical Sciences*, *73*(10), 1352–1355.
- Sweeney, T. M., & Downing, D. T. (1970). The role of lipids in the epidermal barrier to water diffusion. *The Journal of Investigative Dermatology*, *55*(2), 135–40.
- Tabbakhian, M., Tavakoli, N., Jaafari, M. R., & Daneshamouz, S. (2006). Enhancement of follicular delivery of finasteride by liposomes and niosomes 1. In vitro permeation and in vivo deposition studies using hamster flank and ear models. *International Journal of Pharmaceutics*, *323*(1–2),

1–10.

Takahashi, K., Sakano, H., Numata, N., Kuroda, S., & Mizuno, N. (2002a). Effect of Fatty Acid Diesters on Permeation of Anti-Inflammatory Drugs Through Rat Skin. *Drug Development and Industrial Pharmacy*, 28(10), 1285–1294.

Takahashi, K., Sakano, H., Numata, N., Kuroda, S., & Mizuno, N. (2002b). Effect of Fatty Acid Diesters on Permeation of Anti-Inflammatory Drugs Through Rat Skin. *Drug Development and Industrial Pharmacy*, 28(10), 1285–1294.

Tan, J. K. L., & Bhate, K. (2015). A global perspective on the epidemiology of acne. *British Journal of Dermatology*, 172(1), 3–12.

Teichmann, A., Jacobi, U., Ossadnik, M., Richter, H., Koch, S., Sterry, W., & Lademann, J. (2005). Differential stripping: determination of the amount of topically applied substances penetrated into the hair follicles. *The Journal of Investigative Dermatology*, 125(2), 264–9.

Teichmann, A., Ossadnik, M., Richter, H., Sterry, W., & Lademann, J. (2006). Semiquantitative determination of the penetration of a fluorescent hydrogel formulation into the hair follicle with and without follicular closure by microparticles by means of differential stripping. *Skin Pharmacology and Physiology*, 19(2), 101–5.

Thiboutot, D. (2001). Hormones and acne: pathophysiology, clinical evaluation, and therapies. *Seminars in Cutaneous Medicine and Surgery*, 20(3), 144–53.

Tongaree, S., Flanagan, D. R., & Poust, R. I. (1999). The Interaction Between Oxytetracycline and Divalent Metal Ions in Aqueous and Mixed Solvent Systems. *Pharmaceutical Development and Technology*, 4(4), 581–591.

Tongaree, S., Goldberg, A. M., Flanagan, D. R., & Poust, R. I. (2000). The effects of pH and PEG 400-water cosolvents on oxytetracycline-magnesium complex formation and stability.

- Pharmaceutical Development and Technology*, 5(2), 189–99.
- Traish, A. M., Melcangi, R. C., Bortolato, M., Garcia-Segura, L. M., & Zitzmann, M. (2015). Adverse effects of 5 $\alpha$ -reductase inhibitors: What do we know, don't know, and need to know? *Reviews in Endocrine and Metabolic Disorders*, 16(3), 177–198.
- Trottet, L., Merly, C., Mirza, M., Hadgraft, J., & Davis, A. . (2004). Effect of finite doses of propylene glycol on enhancement of in vitro percutaneous permeation of loperamide hydrochloride. *International Journal of Pharmaceutics*, 274(1–2), 213–219.
- Trüeb, R. M. (2002). Molecular mechanisms of androgenetic alopecia. *Experimental Gerontology*, 37(8–9), 981–90.
- Tsai, J. C., Flynn, G. L., Weiner, N. D., Cappel, M. J., Kreuter, J., & Ferry, J. J. (1992). Drug and Vehicle Deposition from Topical Applications: Use of In Vitro Mass Balance Technique with Minoxidil Solutions. *Journal of Pharmaceutical Sciences*, 81(8), 736–743.
- Tschan, T., Steffen, H., & Supersaxo, A. (1997). Sebaceous-gland deposition of isotretinoin after topical application: an in vitro study using human facial skin. *Skin Pharmacology*, 10(3), 126–34.
- Tuntiyasawasdikul, S., Limpongsa, E., Jaipakdee, N., & Sripanidkulchai, B. (2014). Transdermal permeation of Kaempferia parviflora methoxyflavones from isopropyl myristate-based vehicles. *AAPS PharmSciTech*, 15(4), 947–55.
- Turner, D. L., Ford, W. R., Kidd, E. J., Broadley, K. J., & Powell, C. (2017). Effects of nebulised magnesium sulphate on inflammation and function of the guinea-pig airway. *European Journal of Pharmacology*, 801, 79–85.
- Twist, J. N., & Zatz, J. L. (1988). Membrane–solvent–solute interaction in a model permeation system. *Journal of Pharmaceutical Sciences*, 77(6), 536–540.

- Tyle, P., & Agrawala, P. (1989). Drug delivery by phonophoresis. *Pharmaceutical Research*, 6(5), 355–61.
- Unger, W. P., & Unger, R. H. (2003). Hair transplanting: an important but often forgotten treatment for female pattern hair loss. *Journal of the American Academy of Dermatology*, 49(5), 853–860.
- van de Sandt, J. J. M., van Burgsteden, J. A., Cage, S., Carmichael, P. L., Dick, I., Kenyon, S., ... Williams, F. M. (2004). In vitro predictions of skin absorption of caffeine, testosterone, and benzoic acid: a multi-centre comparison study. *Regulatory Toxicology and Pharmacology*, 39(3), 271–81.
- van Eden, W., van der Zee, R., & Prakken, B. (2005). Heat-shock proteins induce T-cell regulation of chronic inflammation. *Nature Reviews Immunology*, 5(4), 318–330.
- van Smeden, J., Janssens, M., Gooris, G. S., & Bouwstra, J. A. (2014). The important role of stratum corneum lipids for the cutaneous barrier function. *Biochimica et Biophysica Acta (BBA) - Molecular and Cell Biology of Lipids*, 1841(3), 295–313.
- Vecchia, B. E., & Bunge, A. L. (2003). Skin absorption databases and predictive equations. In R. H. Guy & J. Hadgraft (Eds.), *Transdermal drug delivery* (2nd ed., pp. 57–141). New York: Marcel Dekker.
- Vimal, K. R., Sankar, V., Srinivas, C. R., & Kumaresan, M. (2012). Enhancement of follicular delivery of finasteride in niosomal and proniosomal gel form for treating androgenetic alopecia. *Indian Drugs*, 49(5), 47–55.
- Vogt, A., Mandt, N., Lademann, J., Schaefer, H., & Blume-Peytavi, U. (2005). Follicular targeting--a promising tool in selective dermatotherapy. *The Journal of Investigative Dermatology*.
- Walters, K. A., & Roberts, M. S. (2002). The structure and function of the skin. In K. A. Walters & M. S. Roberts (Eds.), *Dermatological and Transdermal Formulations* (pp. 1–39). New York: Marcel Dekker Inc.
- Warner, R. R., Stone, K. J., & Boissy, Y. L. (2003). Hydration disrupts human stratum corneum

- ultrastructure. *The Journal of Investigative Dermatology*, 120(2), 275–84.
- Watt, F. M. (1989). Terminal differentiation of epidermal keratinocytes. *Current Opinion in Cell Biology*, 1(6), 1107–1115.
- Wessels, J. M., Ford, W. E., Szymczak, W., & Schneider, S. (1998). The Complexation of Tetracycline and Anhydrotetracycline with Mg<sup>2+</sup> and Ca<sup>2+</sup> : A Spectroscopic Study. *The Journal of Physical Chemistry B*, 102(46), 9323–9331.
- White, J. P., & Cantor, C. R. (1971). Role of magnesium in the binding of tetracycline to Escherichia coli ribosomes. *Journal of Molecular Biology*, 58(1), 397–400.
- Wiechers, J. W. (1989). The barrier function of the skin in relation to percutaneous absorption of drugs. *Pharmaceutisch Weekblad*, 11(6), 185–98.
- Williams, A. C. (2003). *Transdermal and topical drug delivery from theory to clinical practice*. London: Pharmaceutical Press.
- Williams, A. C., & Barry, B. W. (1992). Skin absorption enhancers. *Critical Reviews in Therapeutic Drug Carrier Systems*.
- Williams, A. C., & Barry, B. W. (2004). Penetration enhancers. *Advanced Drug Delivery Reviews*, 56(5), 603–18.
- Williams, A. C., & Barry, B. W. (2012a). Penetration enhancers. *Advanced Drug Delivery Reviews*, 64, 128–137.
- Williams, H. C. (1997). Dermatology. In A. Stevens & J. Raftery (Eds.), *Health Care Needs Assessment: The Epidemiologically Based Needs Assessment Reviews*. (Second Ser, pp. 261–348). Oxford: Radcliffe Publishing.
- Wolff, H. (2008). Male and female androgenetic alopecia. In H. C. Williams, M. E. Bigby, T. Diepgen, A.

- Herxheimer, L. Naldi, & B. Rzany (Eds.), *Evidence-based dermatology* (2nd ed., pp. 513–517). Singapore: Blackwell Publishing.
- Wood, A. J. J., & Rittmaster, R. S. (1994). Finasteride. *New England Journal of Medicine*, *330*(2), 120–125.
- Wood, D. G., Brown, M. B., & Jones, S. A. (2012). Understanding heat facilitated drug transport across human epidermis. *European Journal of Pharmaceutics and Biopharmaceutics*, *81*(3), 642–649.
- Wood, D. G., Brown, M. B., Jones, S. A., & Murnane, D. (2011). Characterization of Latent Heat-Releasing Phase Change Materials for Dermal Therapies. *The Journal of Physical Chemistry C*, *115*(16), 8369–8375.
- Wood, D. G., Jones, S. A., & Brown, M. B. (2012). Drug delivery formulations. United states of America: WIPO/PCT.
- Wosicka, H., & Cal, K. (2010). Targeting to the hair follicles: current status and potential. *Journal of Dermatological Science*, *57*(2), 83–9.
- Wu, Y., & Fassihi, R. (2005). Stability of metronidazole, tetracycline HCl and famotidine alone and in combination. *International Journal of Pharmaceutics*, *290*(1–2), 1–13.
- Yeoh, T. (2012). Current landscape and trends in transdermal drug delivery systems. *Therapeutic Delivery*, *3*(3), 295–7.
- Zauli, S., Caracciolo, S., Borghi, A., Ricci, M., Giari, S., Virgili, A., & Bettoli, V. (2014). Which factors influence quality of life in acne patients? *Journal of the European Academy of Dermatology and Venereology*, *28*(1), 46–50.
- Zewert, T. E., Pliquett, U. F., Vanbever, R., Langer, R., & Weaver, J. C. (1999). Creation of transdermal pathways for macromolecule transport by skin electroporation and a low toxicity, pathway-enlarging molecule. *Bioelectrochemistry and Bioenergetics (Lausanne, Switzerland)*, *49*(1), 11–

20.

Zhang, J., Hao, Z., Hull, A., & Rigby, L. (2003). Integrated apparatus for controlled heat aided dermal drug delivery. United States: United States Patent.

Zhang, Q., Li, P., Liu, D., & Roberts, M. S. (2013). Effect of Vehicles on the Maximum Transepidermal Flux of Similar Size Phenolic Compounds. *Pharmaceutical Research*, 30(1), 32–40.

Zhang, Q., Li, P., & Roberts, M. S. (2011). Maximum transepidermal flux for similar size phenolic compounds is enhanced by solvent uptake into the skin. *Journal of Controlled Release*, 154(1), 50–57.